

**INFRARED STUDIES ON THE SPECTRA AND STRUCTURES OF NOVEL
CARBON MOLECULES**

by

RAFAEL CARDENAS

Bachelor of Science, 1999
(UMNSH) University
Michoacán, México

Master of Science, 2002
(UTEP) University
Texas, USA

Submitted to the Graduate Faculty of the
College of Sciences and Engineering
Texas Christian University
in partial fulfillment of the requirements
for the degree of

DOCTOR OF PHILOSOPHY

December, 2007

Copyright by
Rafael Cárdenas
2007

ACKNOWLEDGEMENTS

I would like to express all my deep gratitude to my adviser Dr. W. R. M Graham for all the time and effort that he dedicated to my professional formation, without his commitment to help me every time I needed, my endeavor would not be possible. I would also like to thank to Dr. C. M. L. Rittby for his many helpful observations and suggestions I have received over my entire research concerning critical aspects of my work. The team of professional technicians Mr. Mike Murdock, Mr. David Yale and Mr. Jerry Katchinska perform and fabricate different mechanical apparatus and mechanisms to optimize the results of the material used in my research for which I thank them. For me to stay in Texas Christian University it would not be achievable if my wife, daughter and son would not be supporting me all the way. I also extend my appreciation to several sources which provided various kinds of financial support for me during my period reading for the degree, including my brothers and sisters. I would like to devote this work to the loving memory of my mother and to my father for all his support. Finally I would like thanks the Welch Foundation, the TCU Research found and the W.M. Keck Foundation for supporting of my work.

TABLE OF CONTENTS

ACKNOWLEDGMENTS.....	ii
LIST OF FIGURES.....	vi
LIST OF TABLES.....	xix
CHAPTER I. INTRODUCTION.....	1
1.1 Introduction.....	2
1.2 Development of the procedure to produce carbon rods with ¹³ C enrichment.....	9
CHAPTER II. EXPERIMENTAL PROCEDURES AND TECHNIQUES.....	16
2.1 Experimental setup.....	16
CHAPTER III. FTIR SPECTROSCOPIC STUDIES OF THE $\nu_4(\sigma_u)$ MODE OF C ₇	21
3.1 Introduction.....	21
3.2 Theoretical calculations.....	22
3.2.1 Deperturbation Method.....	26
3.3 Experimental procedure.....	29
3.4 Results and discussion.....	31
3.5 Assignment of the isotopomer for the $\nu_4(\sigma_u)$ mode of C ₇	33
3.6 Conclusion.....	42
CHAPTER IV. FTIR SPECTROSCOPIC STUDY OF THE $\nu_5(\sigma_u)$, $\nu_6(\sigma_u)$ AND $\nu_7(\sigma_u)$ MODES OF LINEAR C ₉	43
4.1 Introduction.....	43
4.2 Discussion an experimental procedure.....	46
4.3 Results and discussion.....	47
4.4 Assignment of the isotopomers for the $\nu_6(\sigma_u)$ mode of C ₉	48

4.5 Assignment of the isotopomers for the $\nu_5(\sigma_u)$ mode of C_9	60
4.6 Assignment of the isotopomers for the $\nu_7(\sigma_u)$ mode of C_9	68
4.7 Conclusions.....	70
CHAPTER V. FTIR SPECTROSCOPIC STUDY OF THE $\nu_6(\sigma_u)$ AND $\nu_7(\sigma_u)$ MODES OF LINEAR C_{10}	72
5.1 Introduction.....	72
5.2 Results and discussion.....	73
5.3 Assignment of the isotopomers for the $\nu_7(\sigma_u)$ mode of C_{10}	75
5.4 Assignment of the isotopomers for the $\nu_6(\sigma_u)$ mode of C_{10}	83
5.5 Conclusions.....	98
CHAPTER VI. FTIR SPECTROSCOPIC STUDY OF THE $\nu_7(\sigma_u)$, $\nu_8(\sigma_u)$ AND $\nu_9(\sigma_u)$ MODES OF LINEAR C_{11}	99
6.1 Introduction.....	99
6.2 Results and discussion.....	100
6.3 Assignment of the isotopomers for the $\nu_7(\sigma_u)$ mode of C_{11}	103
6.4 Assignment of the isotopomers for the $\nu_8(\sigma_u)$ mode of C_{11}	115
6.5 Assignment of the isotopomers for the $\nu_9(\sigma_u)$ mode of C_{11}	121
6.6 Conclusions.....	124
CHAPTER VII. FTIR SPECTROSCOPIC STUDY OF THE $\nu_5(\sigma_u)$ AND $\nu_6(\sigma_u)$ MODES OF OF LINEAR C_8 AND THE $\nu_7(\sigma_u)$, $\nu_8(\sigma_u)$ AND $\nu_9(\sigma_u)$ MODES OF OF LINEAR C_{12}	126
7.1 Introduction.....	126
7.2 Results and discussion for C_8	127

7.3 Assignment of the isotopomers for the $\nu_5(\sigma_u)$ mode of C_8	131
7.4 Assignment of the isotopomers for the $\nu_6(\sigma_u)$ mode of C_8	137
7.5 Results and discussion for C_{12}	141
7.6 Assignment of the isotopomers for the $\nu_7(\sigma_u)$ mode of C_{12}	142
7.7 Assignment of the isotopomers for the $\nu_8(\sigma_u)$ mode of C_{12}	151
7.8 Assignment of the isotopomers for the $\nu_9(\sigma_u)$ mode of C_{12}	156
7.9 Conclusions.....	160
CHAPTER VIII. FTIR SPECTROSCOPIC STUDY OF THE $\nu_{10}(\sigma_u)$ MODE OF LINEAR C_{15} AND THE $\nu_{12}(\sigma_u)$ MODE OF C_{18}	
8.1 Introduction.....	161
8.2 Results and discussion.....	162
8.3 Assignment of the isotopomers for the $\nu_{10}(\sigma_u)$ mode of C_{15}	166
8.4 Assignment of the isotopomers for the $\nu_{12}(\sigma_u)$ mode of C_{18}	175
8.5 Conclusions.....	189
CHAPTER IX. CONCLUSIONS AND FUTURE STUDIES.....	
9.1 Conclusions.....	190
9.2 Summary of Results.....	191
9.3 Future work.....	194
9.3.1 Future work on cyclic C_n molecules.....	196
APPENDIX. A. DEPERTURBATION METHOD (DPM).....	198
REFERENCES.....	202

LIST OF FIGURES

Figures	Page
Figure 1. Probability of observing the singly-substituted isotopomers for different C_n chains for the values $q = 1, 3 \leq n \leq 6$ and $0\% \leq c \leq 100\%$	6
Figure 2. Probability of observing the singly-substituted isotopomers for different C_n chains for the values $q = 1, 6 \leq n \leq 10$ and $0\% \leq c \leq 100\%$	7
Figure 3. Probability of observing the (where is $q = 1$) singly-substituted isotopomers for different C_n chains for the values $q = 1, 3 \leq n \leq 20$ and $0\% \leq c \leq 100\%$	8
Figure 4. Renovated furnace with heavy-duty welding cables and water-cooling lines.....	11
Figure 5. The temperature reached in the refitted cell is $2100\text{ }^{\circ}\text{C}$ for more than 30 days.....	12
Figure 6. General schematic for the cluster generator.....	18
Figure 7. General schematic for the cluster generator and FTIR Spectrometer (Bomem DA3.16).....	19
Figure 8. FTIR Spectrometer (Bomem DA3.16).....	43
Figure 9. Comparison of the FTIR spectra of the $\nu_4(\sigma_u)$ mode of the linear C_7 and its ^{12}C and ^{13}C isotopic shifts with carbon enrichments (a) $90\%^{13}\text{C}$ and $10\%^{12}\text{C}$ and $10\%^{13}\text{C}$ and $90\%^{12}\text{C}$ (c) and the simulations (b) and (d) derived from the DFT calculations at the B3YLP/cc-pVDZ level for the same enrichment values. The lower case letter c in the labels c1, c2..., indicates a single ^{12}C or ^{13}C carbon isotope and the number 1, 2... stands for the location (starting form left to right) where the carbon isotope is positioned for both complimentary spectrum, left [$90\%^{13}\text{C}$ and $10\%^{12}\text{C}$ (a)] and right [$10\%^{13}\text{C}$ and $90\%^{12}\text{C}$ (b)] of the spectra. The labels A and B will be used only for the vibrational	

fundamentals of ^{12}C and ^{13}C carbon chains respectively. The label $\text{C}_5,\text{c1}$ is related to the single substituted 12-13-13-13-13 isotopomer of the $\nu_4(\sigma_u)$ mode of linear C_5 obtained with a carbon enrichment of 90% ^{13}C and 10% ^{12}C and the label C_5,d refers to a double substituted isotopomer of the $\nu_4(\sigma_u)$ mode of linear C_5	32
Figure 10. Comparison of the observed FTIR spectrum of the $\nu_4(\sigma_u)$ mode of the linear C_7 and its single ^{13}C isotopic shifts using 90% ^{12}C and 10% ^{13}C (a) enrichment, and (b) a simulated spectrum derived from the DFT calculations at the B3YLP/cc-pVDZ level using the same enrichment values. Also the label C_5,d refers to a double substituted isotopomer of the $\nu_4(\sigma_u)$ mode of linear C_5	33
Figure 11. Comparison of the FTIR spectrum of the $\nu_4(\sigma_u)$ mode of the linear C_7 and its single ^{12}C isotopic shifts with (a) 10% ^{12}C /90% ^{13}C enrichment, and (b) a DFT B3YLP/cc-pVDZ simulation using the same enrichment.....	36
Figure 12. Comparison of the FTIR spectra of the $\nu_4(\sigma_u)$ mode of the linear C_7 and the $\nu_4(\sigma_u)$ mode of the linear C_5 and its single ^{12}C isotopic shifts with (a) 90% ^{13}C :10% ^{12}C enrichment, and (b) a DFT B3YLP/cc-pVDZ simulation using the same enrichment. Additionally the for the $\nu_4(\sigma_u)$ mode of the linear C_7	41
Figure 13. Comparison of the FTIR spectrum of the $\nu_6(\sigma_u)$ mode of linear C_9 and its single ^{13}C isotopic shifts with carbon enrichments (a) 90% ^{12}C and 10% ^{13}C and a simulation (b) derived from the DFT calculations at the B3YLP/cc-pVDZ level for the same enrichment values.....	49
Figure 14. Comparison of observed FTIR annealed spectra (a) 30 K (b) 28 K and (c) 22 K of .the $\nu_6(\sigma_u)$ mode of linear C_9 and its single ^{13}C isotopic shifts using 90% ^{12}C and 10% ^{13}C	

carbon enrichments, and (e) a simulated spectrum derived from the DFT calculations at the B3YLP/cc-pVDZ level using the same enrichment values.....	51
Figure 15. Comparison of observed FTIR annealed spectra (a)39.5 K (b) 39.0 K and (c) 10.0 K of the $\nu_6(\sigma_u)$ mode of linear C ₉ and its single ¹³ C isotopic shifts using 90% ¹² C and 10% ¹³ C carbon enrichments, and (e) a simulated spectrum derived from the DFT calculations at the B3YLP/cc-pVDZ level using the same enrichment values.....	52
Figure 16. Observed FTIR spectrum of the $\nu_6(\sigma_u)$ mode of linear C ₉ and $\nu_8(\sigma_u)$ mode and the its single ¹³ C-substituted (¹³ C ¹² C ₈) carbon clusters and the $\nu_8(\sigma_u)$ mode of linear C ₁₂ ⁵ and its isotopic shifts using 90% ¹² C and 10% ¹³ C enrichment.....	54
Figure 17. Comparison of an FTIR spectrum of the $\nu_6(\sigma_u)$ mode of the linear C ₉ and its isotopic shifts with (a) 10% ¹² C /90% ¹³ C and (b) a DFT calculations at the B3YLP/cc-pVDZ simulation using the same enrichment.....	55
Figure 18. Comparison of observed FTIR annealed spectra (a)(35 K) and (b) (10 K) of the $\nu_6(\sigma_u)$ mode of linear C ₉ and its single ¹² C isotopic shifts using 90% ¹³ C and 10% ¹² C carbon enrichments and (c) a DFT calculations at the B3YLP/cc-pVDZ simulation using the same enrichment.....	58
Figure 19. Comparison of an FTIR spectrum of the $\nu_5(\sigma_u)$ mode of linear C ₉ and its single ¹³ C isotopic shifts with (a) 10% ¹³ C and 90% ¹² C enrichment, and (b) a DFT B3YLP/cc-pVDZ simulation using the same enrichment.....	61
Figure 20. A section of Fig. 18 has been enlarged to visually emphasize the preliminary selection of the 13-12-12-12-12-12-12-12-12 (c1) and the12-13-12-12-12-12-12-12-12 (c2) isotopomers correspondent to the $\nu_5(\sigma_u)$ mode of linear C ₉	62

Figure 21. Comparison of an FTIR spectrum of the $\nu_5(\sigma_u)$ mode of linear C_9 its single ^{12}C isotopic shifts with (a) 90% ^{13}C and 10% ^{12}C enrichment, and (b) DFT B3YLP/cc-pVDZ simulation using the same enrichment.....65

Figure 22. The partial spectrum of the ^{13}C shifts for the $\nu_7(\sigma_u)$ mode of $^{12}C_9$ showing the overlapping H_2O bands (from Kranze *et al.*)⁷.....68

Figure 23. Comparison of the FTIR spectra of the $\nu_7(\sigma_u)$ mode of the linear C_9 and its ^{12}C and ^{13}C isotopic shifts with carbon enrichments (a) 10% ^{12}C and 90% ^{13}C (c) and 90% ^{12}C and 10% ^{13}C (c) and a simulations (b) and (d) derived from the DFT calculations at the B3YLP/cc-pVDZ level for the same enrichment values.....69

Figure 24. Comparison of observed FTIR of the of the $\nu_7(\sigma_u)$ mode of the linear C_{10} and its single ^{12}C and ^{13}C isotopic shifts with carbon enrichments (a) 90% ^{13}C and 10% ^{12}C and a simulation (b) derived from the DFT calculations at the B3YLP/cc-pVDZ level for the same enrichment values.....74

Figure 25. Comparison of observed FTIR annealed spectra (a) 34 K (b) 10 K of the of the $\nu_7(\sigma_u)$ mode of the linear C_{10} and its single ^{12}C and ^{13}C isotopic shifts with carbon enrichments (a) 90% ^{13}C and 10% ^{12}C and a simulation (b) derived from the DFT calculations at the B3YLP/cc-pVDZ level for the same enrichment values.....76

Figure 26. Comparison of the FTIR spectra of the $\nu_7(\sigma_u)$ mode of the linear C_{10} and its isotopic shifts with (a) 90% ^{13}C and 10% ^{12}C mixture and (b) a DFT calculations at the B3YLP/cc-pVDZ level simulation using the same enrichment.....78

Figure 27. Comparison of observed FTIR annealed spectra (a)(38 K) and (b) (10 K) of the $\nu_6(\sigma_u)$ mode of linear C_{10} and its single ^{12}C isotopic shifts using 90% ^{13}C and 10% ^{12}C

carbon enrichments and (c) a DFT calculations at the B3YLP/cc-pVDZ simulation using the same enrichment.....	81
Figure 28. DFT calculation at the B3YLP/cc-pVDZ level for the enrichment values 90% ¹² C and 10% ¹³ C of the $\nu_6(\sigma_u)$ mode of the linear C ₁₀ and its single ¹³ C isotopic shifts. To show the existence of the c3' and c5' not easily seeing.....	84
Figure 29. Two spectrums (a) (increase vertical gain) and (b) of the same DFT calculation at the B3YLP/cc-pVDZ level for the enrichment values 90% ¹² C and 10% ¹³ C of the $\nu_6(\sigma_u)$ mode of the linear C ₁₀ and its single ¹³ C isotopic shifts. To show the existence of the c2', c3', c4' and c5' not easily seeing.....	85
Figure 30. Two spectrums (a) (increase vertical gain) and (b) of the same DFT calculation at the B3YLP/cc-pVDZ level for the enrichment values 90% ¹² C and 10% ¹³ C of the $\nu_6(\sigma_u)$ mode of the linear C ₁₀ and its single ¹³ C isotopic shifts. To show the existence of the c2', c3', c4' and c5' not easily seeing.....	86
Figure 31. Comparison of the observed FTIR spectrum of the of the $\nu_6(\sigma_u)$ mode of the linear C ₁₀ and its single ¹² C and ¹³ C isotopic shifts with carbon enrichments (a) 90% ¹³ C and 10% ¹² C and a simulation (b) derived from the DFT calculations at the B3YLP/cc-pVDZ level for the same enrichment values. The lower case letter c in the labels c1, c2..., indicates a single ¹² C or ¹³ C carbon isotope and the number 1, 2... stands for the location (starting form left to right) where the carbon isotope is positioned. c1, c2... belong to the $\nu_6(\sigma_u)$ mode of the linear ¹³ C ₁₀ and c1', c2'... belong to the infrared active shifts of the $\nu_1(\sigma_g)$ mode of the linear ¹² C ₁₀	87
Figure 32. Comparison of observed FTIR of the of the $\nu_6(\sigma_u)$ mode of the linear C ₁₀ and its single ¹² C and ¹³ C isotopic shifts with carbon enrichments (a) 90% ¹³ C and 10% ¹² C and	

a simulation (b) derived from the DFT calculations at the B3YLP/cc-pVDZ level for the same enrichment value.....89

Figure 33. FTIR spectra obtained with 90%¹³C and 10%¹²C carbon enrichment, where the $\nu_6(\sigma_u)$ mode of the linear C₁₀ and its single ¹²C-isotopic shifts suppose to lie.....91

Figure 34. Comparison of the FTIR spectra of the $\nu_6(\sigma_u)$ mode of the linear ¹³C₁₀ and its isotopic shifts with (a) 10%¹²C and 90%¹³C mixture and (b) a DFT calculations at the B3YLP/cc-pVDZ level simulation using the same enrichment. The label B will be used only for the vibrational fundamentals of $\nu_6(\sigma_u)$ mode of the linear ¹³C₁₀. The lower case letter c in the labels c1, c2..., indicates a single ¹²C or ¹³C carbon isotope and the number 1, 2... stands for the location (starting from left to right) where the carbon isotope is positioned. c1, c2... belong to the $\nu_6(\sigma_u)$ mode of the linear ¹³C₁₀ and c1', c2'... that belong to the infrared active shifts of the $\nu_1(\sigma_g)$ mode of the linear ¹³C₁₀. The square, dot and rectangle corresponds to the $\nu_{14}(\sigma_u)$ mode of the ¹³C₁₀, $\nu_5(\sigma_u)$ mode of the linear ¹³C₉ and $\nu_3(\sigma_u)$ mode of the linear ¹³C₃ respectively.....93

Figure 35. Both (a)(red) and (b)(blue) are spectra derived from the DFT calculations at the B3YLP/cc-pVDZ level and its isotopic shifts with (a) 10%¹²C and 10%¹³C mixture (b) 90%¹³C and 10%¹²C. The bars in black and yellow are only for the purpose of illustrate where the interacting non infrared active $\nu_1(\sigma_g)$ mode and the observed single ¹²C (a) and ¹³C (b) isotopic shifts would appear. We can see also the repulsion between the shifts of the interacting ν_1 and ν_6 modes.....97

Figure 36. Both (a)(red) and (b)(blue) are spectra derived from the DFT calculations at the B3YLP/cc-pVDZ level and its isotopic shifts with (a) 10%¹²C and 90%¹³C mixture (b) 90%¹³C and 10%¹²C. The bar in black is only for the purpose of illustrate where the

interacting non infrared active $\nu_2(\sigma_g)$ mode would appear. We can see also a representation of the repulsion between the shifts of the interacting ν_2 and ν_7 modes....102

Figure 37. Comparison of observed FTIR of the of the $\nu_7(\sigma_u)$ mode of the linear C_{11} and its single ^{12}C and ^{13}C isotopic shifts with carbon enrichments (a) 90% ^{12}C and 10% ^{13}C and a simulation (b) derived from the DFT calculations at the B3YLP/cc-pVDZ level for the same enrichment values.....105

Figure 38. Comparison of the FTIR spectra of the $\nu_7(\sigma_u)$ mode of the linear C_{11} and its isotopic shifts with (a) 90% ^{13}C and 10% ^{12}C mixture and (b) a DFT calculations at the B3YLP/cc-pVDZ level simulation using the same enrichment.....109

Figure 39. Both (a)(red) and (b)(blue) are spectra derived from the DFT calculations at the B3YLP/cc-pVDZ level and its isotopic shifts with (a) 10% ^{12}C and 10% ^{13}C mixture (b) 90% ^{13}C and 10% ^{12}C . The bars in black and yellow are only for the purpose of illustrate where the interacting non infrared active $\nu_2(\sigma_g)$ mode and the observed single ^{12}C (a) and ^{13}C (b) isotopic shifts would appear. We can see also the repulsion between the shifts of the interacting ν_2 and ν_7 modes.....114

Figure 40. Comparison of observed FTIR annealed spectra (a)35.0 K and (b) 10.0 K of the $\nu_6(\sigma_u)$ mode of linear C_{11} and its single ^{13}C isotopic shifts using 90% ^{12}C and 10% ^{13}C carbon enrichments, and (c) a simulated spectrum derived from the DFT calculations at the B3YLP/cc-pVDZ level using the same enrichment116

Figure 41. Comparison of observed FTIR annealed spectra (a)38 K (b) 34 K and (c) 10 °K of the $\nu_6(\sigma_u)$ mode of linear C_{11} and its single ^{13}C isotopic shifts using 10% ^{12}C and 90% ^{13}C carbon enrichments, and (d) a simulated spectrum derived from the DFT calculations at the B3YLP/cc-pVDZ level using the same isotopic enrichments.....118

- Figure 42. Comparison of observed FTIR annealed spectra (a)40 K (b) 38 K and (c) 10 K of the $\nu_9(\sigma_u)$ mode of linear C_{11} and its single ^{13}C isotopic shifts using 90% ^{12}C and 10% ^{13}C carbon enrichments, and (d) a simulated spectrum derived from the DFT calculations at the B3YLP/cc-pVDZ level using the same enrichment values.....122
- Figure 43. The spectra are derived from DFT calculations at the B3YLP/cc-pVDZ level of the isotopic shifts with a (a) 10% ^{12}C /10% ^{13}C mixture (b) 90% ^{13}C /10% ^{12}C mixture. The bar in black is only for the purpose of illustrating where the interacting infrared forbidden $\nu_1(\sigma_g)$ mode would appear. We can see also a representation of the repulsion between the shifts of the interacting ν_1 and ν_5 modes.....130
- Figure 44. . Comparison of observed FTIR annealed spectra (a) 43K (b) 30 K and (c) 10 K of the $\nu_5(\sigma_u)$ mode of linear C_8 and its single ^{13}C -isotopic shifts using 90% ^{12}C and 10% ^{13}C carbon enrichments, and (d) a simulated spectrum derived from the DFT calculations at the B3YLP/cc-pVDZ level using the same enrichment values.132
- Figure 45. Comparison of observed FTIR annealed spectra (a)35 K (b) 32 K and (c) 10 K of the $\nu_5(\sigma_u)$ mode of linear C_8 and its single ^{12}C -isotopic shifts using 10% ^{12}C and 90% ^{13}C carbon enrichments, and (d) a simulated spectrum derived from the DFT calculations at the B3YLP/cc-pVDZ level using the same enrichment values.....134
- Figure 46. Both (a)(red) and (b)(blue) are spectra derived from the DFT calculations at the B3YLP/cc-pVDZ level and its isotopic shifts with (a) 10% ^{12}C and 10% ^{13}C mixture (b) 90% ^{13}C and 10% ^{12}C , in comparison with the observed shifts, obtained by using the same isotopic mixtures. The bar in black is only for the purpose of illustrate where the interacting non infrared active $\nu_1(\sigma_g)$ mode would appear. We can see also a

representation of the repulsion between the shifts of the interacting ν_1 and ν_5 modes.....	136
Figure 47. Comparison of observed FTIR annealed spectra (a) the $\nu_5(\sigma_u)$ mode of linear C_8 and its single ^{13}C -isotopic shifts using 90% ^{12}C and 10% ^{13}C carbon enrichments, and (b) a simulated spectrum derived from the DFT calculations at the 3YLP/cc-pVDZ level using the same enrichment values.....	138
Figure 48. Comparison of observed FTIR annealed spectra (a)35.5 K and (b) 10.0 K of the $\nu_6(\sigma_u)$ mode of linear C_8 and its single ^{13}C isotopic shifts using 90% ^{12}C and 10% ^{13}C carbon enrichments, and (c) a simulated spectrum derived from the DFT calculations at the B3YLP/cc-pVDZ level using the same enrichment values.....	139
Figure 49. Both (a)(red) and (b)(blue) are spectra derived from the DFT calculations at the B3YLP/cc-pVDZ level and its isotopic shifts with (a) 10% ^{12}C and 10% ^{13}C mixture (b) 90% ^{13}C and 10% ^{12}C . The bar in black is only for the purpose of illustrate where the interacting non infrared active $\nu_1(\sigma_g)$ mode would appear. We can see also a representation of the repulsion between the shifts of the interacting ν_1 and ν_7 modes...	144
Figure 50. Comparison of observed FTIR annealed spectra (a)30 K, 28 K (b) and (c)10 K of the $\nu_6(\sigma_u)$ mode of linear C_{12} and its single ^{13}C isotopic shifts using 90% ^{12}C and 10% ^{13}C carbon enrichments, and (c) a simulated spectrum derived from the DFT calculations at the B3YLP/cc-pVDZ level using the same enrichment values.....	146
Figure 51. Comparison of observed FTIR annealed spectra (a)35.5 K and (b) 10.0 K of the $\nu_7(\sigma_u)$ mode of linear C_{12} and its single ^{13}C isotopic shifts using 90% ^{12}C and 10% ^{13}C carbon enrichments, and (c) a simulated spectrum derived from the DFT calculations at the B3YLP/cc-pVDZ level using the same enrichment values.....	148

Figure 52. Both (a)(red) and (b)(blue) are spectra derived from the DFT calculations at the B3YLP/cc-pVDZ level and its isotopic shifts with (a) 10%¹²C and 10%¹³C mixture (b) 90%¹³C and 10%¹²C. The bars in yellow are to show where the observed frequencies would be located. The bar in black is only for the purpose of illustrate where the interacting non infrared active $\nu_1(\sigma_g)$ mode would appear. We can see also a representation of the repulsion between the shifts of the interacting ν_1 and ν_7 modes...150

Figure 53. Comparison of observed FTIR annealed spectra (a)39.5 K and (b) 10.0 K of the (a) the $\nu_8(\sigma_u)$ mode of linear C₁₂ and its single ¹³C-isotopic shifts using 90%¹²C and 10%¹³C carbon enrichments, and (b) and (c) are simulated spectra derived from the DFT calculations at the B3YLP/cc-pVDZ level using the same enrichment values, for the $\nu_6(\sigma_u)$ mode of linear C₉ and $\nu_8(\sigma_u)$ mode of linear C₁₂ in that order.....152

Figure 54. Comparison of observed FTIR annealed spectra (a)32.5 K and (b) 27.0K and (c)10.0 K of the $\nu_8(\sigma_u)$ mode of linear C₁₂ and its single ¹³C isotopic shifts using 90%¹²C and 10%¹³C carbon enrichments, and (d) and (f) a simulated spectrum derived from the DFT calculations at the B3YLP/cc-pVDZ level using the same enrichment values for the $\nu_6(\sigma_u)$ mode of linear C₉ and $\nu_8(\sigma_u)$ mode of linear C₁₂ in that order.....154

Figure 55. Comparison of observed FTIR (a) the $\nu_9(\sigma_u)$ mode of linear C₁₂ and its single ¹³C-isotopic shifts using 90%¹²C and 10%¹³C carbon enrichments, and (b) is a simulated spectra derived from the DFT calculations at the B3YLP/cc-pVDZ level using the same enrichment values.....157

Figure 56. Comparison of observed FTIR spectra (a)38 K and (b) 10 K and for the $\nu_9(\sigma_u)$ mode of linear C₁₂ and its single ¹³C isotopic shifts using 90%¹²C and 10%¹³C carbon

enrichments, and (c) is a simulated spectrum derived from the DFT calculations at the B3YLP/cc-pVDZ level using the same enrichment values.....	158
Figure 57. Comparison of observed FTIR spectra (a) and (b) obtained through different experiments using same 90% ¹² C and 10% ¹³ C carbon enrichments, and (c) DFT calculations at the B3YLP/cc-pVDZ level using the same enrichment values of different C _n molecules.....	162
Figure 58. Comparison of a collection of different observed FTIR spectra (a)...(e) obtained through different experiments using 90% ¹² C and 10% ¹³ C carbon enrichments, and (f) a collection of simulated spectrum derived from the DFT calculations at the B3YLP/cc-pVDZ level using the same enrichment values of different C _n molecules.....	163
Figure 59. Comparison of observed FTIR and DFT calculated vibrational fundamentals at the B3YLP/cc-pVDZ level for linear C _n chains with an odd number of atoms. (Courtesy of C. M. L Rittby).....	164
Figure 60. Comparison of observed FTIR and DFT calculated vibrational fundamentals at the B3YLP/cc-pVDZ level for linear C _n chains with an even number of atoms. (Courtesy of C. M. L Rittby).....	165
Figure 61. Comparison of observed FTIR annealed spectra (a)42.0 K and (b) 10.0 K of the ν ₁₀ (σ _u) mode of linear of C ₁₅ and its single ¹³ C isotopic shifts using 90% ¹² C and 10% ¹³ C carbon enrichments, and (c) a simulated spectrum derived from DFT calculations at the B3YLP/cc-pVDZ level using the same enrichment values.....	168
Figure 62. Comparison of observed FTIR annealed spectra (a)43.0 K and (b) 10.0 K of the ν ₁₀ (σ _u) mode of linear of C ₁₅ and its single ¹³ C isotopic shifts using 90% ¹² C and 10% ¹³ C carbon enrichments, and (c) a simulated spectrum derived from the DFT calculations at the B3YLP/cc-pVDZ level using the same enrichment values.....	170

- Figure 63. Comparison of observed FTIR annealed spectra (a) 36 K and (b) 10 K of the $\nu_8(\sigma_u)$ mode of linear C_{12} and its single ^{13}C isotopic shifts using 90% ^{12}C and 10% ^{13}C carbon enrichments and a simulated spectrum derived from the DFT calculations at the B3YLP/cc-pVDZ level using the same enrichment values for the $\nu_{10}(\sigma_u)$ mode of linear C_{10}171
- Figure 64. Both (a)(red) and (b)(blue) are spectra derived from DFT calculations at the B3YLP/cc-pVDZ level of the isotopic shifts with a (a) 10% ^{12}C /10% ^{13}C mixture (b) 90% ^{13}C /10% ^{12}C mixture. The bar in black is only for the purpose of illustrating where the interacting infrared forbidden $\nu_1(\sigma_g)$ mode would appear. We can see also a representation of the repulsion between the shifts of the interacting ν_3 mode.....176
- Figure 65. Comparison of observed FTIR annealed spectra (a)37 K, (b) 35K and (c) 35 K of the $\nu_{12}(\sigma_u)$ mode of linear of C_{18} and its single ^{13}C isotopic shifts using 90% ^{12}C and 10% ^{13}C carbon enrichments, and (d) a simulated spectrum derived from the DFT calculations at the B3YLP/cc-pVDZ level using the same enrichment values.....78
- Figure 66. Is a comparison of observed FTIR annealed spectra (a) 37.0 K, (b) 35.0 K and (c) 35.0 K of the not IR-allowed $\nu_3(\sigma_g)$ mode of linear of C_{18} and its single ^{13}C isotopic shifts using 90% ^{12}C and 10% ^{13}C carbon enrichments, and (d) a simulated spectrum derived from the DFT calculations at the B3YLP/cc-pVDZ level using the same enrichment values.....180
- Figure 67. Comparison of observed FTIR annealed spectra (a) 36 K and (b) 10 K of the $\nu_6(\sigma_u)$, $\nu_8(\sigma_u)$, $\nu_{10}(\sigma_u)$ and $\nu_{12}(\sigma_u)$ mode of linear C_9 , C_{12} , C_{15} and C_{18} and its single ^{13}C isotopic shifts using 90% ^{12}C and 10% ^{13}C carbon enrichments and a simulated spectra derived from the DFT calculations at the B3YLP/cc-pVDZ level using the same enrichment

values for the $\nu_6(\sigma_u)$, $\nu_8(\sigma_u)$, $\nu_{10}(\sigma_u)$ and $\nu_{12}(\sigma_u)$ mode of linear C ₉ , C ₁₂ , C ₁₅ and C ₁₈	182
Figure 67. Comparison of observed FTIR annealed spectra (a) 36 K and (b) 10 K of the $\nu_{12}(\sigma_u)$ mode of linear C ₁₈ and its single ¹³ C isotopic shifts using 90% ¹² C and 10% ¹³ C carbon enrichments and a simulated spectra derived from the DFT calculations at the B3YLP/cc-pVDZ level using the same enrichment values for the $\nu_{12}(\sigma_u)$ mode of linear C ₁₈	185
Fig. 69. Both (a)(red) and (b)(blue) are spectra derived from DFT calculations at the B3YLP/cc-pVDZ level of the isotopic shifts with a (a) 10% ¹² C/10% ¹³ C mixture (b) 90% ¹³ C/10% ¹² C mixture. The bars in yellow are only to represent where the observed frequencies would be located. The bar in black is also for the purpose of illustrating where the interacting infrared forbidden $\nu_1(\sigma_g)$ mode would appear. We can see also a representation of the repulsion between the shifts of the interacting ν_3 and ν_{12} modes.	188
Figures in the Appendix A.	Page
Appendix A. Figure A.1. Energy corrections to first (middle) and second order (right) in perturbation theory after the system is subjected to a positive perturbation (a) W^+ (adding mass) and to a negative perturbation (b) W^- (subtracting mass) (Fig. courtesy of G. García).....	199
Appendix A. Figure A.2. Elimination of the coupling effects of E_2 on E_1^+ and E_1^- by “mirroring” the energy E_1^- and taking the average between the “mirrored” energy $E_{1,m}^-$ and the energy E_1^+ . (Fig. courtesy of G. García).....	201

LIST OF TABLES

Table I. DFT B3LYP/cc-pVDZ predicted vibrational frequencies and band intensities for (ℓ -C ₇).....	25
Table II. Comparison of observed and predicted DFT (B3LYP/cc-pVDZ) frequencies for single ¹³ C-substituted isotopomers of ¹² C ₇ and single ¹² C-substituted isotopomers of ¹³ C ₇ for the ν_4 mode.....	37
Table III. DFT B3LYP/cc-pVDZ predicted vibrational frequencies and band intensities for (ℓ -C ₉).....	45
Table IV. Comparison of observed and predicted DFT (B3LYP/cc-pVDZ) frequencies for single ¹³ C-substituted isotopomers of ¹² C ₉ and single ¹² C-substituted isotopomers of ¹³ C ₉ for the ν_6 mode.....	56
Table V. Comparison of observed and predicted DFT (B3LYP/cc-pVDZ) frequencies for single ¹³ C-substituted isotopomers of ¹² C ₉ and single ¹² C-substituted isotopomers of ¹³ C ₉ for the ν_5 mode.....	66
Table VI. Comparison of observed and predicted DFT (B3LYP/cc-pVDZ) frequencies for single ¹³ C-substituted isotopomers of ¹² C ₉ and single ¹² C-substituted isotopomers of ¹³ C ₉ for the ν_7 mode.....	70
Table VII. DFT B3LYP/cc-pVDZ predicted vibrational frequencies and band intensities for (ℓ -C ₁₀).....	97
Table VIII. Comparison of observed and predicted DFT (B3LYP/cc-pVDZ) frequencies for single ¹³ C-substituted isotopomers of ¹² C ₁₀ and single ¹² C-substituted isotopomers of ¹³ C ₁₀ for the ν_7 mode.....	79

Table IX. Comparison of observed and predicted DFT (B3LYP/cc-pVDZ) frequencies for single ^{13}C -substituted isotopomers of $^{12}\text{C}_{10}$ and single ^{12}C -substituted isotopomers of $^{13}\text{C}_{10}$ for the ν_6 mode.....	94
Table X. DFT B3LYP/cc-pVDZ predicted vibrational frequencies and band intensities for ($\ell\text{-C}_{11}$).....	101
Table XI. Comparison of observed and predicted DFT (B3LYP/cc-pVDZ) frequencies for single ^{13}C -substituted isotopomers of $^{12}\text{C}_{11}$ and single ^{12}C -substituted isotopomers of $^{13}\text{C}_{11}$ for the ν_8 mode.....	110
Table XII. Comparison of observed and predicted DFT (B3LYP/cc-pVDZ) frequencies for single ^{13}C -substituted isotopomers of $^{12}\text{C}_{11}$ and single ^{12}C -substituted isotopomers of $^{13}\text{C}_{11}$ for the ν_7 mode.....	119
Table XIII. Comparison of observed and predicted DFT (B3LYP/cc-pVDZ) frequencies for single ^{13}C -substituted isotopomers of $^{12}\text{C}_{11}$ and single ^{12}C -substituted isotopomers of $^{13}\text{C}_{11}$ for the ν_9 mode.....	124
Table XIV. DFT B3LYP/cc-pVDZ predicted vibrational frequencies and band intensities for ($\ell\text{-C}_8$).....	128
Table XV. Comparison of observed and predicted DFT (B3LYP/cc-pVDZ) frequencies for single ^{13}C -substituted isotopomers of $^{12}\text{C}_8$, and single ^{12}C -substituted isotopomers of $^{13}\text{C}_8$, for the ν_8 mode.....	135
Table XVI. Comparison of observed and predicted DFT (B3LYP/cc-pVDZ) frequencies for single ^{13}C -substituted isotopomers of $^{12}\text{C}_8$, and single ^{12}C -substituted isotopomers of $^{13}\text{C}_8$, for the ν_6 mode.....	140

Table XVII. DFT B3LYP/cc-pVDZ predicted vibrational frequencies and band intensities for (ℓ -C ₁₂).....	142
Table XVIII. Comparison of observed and predicted DFT (B3LYP/cc-pVDZ) frequencies for single ¹³ C-substituted isotopomers of ¹² C ₁₂ , and single ¹² C-substituted isotopomers of ¹³ C ₁₂ , for the ν_6 mode.....	149
Table XIX. Comparison of observed and predicted DFT (B3LYP/cc-pVDZ) frequencies for single ¹³ C-substituted isotopomers of ¹² C ₁₂ , and single ¹² C-substituted isotopomers of ¹³ C ₁₂ , for the ν_8 mode.....	155
Table XX. Comparison of observed and predicted DFT (B3LYP/cc-pVDZ) frequencies for single ¹³ C-substituted isotopomers of ¹² C ₁₂ , and single ¹² C-substituted isotopomers of ¹³ C ₁₂ , for the ν_9 mode.....	159
Table XXI. DFT B3LYP/cc-pVDZ predicted vibrational frequencies and band intensities for (ℓ -C ₁₅).....	166
Table XXII. Comparison of observed and predicted DFT (B3LYP/cc-pVDZ) frequencies for single ¹³ C-substituted isotopomers of ¹² C ₁₅ , and single ¹² C-substituted isotopomers of ¹³ C ₁₈ , for the ν_{10} mode.....	173
Table XXIII. DFT B3LYP/cc-pVDZ predicted vibrational frequencies and band intensities for (ℓ -C ₁₈).....	175
Table XXIV. Comparison of observed and predicted DFT (B3LYP/cc-pVDZ) frequencies for single ¹³ C-substituted isotopomers of ¹² C ₁₈ , and single ¹² C-substituted isotopomers of ¹³ C ₁₈ , for the ν_{12} mode.....	184

Table XXV. Observed results for full $^{12}\text{C}_n$ and $^{13}\text{C}_n$ and their single substituted $^{12}\text{C}_{n-1}^{13}\text{C}$ and $^{12}\text{C}^{13}\text{C}_{n-1}$ isotopomers for C_n clusters with $n \leq 12$, obtained by the laser ablation technique on carbon rods with high ^{13}C enrichment.....	193
Table XXVI. Observed unknown bands of $^{12}\text{C}_n$ species and its correspondent $^{13}\text{C}_n$ scaled via $\nu(^{12}\text{C}) = \sqrt{\frac{13.0}{12.0}}[\nu(^{13}\text{C})]$	196
Table XXVII. Proposed results for the cyclic C_n carbon chains obtained by the laser ablation.....	197

CHAPTER I INTRODUCTION

1.1 Introduction

Carbon clusters have been the subjects of extensive theoretical and experimental studies for over 35 years.^{1,2,3} Carbon chains, which can be experimentally formed by trapping the products from the evaporation of graphite in argon and neon matrices, have drawn particular attention from astrophysicists who are trying to understand the atmospheres of late-type carbon-rich stars like CW Leonis (IRC + 10216), the molecular cloud TMC-1 in Taurus,^{1,5} and interstellar space where molecules with carbon-chain backbones are abundant.^{4,5,6} However, observation of this rich variety of molecules faces two problems. First, since Earth's atmosphere blocks a large part of the incident infrared radiation, most of the molecules cannot be observed from the ground. Second, vast regions of space filled with dense clouds of gas and dust can block the view of optical telescopes. Space-based infrared telescopes, like the Space Infrared Telescope Facility (SIRTF) (launched August 2003), are equipped with infrared detectors to examine the infrared radiation that can penetrate the clouds, thus revealing valuable information about their molecular composition. By increasing the amount of data by using this new observations frequently result on the recognition of possible new molecules, and a rich variety of Unidentified Infrared Bands (UIB)^{7,8,9,10,11,12,13} as well.

It is also important from a purely spectroscopic perspective to establish the vibrational fundamentals and to determine the novel structures of carbon chains and rings. A well known example of the importance of basic spectroscopy studies was the discovery of a new form of pure

carbon in 1985 by Robert Curl, Harold Kroto, and Richard Smalley, who were awarded the Nobel Prize in chemistry in 1996. They provided strong experimental evidence to suggest that carbon chains and rings are precursors to the formation of more complicated structures such as multi-fullerenes and nanotubes.^{14,15,16} Engineers are trying to understand the chemical processes that take place during the combustion of hydrocarbon fuels, the formation of soot and the deposition of carbide microfilms, which have potential application in semiconductor technology and microelectronics products.^{17,18,19,20,21,22,23,24} They also study the structures and properties of the chemical bonds of carbon species and the possibility of predicting the structures and properties of as yet, undiscovered larger C_n ($n \geq 60$) molecules. In spite of these studies, there are still incomplete experimental measurements of the fundamental vibrations of C_n species, which can be identified using infrared spectroscopy and matrix isolation. Specifically needed are measurements on neutral linear C_n ($n = 7-12$)^{15,16,17,18,19,20} and cyclic C_n ($n = 6-8$)^{24,25,27} species. Furthermore, little information is known about isotopic experimental measurements of the fundamental vibrations of larger neutral linear C_n ($n > 12$) and cyclic C_n ($n > 8$) molecules. In our present work we will present new studies on the fundamental vibrational modes of the linear C_n ($n = 7,9$) (see chapters III, IV) and potential candidates for some of the vibrational fundamentals for even longer linear C_n ($n = 10,11,15,18$) see chapter VI species, with the aim of contributing to a broader information of the C_n species.

Assignment of frequencies to specific molecules using matrix isolation can be a challenging task since matrices usually contain a mixture of carbon clusters of varying sizes. The complete characterization of C_n species is a challenge for experimentalists because it is not always possible to identify every mode for a given C_n species, especially when trying to include the

associated isotopic frequencies. However, the symbiosis between Fourier transform infrared (FTIR) spectroscopy of molecules formed by laser ablation and trapped in a rare gas matrix and *ab initio* theory has proven to be one of the most effective ways identify the vibrational fundamentals of carbon clusters.²⁵ Comparison between measured and predicted ¹²C and ¹³C isotopic shifts has been crucial to the correct identifications of the vibrational fundamentals of specific C_n species. The laser ablation technique²⁶ provides a particularly effective way to produce trapped carbon clusters for matrix infrared investigations. Using these techniques, vibrational fundamentals for the C_n , ($3 \leq n \leq 7$, $n=9,12$) linear carbon chains as well as the cyclic C_6 and C_8 clusters have been identified in the TCU Molecular Physics Laboratory.^{27,28,29,30,31,32,33,34} Additionally, vibrational fundamentals have been identified for clusters based on the Group IVA atoms, such as Si_nC_m ,³⁵ Ge_nC_m ,^{36,37} and $Si_nC_mGe_l$.³⁸

Recent, substantial improvements in experimental techniques³⁹ and the development of a process to fabricate carbon rods, with specific ¹³C enrichments in the TCU Molecular Physics Laboratory,³² now offer us the possibility of routinely achieving experimental reproducibility, which will allow better comparisons between spectra and may lead to the possible identification of new vibrational fundamentals of larger C_n ($n \geq 9$) species. The author's aim with this work is to present new experimental measurements and DFT calculations⁴⁰ for the $\nu_4(\sigma_u)$ modes of C_7 at 2128.1 cm^{-1} ,⁴¹ for the $\nu_6(\sigma_u)$ and $\nu_7(\sigma_u)$ modes of C_9 located at 1601.0 , and 1998.0 cm^{-1} , respectively,^{42,43} and for the $\nu_5(\sigma_u)$ vibrational fundamental of C_9 located at 2078.2 cm^{-1} . Furthermore, we will present recent advances for larger molecules such as the linear C_n ($n \geq 12$) and cyclic C_n ($n > 8$) carbon molecules which might contribute to an understanding the formation mechanisms of molecules as large as the fullerenes C_{60} , C_{70} , or C_{120} .

In the quest to identify the vibrational fundamentals of long carbon molecules we have

faced two main problems. The first one is that the main frequency of the carbon molecule is shifted when ^{13}C isotopic substitutions are made for one or more of the atoms forming the molecule. Different shifts arise, depending on the arrangement of ^{12}C and ^{13}C atoms in the molecule. By adjusting the percentages utilized in the mixture of ^{12}C and ^{13}C isotopes, we can potentially obtain all possible isotopic shifts. For example, in the simple case of C_3 , using a $^{12}\text{C}/^{13}\text{C}=50/50\%$ mixture, all isotopomers have the same probability of being formed. There are five possible shifts corresponding to two different single substitutions, two different double substitutions, and a full substitution. For C_6 will be 36 different shifts, and for C_n species with $n>6$, we will have a rapidly growing number of different shifts.⁷³ Therefore, the unambiguous identification of a new carbon cluster, and assignment of its vibrational fundamentals, will be critically dependent on measuring all the possible isotopic shifts, a task of paramount importance. The second problem in identifying fundamentals is that some of the vibrational modes of different C_n species with similar frequencies, tend to collect within in the same frequency interval in the infrared spectrum and “...the presence of a large number of absorptions in these regions of the infrared spectrum, corresponding to vibrational fundamentals of different C_n chains and some of their isotopically shifted frequencies, produces a collection of overlapping isotopic shifts”.⁴⁴ This makes distinguishing different molecules from one another increasingly difficult.

In order to investigate the first problem, it is necessary to have a better control of carbon isotopic concentrations. A method to measure more accurately the ratio of the carbon mixtures was recently developed by Gonzalez.⁴⁵ It is assumed that the carbon isotopic concentrations are given by c and $100-c$ for ^{13}C and ^{12}C , respectively, to obtain a mixture ratio given by

$$r = \frac{\%^{13}\text{C}}{\%^{12}\text{C}} = \frac{c}{100-c}.$$

Additionally, a theoretical model has been developed⁴⁶ to calculate the probability $P_{n,q}$ of observing single ^{13}C -substituted ($^{12}\text{C}^{13}\text{C}_{n-1}$) or single ^{12}C -substituted ($^{13}\text{C}^{12}\text{C}_{n-1}$) for C_n species as a function of the ^{13}C , or ^{12}C concentration to be used (see Equation 1).

$$P_{n,q} = \left(\frac{100-c}{100} \right)^{n-q} \left(\frac{c}{100} \right)^q \quad (1)$$

where

$$\frac{c}{100} = \text{probability of evaporate } ^{12}\text{C}$$

$$\frac{100-c}{100} = \text{probability of evaporate } ^{13}\text{C}$$

n = total number of carbon atoms in the C_n species

q = number of ^{13}C or ^{12}C atoms

c = ^{13}C or ^{12}C concentration

Assuming a complete randomization of ^{12}C and ^{13}C atoms in the mixture to achieve similar evaporation rates, we can see that for the trivial case, (for each ^{12}C atom we have a ^{13}C atom) only one single substituted isotopomer is obtained. Whereas, for the cases where the values $q=1$ and $3 \leq n \leq 6$ and $0\% \leq c \leq 100\%$, $q=1$, $6 \leq n \leq 10$, and $0\% \leq c \leq 100\%$, finally for the values $q=1, 6 \leq n \leq 10$ and $0\% \leq c \leq 100\%$ represented in Figs. 1,2 and 3 respectively. We can see that when the value of c is close to 50% of either ^{13}C or ^{12}C carbon isotopes there is a high probability of observe all carbon isotopomers for a given C_n species. Conclusively Figs. 1-3 show that the carbon isotopic percentage should be maintained at $c \leq 10\%$ to produce only single ^{13}C -substituted ($^{12}\text{C}^{13}\text{C}_{n-1}$) or single ^{12}C -substituted ($^{13}\text{C}^{12}\text{C}_{n-1}$) carbon clusters in order to limit the number of shifts, (as will be illustrated in CHAPTER III).

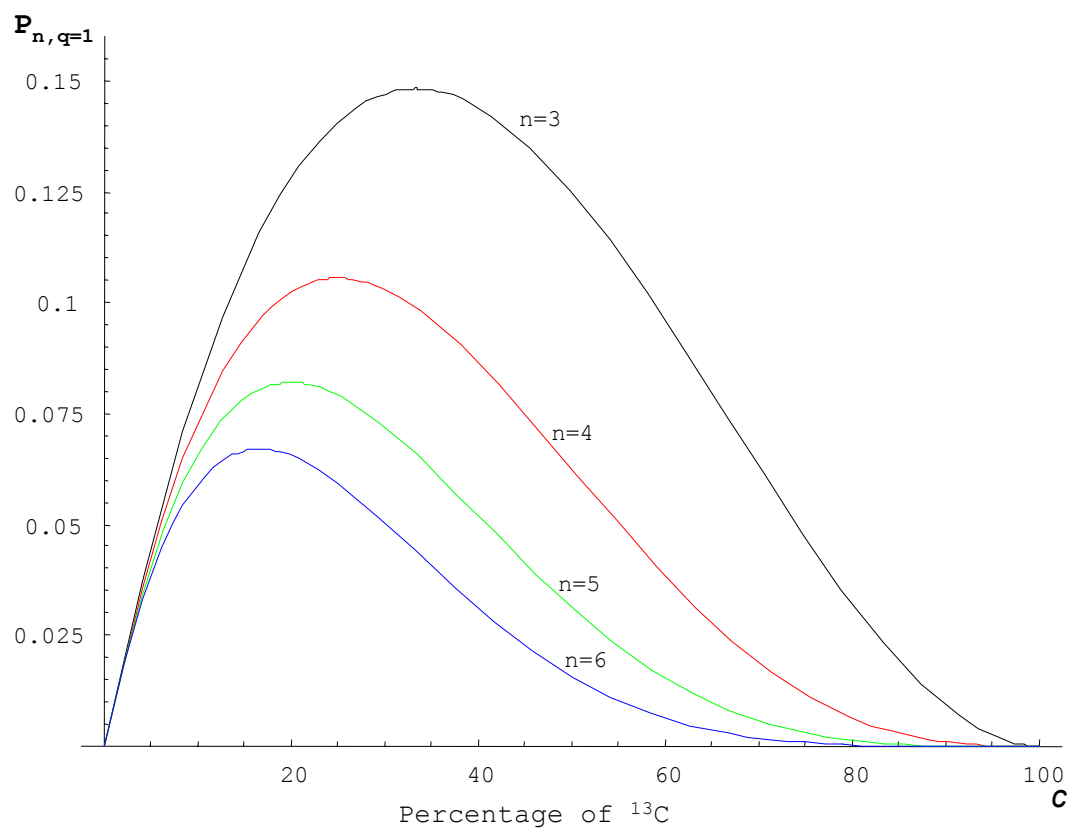


Fig. 1. Probability of observing the singly-substituted isotopomers for different C_n chains for the values $q = 1, 3 \leq n \leq 6$ and $0\% \leq c \leq 100\%$ (From Ref. 47).

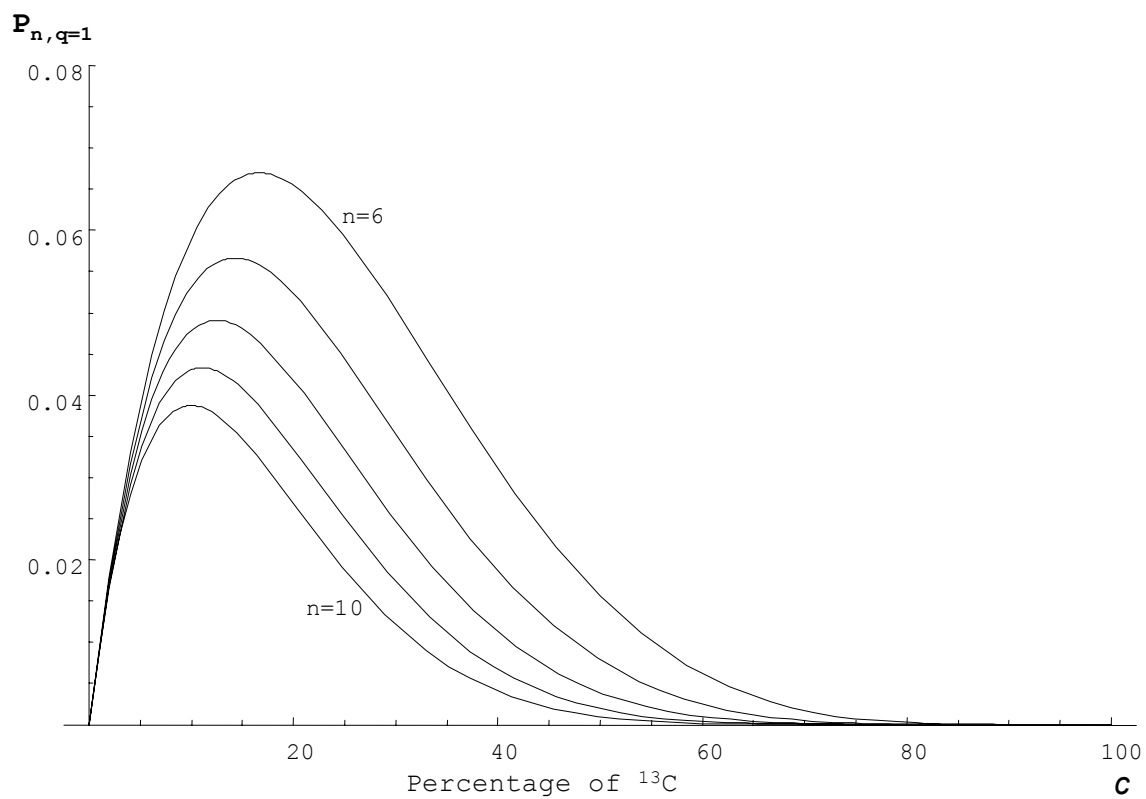


Fig. 2. Probability of observing the singly-substituted isotopomers for different C_n chains for the values $q=1, 6 \leq n \leq 10$ and $0\% \leq c \leq 100\%$ (From Ref. 47).

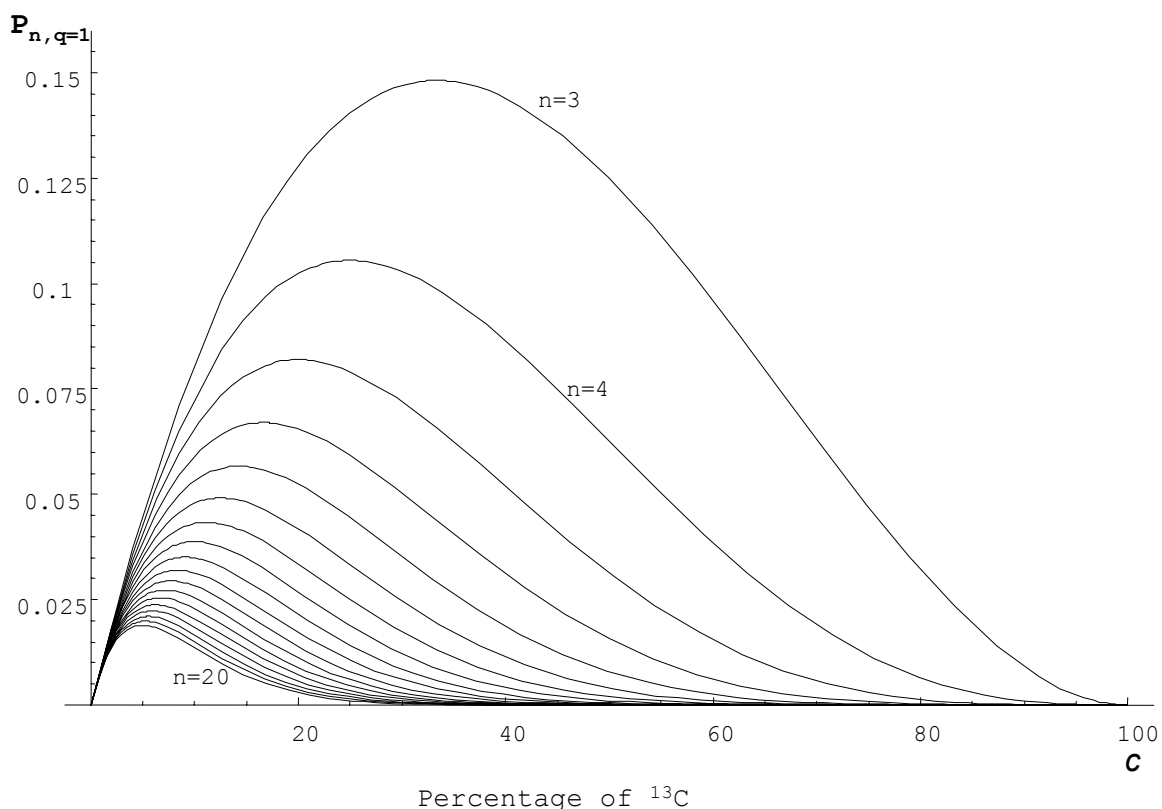


Fig. 3. Probability of observing the singly-substituted isotopomers for different C_n chains for the values $q = 1, 3 \leq n \leq 20$ and $0\% \leq c \leq 100\%$. From Ref. 47.

Now, it is necessary get those carbon bars with the prescribed isotopic percentages ($c \leq 10\%$) and submitted them to the experimental processes, but, since commercial carbon rods with specific ^{13}C enrichments are unavailable, it was necessary to develop a process to fabricate them in the laboratory. Previously²⁸, rods with 90% ^{12}C / 10% ^{13}C enrichment had been made by pressing a premixed powder under high pressure ($\sim 10 \text{ tons/cm}^2$). Rods with 90/10 % or 10/90 %, $^{12}\text{C} / ^{13}\text{C}$, however, have very different rates of evaporation because the ^{13}C isotopic carbon is amorphous in contrast to the crystalline ^{12}C material, and tends to sputter during laser evaporation rather than producing C_n species. Reproducibility in evaporation characteristics was

therefore difficult to achieve. In a single preliminary attempt the established procedure was used to achieve 90% ^{13}C enrichment of the rod, and a spectrum of fully substituted $^{13}\text{C}_n$ species was produced.²⁸

Despite this promising result, it proved impossible to reproduce the spectrum in subsequent attempts. The difficulty in routinely obtaining carbon rods with high ^{13}C enrichment using the existing procedure prompted us to review the whole process of fabrication. Aspects that were considered included factors like the pressure at which the rod should be compressed (8-10 tons/ cm^2), the temperature (1450 to 1750⁰ C) and time at which the rods should be exposed (2 to 3 days), and the differences already noted between the physical states of the ^{12}C and ^{13}C powders used.

1.2 Development of the procedure to produce carbon rods with ^{13}C enrichment

It is known that one form of carbon, graphite, shows a well-developed layer structure in which the atoms are arranged in open hexagons and the layers exhibit some order in stacking sequence. The graphite crystal structure shows a planar morphology and a brilliant silvery surface. Some carbon based materials present strong evidence of graphitization after they have been exposed to pressures of 8 Tn/ cm^2 and temperatures of 1300⁰ C.⁴⁷ Commercial rods containing 98.9 % ^{12}C with a 1.1% natural abundance of the isotope ^{13}C may produce observable single ^{13}C substitution bands when the ^{12}C fundamentals are particularly strong. In contrast, carbon rods made of 5-20% ^{12}C /80-95% ^{13}C does not exist in the market; therefore, the need to fabricate “home made rods” arose. In earlier work in the TCU Physics Lab a fabrication process

was developed which produced “home made rods” with 10-15% ^{12}C /85-90% ^{13}C enrichments. However, the rapid degradation and destruction of these rods after one or two experiments evaporating the rods by the laser ablation technique made it difficult to achieve reproducible evaporation characteristics in the course of a series of experiments in which several different rods were used. The principal difficulty in the fabrication process was the fact that, as mentioned earlier, the isotopes have very different rates of evaporation: the ^{13}C isotopic carbon is amorphous in contrast to the crystalline ^{12}C material and tends to sputter during laser evaporation rather than producing C_n species. When the carbon rods were heated at 1400^0C for 3 days we found that only the surface of the rods was graphitized.

As the result of reviewing all of the steps in the fabrication process, we focused on improving graphitization by heating the rods for a prolonged period of time (≥ 30 days) at a sustained temperature of $\sim 2100^0\text{C}$. For this purpose the furnace, which had previously been used for the evaporation of graphite samples, was refitted with a graphite cell to contain the graphite rod while it was resistance heated during graphitization. A complete renovation of the water-cooling lines to the furnace was undertaken, and new heavy-duty welding cables were installed to permit the 350 amps current necessary to achieve 2100^0C . After completing these improvements, it has been possible to operate the furnace at 2100^0C for over 30 days (see Fig. 4 and 5).

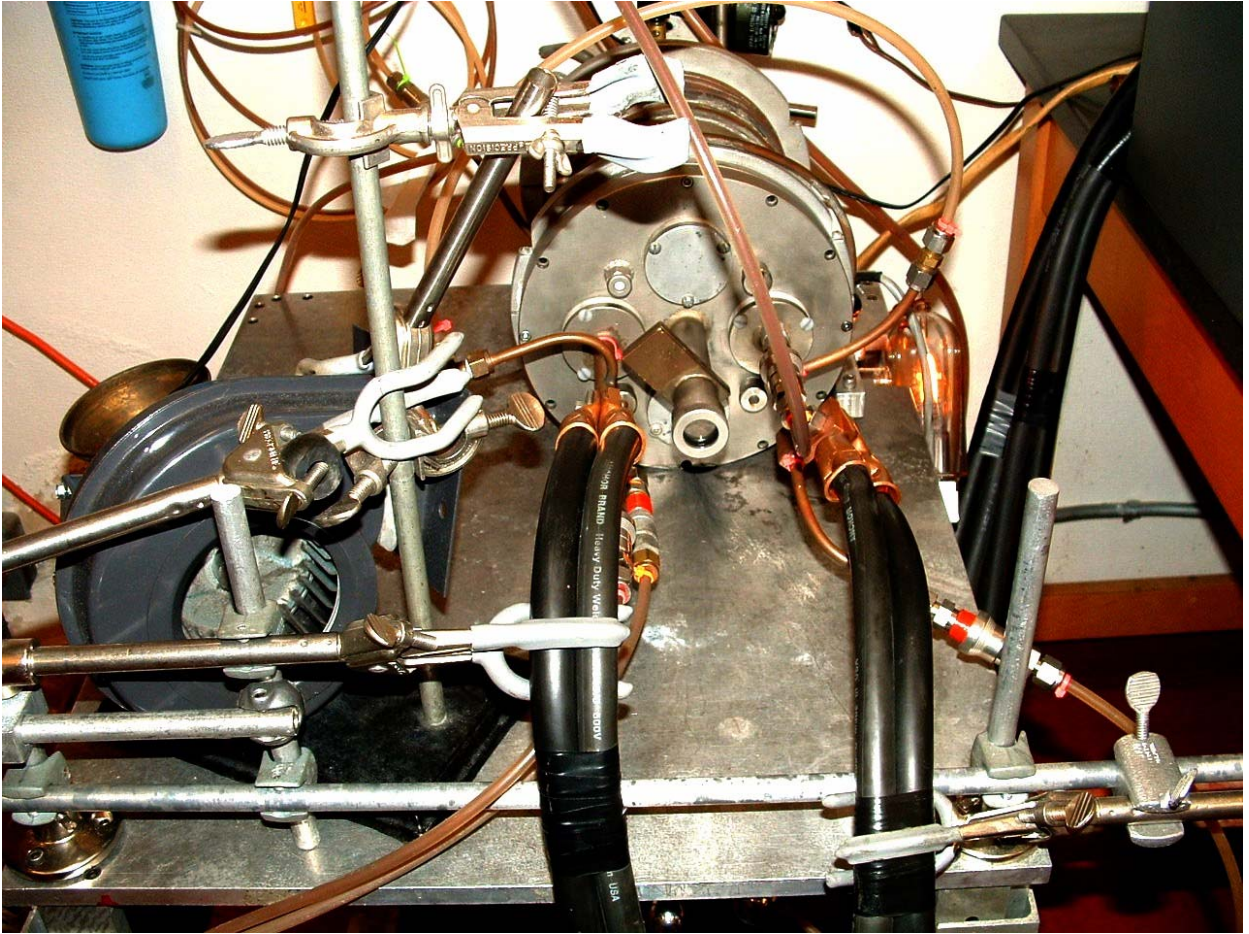


Fig. 4. Renovated furnace with heavy-duty welding cables and water-cooling lines.

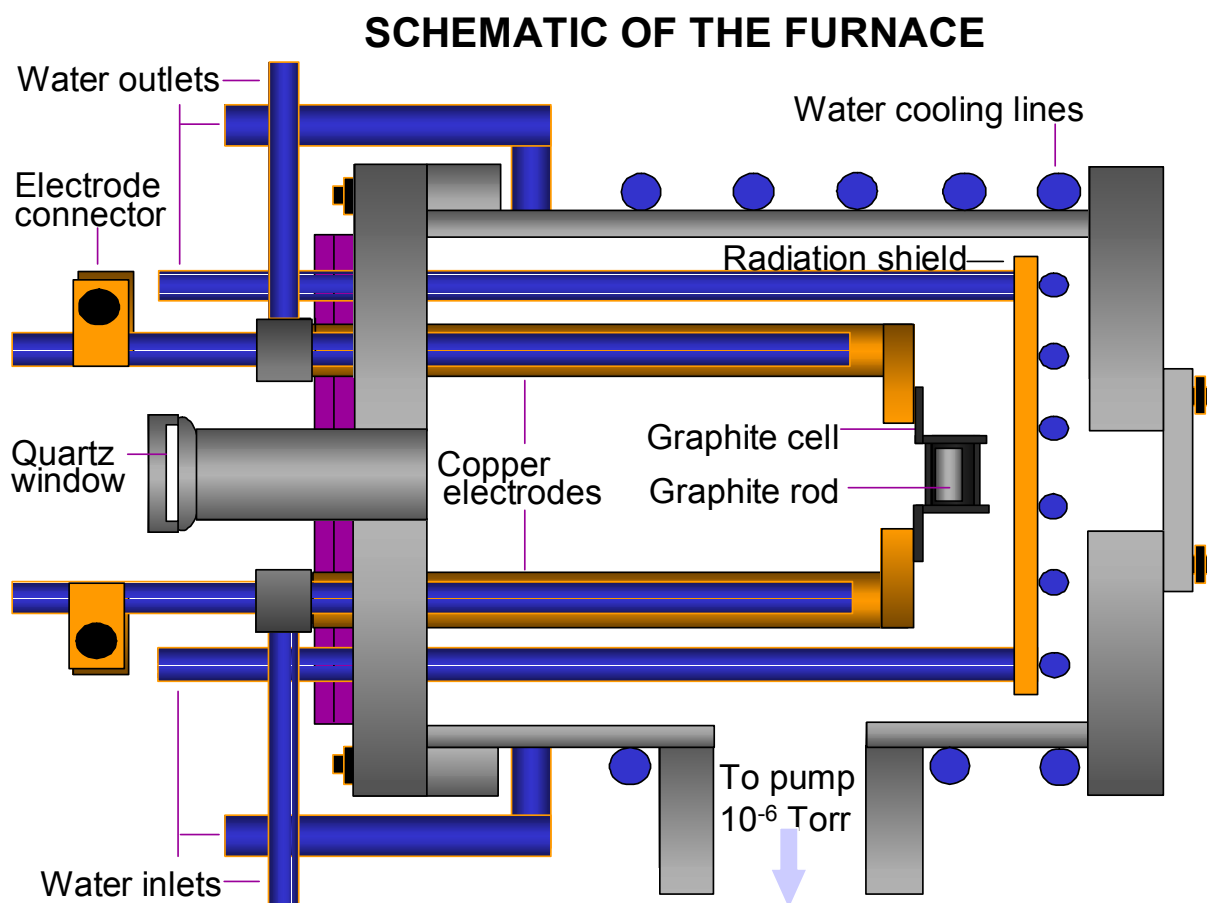


Fig. 5. The temperature reached in the refitted cell is 2100°C for more than 30 days.

In addition to the new heating procedure, the pressures at which the rods were fabricated before graphitization has been increased from 10 to 18 Tn/cm^2 . In contrast to earlier carbon rods, which were quite fragile, these new rods were hard enough to manipulate even before graphitization. Since graphite rods highly enriched with ^{13}C are important to limiting isotopic substitutions to single ^{12}C atoms in an otherwise all ^{13}C molecule, our first attempt to produce

“home made rods” was a mixture of 18% ^{12}C / 82% ^{13}C , with 4 days of exposure to a temperature of 1600⁰ C. Our hope was that after being exposed to high temperatures the amorphous ^{13}C , would become crystallized and be hard enough to handle and evaporate rather than sputter under laser ablation. The outcome was that they were still fragile, but a silvery color over the exterior surface of the rod visible to the naked eye and microcrystallites visible under a microscope, confirmed the beginning of graphitization. Several attempts heating the rods from 1600 to 1750⁰ C for 4 to 8 days resulted in the formation of the first complete lengths of carbon rod, which showed increasing graphitization. An experiment trapping the products of laser ablation of these rods produced spectra with fully substituted $^{13}\text{C}_n$ species. Further refinements increased the temperature from 1750 to 2100⁰ C and the period of heating from 12 to more than 30 days. Microscopic examination of the cross-sections of rods produced under these conditions indicated the crystalline character extended for 2.0 mm into the 10 mm diameter rod.

The inhomogeneity of the $^{12}\text{C}/^{13}\text{C}$ rods produced in earlier work resulted in considerable deviation in the observed isotopic enrichment of the C_n species trapped in Ar from the enrichment of the starting material. In addition, because of the different evaporation characteristics of the two isotopes, the isotopes were not a completely randomized mixture. This often resulted in anomalous relative intensities among singly substituted isotopomers absorptions. Tests to confirm the percentage enrichment in the starting material and in the resulting spectra using the new procedures showed much greater consistency and the observed enrichment in the trapped species was typically $10 \pm 1\%$ for nominal 10% enrichment of the starting mixture. These tests were performed for vibrational fundamentals of the molecules C_5 and C_6 . The crystallization of the “home made rods” also slowed the degradation of the rod

during the performance of the experiments, increasing reproducibility for different runs and rods fabricated at different times.

Conclusively, by using the suggested isotopic percentages ($c \leq 10\%$) together with the mentioned fabrication process the carbon rods were optimized and the production of single ^{12}C -substituted ($^{12}\text{C}^{13}\text{C}_{n-1}$) and the ^{12}C -substituted ($^{12}\text{C}^{13}\text{C}_{n-1}$) carbon clusters during the laser ablation process was achieved. The control of this preferred carbon concentration is of fundamental importance to better experimental design.

The approach to limit the number of isotopic shifts described above alleviates partially the problem of distinguishing between peaks in a carbon infrared spectrum. But as mentioned before, the number of nearby vibrational stretching modes, accumulates in a relatively small region of the infrared spectrum. This situation complicates the analysis in at least two different ways: one is that induced perturbations from nearby modes may produce a complicated shift spectrum for a specific C_n chain, and the other is that in very congested regions of the infrared spectrum it can be very difficult to unambiguously select the shift frequencies for a target molecule. Thus when the observed spectrum is compared to the simulations, due to the existence of multiple peaks with similar characteristics in the same region, there may be several peaks that within experimental error are potential candidates for a single predicted shift, thus complicating the proper identification of a new molecule.

In order to compensate for the loss of data caused by limiting the spectrum to single ^{13}C shifts using the 90% ^{12}C /10% ^{13}C enrichment, we also measure the complementary isotopic shift pattern for 10% ^{12}C /90% ^{13}C enrichment. The latter mixture gives the mirror isotopic pattern for single ^{12}C substitutions in otherwise fully substituted $^{13}\text{C}_n$ clusters. We thus have two different isotopic patterns for the unknown carbon chain. Additionally we superimpose predicted isotopic

shift patterns for comparison with the experimentally observed pattern. The analysis of the behavior of overlapping band patterns produced in different experiments under thermal annealing can also assist in sorting out which bands belong to the same pattern. We have found that these strategies can be crucial for a preliminary selection of a possible set of isotopic shifts that may belong to a specific molecule. Usually for short molecules, the selection of the isotopic shifts is fairly clear. It is also true that some molecular vibrations are located in non-congested frequency intervals and the selection of shifts does not represent a big problem. However in a highly congested frequency interval, all of the aforementioned precautions are not necessarily sufficient to be able to unambiguously assign a specific set of isotopic shifts to a particular C_n species.

With the aim of a better understanding the experimental data, we use the help of well known theoretical approaches such as density functional theory (DFT) to calculate the fundamental frequencies and intensities. A recently theoretical strategy developed by García and Rittby called the *deperturbation method* (DPM),⁴⁸ offers a tool for the interpretation of the isotopic spectra, especially when we have the presence of large numbers of isotopic absorptions in a small region of the measured infrared spectrum, where there are different shifts that can match a single predicted value. Under these conditions having a “one-to-one peak assignment between simulated and observed isotopic spectra becomes a daunting task. A preliminary selected shift set for a specific vibrational fundamental can be filtered through the DPM to assure accuracy in the selection.

CHAPTER II

EXPERIMENTAL PROCEDURES AND TECHNIQUES

2.1 Experimental setup

Matrix samples are prepared in a Displex closed cycle refrigerator, which maintains the samples at a temperature of ~ 10 K and a pressure of 10^{-7} torr, or better (see Fig. 2). The surface of a “home made rod” of composition $^{12}\text{C} / ^{13}\text{C} = 90/10\%$ or $10/90\%$ is ablated using the focused beam from a pulsed Nd-YAG laser (GCR-11 Spectra Physics). The vapor, which is predominantly comprised of pure carbon species, is co-deposited with an excess of Ar (99.999% purity) on a gold plated mirror held at 10 K by the closed cycle refrigerator (APD Cryogenics, Displex).

The flow of Ar atoms regulated by a very precise needle valve is introduced into the Displex chamber through a small inlet located directly behind the rod to be ablated. Ar is supplied to the inlet by a stainless-steel delivery system that is periodically flushed out and then pumped down to 10^{-6} Torr or better to maintain the purity of the Ar entering the system.

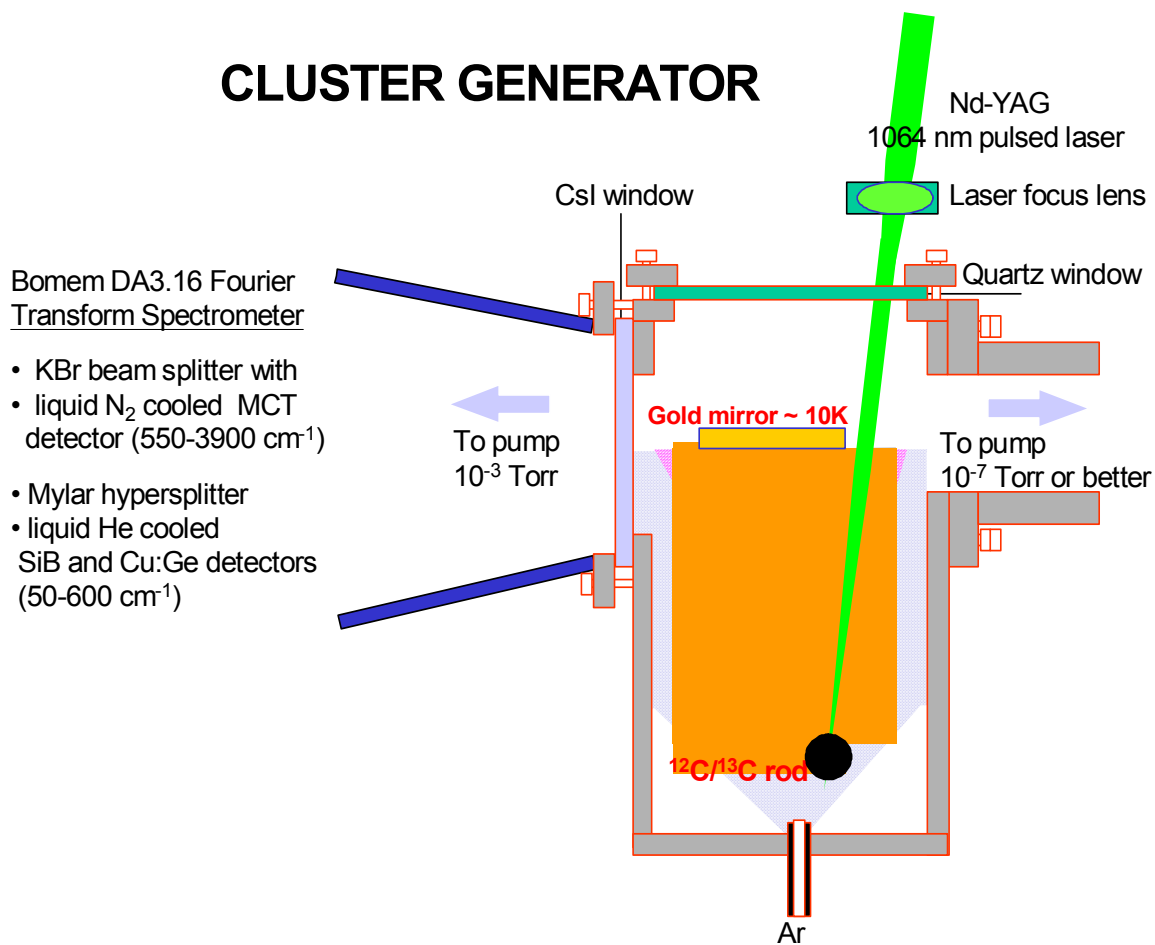


Fig. 6. General schematic for the cluster generator.

Laser ablation of the sample rods varies from 5 to 240 min depending on the optimum conditions for a particular cluster. Once the sample is deposited on the gold mirror absorption spectra are measured using a vacuum Fourier transform infrared spectrometer (Bomem DA3.16) (see Figs. 6 and 7.)

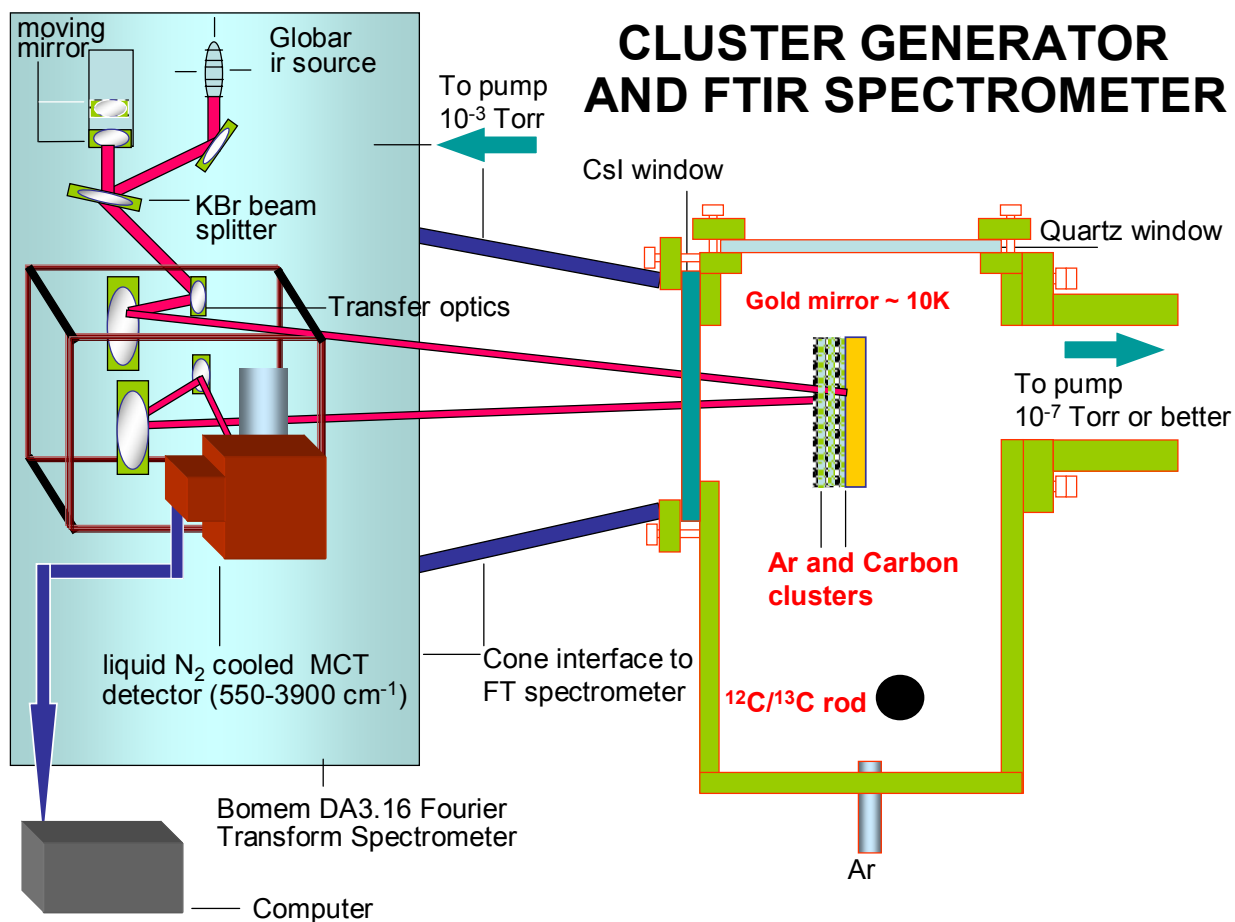


Fig. 7. General schematic for the cluster generator and FTIR Spectrometer (Bomem DA3.16).



Fig. 8. Spectrometer (Bomem DA3.16).

The spectrometer covers the region of the electromagnetic spectrum from 10 cm^{-1} in the far infrared to $50,000\text{ cm}^{-1}$ in the ultraviolet. The source beam providing the continuum for the absorption spectrum of the sample deposited on the gold plated mirror is directed out of the spectrometer and into the sample chamber by an optical transfer bench adjusted to give the maximum throughput. The spectrometer is equipped to operate with excellent sensitivity using various combinations of detectors, beamsplitters, and light sources. In this work, measurements were performed in the region of $500\text{-}3500\text{ cm}^{-1}$, in which almost all the stretching modes of

carbon clusters are located. A liquid N₂ cooled MCT (Hg-Cd-Te) detector and a globar light source were used. The bending modes, which lie principally at 165-370 cm⁻¹, are outside the range of the MCT detector used in this work. The spectrometer system is separated from the evaporation and Displex chambers by a CsI window, and by a magnetic shutter in order to maintain the very high vacuum (up to 10⁻⁸ torr) required during the evaporation process, to avoid possible sample contamination. Typically spectra are recorded using 100 to 300 scans at a resolution of 0.200 cm⁻¹. All frequencies reported here have been measured to an accuracy of ± 0.1 cm⁻¹.

Frequently the deposited sample is annealed by raising the temperature to between 25 and 40 K for 5 – 10 min and then quenching to 10 – 12 K. Generally, the annealing temperature is increased in increments of 1– 4 K. The spectrum is recorded about 5 min after the completion of each annealing cycle in order to allow the mirror to fully equilibrate at the quenching temperature. Annealing tends to sharpen absorption bands as subsidiary features arising from multiple secondary trapping sites collapse into the band corresponding to the minimum energy trapping site. More importantly, spectra often change after annealing because of the reaction of the species trapped in the Ar matrix, resulting in the formation of additional clusters, diffusion and combination of small clusters and the destruction of others. The results can be very useful in identifying unknown species by comparing the relative intensities of unidentified bands as they either grow in intensity or decrease with annealing. The spectra that will be presented here, exhibit relatively narrow lines, which were enhanced by annealing.

CHAPTER III

FTIR SPECTROSCOPIC STUDIES OF THE $\nu_4(\sigma_u)$ MODE OF C_7

3.1 Introduction

Linear carbon chains have been the center of considerable experimental and theoretical interest^{49,50,51,52,53} for a variety of researchers such as, astrophysicists,^{54,55} chemists, and engineers,^{56,57,58,59} who, are trying to understand the role that carbon chains play as precursors to novel structures, astrophysical molecules or their potential applications in semiconductor technology and microelectronics products.^{60,61,62,63,64} There is strong experimental evidence to suggest that carbon chains and rings are precursors to the formation of more complicated structures such as fullerenes and nanotubes.^{65,66,67}

The symbiosis between FTIR matrix isolation technique in rare gases and *ab initio* theory has proven to be one of the most effective ways to identify and the vibrational fundamentals of carbon clusters, formed by laser ablation. At the same time, the complete characterization of C_n species, has proven to be a challenge to experimentalists because it is not always possible to determine every mode a of specific C_n species using ^{13}C isotopic shifts. Intensive experimental measurements and DFT calculations for the $\nu_5(\sigma_u)$ and $\nu_4(\sigma_u)$ modes of C_7 proposed at 1894.3 and at 2128.1 cm^{-1} respectively⁶⁸ and for the modes $\nu_5(\sigma_u), \nu_6(\sigma_u), \nu_7(\sigma_u)$ modes of linear C_9 , proposed to be located at 2078.2, 1998.0 and 1601.0 cm^{-1} respectively,^{69,70} have been done earlier. Although, providing us with quite significant information on the vibrational modes there are discrepancies between experimentally measured ^{13}C isotopic shifts and theoretical predictions that are encountered when we start to study long C_n , ($n \geq 6$) carbon chains. Previous work in this lab has suggested that interactions with the nearby modes which increase with

longer chains contribute to these discrepancies between calculated and observed isotopic shifts frequencies. The author's aim with the present and next chapters has been to make new isotopic measurements for the vibrational fundamental $\nu_4(\sigma_u)$ mode of C_7 and the $\nu_5(\sigma_u)$, $\nu_6(\sigma_u)$ and $\nu_7(\sigma_u)$ fundamentals of C_9 respectively, and with the improved and extended data, to positively identify isotopomer shifts.

3.2 Theoretical calculations

Theoretical and experimental studies of linear C_7 , have previously been performed by various researchers.^{2,71,72,73} In the TCU Molecular Physics Lab, Kranze and co-workers⁷³, performed a very careful comparison between the theoretical and experimental isotopic measurements confirming the assignment for the second most intense mode of C_7 , $\nu_5(\sigma_u)=1894.3\text{ cm}^{-1}$ and a complete analysis of both the single ^{13}C -substituted $^{12}\text{C}^{13}\text{C}_6$ and single ^{12}C -substituted $^{13}\text{C}^{12}\text{C}_6$ isotopomers. It was found for the most intense $\nu_4(\sigma_u)$ mode of C_7 , however, that the shifts were highly sensitive to the level of the calculation. Why is there such an unexpectedly different behavior for the two modes? It was suspected that the origin of this phenomenon could be the influence of other nearby vibrational states on the isotopic shifts predicted for linear C_n carbon chains. In an attempt to measure and predict the different behavior of the two modes, a tool, called the "isotopic sensitivity index" (i_s) is defined;

$$i_s = \left| 1 - \frac{\Delta\omega_\infty}{\Delta_1} \right|, \quad (3.1)$$

$\Delta\omega_\infty$ is the infinite order shift and

$$\Delta_1 = \frac{\omega}{2} \left(1 - \frac{m_i}{m_f} \right) |\mathbf{u}|^2 \quad (3.2)$$

is the first order contribution to the isotopic shift, where ω is the original unperturbed frequency, m_i and m_f are the initial and final mass, and \mathbf{u} is the mass-weighted normal mode displacement for the nucleus in question (see Ref. 72). The findings were that when the isotopic sensitivity index has a value of $i_s \leq 0.1$, then the effects of perturbation by the nearby vibrational modes are small and the agreement between the predicted and observed shifts is good (see Eq. 3.2). In the case of the $\nu_5(\sigma_u)$ mode of C_7 it was found that the isotopic sensitivity index was $i_s \leq 0.1$, and therefore the predicted isotopic shifts should agree well with experimentally measured shifts. However, the $\nu_4(\sigma_u)$ mode has a value $i_s \geq 0.24$; consequently, it is expected that the $\nu_4(\sigma_u)$ mode could have a highly complicated shift behavior and the shift intensity information may be very different from that predicted. Our preliminary conclusion is that, these “irregularities” in the intensities of the observed shifts may be due to coupling effects with nearby modes, which can cause serious discrepancies between calculated and observed isotopic shift frequencies.

It is also essential to take into consideration how isotopic substitution can affect the symmetry of linear C_n carbon chains. In an earlier paper from this lab on C_7 (Ref. 72) the effects of nearby modes on C_n shift patterns were discussed: “The symmetry of a linear C_n carbon chain is affected when a single ^{12}C or ^{13}C isotopic substitution takes place. The symmetric vibration is infrared inactive when the symmetry remains $D_{\infty h}$; however, when a single ^{13}C is substituted anywhere except at the central atom where the symmetry holds under inversion, the symmetry changes to $C_{\infty v}$ symmetry. Under this point group, the symmetry of the vibrations change from σ_u or σ_g to σ , and the isotopic shifts for the σ_g mode become infrared active. This is true for all the linear molecules with $D_{\infty h}$ symmetry and generally causes no difficulties because of the small

intensity associated with such transitions. The problem in our present case is that the $\nu_1(\sigma_u)$ mode, and $\nu_4(\sigma_g)$ modes are so close in energy (38.6 cm^{-1} at the level of the DFT B3LYP/cc-pVDZ, see Table I), that when their symmetry changes to σ under isotopic substitution, the intensity of the $\nu_4(\sigma_u)$ isotopomer absorptions is “shared” with those of the $\nu_1(\sigma_u)$ mode. As a result, the isotopomers from both vibrational modes should in principle be observable. Not only is the intensity affected but the isotopic frequencies may also change significantly. When the two modes have the same symmetry, the individual isotopomer energy levels may “repel” each other and the resulting isotopic shift may be highly unpredictable. In extreme cases, the isotopomer absorptions may even be observed at a higher frequency than the total ^{12}C band.”

So any effort to identify all possible candidates for the single ^{13}C or ^{12}C isotopomers should be done with extreme care.

TABLE I. DFT B3LYP/cc-pVDZ^a predicted vibrational frequencies and band intensities for (*l*-C₇)

Vibrational mode	Frequency (cm ⁻¹)	Infrared intensity (km/mol)
$\nu_1(\sigma_g)$	2221.4	0.0
$\nu_2(\sigma_g)$	1609.5	0.0
$\nu_3(\sigma_g)$	588.84	0.0
$\nu_4(\sigma_u)$	2258.2	4656.5
$\nu_5(\sigma_u)$	1988.4	1303.1
$\nu_6(\sigma_u)$	1118.8	15.5
$\nu_7(\pi_g)^a$	574.4	(0.0)2
$\nu_8(\pi_g)$	190.2	(0.0)2
$\nu_9(\pi_u)$	708.0	(6.12)2
$\nu_{10}(\pi_u)$	293.1	(6.18)2
$\nu_{11}(\pi_u)$	80.1	(9.93)2

^aall the π modes are doubly degenerate

These conclusions will be immediately applied in the present work in a new attempt to complete studies on the “problematic” $\nu_4(\sigma_u)$ mode, the most intense fundamental of linear C₇ which is predicted at the B3LYP/cc-pVDZ level (see Table I) to be only 36.8 cm⁻¹ lower than the $\nu_1(\sigma_u)$ mode. That small energy difference precludes a difficult isotopic analysis, such that it has not been possible until now to assign the isotopic shifts for the $\nu_4(\sigma_u)$ mode appearing in solid Ar at 2128.1 cm⁻¹. We will focus on the analysis of this mode that has a very complicated isotopic shift pattern in an attempt to make definite assignments and then use a similar strategy to analyze the spectra of other C_{*n*} carbon chains, later in this work. The theoretical vibrational spectrum based upon isotopic substitution, was calculated by performing DFT calculations with the standard B3LYP/cc-pVDZ functional using the GAUSSIAN 03 program suite.⁷⁴ Also, we

used a recently developed method developed by Garcia and Rittby called the *deperturbation method*,⁴⁸ a useful tool to help in the interpretation of the isotopic spectra.

3.2.1 The Deperturbation Method

The number of vibrational fundamentals for long linear C_n ($n \geq 6$) carbon chains increases when n is large and they tend to accumulate within small regions of the infrared spectrum together with other near-lying modes sensitive to isotopic substitutions⁷⁵. This situation leads to coupling effects (interactions) between stretching modes.⁷⁶ Frequently, the observed peaks coincidentally overlap with other bands within these small energy intervals generating a rather complex problem for interpretation. For example, a non infrared active stretching mode of a centrosymmetric linear molecule can become infrared active when a ^{13}C is substituted. Such substitutions produce isotopomers bands, now infrared active, that might be observable, increasing the possibility of incorrectly assigning isotopomers to a vibrational fundamental. On the other hand, the observation of those “extra” isotopomers, might in fact, reinforce a possible band assignment, since it would be highly improbable that another vibrational fundamental would have the same isotopic pattern, thus establishing its distinctiveness. However it is clear now, that when we have a large number of observed isotopic absorptions of C_n chains within a narrow energy interval of the infrared spectra; it is possible to observe several different shifts that are potential candidates for a theoretically predicted shift. This presents a serious problem when attempting to identify molecular species by comparing the observed isotopic shifts and the calculated isotopomers. Establishing a “one-to-one peak comparison” becomes an extremely difficult task.

As mentioned earlier, it has been suspected that in order to investigate the coupling effects for molecules whose vibrational modes have near-lying fundamental frequencies, such as long C_n ($n > 6$) carbon chain, it is necessary to take into consideration the energy separation between the fundamental frequencies in order to consider how weak or strong this interaction may be.

Recently an approach to this problem through perturbation theory, called the “*deperturbation Method*” (DPM), (See. Ref. 48) has been developed in an attempt to measure the magnitude of such coupling effect (perturbation), upon isotopic substitution, on an atom by atom basis for a C_n carbon chain and its impact on the isotopic shifts. In this method the isotopic shifts are considered as variations in the molecular mass for the vibrational modes of a linear C_n carbon chain. Isotopic substitutions induce frequency deviations of the vibrational fundamentals to a lower frequency (by adding mass) or to a higher frequency (subtracting mass). To calculate these mentioned isotopic shifts, two different methods have been used by theorists. One consists of finding the fundamental vibrational frequencies of the normal modes, by solving an algebraic problem consisting of the diagonalization of the mass-weighted Cartesian Hessian matrix, meaning that by variations of the mass, it generates another mass-weighted Cartesian Hessian matrix, which diagonalization gives as result the shifts for a particular vibrational fundamental. The other, is a perturbation theory calculation carried out up to second order, where if we consider that the vibrational fundamentals are the unperturbed energies and the mass variations are the perturbation in a finite order expression, is possible to calculate isotopically shifted frequencies like the single ^{13}C -substituted isotopomers ($^{13}\text{C}^{12}\text{C}_{n-1}$) and single ^{12}C -substituted isotopomers ($^{12}\text{C}^{13}\text{C}_{n-1}$). Both methods make use of the harmonic approximation. It was established before that an isotopic substitution has two effects; one, it turns a non-infrared active

mode of a given linear molecule into an infrared active mode (affecting its symmetry as discussed before) and consequently its shifts become potentially observable. The other one is that this mode now infrared active will be capable of interacting with other near-by modes, and the closer the vibrational fundamental energy values are for a given molecule the stronger will be the coupling effects between them. The objective of the DPM is to reduce or even eliminate the coupling effects displayed between nearby vibrational modes of a molecule upon isotopic substitution to allow better comparisons with the experimental results (see Appendix A).

The development of techniques in this dissertation research for the laser evaporation of highly enriched ^{13}C (10% ^{12}C /90% ^{13}C) carbon rods as well as the low enriched rods (90% ^{12}C C/10% ^{13}C) means that we can experimentally obtain complementary sets of shifts for C_n carbon clusters: the single ^{12}C -substituted isotopomers ($^{12}\text{C}^{13}\text{C}_{n-1}$) from the “90/10 spectrum” and the single ^{13}C -substituted isotopomers ($^{13}\text{C}^{12}\text{C}_{n-1}$) from the “10/90 spectrum”. Applying the DPM to these complementary measurements can reduce the coupling effects occurring between vibrational modes upon ^{13}C substitution. The substitution of a ^{13}C atom for a ^{12}C in an otherwise all- ^{12}C molecule corresponds to a positive mass perturbation causing a shift to lower frequency and the substitution of a ^{12}C for a ^{13}C corresponds to a negative mass perturbation. As shown by Garcia and Rittby, the mass perturbations, which are opposite in sign, are approximately equal. In the application of their Mass Perturbation theory then, a vibrational fundamental corresponds to the unperturbed energy $E_1^{(0)}$; a single ^{13}C shift in the all ^{12}C molecule, to the second order energy E_1^+ ; a single ^{13}C shift in the all ^{13}C molecule, to E_1^+ ; and the unperturbed energy $E_2^{(0)}$, to another mode perturbing the fundamental. The repulsion of the energy levels E_1^+ and E_1^+ from the $E_2^{(0)}$ level that we noted earlier is reflected in the repulsion of the shifts in the 90/10 and 10/90 spectra in the opposite direction away from the perturbing fundamental. The

coupling effect is the same so that by mirroring the 10/90 spectrum to the opposite sign using the “mirror transformation” developed by Garcia and Rittby and averaging with the 90/10 spectrum the coupling can be eliminated.

A tremendous disadvantage in the experimental results observed for the study of carbon spectra, is that in the highly congested interval of carbon-carbon stretching modes at 1900 to 2100 cm^{-1} , it is possible to observe more than one peak that is a candidate for a specific calculated isotopomer shift. We can thus have more than one possible set of isotopic shifts that can potentially be assigned to a vibrational fundamental. From now on, for the purpose of distinguishing among these possible shift-set selections, we will use the notation of *SSC12*, *SSC12'*, *SSC12''*... to represent different possible shift-sets for the single ^{12}C -substituted isotopomers ($^{12}\text{C}^{13}\text{C}_{n-1}$) and *SSC13*, *SSC13'*, *SSC13''*... for the single ^{13}C -substituted isotopomers ($^{13}\text{C}^{12}\text{C}_{n-1}$) that can be correlated to specific vibrational fundamentals. This nomenclature will be useful when we apply the DPM to eliminate possible extra observed frequency shifts, leaving only those which can best match the predicted values. In other words, a preliminary single shift-set selected for a specific vibrational fundamental of a C_n chain can be “filtered” through this method to ensure accuracy in the shift assignments.

3.3 Experimental procedure

The linear C_7 cluster was produced using a laser ablation setup that has been described previously,⁶⁸ in which, the carbon rods are rotated and translated while being ablated by Nd:YAG lasers (CGR-11, Spectra Physics) operating at 1064 nm in the pulsed mode. The evaporated species are condensed in solid Ar (Matheson, 99.9995% purity) on a gold surfaced

mirror previously cooled to ~ 10 K by a closed cycle refrigeration system (ARS, Displex). The mirror is enclosed in a vacuum chamber maintained at a pressure of $\sim 10^{-8}$ Torr. In order to unambiguously characterize the vibrational fundamentals of C_n species when ($n \geq 6$), it is crucial to limit the carbon enrichments during the fabrication of the carbon rods to 10% of either ^{13}C or ^{12}C carbon isotopes in order to produce, only single ^{13}C -substituted ($^{12}\text{C}^{13}\text{C}_{n-1}$) or single ^{12}C -substituted ($^{13}\text{C}^{12}\text{C}_{n-1}$) carbon clusters. Other experimental parameters such as laser focus, laser power, and Ar flow were adjusted to favor the production of predominantly long chains of C_n ($n \geq 6$) species. During the cluster deposition, the Ar flow rate was adjusted by opening a needle valve until the chamber pressure increased from $\sim 10^{-8}$ to $\sim 6.0 \times 10^{-5}$ Torr, in order to maintain a controlled Ar flow that swept the laser ablation products and deposited them on the gold plated mirror.

Two different carbon rods were fabricated using mixtures of ^{12}C (Alfa Aesar, 99.9995% purity) and ^{13}C (Isotec, 99.3% purity), one with $\sim 10\%$ ^{13}C enrichment to produce the single ^{12}C -substituted ($^{13}\text{C}^{12}\text{C}_{n-1}$) carbon clusters and the other with $\sim 90\%$ ^{13}C to produce the mirror image isotopic shift pattern for the single ^{13}C -substituted ($^{12}\text{C}^{13}\text{C}_{n-1}$) or single ^{12}C -substituted ($^{13}\text{C}^{12}\text{C}_{n-1}$) carbon clusters. The carbon powder mixtures were pressed into cylindrical rods (2 cm long and 1 cm in diameter) and then the rods were baked for 30 days at $\sim 2100^\circ\text{C}$ inside a furnace maintained under a vacuum of $\sim 10^{-6}$ Torr or better. FTIR absorption spectra of the products condensed in the Ar matrix were recorded over the range of $500\text{-}3500\text{ cm}^{-1}$ at a resolution of 0.2 cm^{-1} using a Bomem DA3.16 Fourier transform spectrometer equipped with liquid nitrogen cooled MCT (Hg-Cd-Te) detector and KBr beamsplitters. Details of the optical system have been reported previously.⁷⁷

3.4 Results and discussion

Figure 9(a) and (c) shows some of the products resulting from laser ablation of 10%¹²C / 90%¹³C and 90%¹²C / 10%¹³C rods respectively and the predicted spectra 9(b) and (d) at the B3YLP/cc-pVDZ level of the theory with using the same carbon ¹²C / ¹³C ratios. The lower case letter c in the labels c1, c2..., stands for a carbon atom, either ¹²C or ¹³C, and the number 1, 2..., stands for the its position (starting from left to right) and will be applied to both sets of isotopomers obtained with 10%¹²C / 90%¹³C and the set of isotopomers obtained with 90%¹²C / 10%¹³C, since the labels indicates only the position of either ¹³C or ¹²C isotopes within a given isotopomer. The labels A, B... will be used only for the vibrational fundamentals of the full ¹²C or ¹³C isotopomers. For example in Fig. 9(c) the most intense antisymmetric $\nu_4(\sigma_u)$ mode of linear ¹²C₇ observed at 2128.1 cm⁻¹ is labeled A and the corresponding vibrational fundamental for ¹³C₇ observed at 2045.9 cm⁻¹ is labeled B. To the low frequency side, the absorption observed at 2095.5 cm⁻¹, which has been assigned (for reasons to be discussed) to the centrosymmetric 12-12-12-13-12-12-12 isotopomer (see Table II) in the 10%¹³C and 90%¹²C enrichment spectrum, is labeled c4, corresponding to the 4th carbon position, with the remaining bands labeled in a similar way for their positions. Other isotopomers are similarly labeled with the position of the substituted carbon atom in the ¹²C or ¹³C isotopomer.

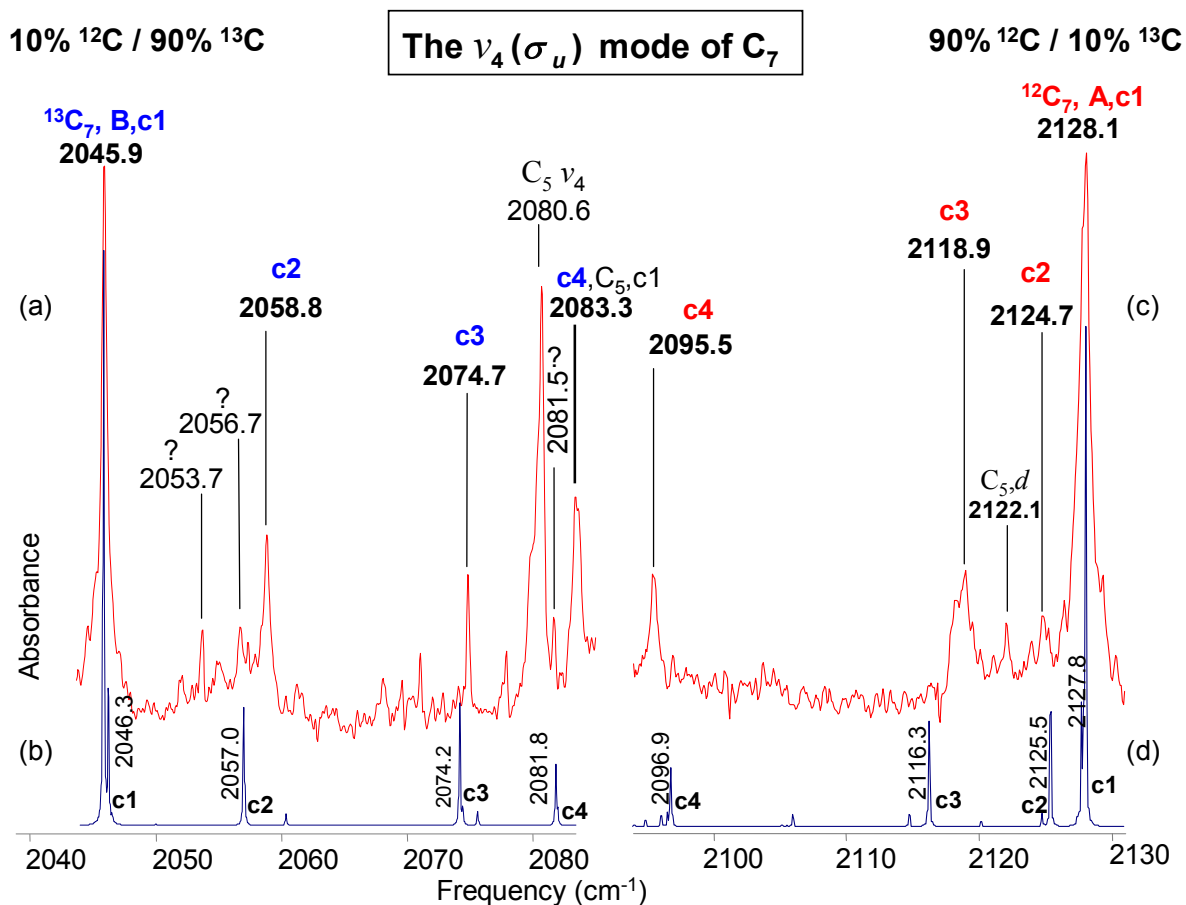


Fig. 9. Comparison of the FTIR spectra of the $\nu_4(\sigma_u)$ mode of the linear C_7 and its ^{12}C and ^{13}C isotopic shifts with carbon enrichments (a) 90% ^{13}C and 10% ^{12}C and 10% ^{13}C and 90% ^{12}C (c) and the simulations (b) and (d) derived from the DFT calculations at the B3YLP/cc-pVDZ level for the same enrichment values. The lower case letter c in the labels c1, c2..., indicates a single ^{12}C or ^{13}C carbon isotope and the number 1, 2... stands for the location (starting from left to right) where the carbon isotope is positioned for both complementary spectrum, left [(90% ^{13}C and 10% ^{12}C (a)] and right [10% ^{13}C and 90% ^{12}C (b)] of the spectra. The labels A and B will be used only for the vibrational fundamentals of ^{12}C and ^{13}C carbon chains respectively. The label $C_{5,c1}$ is related to the single substituted 12-13-13-13-13 isotopomer of the $\nu_4(\sigma_u)$ mode of linear C_5 obtained with a carbon enrichment of 90% ^{13}C and 10% ^{12}C and the label $C_{5,d}$ refers to a double substituted isotopomer of the $\nu_4(\sigma_u)$ mode of linear C_5 .

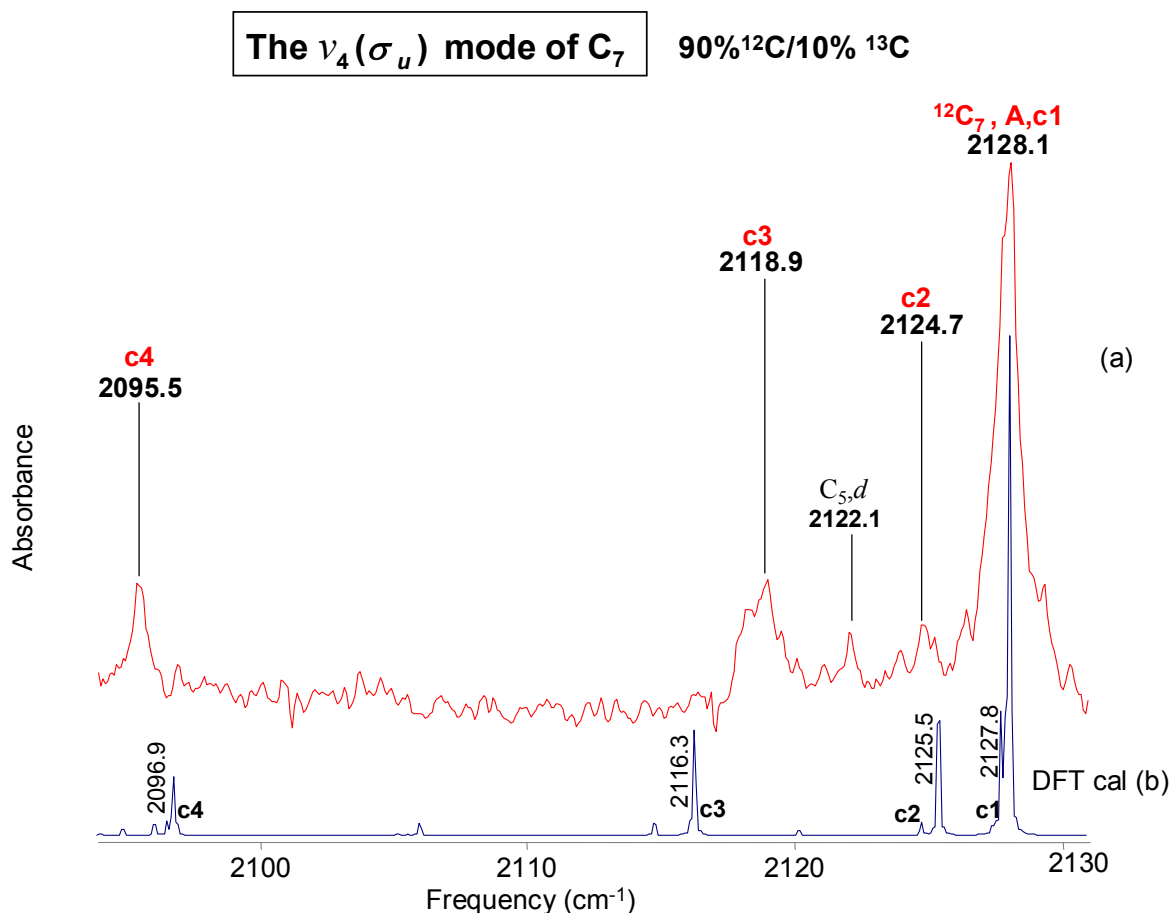


Fig. 10. Comparison of the observed FTIR spectrum of the $\nu_4(\sigma_u)$ mode of the linear C_7 and its single ^{13}C isotopic shifts using 90% ^{12}C and 10% ^{13}C (a) enrichment, and (b) a simulated spectrum derived from the DFT calculations at the B3YLP/cc-pVDZ level using the same enrichment values. Also the label $C_{5,d}$ refers to a double substituted isotopomer of the $\nu_4(\sigma_u)$ mode of linear C_5 .

3.5 Assignment of the isotopomer for the $\nu_4(\sigma_u)$ mode of C_7

An expanded version of the right half of Fig. 9(c) and (d) shows the matrix results produced by the evaporation of a carbon mixture with 90% ^{12}C and 10% ^{13}C in Fig. 10(a) compared with the simulated B3YLP/cc-pVDZ spectrum Fig. 10(b), in the region where the vibrational fundamental of $\nu_4(\sigma_u)$ mode of C_7 and its single ^{13}C -substituted ($^{13}C^{12}C_{n-1}$)

isotopomers are expected to lie. In previous work in the TCU Molecular Physics Lab by Kranze *et al.*⁶⁸ the isotopomer bands for this mode could not be fully analyzed because the signal-to-noise was inferior and also because of the interaction with the $\nu_1(\sigma_g)$ mode, predicted at the DFT level to lie $\sim 54 \text{ cm}^{-1}$ lower. Only the bands for the $^{12}\text{C}_7$ and $^{13}\text{C}_7$ modes for the c4 isotopomer, in which the centrally substituted atom maintains the center of symmetry in the molecule, could be positively identified. Because of the linear centrosymmetric C_7 structure we should observe four single ^{13}C isotopomers. We will consider the absorptions to the low frequency side of the $\nu_4(\sigma_u)$ mode at 2128.1 cm^{-1} for the identification of the four single ^{13}C isotopomers in the spectrum shown in Fig. 10(a). To start with, a preliminary selection of four single ^{13}C -substituted $^{13}\text{C}^{12}\text{C}_6$ isotopomers is chosen, bands at 2127.8 (c1) [overlapped with the main band at 2128.1 (A)], 2124.7 (c2), 2118.9 (c3), and the centrosymmetric 2095.5 cm^{-1} (c4). From now on we will call this selection SSC12 for our first preliminary single ^{13}C shift-set selection. Because of reasons described previously, is possible to have other possible shift-sets for the four single ^{13}C -substituted $^{13}\text{C}^{12}\text{C}_6$ isotopomers, a second selection, still to be chosen, will be named SSC12' or SSC12'' for a possible third selection if necessary.

The absorption observed at 2095.5 cm^{-1} (c4) can be assigned the centrosymmetric 12-12-12-13-12-12-12 (c4) isotopomer, (in this case the ν_4 mode retains its σ_u symmetry upon ^{13}C substitution). At the B3YLP/cc-pVDZ level of the theory the 12-12-12-13-12-12-12 (c4) isotopomer is predicted to lie at 2096.9 cm^{-1} , in acceptable agreement with the observed absorption. Bands of the remaining non-centrosymmetric single ^{13}C substitutions at 2118.9 and 2124.7 cm^{-1} can be reasonably assigned to the 12-12-13-12-12-12-12 (c3) and the 12-13-12-12-12-12-12 (c2) isotopomers since there are no other candidates in this region. The isotopomers corresponding to the $\nu_1(\sigma_g)$ mode now $\nu_1(\sigma)$ and infrared active on isotopic substitution (although

not observed) must lie to the low frequency side of that of the main band located at 2128.1 cm^{-1} , repelling the isotopomer shifts 2118.8 cm^{-1} (c2) and 2124.7 cm^{-1} (c3) of the $\nu_4(\sigma_u)$, pushing them toward the main band so that 2118.8 cm^{-1} (c2) lie at slightly higher frequency than in the simulated spectrum. A similar situation in the complementary spectrum with the corresponding mirrored isotopomers, the 2058.8 cm^{-1} (c2) and 2074.7 cm^{-1} (c3), but this case will be analyzed later.

Absorptions of the 3 non-centrosymmetric isotopomers should have the same intensity and the band of the remaining central-symmetric isotopomer should have an intensity of approximately half that of the others. Fig. 10(a) shows that we do not in fact, observe isotopomer bands with these intensities, in part due to the mode interaction described above, but also because of overlap with other features. In the case of the single ^{13}C isotopomer band at 2118.9 cm^{-1} (c3) an unidentified absorption is growing in on the low frequency shoulder, making it difficult to measure the integrated intensity (see Fig. 10). The band corresponding to the 13-12-12-12-12-12 (c1) is contained in the envelope of the $\nu_4(\sigma_u)$ fundamental observed at 2128.1 cm^{-1} (A).

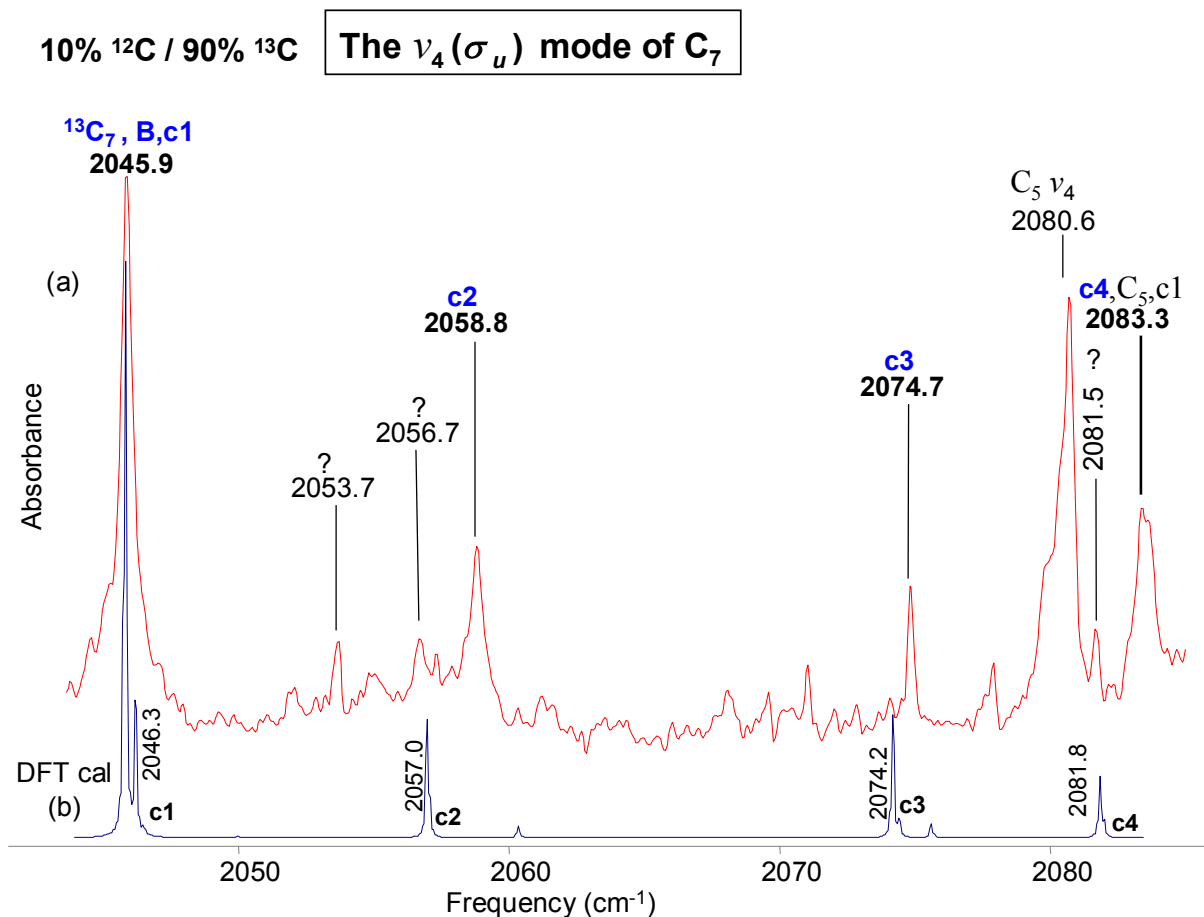


Fig. 11. Comparison of the FTIR spectrum of the $\nu_4(\sigma_u)$ mode of the linear C_7 and its single ^{12}C isotopic shifts with (a) 10% ^{12}C /90% ^{13}C enrichment, and (b) a DFT B3YLP/cc-pVDZ simulation using the same enrichment.

Fig. 11(a), shows the mirror spectrum corresponding to the single (and probably some double) ^{12}C substitutions in the $\nu_4(\sigma_u)$ mode of $^{13}\text{C}_7$ produced by the evaporation of a carbon mixture rod of a 90% of ^{13}C and 10% ^{12}C . The absorption at 2045.9 cm⁻¹, which is a factor $\sim\sqrt{12/13}$ of the 2128.1 cm⁻¹ frequency, is identified as belonging to the fully ^{13}C -substituted isotopomer. In Fig. 11 (a) a tentative set of a possible shifts, SSC13 at 2046.3 cm⁻¹ (c1) [overlapped with the main band at 2045.9 cm⁻¹ (A)], 2058.8 (c2), 2074.7 (c3), and 2081.8 cm⁻¹ (c4) [overlapped by the 12-13-13-13-13 isotopomer of the ν_4 mode of the C_5] (see Table II).

TABLE II. Comparison of observed and predicted DFT (B3LYP/cc-pVDZ) frequencies for single ^{13}C -substituted isotopomers of $^{12}\text{C}_7$, and single ^{12}C -substituted isotopomers of $^{13}\text{C}_7$, for the ν_4 mode.

Isotopomer	ν_{obs}	B3LYP/cc-pVDZ		$\Delta\nu$ $\nu_{\text{obs}} - \nu_{\text{scaled}}$
		ν	ν_{scaled}	
12-12-12-12...(A)	2128.1	2258.4	2128.1 ¹	0.0
13-12-12-12...(c1)	Overlapped ²	2258.1	2127.8	----
12-13-12-12...(c2)	2124.7	2255.6	2125.5	-0.8
12-12-13-12...(c3)	2118.9	2245.9	2116.3	2.6
12-12-12-13...(c4)	2095.5	2225.3	2096.9	-1.4
13-13-13-13...(B)	2045.9	2169.5	2045.9 ³	0.0
12-13-13-13...(c1)	Overlapped ⁴	2169.9	2046.3	----
13-12-13-13...(c2)	2058.8	2181.3	2057.0	1.8
13-13-12-13...(c3)	2074.7	2199.5	2074.2	0.5
13-13-13-12...(c4)	Overlapped ⁵	2207.6	2081.8	----

¹Scaling factor $\nu_{\text{obs}}/\nu \sim 0.94230$

²Overlapped by the by the main band at 2128.1 cm^{-1} (A)

³Scaling factor $\nu_{\text{obs}}/\nu \sim 0.94303$

⁴Overlapped by the main band at 2045.9 cm^{-1} (B)

⁵Overlapped by the 13-12-12-12-12 isotopomer of the $\nu_4(\sigma_u)$ mode of the linear C_5 at 2083.3 cm^{-1} (B)

The top half of Table II, shows a preliminary selection SSC12 for the single ^{13}C -substituted $^{13}\text{C}^{12}\text{C}_6$ isotopomers, and in the bottom half the shift-set SSC13, for the single ^{12}C -substituted $^{12}\text{C}^{13}\text{C}_6$ isotopomers, (in the knowledge that we may have more than one possible shift-sets), which will be tested by applying the DPM. In Table II, the first column lists the isotopomers under consideration for the ν_4 mode of C_7 with their abbreviated isotopomer label in parentheses. In the second column labeled ν_{obs} are the observed frequencies of the absorptions and their isotopomer assignments. The third column labeled ν lists the frequencies predicted by Density functional theory DFT, using the Becke-type exchange functional (B3), coupled with the correlation functional of Lee, Yang and Parr and a double- ζ polarized basis set (DFT-

B3LYP/cc-pVDZ)^{15,78}. The predicted frequencies for the single ¹³C-substituted ¹³C¹²C_{n-1} isotopomers are scaled by a factor of ~0.94230 obtained by taking the ratio of the observed main frequency 2128.1 cm⁻¹ with the corresponding DFT calculated main frequency of 2258.4 cm⁻¹ of the ν_4 mode of ¹²C₇. By similarly taking the ratio of the predicted and observed frequencies for the ν_4 mode of ¹³C₇ we obtain a scaling factor of ~0.94303 for the ¹²C substituted ¹²C¹³C_{n-1} isotopomers. The scaled frequencies are listed in column 4 labeled ν_{scaled} . The discrepancies between the scaled frequencies and the observed frequencies are expected to be large due to the heavy interactions between the nearby modes upon isotopic substitution explained before.

The measured frequencies are compared with the results of the scaled DFT calculation given in the Table II (lower level). As noted, the calculated frequency for the c1 isotopomer at 2046.3 cm⁻¹ in the 10%¹²C / 90%¹³C spectrum of Fig. 11 is not observable because it is overlapped by the main band at 2045.9 cm⁻¹ (B). The next chosen band at 2058.8 cm⁻¹ (c2) presents some anomalies derived from coupling interactions between the $\nu_4(\sigma_u)$ and $\nu_1(\sigma_g)$ modes, now infrared active upon isotopic substitution (see Table I) and described above. The appearance of the 2058.8 cm⁻¹ (c2) and 2074.7 cm⁻¹ (c3) absorptions to the high frequency side of their predicted positions at 2057 and 2074.2 cm⁻¹ in the DFT simulation [Fig. 11(a)] can be attributed to coupling with the ν_1 mode effect. The isotopomers corresponding to the $\nu_1(\sigma_g)$ mode must lie in the low frequency side of the main band located at 2045.9 cm⁻¹ producing a repulsion effect on the frequency shifts 2058.8 cm⁻¹ (c2) and 2074.7 cm⁻¹ (c3) of the $\nu_4(\sigma_u)$ pushing them in the high frequency direction. Also, the integrated intensity value of the c2 isotopomer is affected by a shoulder growing in at the low frequency side caused by another absorption. The difference between the observed and the calculated values of 1.8 cm⁻¹ is a little large, but understandable in view of the coupling with the ν_1 mode.

The band at 2056.7 cm^{-1} can be considered as a possible alternative candidate for assignment to the 13-12-13-13-13-13-13 (c2) isotopomer since it matches with the DFT predicted frequency of 2057.0 cm^{-1} for the c2 isotopomer in the simulation. Thus an alternative shift-set *SSC13'* can be formed including 2046.3 cm^{-1} (c1) (overlapped with the main band B), 2056.7 (c2), 2074.7 (c3) and 2081.5 cm^{-1} (c4). There are therefore two possible shift sets, *SSC13* and *SSC13'*, that can be associated with the shift set *SSC12*. The application of DPM helps in choosing between these alternatives. By taking into consideration each of the two possible pairs of shift sets of a vibrational fundamental, this model can process each of these possible shift-sets. It was found that the frequency of 2056.7 cm^{-1} in the shift-set *SSC13'* was the only frequency that presented the biggest discrepancy when correlated with the corresponding “mirrored” isotopomer at 2124.7 cm^{-1} (c2) correspondent to the shift set *SSC12* [see Fig. 10(a)] and cannot be assigned to the absorption 13-12-13-13-13-13-13(c2); therefore, the shift set *SSC13'* is not a viable alternative. The band at 2053.7 cm^{-1} might be considered as an alternative for the c2 band but can be excluded since the interaction with the ν_1 mode should be repulsive. Also the deviation from the calculated frequency 2057.0 cm^{-1} (c2) is of 3.4 cm^{-1} located to the lower side of the spectrum. Thus the frequency at 2053.7 cm^{-1} cannot be considered to form an alternative shift-set nor as a possible alternative candidate for the 13-12-13-13-13-13-13(c2) isotopomer. The band at 2074.7 cm^{-1} , which has an integrated intensity of $\sim 12\%$, somewhat greater than the expected $\sim 20\%$ but its frequency is in excellent agreement with the DFT calculated frequency of 2074.2 cm^{-1} for the 13-13-12-13-13-13-13 (c3) isotopomer shown in the simulation in Fig 11(b). The centrosymmetric 13-13-13-12-13-13-13 (c4) isotopomer is somewhat more difficult to assign. A band located at 2081.5 cm^{-1} which has an integrated intensity of about half that of the 2074.7 cm^{-1} (c3) consistent with its being a substitution at the unique central site c4 matches well

with the predicted frequency of 2081.8 cm^{-1} , qualifying it as a candidate for the centrosymmetric 13-13-13-12-13-13-13 (c4) isotopomer. Therefore we can form another set of shifts *SSC13''* but when the application of the DPM takes place it was found that when the frequency at 2081.5 cm^{-1} is related to the mirrored frequency 2095.5 cm^{-1} (c4) belonging to the *SSC12* shifts presents also serious discrepancies. Therefore, we need to choose another candidate for the centrosymmetric isotopomer, and another possible candidate for the c4 isotopomer is a band located at 2083.3 cm^{-1} but, the absorption is overlapped by a band assigned⁷⁹ to the 12-13-13-13-13 (c5) isotopomer of the $\nu_4(\sigma_u)$ mode $^{13}\text{C}_5$ located at 2083.3 cm^{-1} (c1) [see Fig. 11(a)]. This band is more intense than another shift corresponding to the 13-12-13-13-13(c2) isotopomer of the $\nu_4(\sigma_u)$ mode $^{13}\text{C}_5$, which is located at 2104.4 cm^{-1} (c2) [see Fig. 12(a)]. This “extra” intensity would be consistent with our hypothesis that the c4 isotopomer band coincides with it. Thus the c4 isotopomer calculated to be at 2081.8 cm^{-1} will be consider to be overlapped by the 12-13-13-13-13 isotopomer of the ν_4 mode of the C_5 .

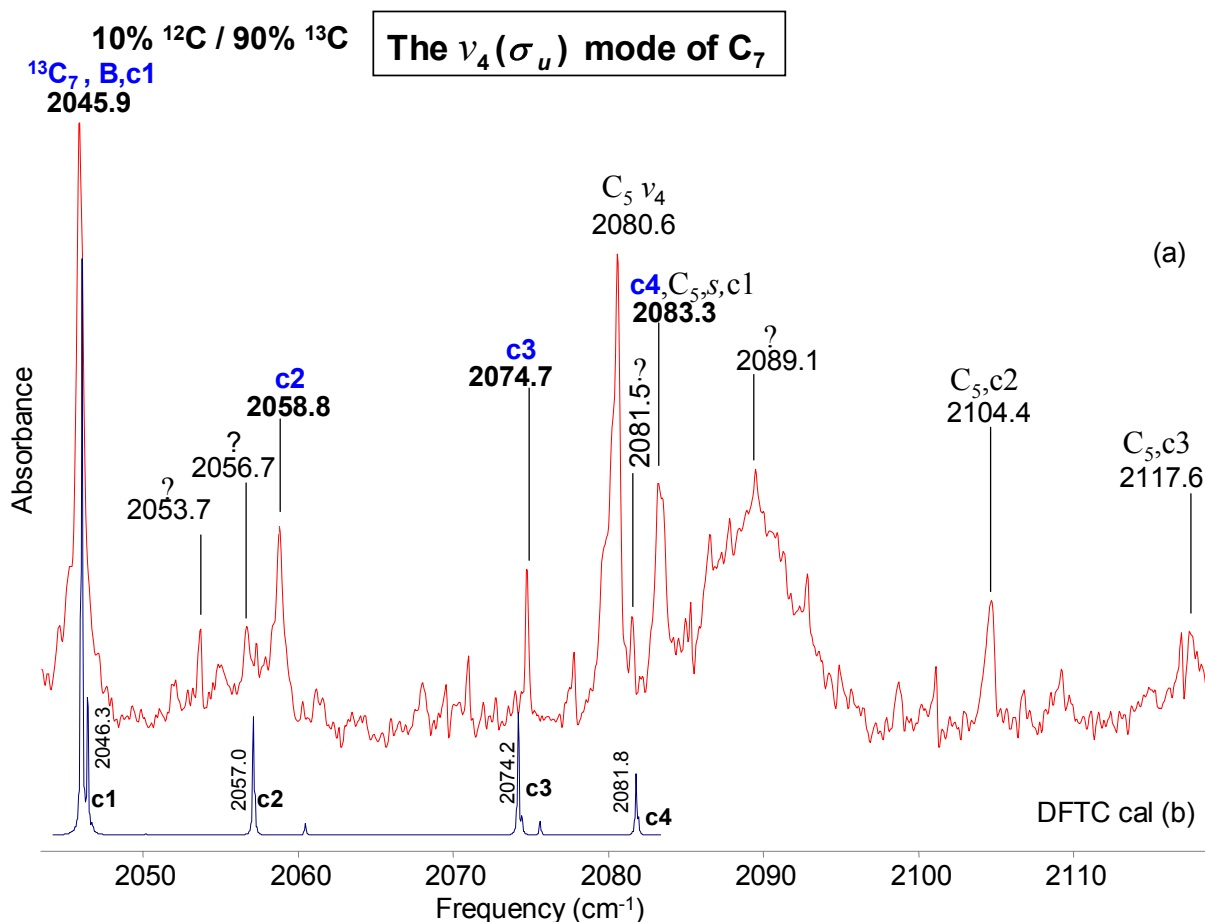


Fig. 12. Comparison of the FTIR spectra of the $\nu_4(\sigma_u)$ mode of the linear C_7 and the $\nu_4(\sigma_u)$ mode of the linear C_5 and its single ^{12}C isotopic shifts with (a) 90% ^{13}C :10% ^{12}C enrichment, and (b) a DFT B3YLP/cc-pVDZ simulation using the same enrichment. Additionally the for the $\nu_4(\sigma_u)$ mode of the linear C_7 .

Thus an alternative shift-set $\text{SSC13}'''$ for the single ^{12}C -substituted $^{12}\text{C}^{13}\text{C}_6$ carbon clusters is now composed of the following frequencies: 2046.3 (c1) [overlapped with the main band at 2045.9 cm^{-1} (A)], 2058.8 (c2), 2074.7(c3), including the 2081.8 cm^{-1} (c4) [overlapped by the 12-13-13-13-13 isotopomer of the ν_4 mode of the C_5] as it can be seeing in Fig. 11(a) and listed in Table III (lower half). Additionally to this analysis, we are now taking the two shift sets $\text{SSC13}'''$ and SSC12 listed in Table III and submitted to DPM. As a result it was found that

those two shift-sets frequencies giving almost no discrepancies and a reasonable match between calculated and observed frequencies.

3.6 Conclusion

A Fourier transform infrared study has been presented for the linear $\nu_4(\sigma_u)$ mode C_7 carbon cluster produced in solid Ar at 10 K through laser ablation of graphite, previously assigned at 2128.1 cm^{-1} , but without any confirming isotopic shifts. Using the much improved spectra obtained for both 90/10 and 10/90 isotopic measurements and by taking into consideration the interaction with the ν_1 mode using the *deperturbation method* it is, possible to make accurate assignments of the isotopic shifts. This provides useful information for subsequent isotopic investigation of other carbon chains whose spectra lie in this region because these isotopic shifts can now be eliminated. Another important conclusion is that the approach taken here can be the basis for future identifications of vibrational modes of longer C_n ($n > 7$) carbon clusters.

CHAPTER IV

FTIR SPECTROSCOPIC STUDY OF THE $\nu_5(\sigma_u)$, $\nu_6(\sigma_u)$ AND $\nu_7(\sigma_u)$ MODES OF LINEAR C_9

4.1 Introduction

It had been proven over several decades that any knowledge and information gained on the studies on long C_n ($n \geq 6$) carbon clusters has been really valuable to support other important studies in chemistry, astrophysics and carbide depositions processes.⁸⁰ In continuing with the theoretical and experimental studies of infrared spectra of carbon clusters produced by laser ablation of graphite and trapped on cold rare gas matrices, (previously decrypted in this work), we will analyze the $\nu_5(\sigma_u)$, $\nu_6(\sigma_u)$, and $\nu_7(\sigma_u)$ modes of linear C_9 . Extensive experimental measurements and DFT calculations have been done^{1,81,82} in an attempt to completely characterize the $\nu_5(\sigma_u)$, $\nu_6(\sigma_u)$ and $\nu_7(\sigma_u)$ modes of linear C_9 reported to be at 2078.1, 1998.0 and 1601.0 cm^{-1} respectively. Other separate studies were done by Maier *et al.*⁸³ (Mass selected) and Vala *et al.*⁸⁴ (matrix-isolated) on the $\nu_5(\sigma_u)$, $\nu_6(\sigma_u)$ modes, but no isotopic information was presented in either case. In a study on the $\nu_7(\sigma_u)$ mode done by Kranze *et al.*⁸⁵ (FTIR, matrix-isolated) only two out of the five single ^{13}C -substituted isotopomers were reported because H_2O contamination.

New obtained experimental spectra, with a better signal to noise ratio and free of contamination, is now providing us with new information that may help to ultimately describe and completely characterize the $\nu_5(\sigma_u)$, $\nu_6(\sigma_u)$ and $\nu_7(\sigma_u)$ modes of linear C_9 . Recent theoretical investigations done by Dr. Rittby using DFT at the standard B3LYP/cc-pVDZ level using the

GAUSSIAN 03 program suite were performed⁸⁶ to investigate its geometry and harmonic frequencies in order to shed more light on the isotopic information of this, rather complicated, C₉ carbon molecule. To aid in the analysis of the proposed studies of the vibrational fundamentals of linear C₉ we will continue with the application of the recently developed method called *Deperturbation method* (DPM),⁴⁷ which already proved to be a useful tool to help in the interpretation of the isotopic spectra (See CHAPTER III).

Any attempt to characterize complete shift sets for any modes of any molecule should start (ideally), by experimentally having all possible isotopomers. Even though, we know now, such a task is of paramount importance, especially for C_n ($n \geq 6$) carbon chains. It is important to have as detailed as possible comparisons between the ¹³C and the ¹²C isotopic measurements with isotopomers predicted by the theory, to conclusively confirm a particular assignment of a possible new C_n molecule. Some times, even long carbon molecules may have vibrational fundamentals that lie in specific frequency regions of the spectra, within a non-congested frequency intervals and the selection of a set of shifts is rather easier. In such conditions a rather good agreement should be expected when calculated and experimental C_n carbon chains are compared. Also, we have shown (see CHAPTER III) that molecules C_n ($n \geq 6$) may be especially sensitive to isotopic substitutions, and when the vibrational fundamentals lie in a highly congested frequency intervals, the analysis of the C_n isotopomers gets more complicated to unequivocally assign a detailed shift set to a C_n species. In the case of the $\nu_5(\sigma_u)$ and $\nu_6(\sigma_u)$ modes of C₉ the situation is even a little more complicated. Both, $\nu_5(\sigma_u)$ and $\nu_6(\sigma_u)$ modes lie in a respectively congested frequency intervals (2040.0-2080 cm⁻¹) and (1975.0-2000.0 cm⁻¹), where there is a conglomeration of overlapping fundamental frequencies and isotopic identification is difficult. Also the $\nu_5(\sigma_u)$ mode has a relatively strong coupling with the $\nu_1(\sigma_g)$ non-infrared

active mode located at 58.8 cm^{-1} to the high frequency side of the spectrum (see Table IV). Therefore is expected to have frequencies disagreements between the calculated and experimental isotopomers.

TABLE III. DFT B3LYP/cc-pVDZ predicted vibrational frequencies and band intensities for (ℓ -C₉)

Vibrational mode	Frequency (cm ⁻¹)	Infrared intensity (km/mol)
$\nu_1(\sigma_g)$	2276.3	0.0
$\nu_2(\sigma_g)$	1970.6	0.0
$\nu_3(\sigma_g)$	1293.9	0.0
$\nu_4(\sigma_g)$	463.9	0.0
$\nu_5(\sigma_u)$	2217.5	4071.4
$\nu_6(\sigma_u)$	2132.4	6527.8
$\nu_7(\sigma_u)$	1669.8	393.2
$\nu_8(\sigma_u)$	895.2	0.2
$\nu_9(\pi_g)^a$	641.6	(0.0)2
$\nu_{10}(\pi_g)$	302.9	(0.0)2
$\nu_{11}(\pi_g)$	129.0	(0.0)2
$\nu_{12}(\pi_u)$	744.2	(7.4)2
$\nu_{13}(\pi_u)$	519.2	(0.3)2
$\nu_{14}(\pi_u)$	225.1	(9.7)2
$\nu_{15}(\pi_u)$	50.9	(7.1)2

^aall the π modes are doubly degenerate

Also the mentioned new DFT calculations show that the $\nu_5(\sigma_u)$ second most intense and $\nu_7(\sigma_u)$ third most intense modes have ~ 62.0 and ~ 6.0 % of intensity respectively, with respect to that of the $\nu_6(\sigma_u)$ mode predicted to be the most intense, but with the worse isotopic substituted index ($i_s=0.22$). To experimentally test this intensity is really difficult, due to the tremendous irregularities obtained in the band line profiles within the mentioned intervals, presenting high difficulty in to have measurements of integrated intensities. So, we will be basically oriented on

analyzing the obtained experimental isotopic information for any of the $\nu_5(\sigma_u)$, $\nu_6(\sigma_u)$ and $\nu_7(\sigma_u)$ modes in order to demonstrate any advance towards to a definite identification.

4.2 Discussion and experimental procedure

The linear C_9 cluster was produced using a laser ablation setup described previously (see CHAPTER III). The above mentioned problems that surround those rather long C_n ($n \geq 6$) carbon chains, demands a step by step analytical process to achieve progress.

With the better control gained of the carbon isotopic concentrations restricted to use specific carbon enrichments to 10% of either ^{13}C or ^{12}C carbon isotopes we can obtain sort of a “chain reaction” of benefits: a) we can restrict the isotopic shift patterns to obtain only the single ^{13}C -substituted isotopomers ($^{13}C^{12}C_{n-1}$) or the complementary (or “mirror”) isotopic shift pattern, usable when the vibrational fundamental under study is located in highly congested frequency interval of the spectra. So by having both set of shifts it is possible to compensate for a possible loss of data. In other words, when one or more of the observed isotopomers may be overlapped with other bands in one “side of its spectrum”, in the mirrored pattern the correspondent isotopomers may be not; b) in case of the existence of a interaction between the near by modes infrared (active upon isotopic substitution) it is possible to analyze the manifestation of such a coupling (which should be present in both “mirrored” sides), therefore, getting a double set of information about such coupling, and increasing the possibility of a potential identification of a vibrational fundamental. Also, it is of fundamental importance (maybe more than ever) to achieve experimental reproducibility, which it can provide us with an analogous results, to compare, different carbon infrared spectra in the quest of the “best” experimental conditions, to

improve our spectrum, in order to better select preliminary shifts-sets. Finally, one of the most important consequences of having both isotopic spectra of the same molecule (as mentioned before) is that it allows us to make use of the DPM, to help in the selection of the “best” isotopomer candidates, which is especially important for long molecules.

4.3 Results and discussion

We will continue with the same notation described in CHAPTER III, where it was introduced that the lower case letter c in the labels c1, c2..., stands for a carbon atom, either ^{12}C or ^{13}C , and the number 1, 2..., stands for its position (starting from left to right). It will be applied to both sets of isotopomers obtained with 10% ^{12}C / 90% ^{13}C and 90% ^{12}C / 10% ^{13}C mixtures. The labels A, B... will be used only for the vibrational fundamentals of the full ^{12}C or ^{13}C isotopomers. Figure 12(a) shows the present FTIR observations in the region where the vibrational fundamental of $\nu_6(\sigma_u)$ mode of C_9 and its single ^{13}C -substituted ($^{13}\text{C}^{12}\text{C}_{n-1}$) isotopomers are expected to lie. In previous work in the TCU Molecular Physics Lab by Kranze *et. al.*⁷ the isotopomer bands for this mode could not be fully analyzed due to several reasons; the signal-to-noise was inferior, the absence of isotopic information of the mirrored side of the mode and the nature of the interaction with the $\nu_1(\sigma_g)$ mode, lying at $\sim 59.0\text{ cm}^{-1}$ in the higher frequency side (see Table IV), difficulty its analysis. In the present work we will see more clearly experimental measures of that particular congested energy interval (1975.0 and 2000.0 cm^{-1}) for a better isotopic identification.

4.4 Assignment of the isotopomers for the $\nu_6(\sigma_u)$ mode of C_9

Figure 13(a) shows some of the products resulting from laser ablation of 90% ^{12}C / 10% ^{13}C rods and the predicted spectra 13(b) at the B3YLP/cc-pVDZ level of the theory with using the same carbon ^{12}C / ^{13}C ratios where the vibrational fundamental of $\nu_6(\sigma_u)$ mode of C_9 and its single ^{13}C -substituted ($^{13}C^{12}C_{n-1}$) isotopomers are expected to lie. The Figure 13 (a) shows a prominent peak at 1998.2 cm^{-1} , which is very close to the 1998.0 cm^{-1} absorption, studied in previous work⁷ and tentatively assigned to the $\nu_6(\sigma_u)$ mode of C_9 , on the basis of *ab initio* calculations and mass selection. This work will present a complete isotopic analysis that will help to definitively assign the 1998.2 cm^{-1} to the $\nu_6(\sigma_u)$ most intense mode of C_9 .

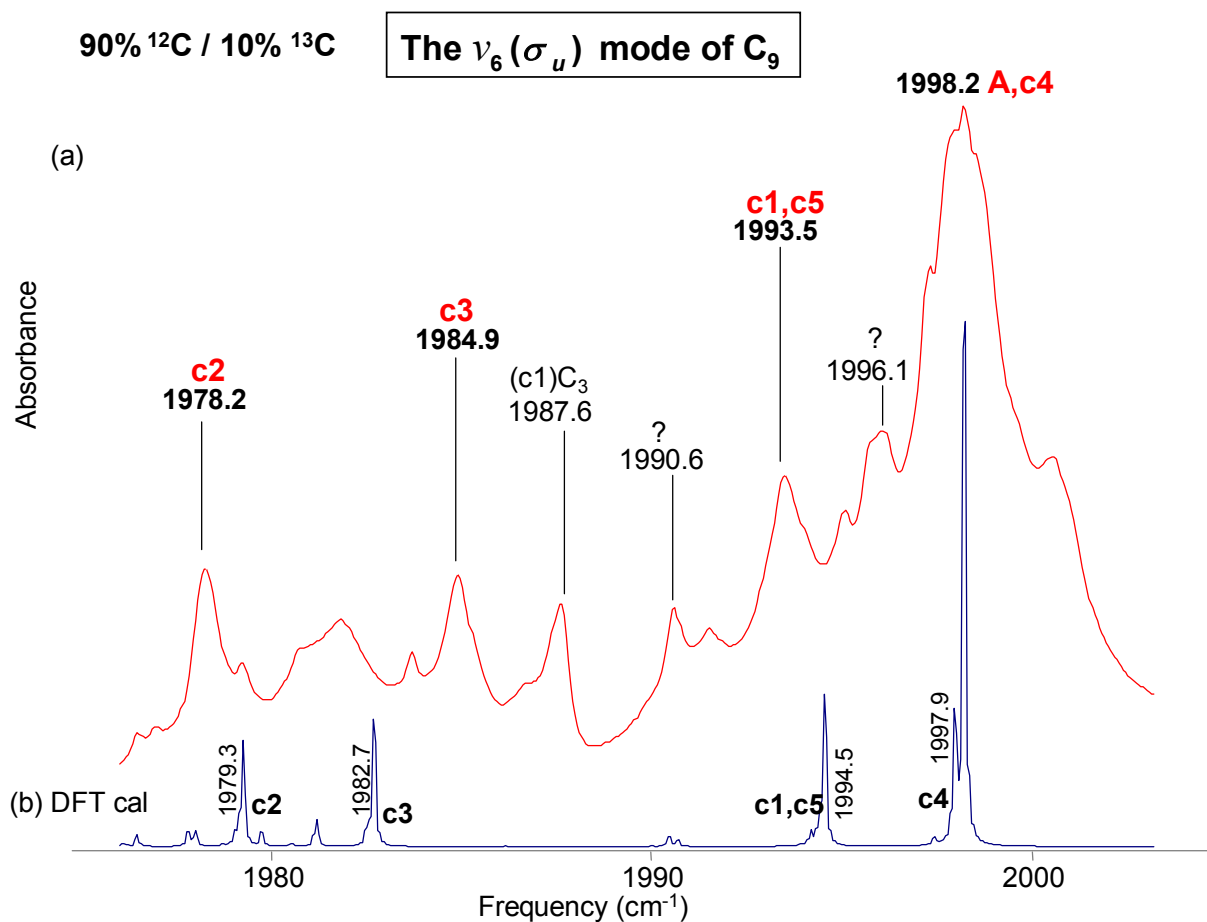


Fig. 13. Comparison of the FTIR spectrum of the $\nu_6(\sigma_u)$ mode of linear C_9 and its single ^{13}C isotopic shifts with carbon enrichments (a) 90% ^{12}C and 10% ^{13}C and a simulation (b) derived from the DFT calculations at the B3YLP/cc-pVDZ level for the same enrichment values.

We will consider the absorptions to the low frequency side of the $\nu_6(\sigma_u)$ mode at 1998.2 cm^{-1} for the identification of the four single ^{13}C isotopomers in the spectrum shown in Fig. 13(a). To start with, a preliminary selection of five single ^{13}C -substituted $^{13}\text{C}^{12}\text{C}_8$ isotopomers is chosen, bands 1978.2 (c2), 1984.9 (c3) and 1998.2 cm^{-1} (c4) [overlapped with the main band 1998.2 (A)] and for the centrosymmetric 1993.5 (c5) overlapped with 1993.5 cm^{-1} (c1). From now on we will call our first preliminary single ^{13}C shift-set selection SSC12. Because of

reasons described previously, it is possible to have other possible set of shifts for the four single ^{13}C -substituted $^{13}\text{C}^{12}\text{C}_8$ isotopomers that may be chosen; in such case they will be named *SSC12'* or *SSC12''* correspondingly.

By symmetry the single ^{13}C -substituted $^{13}\text{C}^{12}\text{C}_8$ isotopomers of the C_9 carbon chain are expected to have double contribution to its integrated intensity, since two isotopomers are contributing to it, except in the case of the centrosymmetric isotopomer, which only has an integrated intensity that should be of a value of only the half of that of other single substituted isotopomer. But in order to obtain the comparative percentiles of the single substituted isotopomers with respect to the main band it is necessary to measure the integrated intensity of the main band at 1998.2 cm^{-1} [Fig. 13(a)] which is precisely difficult to measure, due to its asymmetric line profile. Therefore it is difficult to determine where the base line may be located for the main band or for every one of the chosen isotopomers, as a result, a direct comparison of the integrated intensity between the main band and each of the proposed single ^{13}C -substituted $^{13}\text{C}^{12}\text{C}_8$ isotopomers would be highly inaccurate.

It has been observed under annealing processes (systematic increases of temperature) performed on different experiments [see Fig. 14 and 15] that, the behavior of these preliminary selected bands, seem to be related to each other and to the main band. This consistent behavior of the proposed isotopomers is specially noted in the Fig. 14(a), (b) and (c) where our preliminary shift-set grow in as temperature increases, reflecting a correlation between the isotopomers.

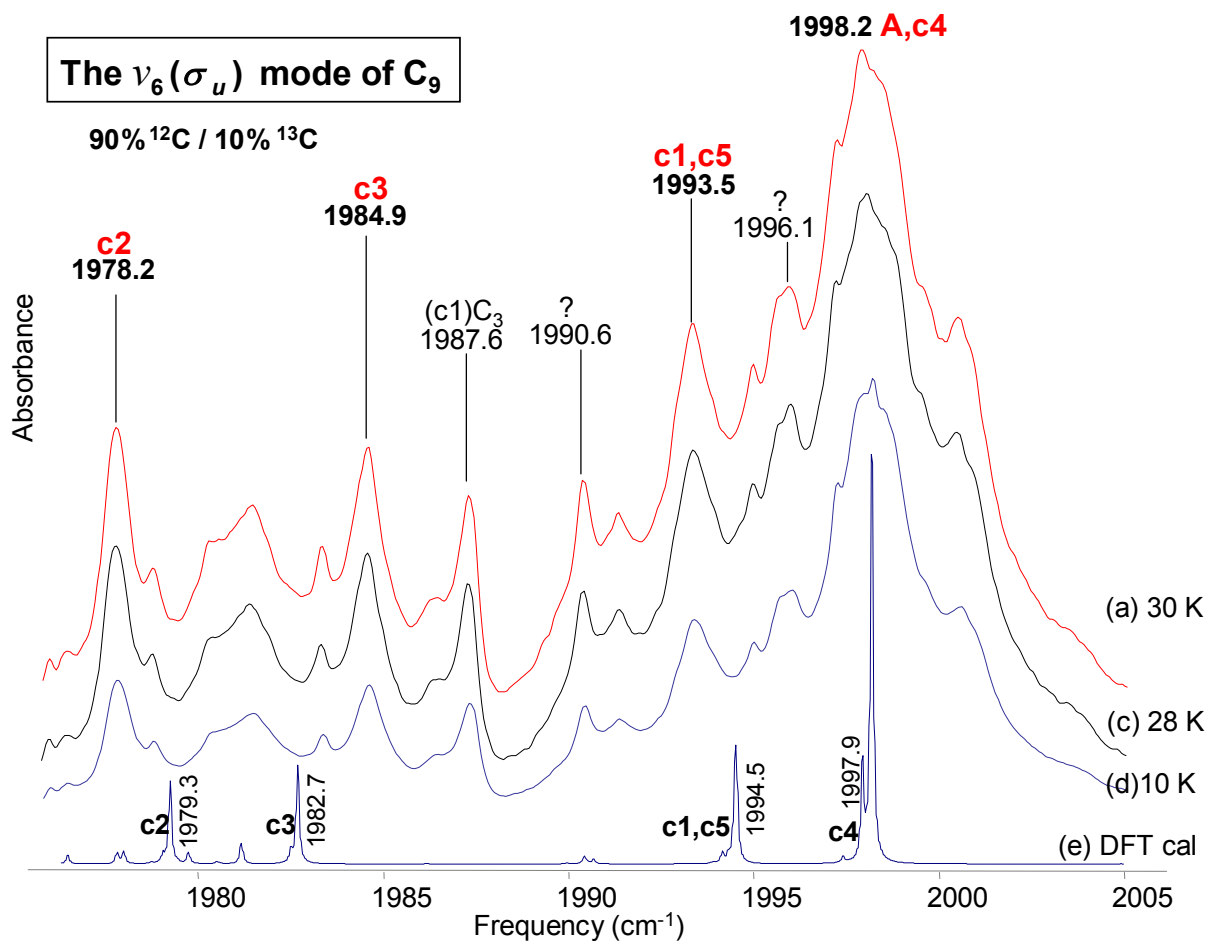


Fig. 14. Comparison of observed FTIR annealed spectra (a) 30 K (b) 28 K and (c) 22 K of the $\nu_6(\sigma_u)$ mode of linear C_9 and its single ^{13}C isotopic shifts using 90% ^{12}C and 10% ^{13}C carbon enrichments, and (e) a simulated spectrum derived from the DFT calculations at the B3YLP/cc-pVDZ level using the same enrichment values.

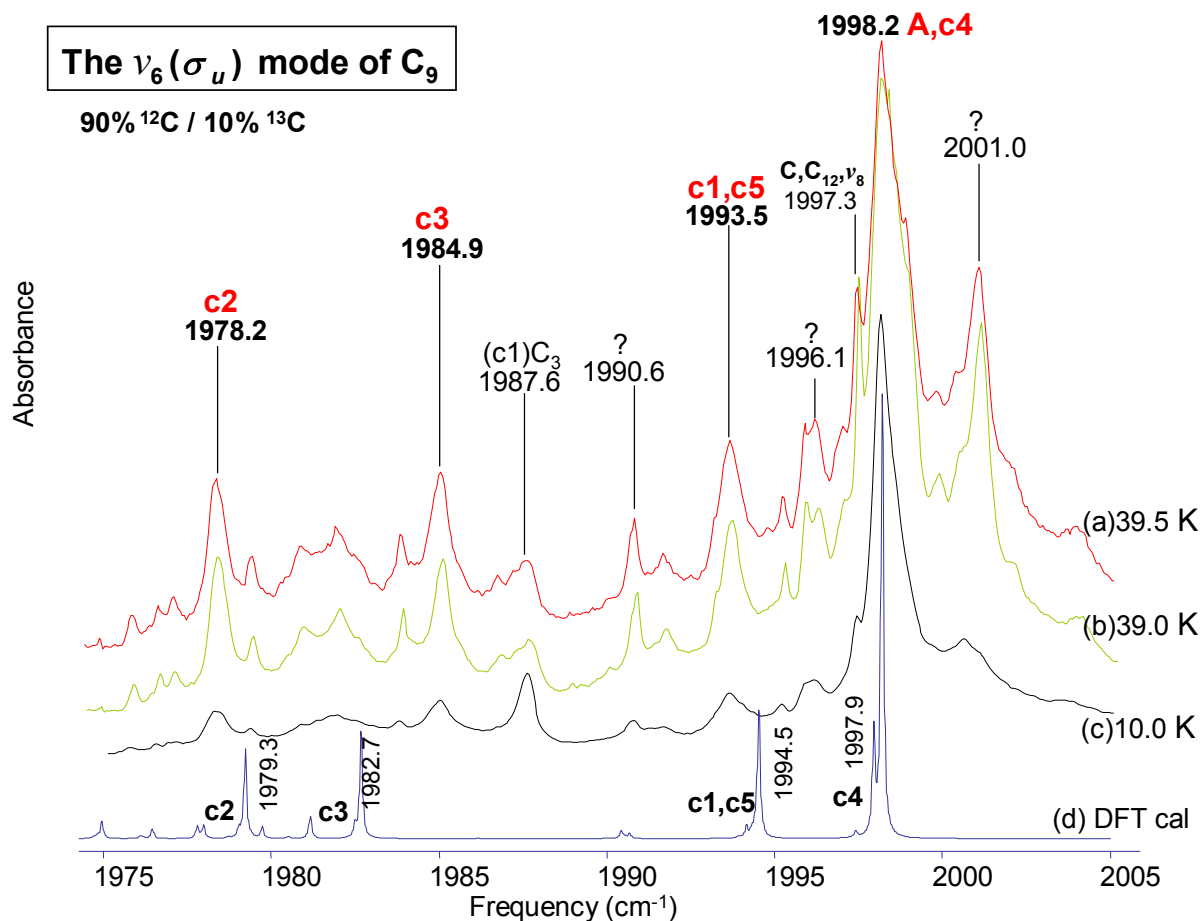


Fig. 15. Comparison of observed FTIR annealed spectra (a) 39.5 K (b) 39.0 K and (c) 10.0 K of the $\nu_6(\sigma_u)$ mode of linear C_9 and its single ^{13}C isotopic shifts using 90% ^{12}C and 10% ^{13}C carbon enrichments, and (d) a simulated spectrum derived from the DFT calculations at the B3LYP/cc-pVDZ level using the same enrichment values.

Those analogous results [see Fig. 14 and 15 (a), (b) and (c)], allow us to compare different carbon infrared spectra in the quest of the “best” experimental analysis to support any preliminary shift-sets selection for this particular vibrational fundamental. Of the five calculated isotopomers we can clearly see only four peaks; we should have then at least one overlapped isotopomers. The simulated spectrum [Fig. 15(d)] shows visually only four peaks instead of five individual peaks, but looking at the peak distribution file from the DFT calculations we can

found that the centrosymmetric c5 isotopomer is overlapped with the c1 isotopomer and close the observed band at 1993.5 cm^{-1} that appears prominently in the observed spectrum [see Fig. 15(a)], this band is wide enough in the base to possible contains two isotopomers the 13-12-12-12-12-12-12-12-12(c1) and the centrosymmetric 12-12-12-12-13-12-12-12-12(c5) isotopomers. The calculated band 12-12-12-13-12-12-12-12 (c4) appears to be located at the 1997.9 cm^{-1} is overlapped with the main band at 1998.2 cm^{-1} (A), corresponding to the $\nu_6(\sigma_u)$ mode of C_9 . The observed bands at 1984.9 and 1978.2 cm^{-1} have the same as the band at 1993.5 cm^{-1} already assigned to the c1 and c5 isotopomers under annealing. Those mentioned bands are close to the calculated bands at 1982.7 and 1978.2 cm^{-1} correspondent to the 12-12-13-12-12-12-12-12-12 (c3) and the 12-12-13-12-12-12-12-12-12 (c3) isotopomer respectively [see Fig. 15(a)]. The isotopomers corresponding to the $\nu_1(\sigma_g)$ mode must lie at the high frequency side of that of the main band located at 1998.2 cm^{-1} (A) producing a repulsion effect on the proposed shifts 1984.9 cm^{-1} (c3) and 1978.2 cm^{-1} (c2) of the $\nu_6(\sigma_u)$ inducing a separation from the calculated bands of 2.2 and 1.1 cm^{-1} respectively, which is still acceptable due to this coupling with the $\nu_1(\sigma_g)$ mode. So the 1984.9 and 1978.2 cm^{-1} will be assigned to the c3 and c2 isotopomers in that order.

We finally end up choosing the observed frequencies for the single ^{13}C -substituted isotopomers of the $\nu_6(\sigma_u)$ mode of $^{12}\text{C}_9$ to be 1993.5 (c1,c5), 1978.2 (c2), 1984.9 (c3), and 1997.9 cm^{-1} (c4)[overlapped with the main band at 1998.2 (A)] called SSC12.

It is necessary to mention that in Fig. 15 (a) and (b) the spectra annealed at 39.0 and 39.5 K some other carbon bands appear in the vicinity of the proposed $\nu_6(\sigma_u)$ mode of C_9 at 1998.2 cm^{-1} (A). One is located to the high frequency side at 2001.0 cm^{-1} and the other to the lower frequency side at 1997.3 cm^{-1} correspondent to the $\nu_8(\sigma_u)$ mode of C_{12}^5 . However, our previous shift-set SSC12 selected for the $\nu_6(\sigma_u)$ mode of C_9 seems to be not related to any of those

mentioned bands. For this reason and only with the aim of memory recall we reproduce in the Fig. 16 the spectrum of the Fig. 15 (b) in order to show that the single substituted isotopomers for the $\nu_6(\sigma_u)$ mode of C_9 at 1998.2 cm^{-1} (A) and the $\nu_8(\sigma_u)$ mode of C_{12}^5 at 1997.3 cm^{-1} clearly, that neither isotopomer from either mode is in fact overlapping or otherwise interfering with their correspondent individual selection.

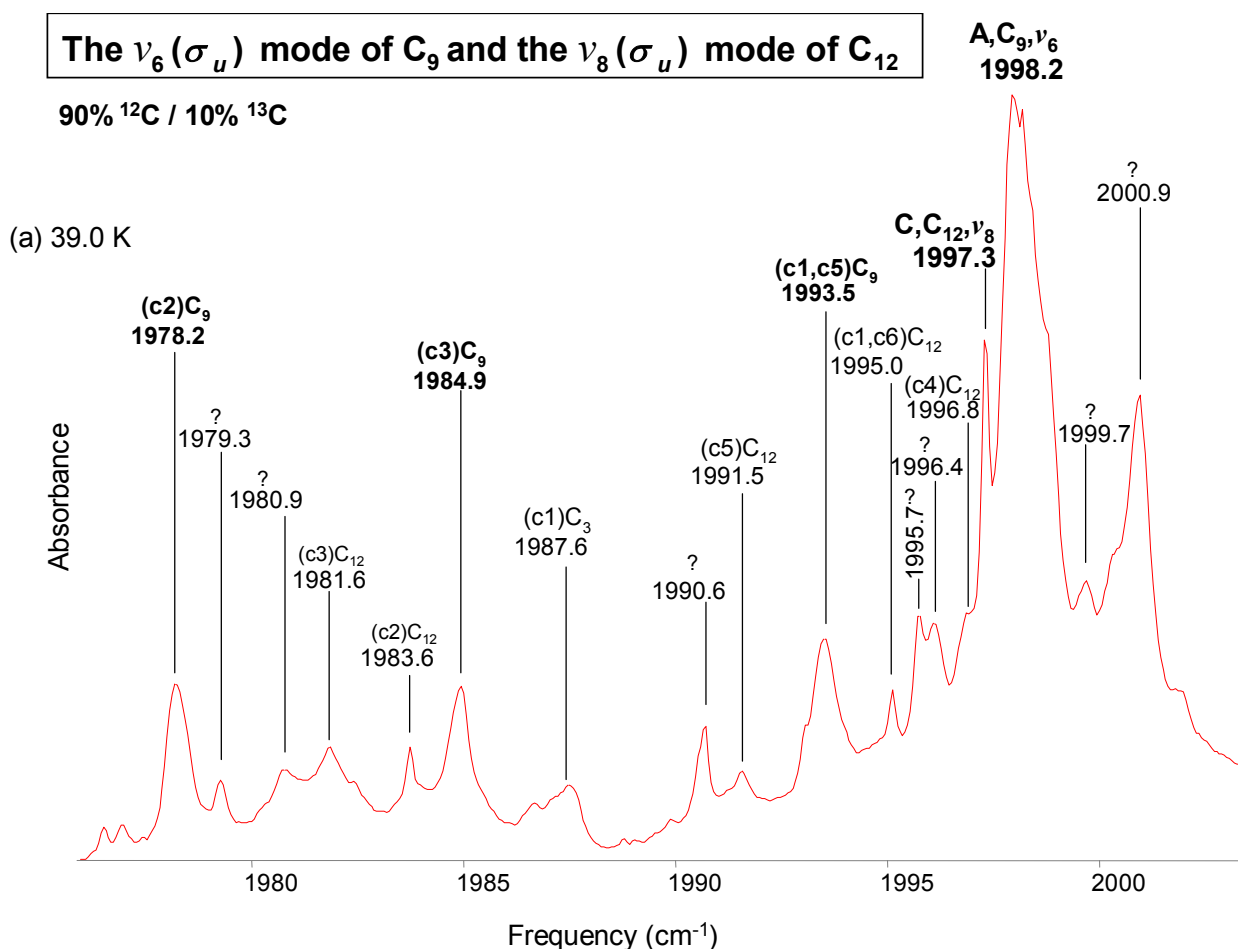


Fig. 16. Observed FTIR spectrum of the $\nu_6(\sigma_u)$ mode of linear C_9 and $\nu_8(\sigma_u)$ mode and the its single ^{13}C -substituted ($^{13}\text{C}^{12}\text{C}_8$) carbon clusters and the $\nu_8(\sigma_u)$ mode of linear C_{12}^5 and its isotopic shifts using 90% ^{12}C and 10% ^{13}C enrichment.

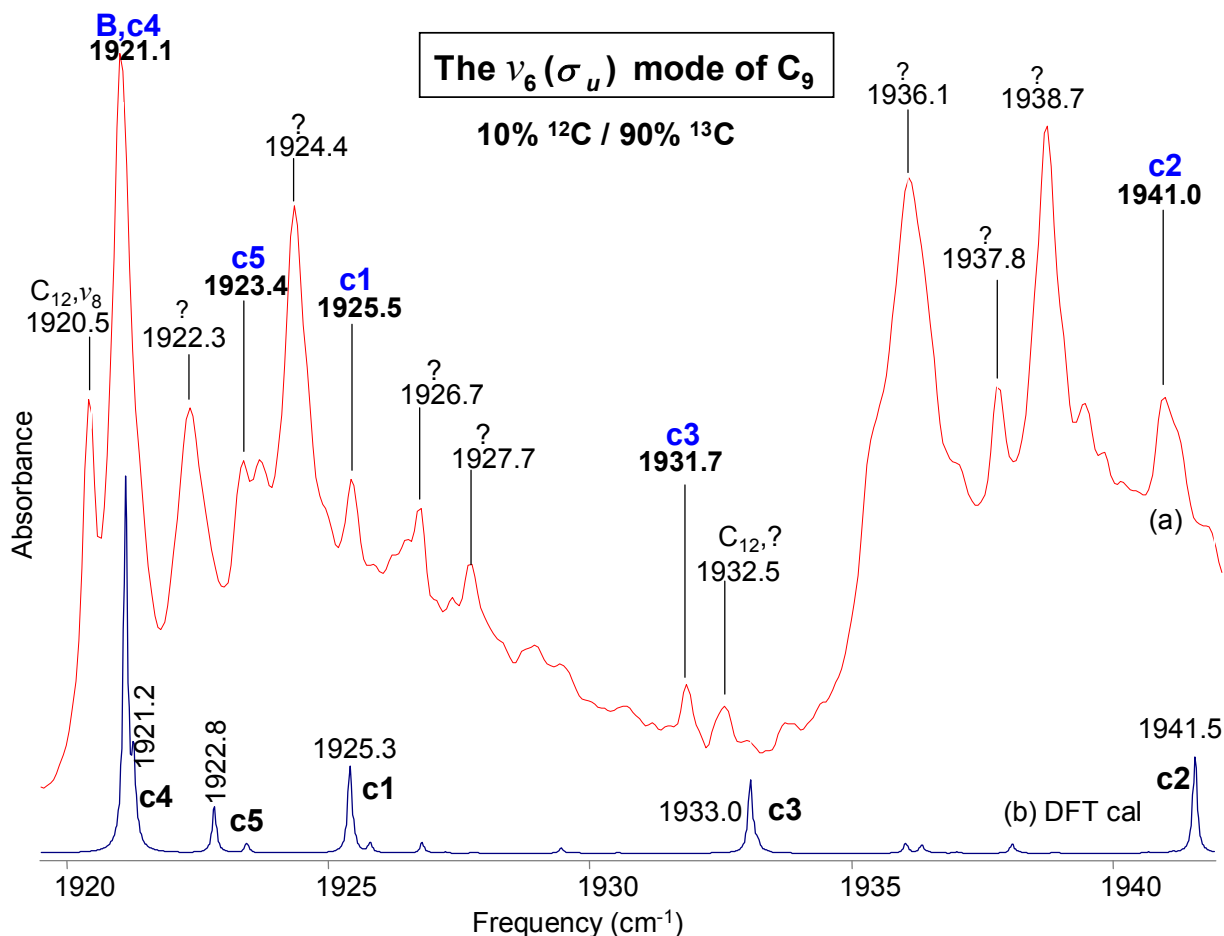


Fig. 17. Comparison of an FTIR spectrum of the $\nu_6(\sigma_u)$ mode of the linear C_9 and its isotopic shifts with (a) 10% ^{12}C / 90% ^{13}C and (b) a DFT calculations at the B3YLP/cc-pVDZ simulation using the same enrichment.

Fig. 17(a), shows the mirror spectrum corresponding to the single (and other peaks yet to be discussed) ^{12}C substitutions in the $\nu_6(\sigma_u)$ mode of $^{13}C_7$ produced by the evaporation of a carbon mixture rod of a 90% of ^{13}C and 10% ^{12}C . The absorption at 1921.1 cm^{-1} , which is a factor $\sim\sqrt{12/13}$ of the 1998.2 cm^{-1} frequency, is identified as belonging to the fully ^{13}C -substituted isotopomer. In Fig. 17 (a) we can see a tentative shift-set that we call SSC13 with the

frequencies for the isotopomers at 1921.1 (c4) 1925.5 (c1) (overlapped by the main band at 1921.1 (B), 1941.0 (c2), 1931.7 (c3) and 1923.4 cm^{-1} (c5) (see Fig. 17). The measured frequencies were compared with the results of the scaled DFT calculation (see Table IV).

TABLE IV. Comparison of observed and predicted DFT (B3LYP/cc-pVDZ) frequencies for single ^{13}C -substituted isotopomers of $^{12}\text{C}_9$, and single ^{12}C -substituted isotopomers of $^{13}\text{C}_9$, for the ν_6 mode.

Isotopomer	ν_{obs}	B3LYP/cc-pVDZ		$\Delta\nu$ $\nu_{\text{obs}} - \nu_{\text{scaled}}$
		ν	ν_{scaled}	
12-12-12-12-12...(A)	1998.2	2132.4	1998.2 ¹	0.0
13-12-12-12-12...(c1)	1993.5	2128.5	1994.5	-1.0
12-13-12-12-12...(c2)	1978.2	2112.2	1979.3	-1.1
12-12-13-12-12...(c3)	1984.9	2115.9	1982.7	2.2
12-12-12-13-12...(c4)	Overlapped ²	2132.1	1997.9	----
12-12-12-12-13...(c5)	Overlapped ³	2128.5	1994.5	----
13-13-13-13-13...(B)	1921.1	2048.5	1921.1 ⁴	0.0
12-13-13-13-13...(c1)	1925.5	2053.0	1925.3	0.2
13-12-13-13-13...(c2)	1941.0	2070.2	1941.5	-0.5
13-13-12-13-13...(c3)	1931.7	2061.2	1933.0	-1.3
13-13-13-12-13...(c4)	Overlapped ⁵	2048.6	1921.2	----
13-13-13-13-12...(c5)	1923.4	2050.3	1922.8	0.6

¹Scaling factor $\nu_{\text{obs}}/\nu \sim 0.93710$

²Overlapped by the main band at 1998.2 cm^{-1} (A)

³Overlapped by the c1 isotopomer

⁴Scaling factor $\nu_{\text{obs}}/\nu \sim 0.93781$

⁵Overlapped by the main band at 1921.1 cm^{-1} (B)

The top half of Table IV, shows a preliminary selection SSC12 for the single ^{13}C -substituted $^{13}\text{C}^{12}\text{C}_8$ isotopomers, and in the bottom half the shift set SSC13, for the single ^{12}C -substituted $^{12}\text{C}^{13}\text{C}_8$ isotopomers, (in the knowledge that we may have more than one possible set of shifts), which will be tested by applying the DPM. In Table IV, the first column lists the isotopomers under consideration for the ν_6 mode of C_9 with their abbreviated isotopomer label in parentheses. The predicted frequencies for the single ^{13}C -substituted $^{13}\text{C}^{12}\text{C}_8$ isotopomers are

scaled by a factor of ~ 0.93710 obtained by taking the ratio of the observed main frequency 1998.2 cm^{-1} with the corresponding DFT calculated main frequency of 2132.4 cm^{-1} of the ν_6 mode of $^{12}\text{C}_9$. By similarly taking the ratio of the predicted and observed frequencies for the ν_6 mode of $^{13}\text{C}_9$ we obtain a scaling factor of ~ 0.93781 for the ^{12}C substituted $^{12}\text{C}^{13}\text{C}_8$ isotopomers. As mentioned before the discrepancies between the calculated frequencies and the observed frequencies are anticipated to be large. The measured frequencies are compared with the results of the scaled DFT calculation given in the Table IV (lower level).

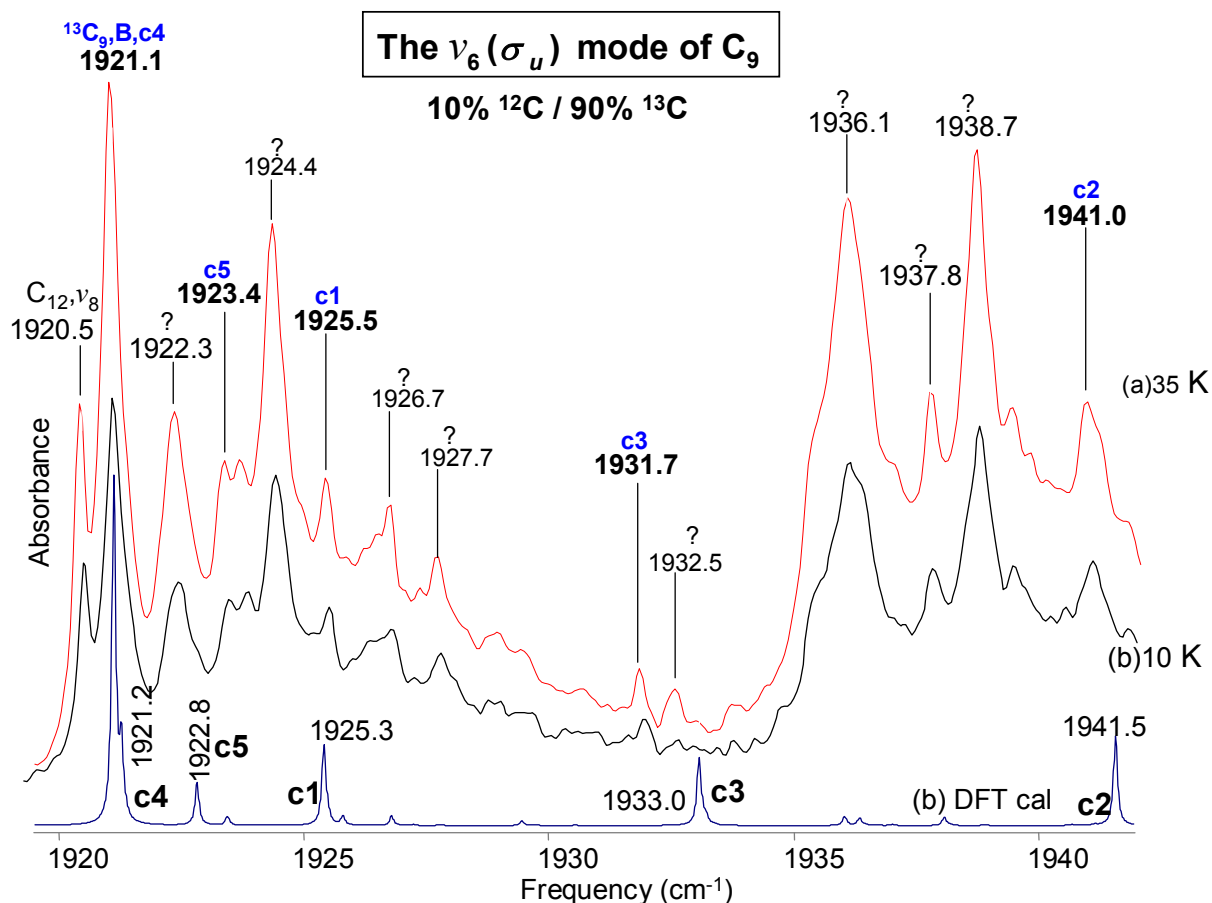


Fig. 18. Comparison of observed FTIR annealed spectra (a) 35 K and (b) 10 K of the $\nu_6(\sigma_u)$ mode of linear C_9 and its single ^{12}C isotopic shifts using 90% ^{13}C and 10% ^{12}C carbon enrichments and (c) a DFT calculations at the B3YLP/cc-pVDZ simulation using the same enrichment.

We will consider the absorptions to the high frequency side of $\nu_6(\sigma_u)$ mode of C_{10} at 1921.1 cm^{-1} (B) for the identification of the five single ^{13}C isotopomers in the spectrum shown in Fig. 18(a), which were produced by the evaporation of a carbon mixture of 10% ^{12}C /90% ^{13}C .

To continue with our task of preliminary select our shift-set it is necessary for us to refer our following considerations to the Figure 18(a) and (b), where we are showing spectra under annealing processes (at 10 and 35 K respectively) to emphasize the correlated behavior

that our selected isotopomers maintain. First of all, it seems that our preliminary shift set selection is not correlated to either of the unknown prominent bands at 1924.4, 1936.1 and 1938.7 cm^{-1} as is shown by the their behavior under annealing processes.

The observed frequency at 1925.5 cm^{-1} is in good agreement with then calculated band at 1925.4 cm^{-1} for the 12-13-13-13-13-13-13-13 (c1) isotopomer [see Fig. 18]. In the other hand, it seems that in the vicinity of this band there is no other peak with similar characteristics. Therefore the band at 1925.5 cm^{-1} will be assigned to the c1 isotopomer. The calculated band at 1941.5 cm^{-1} for the 13-12-13-13-13-13-13-13 (c2) isotopomer seems to have a close agreement with the observed band at 1941.5 cm^{-1} , however, this particular band might contain an extra band growing on its shoulder to the high frequency side, is still related to the c1 isotopomer under annealing. Then band at 1941.5 cm^{-1} will be definitely assigned to the 13-12-13-13-13-13-13-13 (c2) isotopomer. It has been particularly difficult to assign the band at 1931.7 cm^{-1} , due to the existence of other band at 1932.5 cm^{-1} with similar features and closer to the calculated frequency at 1933.0 cm^{-1} corresponding to the 13-13-12-13-13-13-13-13-1(c3) isotopomer. The band at 1932.5 cm^{-1} increases its intensity after annealing as it can be seen in Fig. 18(a), however, this band (which is probably related to the main band of the $\nu_8(\sigma_u)$ mode of $^{13}\text{C}_{12}$) is less intense than its neighbor at 1931.7 cm^{-1} with which it seems not to be related. Therefore, the band at 1931.7 cm^{-1} is assigned to c3 isotopomer. It appears that band corresponding to the 13-13-13-12-13-13-13-13 (c4) isotopomer calculated to be at 1921.3 cm^{-1} for is overlapped by the main band at 1921.1 cm^{-1} (B). The centrosymmetric 13-13-13-13-12-13-13-13-13 (c5) isotopomer calculated to be at 1922.8 cm^{-1} has at least two possibilities to be assigned to two different observed peaks. One is at 1922.3 cm^{-1} , but such a band clearly is not related to the other previously selected c1, c2 and c3 isotopomer [see Fig. 18(b)], besides it is to

big to be centrosymmetric, nor overlapped with. And the observed band at 1923.4 cm^{-1} seems to react after annealing. Therefore it will be assigned to the c5 isotopomer. We finally end up choosing the observed frequencies for the single ^{12}C -substituted isotopomers of the $\nu_6(\sigma_u)$ mode of $^{13}\text{C}_9$ to be 1925.5 (c1), 1941.0 (c2), 1931.7 (c3), 1921.1 (c4)[overlapped by the main band 1921.1 (B)] and 1923.4 cm^{-1} (c5) (see Fig. 18) that we call SSC13 and shown in Table VI. Both shift-sets were submitted to the DPM to support our assignment and it was concluded that the shift-sets reflected in the Table VI had actually a good correlation between the two sets.

4.5 Assignment of the isotopomers for the $\nu_5(\sigma_u)$ mode of C_9

In the absorptions reported by Maier⁸³, Vala⁸⁴ and co-workers in spectra of the products from the evaporation of graphite trapped in Ar, reported the $\nu_5(\sigma_u)$ at 2078.1 cm^{-1} , but no isotopic information was provided. A determination of a definitive assignment of the isotopic shifts of the $\nu_5(\sigma_u)$ mode of linear C_9 can be affected by coupling between the vibrational frequencies corresponding to the $\nu_1(\sigma_g)$ mode and the $\nu_5(\sigma_u)$ mode of C_9 (see Table IV). Therefore, is expected to have significant perturbations with the isotopic shifts of the $\nu_5(\sigma_u)$ vibrational fundamental as a result of the coupling with the $\nu_1(\sigma_g)$ mode.

Figure 19(a) and (b) shows a typical comparison between the matrix results produced by the evaporation of a carbon mixture with 10% ^{13}C /90% ^{12}C and the simulated B3YLP/cc-pVDZ spectrum respectively, in the region where the vibrational fundamental of $\nu_5(\sigma_u)$ mode of C_9 and its single ^{13}C -substituted $^{13}\text{C}^{12}\text{C}_8$ isotopomers are expected to lie.

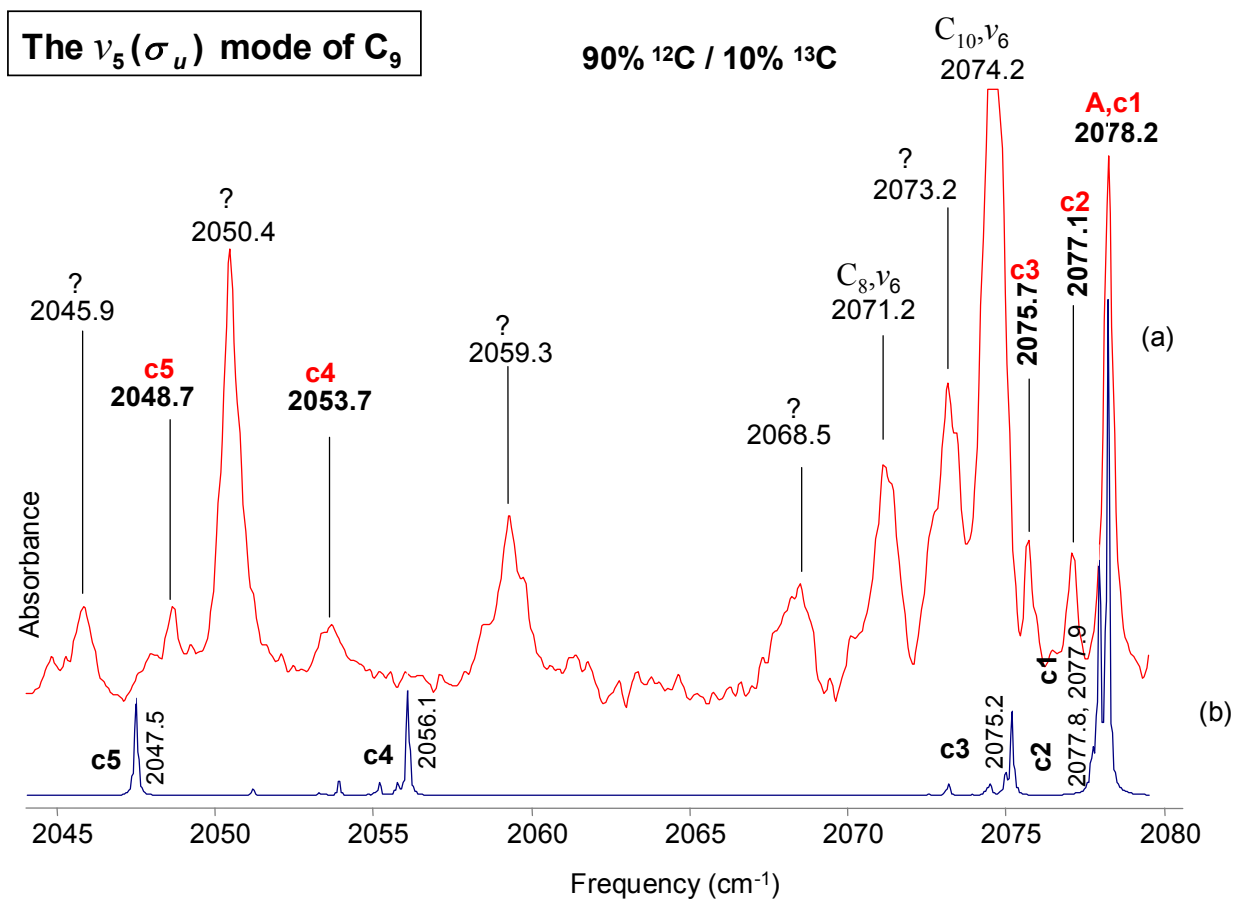


Fig. 19. Comparison of an FTIR spectrum of the $\nu_5(\sigma_u)$ mode of linear C_9 and its single ^{13}C isotopic shifts with (a) 10% ^{13}C and 90% ^{12}C enrichment, and (b) a DFT B3YLP/cc-pVDZ simulation using the same enrichment.

We will consider the absorptions to the low frequency side of the frequency at 2078.2 cm^{-1} for the identification of the preliminary single ^{13}C substituted isotopomers. The two observed bands at 2075.7 and 2077.1 cm^{-1} are similar in intensity, nevertheless the 2077.1 cm^{-1} band is closer to the calculated frequencies 2077.8 , and 2077.9 cm^{-1} that corresponds to the 13-12-12-12-12-12-12(c1) and the 12-13-12-12-12-12-12-12-12 (c2) respectively. The frequency difference of those is $\sim 0.1 \text{ cm}^{-1}$ which in the DFT calculation those two bands appear to be

collapsed in a single peak. The calculated frequency located at 2077.8 cm^{-1} is been “pushed” down due to the action of the not IR- allowed isotopomers for the $\nu_1(\sigma_g)$ mode that lie at 58.8 cm^{-1} to the high frequency side. Then the observed frequency located at 2077.1 cm^{-1} will be assigned to the c2 isotopomer, hence the c1 isotopomer will be considered to be overlapped by the main band at 2078.2 (A) . For a better appreciation of the above decryption we can see in Fig. 20 (c).

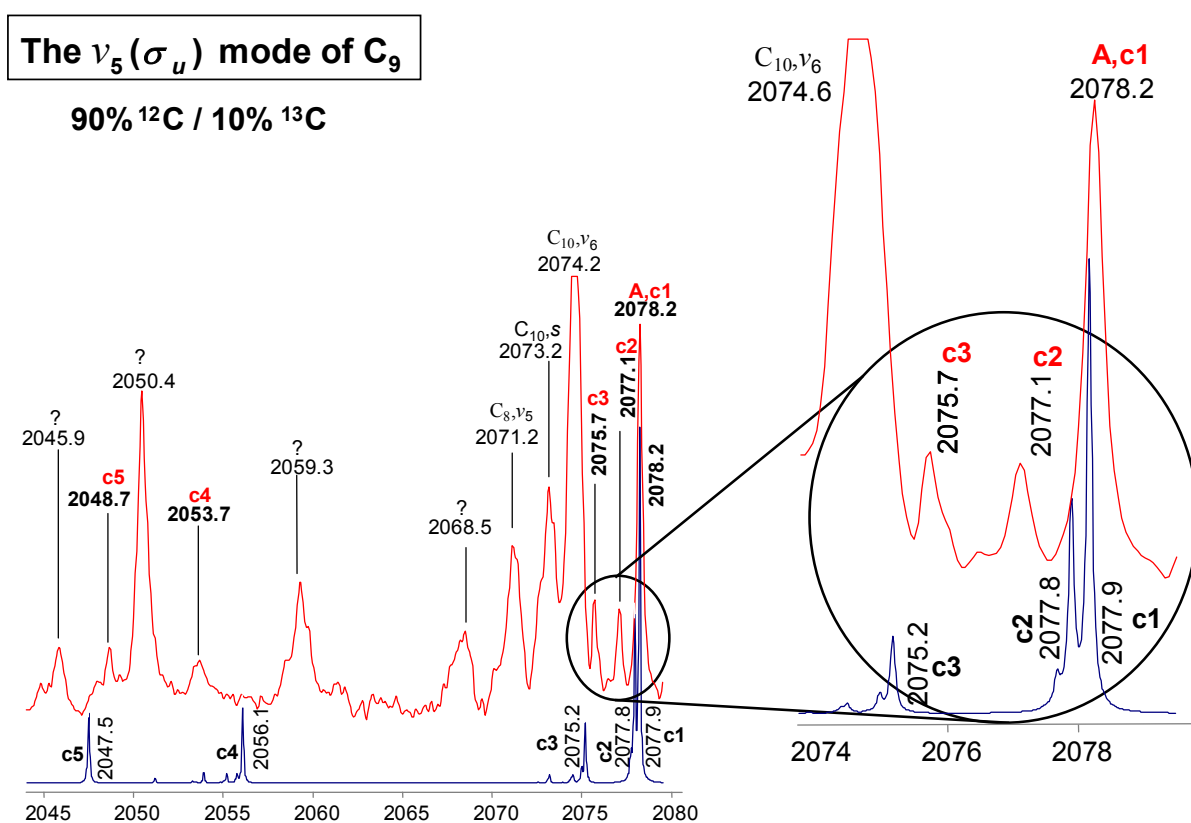


Fig. 20. A section of Fig. 18 has been enlarged to visually emphasize the preliminary selection of the 13-12-12-12-12-12-12-12-12 (c1) and the 12-13-12-12-12-12-12-12-12 (c2) isotopomers correspondent to the $\nu_5(\sigma_u)$ mode of linear C_9 .

The observed band at 2075.7 cm^{-1} is of similar characteristics to the c2 isotopomer already assigned. It is close to the calculated frequency at 2075.2 cm^{-1} correspondent to the isotopomer 12-12-13-12-12-12-12-12 (c3) with a frequency difference of about 0.5 cm^{-1} representing a really good agreement. The observed band at 2059.3 cm^{-1} it is at 3.2 cm^{-1} away from the calculated isotopomer at 2056.1 cm^{-1} for the 12-12-12-13-12-12-12-12 (c4) isotopomer and more intense than those c1 and c2 previously chosen isotopomers, therefore it will not be taken into consideration. The next band to the low frequency side is at 2053.7 cm^{-1} , is at 2.4 cm^{-1} away from the calculated frequency. It is still a rather large frequency difference, but acceptable, since the non infrared active mode $\nu_1(\sigma_g)$ mode of C_9 located at the high frequency side of the $\nu_5(\sigma_u)$ mode of C_9 , is inducing a repulsion between isotopomers. So, the frequency at 2053.7 cm^{-1} will be assigned to the 12-12-12-13-12-12-12-12 (c4) isotopomer. Continuing to the low frequency side [see Fig. 19], we encounter a well-defined, but still unidentified band at 2050.4 cm^{-1} (currently under investigation by the authors of this work). Questions may arise, regarding the possibility that some of the still, unidentified smaller bands at 2045.9 and 2048.7 cm^{-1} may be possible shifts of the 2050.4 cm^{-1} band. But this is where the use of the DPM becomes very helpful; we selected two different shift sets, one formed with the frequencies 2077.1 (c1)[overlapped by the main band at 2078.2 (A)], 2078.2 (c2), 2075.7 (c3), 2053.7 (c4) and 2048.7 (c5) cm^{-1} and named *SSC12* and a second shift-set 2077.1 (c1) [overlapped by the main band at 2078.2 (A)], 2078.2 (c2), 2075.7 (c3), 2053.7 (c4) and 2045.9 (c5) cm^{-1} that we called *SSC12'*. We submitted every one of those shift sets and the shift set *SSC13* (yet to be properly assigned) to the DPM process, and it was founded that in fact the correlated shift-set is the *SSC12*. Therefore the band at 2053.7 cm^{-1} will be assigned to the centrosymmetric 12-12-12-12-13-12-12-12 (c5) isotopomer.

Figure 21 (a) shows the reflected spectrum equivalent to the single ^{12}C - substitutions in the $\nu_5(\sigma_u)$ mode of $^{13}\text{C}_9$, produced by the evaporation of a carbon mixture rod of 10% ^{12}C /90% ^{13}C . The absorption at 1998.0 cm^{-1} , which is a factor $\sim\sqrt{12/13}$ of the 2078.2 cm^{-1} frequency, has been identified as belonging to the fully ^{13}C -substituted isotopomer. We will take in to consideration the bands at higher frequency side of the band at 1998.0 cm^{-1} [see Fig. 21(a)] the bands at 1998.0 cm^{-1} (c1) [overlapped with the main band 1998.0 (B)], 1999.1 (c2), 2000.6 (c3) and 2015.6 cm^{-1} (c4) can be preliminary chosen (see Table V).

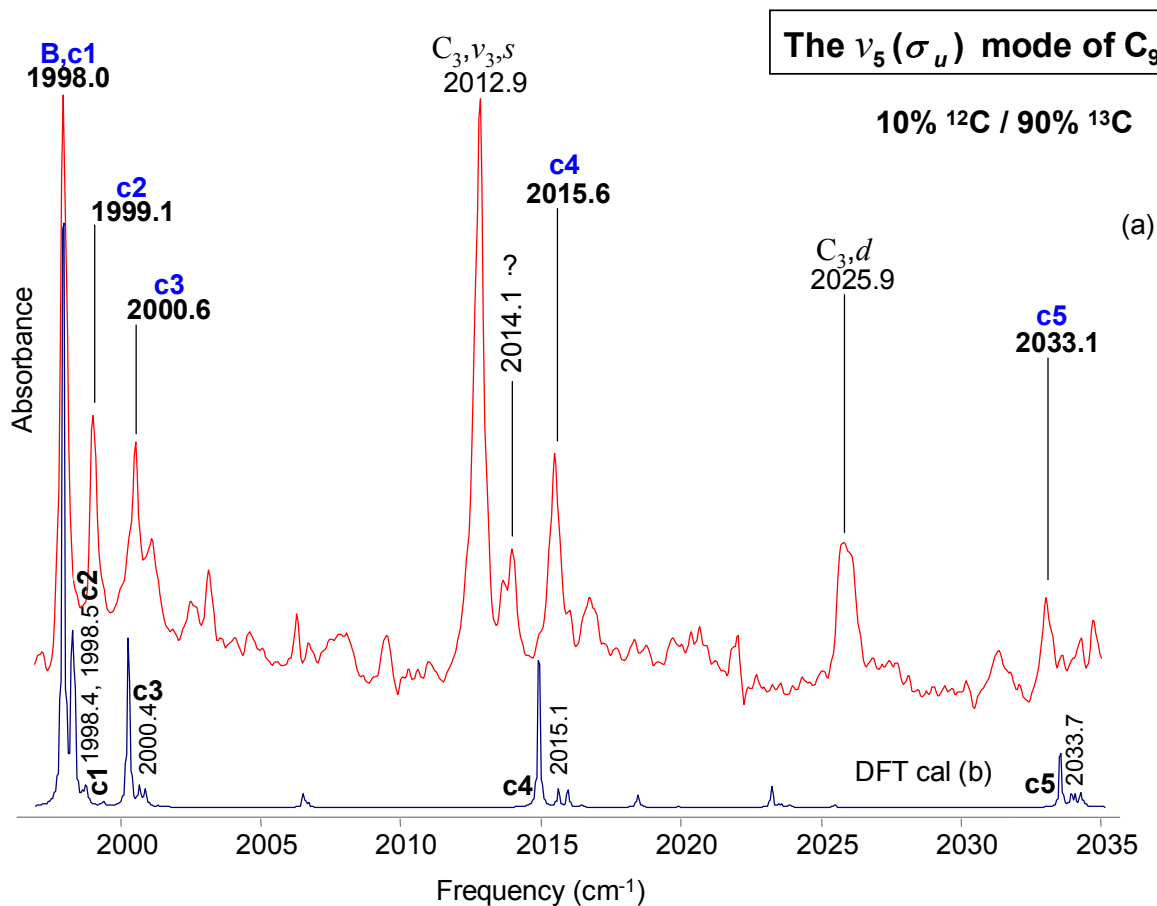


Fig. 21. Comparison of an FTIR spectrum of the $\nu_5(\sigma_u)$ mode of linear C_9 its single ^{12}C isotopic shifts with (a) 90% ^{13}C and 10% ^{12}C enrichment, and (b) DFT B3YLP/cc-pVDZ simulation using the same enrichment.

TABLE V. Comparison of observed and predicted DFT (B3LYP/cc-pVDZ) frequencies for single ^{13}C -substituted isotopomers of $^{12}\text{C}_9$ and single ^{12}C -substituted isotopomers of $^{13}\text{C}_9$ for the ν_5 mode.

Isotopomer	ν_{obs}	B3LYP/cc-pVDZ		$\Delta\nu$ $\nu_{\text{obs}} - \nu_{\text{scaled}}$
		ν	ν_{scaled}	
12-12-12-12-12...(A)	2078.2	2217.5	2078.2 ¹	0.0
13-12-12-12-12...(c1)	Overlapped ²	2217.2	2077.9	0.0
12-13-12-12-12...(c2)	2077.1	2217.1	2077.8	-0.7
12-12-13-12-12...(c3)	2075.7	2214.3	2075.2	0.5
12-12-12-13-12...(c4)	2053.7	2193.9	2056.1	-2.4
12-12-12-12-13...(c5)	2048.7	2184.7	2047.5	1.2
13-13-13-13-13...(B)	1998.0	2130.2	1998.0 ³	0.0
12-13-13-13-13...(c1)	Overlapped ⁴	2130.5	1998.4	0.0
13-12-13-13-13...(c2)	1999.1	2130.6	1998.5	0.6
13-13-12-13-13...(c3)	2000.6	2132.7	2000.4	0.2
13-13-13-12-13...(c4)	2015.6	2148.3	2015.1	0.5
13-13-13-13-12...(c5)	2033.1	2168.2	2033.7	-0.6

¹Scaling factor $\nu_{\text{obs}}/\nu \sim 0.93718$

²Overlapped by the main band at 2078.2 cm^{-1} (A)

³Scaling factor $\nu_{\text{obs}}/\nu \sim 0.93794$

⁴Overlapped by the main band at 1921.1 cm^{-1} (B)

The top half of Table V, shows a preliminary selection for the shift set SSC12 consisted of the single ^{13}C -substituted $^{13}\text{C}^{12}\text{C}_8$ isotopomers, and in the bottom half the shift-set SSC13, for the single ^{12}C -substituted $^{12}\text{C}^{13}\text{C}_8$ isotopomers, (in the knowledge that we may have more than one possible shift-sets), which will be tested by applying the DPM. Let's start at by taking a careful look at the group of frequencies located in the interval from 1997.0 to 2001.0 cm^{-1} [see Fig. 21(a)] where the situation is similar to that of the previously discussed spectrum obtained with the mixture 90% ^{12}C / 10% ^{13}C (see Fig. 18). There are two observed peaks of similar features located at 1999.1 and 2000.6 cm^{-1} , both are close to the peak 1998.4 and 1998.5 cm^{-1} , corresponding to the calculated 12-13-13-13-13-13-13-13-13(c1) and 13-12-13-13-13-13-13-13-

$^{13}\text{C}(2)$ isotopomers respectively [see Figure 21(b)]. Following the same arguments (as in the previous counterpart), it is clear that the 12-13-13-13-13-13-13-13-13 (c1) isotopomer with a calculated frequency at 1998.4 cm^{-1} is overlapped with the main band at 1998.0 cm^{-1} (B) and the calculated frequency at 1998.5 cm^{-1} correspondent to the 13-12-13-13-13-13-13-13-13(c2) isotopomer can be assigned to the observed frequency at 1999.1 cm^{-1} . An the observed band located at 2000.6 cm^{-1} can be assigned to 13-13-13-12-13-13-13-13-13(c3) isotopomer due to its proximity with the calculated frequency at 2000.4 cm^{-1} with, which is in good agreement. The observed band at 2014.1 cm^{-1} is a potential candidate that due to its proximity to the calculated band 2015.1 cm^{-1} can be assigned to the 13-13-13-12-13-13-13-13-13(c4) isotopomer but it is less intense than the previously selected c2 and c3 isotopomers and it can be eliminated from consideration. The observed band located at 2015.6 cm^{-1} has similar characteristics of the c2 and c3 isotopomers. It is close to the calculated band at 2015.1 cm^{-1} for the 13-13-13-12-13-13-13-13-13 (c4) isotopomer. Therefore the band at 2015.6 cm^{-1} can be assigned to the c4 isotopomer. The band observed at 2033.1 cm^{-1} has an intensity smaller than those of the other c2, c3 and c4 as expected for the centrosymmetric 13-13-13-13-13-12-13-13-13-13 (c5) isotopomer. It is also in an excellent agreement with the calculated frequency at 2033.6 cm^{-1} . Finally we can conclude that two shift-sets reported in Table V can be consider as the ^{13}C -substituted $^{13}\text{C}^{12}\text{C}_8$ isotopomers (high part of the Table V) and the single ^{12}C -substituted $^{12}\text{C}^{13}\text{C}_8$ isotopomers (lower part of the table).

4.6 Assignment of the isotopomers for the $\nu_7(\sigma_u)$ mode of C_9

The third stretching fundamental, the $\nu_7(\sigma_u)$ mode of C_9 , was presented by Kranze *et al.*⁸⁵ (see Fig. 21). They reported the vibrational fundamental to be located at 1601.0 cm^{-1} . In spite of such fine work performed by those researchers, only two of the possible five single ^{13}C shifts were observed, with frequencies at $1600.4(\text{c4})$ and 1585.8 cm^{-1} (c1) and the main band was reported at $1601.0\text{ cm}^{-1}(\text{A})$. The other three single substituted isotopomers, whose frequencies were predicted to occur at 1593.0 (c1), 1595.0 , and 1589.8 cm^{-1} , were hypothesized to lie in a frequency interval dominated by strong bands of H_2O , which prevented any possibility of observing them.

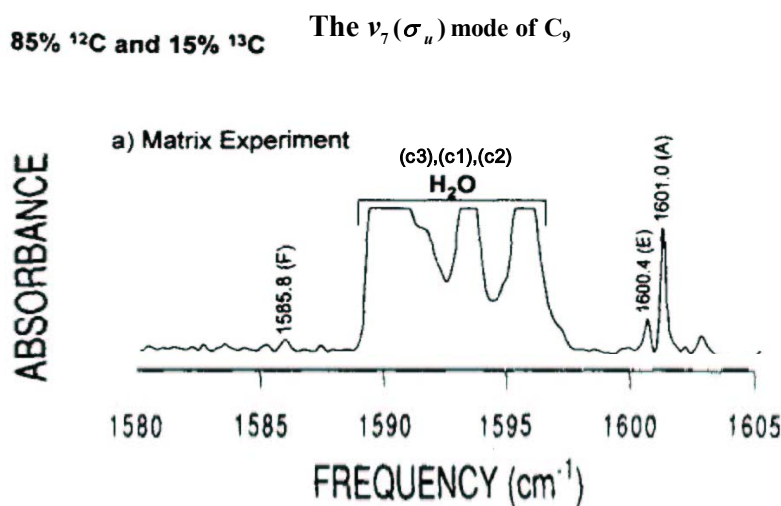


Fig. 22. The partial spectrum of the ^{13}C shifts for the $\nu_7(\sigma_u)$ mode of $^{12}\text{C}_9$ showing the overlapping H_2O bands (from Kranze *et al.*)⁸⁵.

The present experiments [see Fig. 23] permitted the observation of these overlapped three bands at 1593.0 cm^{-1} (c1), 1595.0 cm^{-1} (c2) and 1590.8 cm^{-1} (c3). Also shown is the mirror image of the $\nu_7(\sigma_u)$ mode for $^{13}\text{C}_9$ and its single ^{12}C -substituted $^{12}\text{C}^{13}\text{C}_8$ carbon.

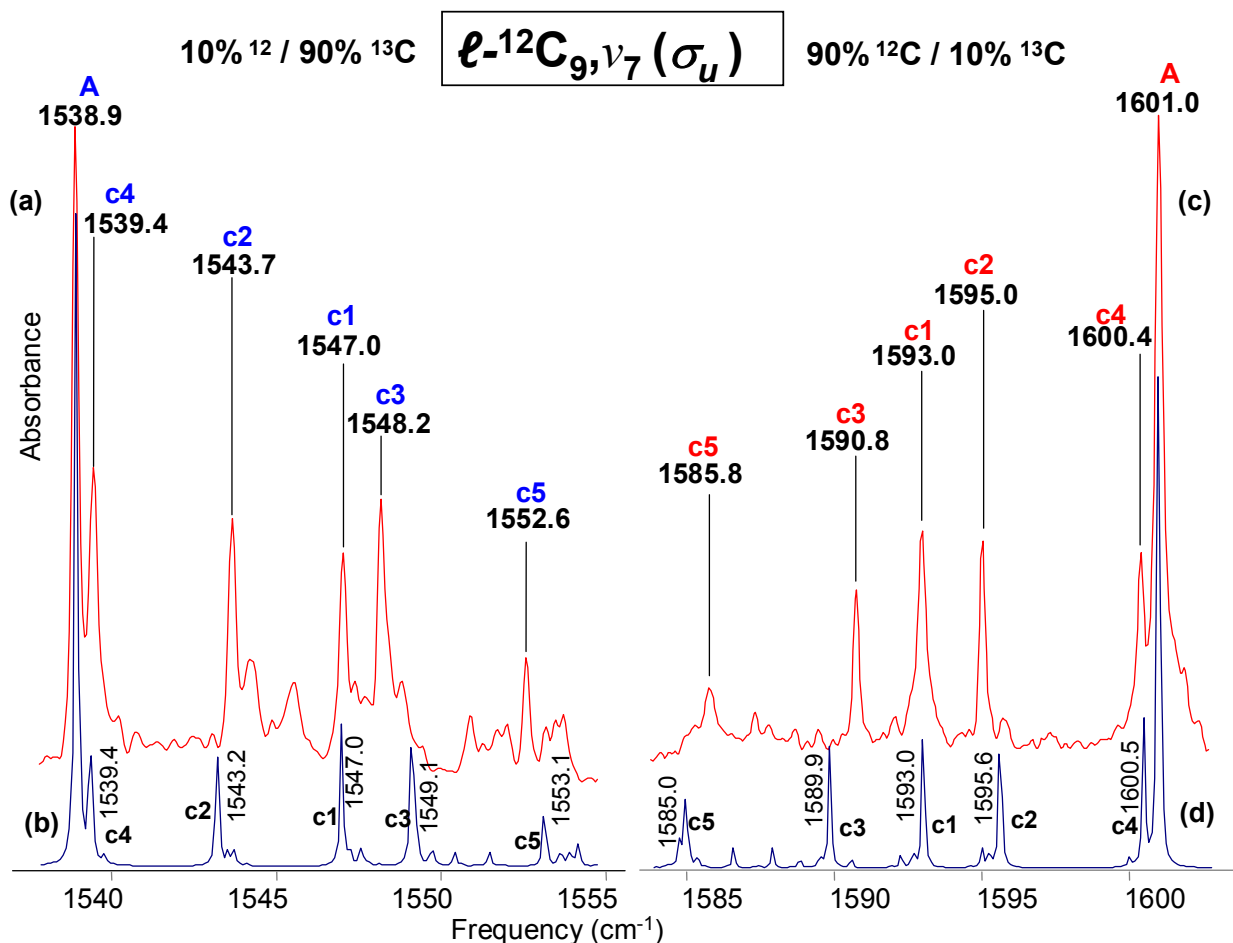


Fig. 23. Comparison of the FTIR spectra of the $\nu_7(\sigma_u)$ mode of the linear C_9 and its ^{12}C and ^{13}C isotopic shifts with carbon enrichments (a) $10\%^{12}\text{C}$ and $90\%^{13}\text{C}$ (c) and $90\%^{12}\text{C}$ and $10\%^{13}\text{C}$ (c) and a simulations (b) and (d) derived from the DFT calculations at the B3YLP/cc-pVDZ level for the same enrichment values.

Table VI, shows the frequencies of the main bands for both shift-sets the single ^{13}C -substituted $^{13}\text{C}^{12}\text{C}_8$ (higher level) and the single ^{12}C -substituted $^{12}\text{C}^{13}\text{C}_8$ carbon clusters (lower level) which are in good agreement.

TABLE VI. Comparison of observed and predicted DFT (B3LYP/cc-pVDZ) frequencies for single ^{13}C -substituted isotopomers of $^{12}\text{C}_9$, and single ^{12}C -substituted isotopomers of $^{13}\text{C}_9$, for the ν_7 mode.

Isotopomer	ν_{obs}	B3LYP/cc-pVDZ		$\Delta\nu$ $\nu_{\text{obs}} - \nu_{\text{scaled}}$
		ν	ν_{scaled}	
12-12-12-12-12...(A)	1601.0	1669.8	1601.0 ¹	0.0
13-12-12-12-12...(c1)	1593.0	1661.5	1593.0	0.0
12-13-12-12-12...(c2)	1595.0	1664.2	1595.6	-0.6
12-12-13-12-12...(c3)	1590.8	1658.2	1589.9	0.9
12-12-12-13-12...(c4)	1600.4	1669.3	1600.5	-0.1
12-12-12-12-13...(c5)	1585.8	1653.1	1585.0	0.8
13-13-13-13-13...(B)	1538.9	1604.1	1538.9 ²	0.0
12-13-13-13-13...(c1)	1547.0	1612.5	1547.0	0.0
13-12-13-13-13...(c2)	1543.7	1608.6	1543.2	0.5
13-13-12-13-13...(c3)	1548.2	1614.7	1549.1	-0.9
13-13-13-12-13...(c4)	1539.4	1604.6	1539.4	0.0
13-13-13-13-12...(c5)	1552.6	1618.9	1553.1	-0.5

¹Scaling factor $\nu_{\text{obs}}/\nu \sim 0.99994$

²Scaling factor $\nu_{\text{obs}}/\nu \sim 0.99993$

4.7 Conclusions

Fourier transform infrared study has been presented for the linear $\nu_5(\sigma_u)$, $\nu_6(\sigma_u)$ and $\nu_7(\sigma_u)$ modes of C_9 carbon clusters produced in solid Ar at 10 K through laser ablation of graphite, now assigned to the 2078.2, 1998.2 and 1601.0 cm^{-1} , with a complete isotopic shift-sets in the first two cases and completing the isotopic information for the last case. Using the much improved

spectra obtained for both 90/10 and 10/90 isotopic measurements and by taking into consideration the interaction with the ν_1 mode [for the cases $\nu_5(\sigma_u)$, $\nu_6(\sigma_u)$] by using DPM has been particularly useful during the endeavor of looking for accurate assignments of their isotopic shifts. This provides useful information for subsequent isotopic investigations of other C_n species whose spectra lie in this region, since these now known, isotopic shifts can be eliminated. We can use the approach taken here as the basis for future identifications of vibrational modes of longer C_n ($n > 9$) carbon clusters.

CHAPTER V

FTIR SPECTROSCOPIC STUDY OF THE $\nu_6(\sigma_u)$ AND $\nu_7(\sigma_u)$ MODES OF LINEAR C_{10}

5.1 Introduction

In previous chapters the importance has been established of having as complete as possible isotopic shift data in order to assign the vibrational fundamentals of C_n carbon molecules. This is one of the most effective ways of characterizing molecules, particularly the larger carbon molecules, C_n ($n \geq 6$). The vibrational fundamentals of interest in this chapter are the $\nu_6(\sigma_u)$ and $\nu_7(\sigma_u)$ modes of C_{10} previously assigned by Maier *et. al.*⁸⁷ by means of mass-selection to absorptions at 2074.5 and 1915.4 cm^{-1} respectively, although no isotopic information was provided for any of those vibrational fundamentals. New experimental information obtained in the present work confirms the identification of the vibrational fundamentals based on extensive ^{13}C isotopic shift measurements combined with DFT theoretical calculations including the *deperturbation method*.

5.2 Results and discussion

Let us start with the $\nu_7(\sigma_u)$ the second most intense mode of C_{10} . On ^{13}C isotopic substitutions which eliminate the center of symmetry, it has an interaction with the $\nu_2(\sigma_g)$ mode calculated at 2069.4 cm^{-1} , which is only 72.0 cm^{-1} to the high frequency side of $\nu_7(\sigma_u)$ (see Table

VII).

TABLE VII. DFT B3LYP/cc-pVDZ predicted vibrational frequencies and band intensities for (ℓ -C₁₀)

Vibrational mode	Frequency (cm ⁻¹)	Infrared intensity (km/mol)
$\nu_1(\sigma_g)$	2162.4	0.0
$\nu_2(\sigma_g)$	2069.4	0.0
$\nu_3(\sigma_g)$	1805.4	0.0
$\nu_4(\sigma_g)$	1167.5	0.0
$\nu_5(\sigma_g)$	417.6	0.0
$\nu_6(\sigma_u)$	2196.4	2839.2
$\nu_7(\sigma_u)$	1997.4	2021.4
$\nu_8(\sigma_u)$	1499.8	294.1
$\nu_9(\sigma_u)$	806.2	0.1
$\nu_{10}(\pi_g)$	751.4	0.0
$\nu_{11}(\pi_g)$	532.7	0.0
$\nu_{12}(\pi_g)$	282.7	0.0
$\nu_{13}(\pi_g)$	110.3	0.0
$\nu_{14}(\pi_u)$	650.1	0.1
$\nu_{15}(\pi_u)$	402.2	2.6
$\nu_{16}(\pi_u)$	195.9	11.1
$\nu_{17}(\pi_u)$	42.5	6.3

The linear C₁₀ cluster was produced using the laser ablation setup described previously in this work (see CHAPTER III and IV). We will continue with the same notation described in CHAPTER III for the analysis of the spectrum. Figure 24 (a) shows the frequency range where the vibrational fundamental of $\nu_7(\sigma_u)$ mode of C₁₀ and its single ¹³C-substituted ¹³C¹²C₉ are expected to lie. We will consider the absorptions to the low frequency side of the $\nu_7(\sigma_u)$ mode at 1915.7 cm⁻¹ for the identification of the single ¹³C-isotopomers in the spectrum in Fig. 24(a).

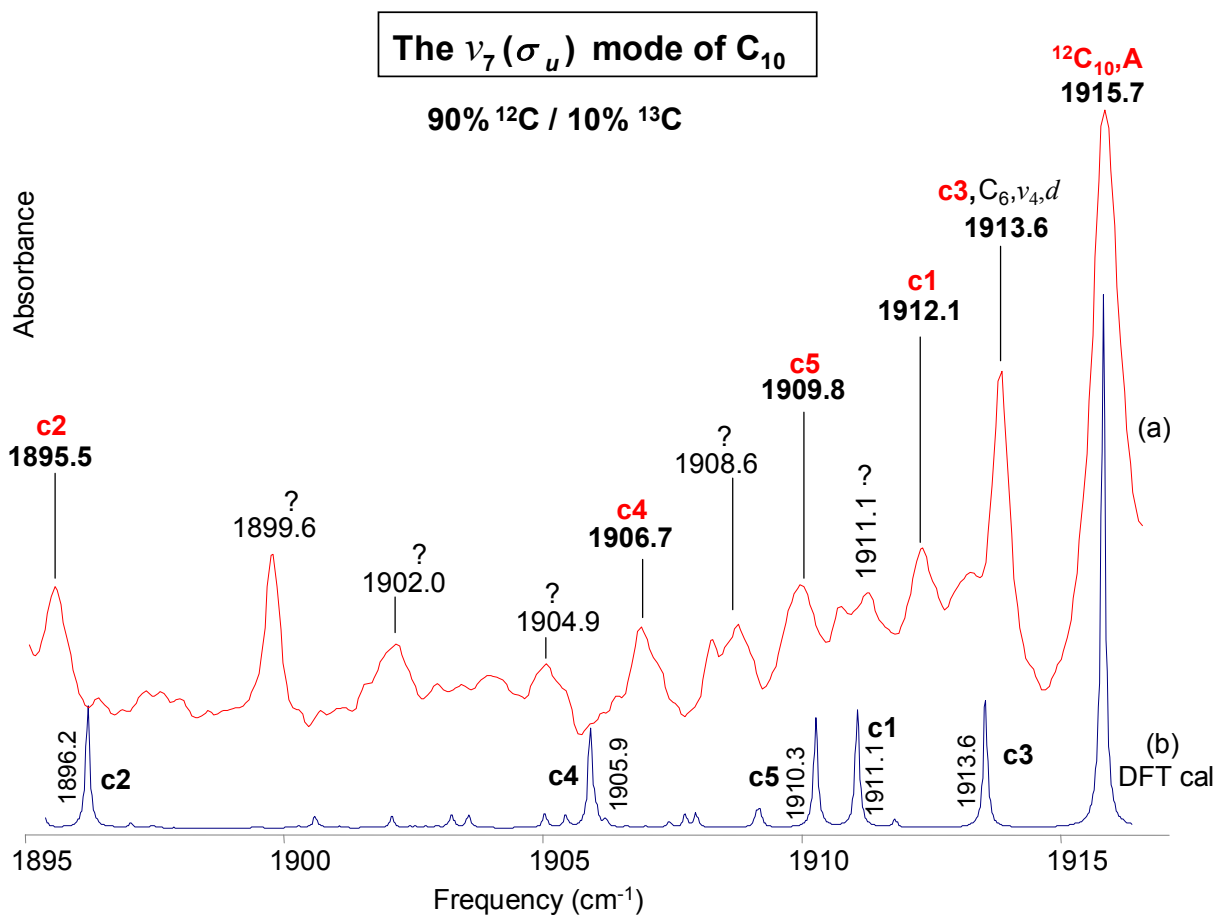


Fig. 24. Comparison of observed FTIR of the of the $\nu_7(\sigma_u)$ mode of the linear C_{10} and its single ^{12}C and ^{13}C isotopic shifts with carbon enrichments (a) 90% ^{13}C and 10% ^{12}C and a simulation (b) derived from the DFT calculations at the B3YLP/cc-pVDZ level for the same enrichment values.

Let us start with, a preliminary selection called *SSC12* of the observed single ^{13}C -substituted $^{13}C^{12}C_9$ isotopomers [see Fig. 24(a)] at 1912.1(c1), 1895.5 (c2), 1913.6 (c3) [overlapped with a double substituted 13-12-13-12-12-12 isotopomer of the $\nu_4(\sigma_u)$ mode of C_6], 1906.7 (c4) and 1909.8 cm^{-1} (c5). It is clear from the spectrum in Fig. 24(a) that at least four of our proposed isotopomers lie within a congested interval of the spectra (1905.0 to 1915.0 cm^{-1}),

where other possible absorptions, could potentially be used to form different shift-sets. The *deperturbation method* can be used to test the potential sets.

5.3 Assignment of the isotopomers for the $\nu_7(\sigma_u)$ mode of C_{10}

Fig. 25 shows the experimental results obtained, before and after annealing in order to find any possible intensity correlation, between bands in our preliminary shift selections. A prominent peak at 1915.7 cm^{-1} (A) is assigned to the $\nu_7(\sigma_u)$ mode of C_{10} . In both observed spectrum in [see Fig. 25 (a) and (b)], is difficult to utilize the base line in order to correctly measure the integrated intensity of the isotopomer bands. It is probably safe to say that, the integrated intensity of the proposed shifts are of about the same intensity except, for the c3 isotopomer located at 1913.6 cm^{-1} , which is overlapped with the double substituted 13-12-13-12-12-12 isotopomer of the $\nu_4(\sigma_u)$ mode of C_6 .⁸⁸

The assignment of the band located at 1912.1 cm^{-1} to the 13-12-12-12-12-12-12-12-12(c1) isotopomer with calculated frequency at 1911.1 cm^{-1} is not obvious, since another peak is observed at 1911.1 cm^{-1} [see Fig. 25 (a)] matching perfectly the calculated frequency. However, in Figure 25(b) (annealed at 34.0 K) this latter band is significantly less intense than the 1912.1 cm^{-1} band and the rest of the proposed isotopomer bands. The discrepancy of 1.0 cm^{-1} between the observed and the calculated bands is probably due to the repulsion caused by the coupling with $\nu_2(\sigma_g)$ mode calculated to be to the higher frequency side (see Table VII) that “pushes” all the isotopomers of $\nu_7(\sigma_g)$ down to the low frequency side of the spectrum. Therefore frequency band at 1912.1 cm^{-1} is assigned to the c3 isotopomer.

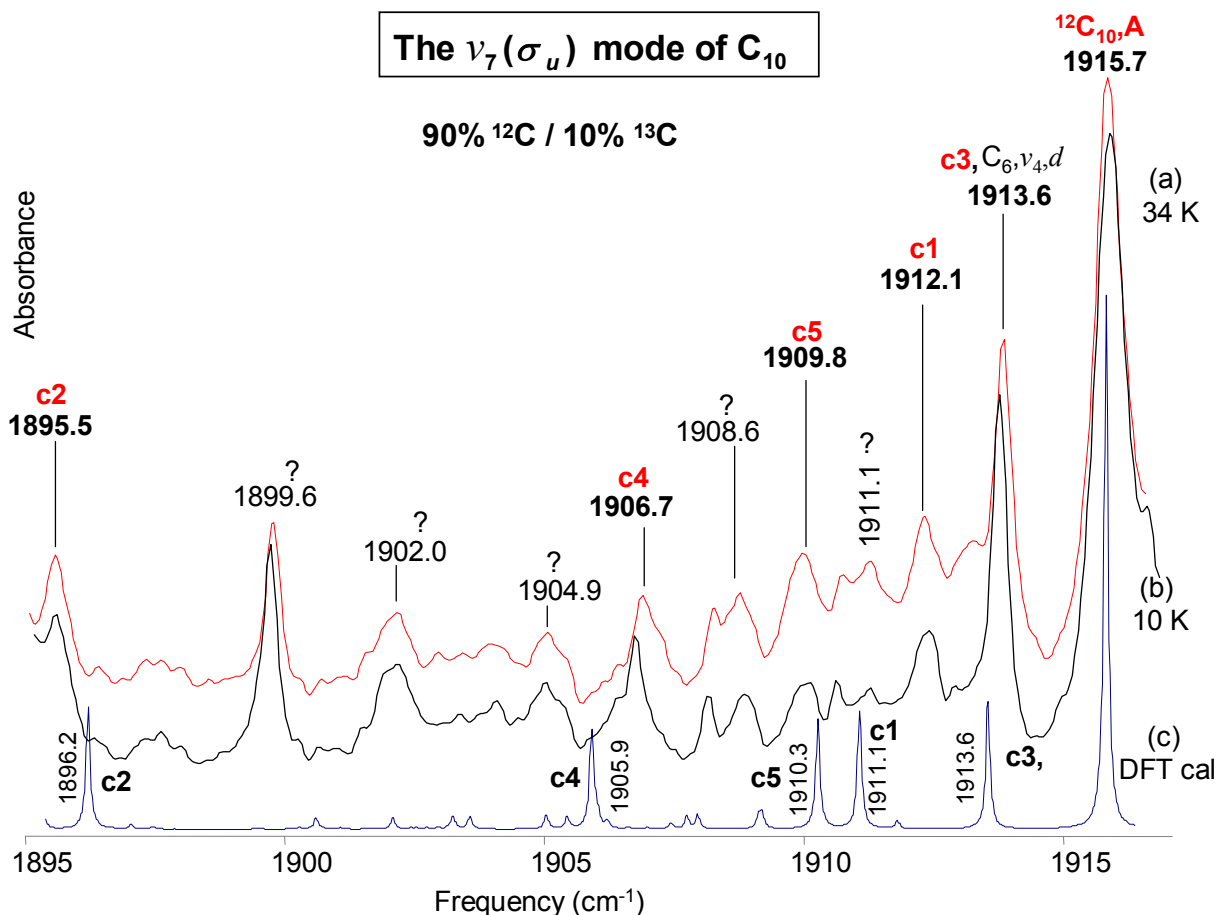


Fig. 25. Comparison of observed FTIR annealed spectra (a) 34 K (b) 10 K of the of the $\nu_7(\sigma_u)$ mode of the linear C_{10} and its single ^{12}C and ^{13}C isotopic shifts with carbon enrichments (a) 90% ^{13}C and 10% ^{12}C and a simulation (b) derived from the DFT calculations at the B3YLP/cc-pVDZ level for the same enrichment values.

The observed band at 1895.5 from the rest of the isotopomers and its intensity correlates with the other proposed isotopomer bands under annealing. It is closed to the 1896.2 cm^{-1} frequency calculated for the 12-12-13-12-12-12-12-12-12-12 (c2) isotopomer. Therefore, the absorption at 1895.5 cm^{-1} is assigned to the c2 isotopomer. The calculated frequency at 1913.6 cm^{-1} corresponding to the 12-12-13-12-12-12-12-12-12-12 (c3) isotopomer matches the band located at 1913.6 cm^{-1} . Its higher intensity is the result of the overlapped bands of two

isotopomers, the double substituted 12-13-13-12-12-12 isotopomer of the $\nu_4(\sigma_u)$ mode of C_6 ,⁸⁸ and our proposed 12-12-13-12-12-12-12-12-12(c3) isotopomer. The band at 1906.7 cm^{-1} has a band growing in under annealing on its shoulder at the high frequency side, which is visible in Figure 25 (a). It shows a characteristically broad line profile like the rest of the previously assigned isotopomers. There is a peak at 1904.9 cm^{-1} that may compete, for assignment to the c4 isotopomer, since it is also, close to the calculated frequency at 1905.9 cm^{-1} for the 12-12-12-13-12-12-12-12-12 (c4) isotopomer; however, the annealed spectrum [see Fig. 25 (a)] does not exhibit the sharpening and increase in intensity shown by the rest of the already selected c1, c2 and c3 bands. Therefore the band at 1906.7 cm^{-1} will be assigned to the 12-12-12-13-12-12-12-12-12 (c4) isotopomer. The observed band at 1909.8 cm^{-1} although somewhat less sharp than the c4, c5, c2 and c1 isotopomer bands, already selected it emerges after annealing as it can be seen in Fig. 25 (b) and correlates well with the intensity and width of the c4, c5, c2 and c1 isotopomer bands, its frequency matches well with the calculated frequency of 1910.3 cm^{-1} for the 12-12-12-12-13-12-12-12-12 (c5) isotopomer. Therefore the band 1910.3 cm^{-1} will be assigned c5 isotopomer.

We now have a complete shift-set composed of the frequencies $1912.1(\text{c1})$, $1895.5(\text{c2})$, $1913.6(\text{c4})$ and $1909.8\text{ cm}^{-1}(\text{c5})$ called SSC12. At this point, is necessary to mention that in spite of all our experimental considerations by which, we obtained the set of isotopomers, we formed alternative sets of shifts using the frequencies 1911.1 , 1908.6 and 1904.9 cm^{-1} , for testing with the DPM. However, as will be shown none of the alternative sets of shifts are sustained when the mirror single ^{13}C -substituted $^{13}\text{C}^{12}\text{C}_9$ isotopomers are considered (yet to be shown).

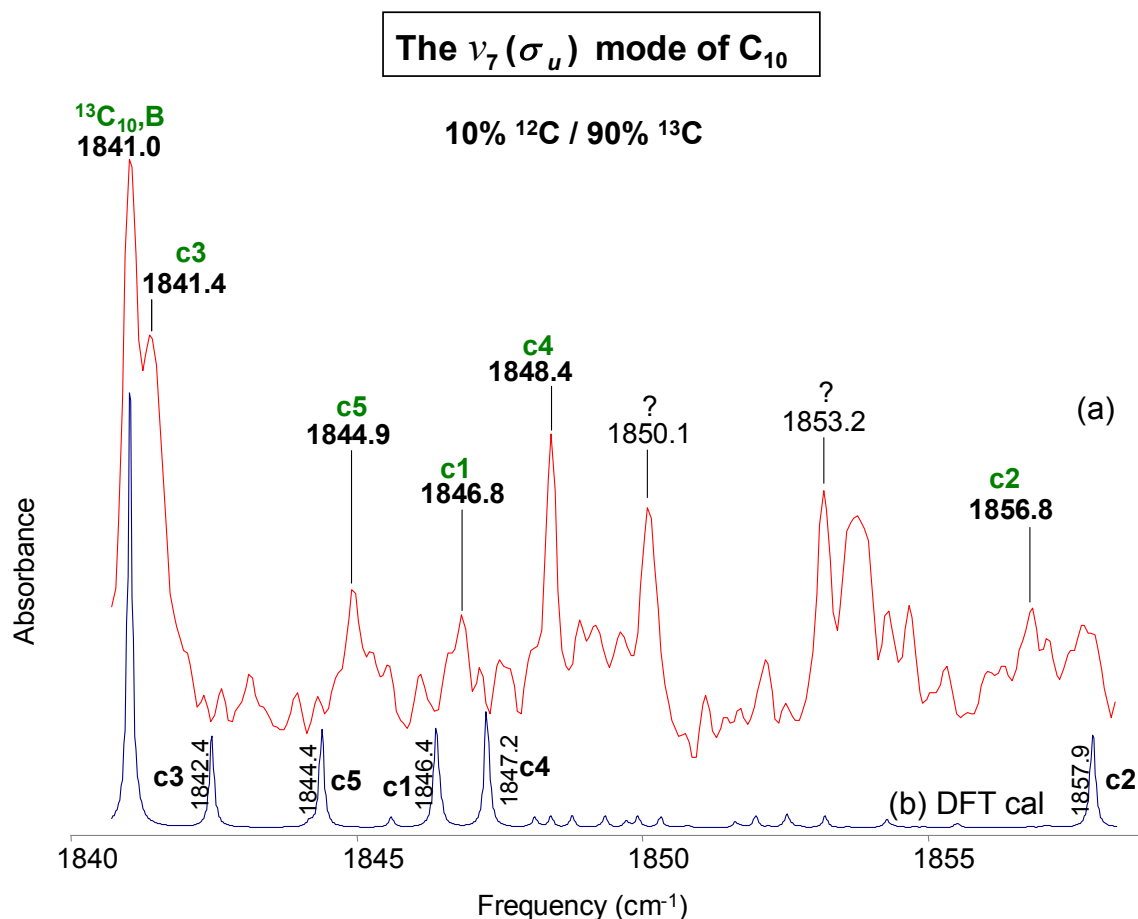


Fig. 26. Comparison of the FTIR spectra of the $\nu_7(\sigma_u)$ mode of the linear C_{10} and its isotopic shifts with (a) 90% ^{13}C and 10% ^{12}C mixture and (b) a DFT calculations at the B3YLP/cc-pVDZ level simulation using the same enrichment.

Figure 26(a), shows the mirror spectrum corresponding to the single ^{12}C substitutions in $^{13}C_{10}$ for the $\nu_7(\sigma_u)$ mode produced by the evaporation of a rod with a 90% of ^{13}C and 10% ^{12}C mixture. The frequency of the absorption at 1841.0 cm^{-1} , which is a factor $\sim \sqrt{12/13}$ of the 1915.7 cm^{-1} frequency, is identified as belonging to the fully ^{13}C -substituted isotopomer $^{13}C_{10}$. In Fig. 26 (a) we can see a provisional set of shifts that we call SSC13 with the frequencies for the isotopomers at $1846.8(\text{c1})$, $1856.8(\text{c2})$, $1841.4(\text{c3})$, and 1844.9 cm^{-1} (c5). The measured frequencies are compared with the results of the scaled DFT calculation in Table VIII.

TABLE VIII. Comparison of observed and predicted DFT (B3LYP/cc-pVDZ) frequencies for single ^{13}C -substituted isotopomers of $^{12}\text{C}_{10}$, and single ^{12}C -substituted isotopomers of $^{13}\text{C}_{10}$, for the ν_7 mode.

Isotopomer	ν_{obs}	B3LYP/cc-pVDZ		$\Delta\nu$ $\nu_{\text{obs}} - \nu_{\text{scaled}}$
		ν	ν_{scaled}	
12-12-12-12-12...(A)	1915.7	1997.4	1915.7 ¹	0.0
13-12-12-12-12...(c1)	1912.1	1992.5	1911.0	1.1
12-13-12-12-12...(c2)	1895.5	1977.0	1896.1	-0.6
12-12-13-12-12...(c3)	Overlapped ²	1995.1	1913.5	----
12-12-12-13-12...(c4)	1906.7	1987.1	1905.8	0.9
12-12-12-12-13...(c5)	1909.8	1991.7	1910.2	-0.4
13-13-13-13-13...(B)	1841.0	1918.8	1841.0 ³	0.0
12-13-13-13-13...(c1)	1846.8	1924.4	1846.4	0.4
13-12-13-13-13...(c2)	1856.8	1936.4	1857.9	-1.1
13-13-12-13-13...(c3)	Overlapped ⁴	1920.3	1842.4	----
13-13-13-12-13...(c4)	1848.4	1925.3	1847.2	1.2
13-13-13-13-12...(c5)	1844.9	1922.3	1844.4	0.5

¹Scaling factor $\nu_{\text{obs}}/\nu \sim 0.95945$

²Overlapped by the 13-12-13-12-12-12 isotopomer of the $\nu_4(\sigma_u)$ mode of C_6 at 1913.6 cm^{-1}

³Scaling factor $\nu_{\text{obs}}/\nu \sim 0.95915$

⁴Overlapped by the unknown band at 1840.0 cm^{-1}

The top half of Table VIII shows the selection *SSC12* for the single ^{13}C -substituted $^{13}\text{C}^{12}\text{C}_6$ isotopomers, and the bottom half, the shift-set *SSC13*, for the single ^{12}C -substituted $^{12}\text{C}^{13}\text{C}_6$ isotopomers, that are necessary for tested with the DPM. In Table VIII, the first column lists the isotopomers under consideration for the ν_6 mode of C_{10} with their abbreviated isotopomer label in parentheses. In the third column (labeled ν) are the predicted frequencies for the single ^{13}C -substituted $^{13}\text{C}^{12}\text{C}_{n-1}$ isotopomers, scaled by a factor of ~ 0.95945 obtained by taking the ratio of the observed main frequency 1915.7 cm^{-1} with the corresponding DFT calculated main frequency of 1997.4 cm^{-1} of the ν_7 mode of $^{12}\text{C}_{10}$. By similarly taking the ratio

of the predicted and observed frequencies for the ν_7 mode of $^{13}\text{C}_{10}$ we obtain a scaling factor of ~ 0.95915 for the ^{12}C substituted $^{12}\text{C}^{13}\text{C}_9$ isotopomers.

We will be considering the absorptions to the high frequency side of the vibrational fundamental at $1841.0\text{ cm}^{-1}(\text{B})$, for the identification of the five single ^{12}C substituted $^{12}\text{C}^{13}\text{C}_{10}$ isotopomers in the spectra shown in Fig. 27(a) annealed at 10 K and (b) annealed at 38 K, respectively, which were produced by the evaporation of a carbon mixture of 10% ^{12}C / 90% ^{13}C .

In selecting a set of shifts it is necessary to examine Fig. 27(a) and (b), showing spectra after annealing at 10 and 38 K, respectively and to note the correlation between the intensity behavior of our selected isotopomer bands and the selected main band at $1841.0\text{ (B) cm}^{-1}$. It is clear that the unidentified bands at 1850.1 , 1853.2 and 1853.7 cm^{-1} are not related to one another or to the main band, nor to the preliminary shift-set selection. SSC13 shown in Fig. 27.

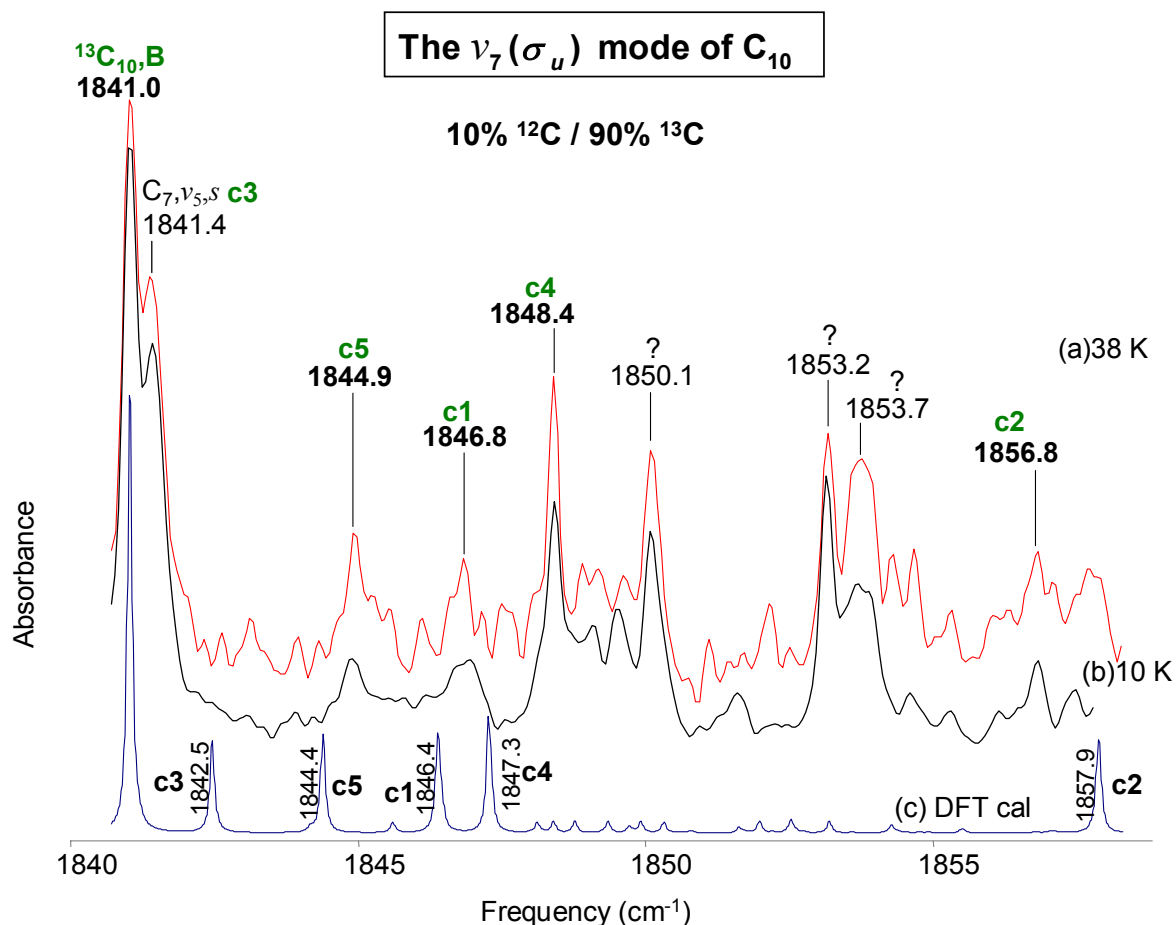


Fig. 27. Comparison of observed FTIR annealed spectra (a) 38 K and (b) 10 K of the $\nu_6(\sigma_u)$ mode of linear C_{10} and its single ^{12}C isotopic shifts using 90% ^{13}C and 10% ^{12}C carbon enrichments and (c) a DFT calculations at the B3YLP/cc-pVDZ simulation using the same enrichment.

The interaction of the $\nu_6(\sigma_g)$ mode with the non infrared active $\nu_2(\sigma_g)$ mode mentioned before in this chapter (see Table VII), induces a repulsion between the energy levels of the corresponding isotopomers. Similar to the mirrored counterpart of the $\nu_6(\sigma_u)$ mode still to be discussed, four of the isotopomers are confined within a frequency region (1840.0 - 1849.0 cm^{-1}), reflecting an analogous behavior characteristic for the C_{10} molecule.

The calculated bands at 1846.4 and 1847.3 cm^{-1} corresponding to the 12-13-13-13-13-13-13-13-13-13(c1) and 13-13-13-12-13-13-13-13-13-13(c4) isotopomers respectively, are close enough to the observed band at 1846.8 cm^{-1} so that both could potentially be assigned to it. The 1846.8 cm^{-1} band in Fig. 27(b) appears broad before annealing, however, after annealing [see Fig. 27(a)] it becomes narrow to result from two overlapping isotopomer bands. The possibility that the 1846.8 cm^{-1} band contains both the (c1) and (c4) was tested by forming an alternative shift set *SSC13'* and testing it along with the *SSC13* set with the DPM. It was found as a result, that the band at 1846.8 cm^{-1} should be assigned to the 12-13-13-13-3-13-13-13-13-13(c1) isotopomer. The calculated frequency 1847.3 cm^{-1} corresponding to the 13-13-13-12-13-13-13-13-13-13(c4) isotopomer must underlie a prominent, unidentified absorption [see Fig. 27(a) and (b)]. An alternative band at 1850.1 cm^{-1} is too far away from the predicted 1847.3 cm^{-1} frequency to be considered. Therefore, the band at 1848.4 cm^{-1} will be assigned to the (c4) isotopomer.

The calculated band at 1857.9 cm^{-1} for the 13-12-13-13-13-13-13-13-13-13(c2) isotopomer seems to be well isolated and close to the observed band at 1856.8 cm^{-1} which exhibits similar behavior to the c1 isotopomer under annealing, showing that they are related. Thus, the band at 1856.8 cm^{-1} will be assigned to the (c2) isotopomer. The shift for the 13-13-12-13-13-13-13-13-13-13(c3) isotopomer calculated with frequency at 1842.4 cm^{-1} probably contributes to the 1841.4 cm^{-1} absorption which is too intense compared to the c1 and c2 isotopomer bands to result exclusively from the (c2) isotopomer for $\nu_5(\sigma_u)$ mode of linear C_7 ⁸⁹ already assigned at this frequency [see Fig. 27 (a)]. The observed band at 1844.9 cm^{-1} is more or less isolated from the rest of the isotopomers and behaves like the c1 and c2 isotopomer bands under annealing [see Fig. 27(a)]. It is close to the calculated band at 1844.4 cm^{-1} corresponding

to the 13-13-13-13-15-13-13-13-13-13(c5) isotopomer, hence, it will be assigned to the c5 isotopomer. The final assignments for 1846.8 (c1), 1856.8 (c2), 1841.4 (c3), 1848.4 (c4) and 1844.9 cm^{-1} (c5) for the single ^{12}C -substituted ($^{12}\text{C}^{13}\text{C}_9$) isotopomers of the $\nu_7(\sigma_u)$ mode of $^{13}\text{C}_{10}$ are shown in Fig. 27 and listed in Table VIII.

5.4 Assignment of isotopomers for the $\nu_6(\sigma_u)$ mode of C_{10}

Maier⁹⁰ and co-workers using the technique of mass-selection reported the $\nu_7(\sigma_u)$ mode at 2074.5 cm^{-1} but no isotopic information was provided to support the assignment. The isotopic shifts of the $\nu_7(\sigma_u)=2196.6 \text{ cm}^{-1}$ can be affected by coupling with the nearby $\nu_1(\sigma_g)=2162.4 \text{ cm}^{-1}$ modes of C_{10} (see Table VIII) only 34.2 cm^{-1} away. The closer the two modes in frequency, the stronger the interaction will be. Under these circumstances, it may be possible to see some of the single ^{12}C or ^{13}C -substituted isotopic shifts for the normally IR-forbidden $\nu_1(\sigma_g)$ mode when the symmetry is broken by the substitution of a single ^{13}C atom in the C_{10} chain. In addition, the spectra should exhibit evidence of significant perturbations and unpredictable isotopic shift behavior, which may be difficult to analyze.

The $\nu_6(\sigma_u)$ mode of linear C_{10} requires a more detailed analysis. In Fig. 28 we present the DFT-calculated spectrum for the $\nu_6(\sigma_u)$ mode of C_{10} . We can see a prominent band at 2074.2 cm^{-1} (A) together with the single ^{13}C substituted $^{13}\text{C}^{12}\text{C}_9$ isotopomers (c1, c2, c3, c4 and c5) appearing to the low frequency side. At $\sim 34.1 \text{ cm}^{-1}$ to lower frequency from the main band at 2074.2 cm^{-1} (A) some of the single ^{13}C substituted $^{13}\text{C}^{12}\text{C}_9$ isotopomers bands that belong to the $\nu_1(\sigma_g)$ mode are seen (see Fig. 28).

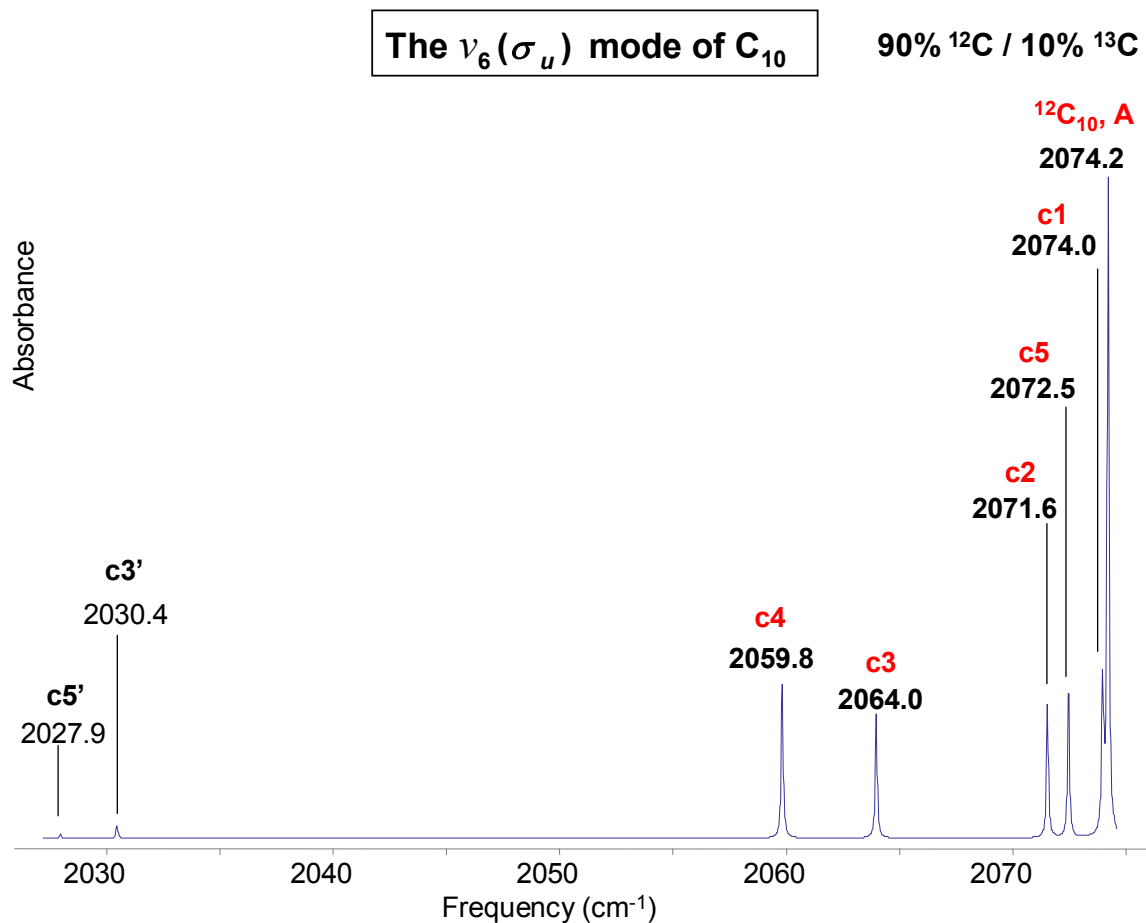


Fig. 28. DFT calculation at the B3YLP/cc-pVDZ level for the enrichment values 90% ^{12}C and 10% ^{13}C of the $\nu_6(\sigma_u)$ mode of the linear C_{10} and its single ^{13}C isotopic shifts. To show the existence of the c3' and c5' not easily seeing

In order to make the single ^{13}C substituted $^{13}C^{12}C_9$ isotopomers corresponding to the $\nu_1(\sigma_g)$ mode fully visible it is necessary to increase the vertical gain of the calculated spectrum by an arbitrary factor (see Fig. 29).

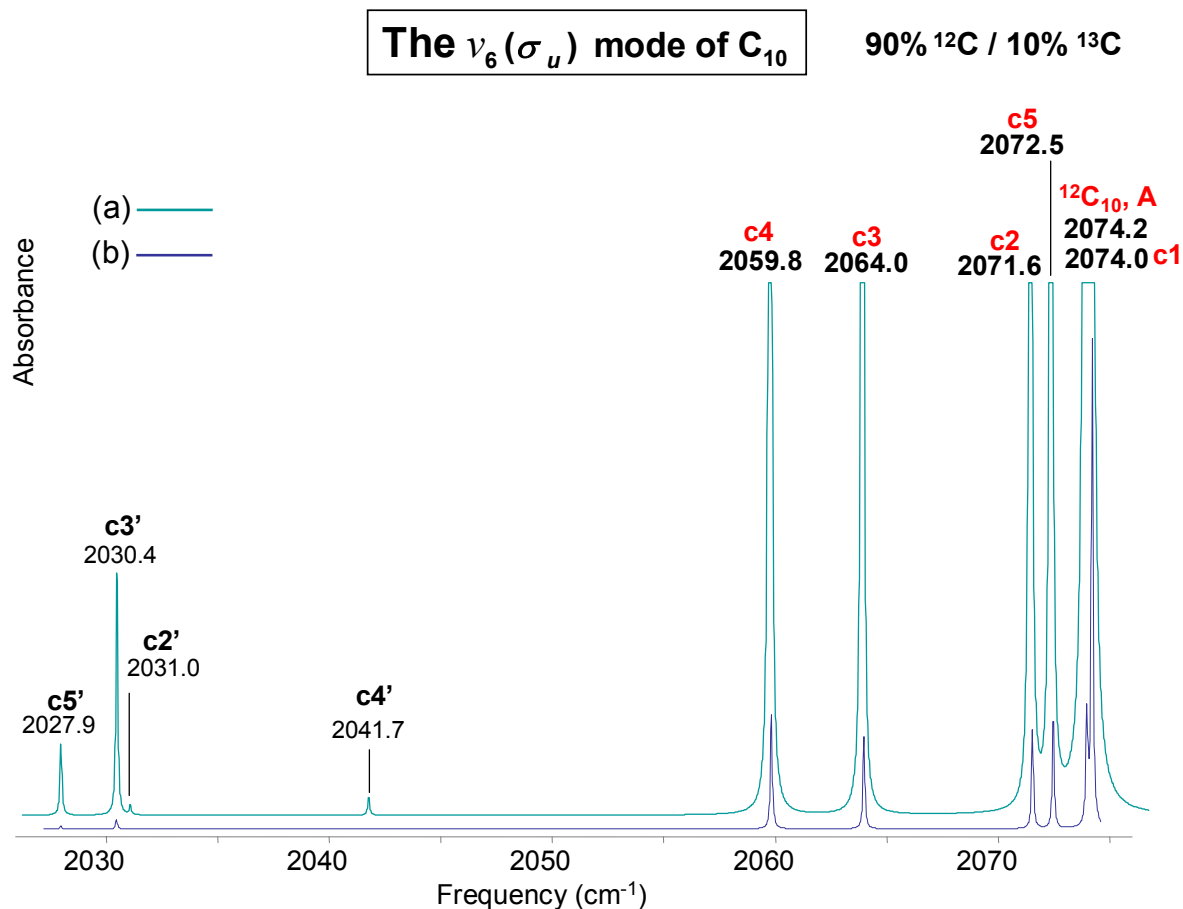


Fig. 29. Two spectrums (a) (increase vertical gain) and (b) of the same DFT calculation at the B3YLP/cc-pVDZ level for the enrichment values 90% ^{12}C and 10% ^{13}C of the $\nu_6(\sigma_u)$ mode of the linear C_{10} and its single ^{13}C isotopic shifts. To show the existence of the $c2'$, $c3'$, $c4'$ and $c5'$ not easily seeing.

Of course, we expect to have the same situation in the mirrored spectrum for the $\nu_1(\sigma_g)$ mode. First of all, in Fig. 30 all the single ^{13}C substituted $^{13}C^{12}C_9$ isotopomers ($c1$, $c2$, $c3$, $c4$, $c5$) corresponding to the $\nu_6(\sigma_u)$ mode appearing to the high frequency side of the main band at 1991.7 cm^{-1} can be seen. Second, we can see also, to the low frequency side of the main band some of the ^{13}C substituted $^{13}C^{12}C_9$ isotopomer bands ($c2'$, $c3'$, $c4'$ and $c5'$) corresponding to

$\nu_1(\sigma_g)$ mode that are now IR allowed because of the change in symmetry from σ_g to σ_u on ^{13}C substitution. In order to see the single ^{12}C substituted $^{12}\text{C}^{13}\text{C}_9$ isotopomers corresponding to the $\nu_1(\sigma_g)$ mode the vertical gain of its calculated spectrum (see Fig. 30) has been increased.

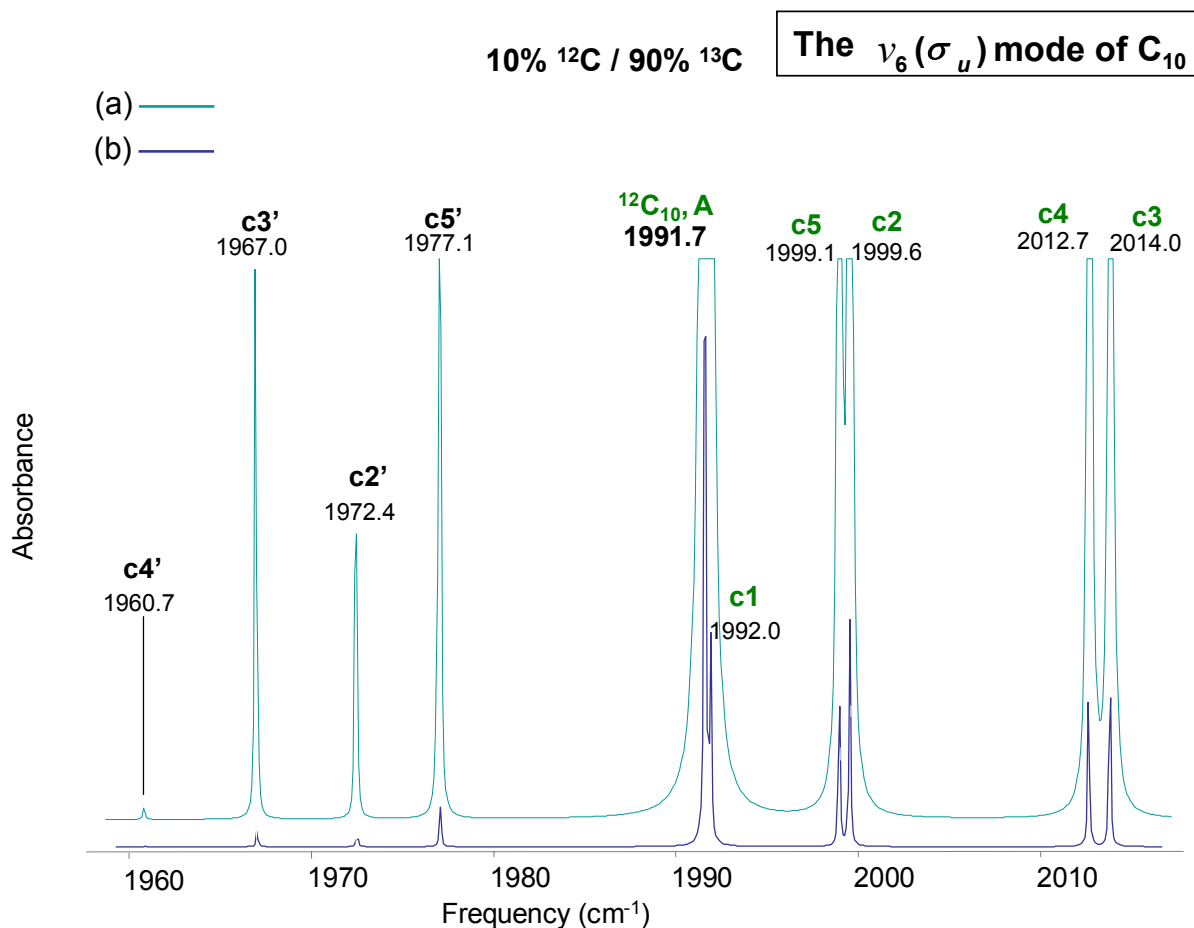


Fig. 30. Two spectrums (a) (increase vertical gain) and (b) of the same DFT calculation at the B3YLP/cc-pVDZ level for the enrichment values 90% ^{12}C and 10% ^{13}C of the $\nu_6(\sigma_u)$ mode of the linear C_{10} and its single ^{13}C isotopic shifts. To show the existence of the $\text{c2}'$, $\text{c3}'$, $\text{c4}'$ and $\text{c5}'$ not easily seeing.

After this theoretical analysis the question arises: Is it possible to observe these isotopomer absorptions? To answer this question, we will start by examining an observed spectrum in the vicinity of the $\nu_6(\sigma_u)$ mode of linear C_{10} (see Fig. 31).

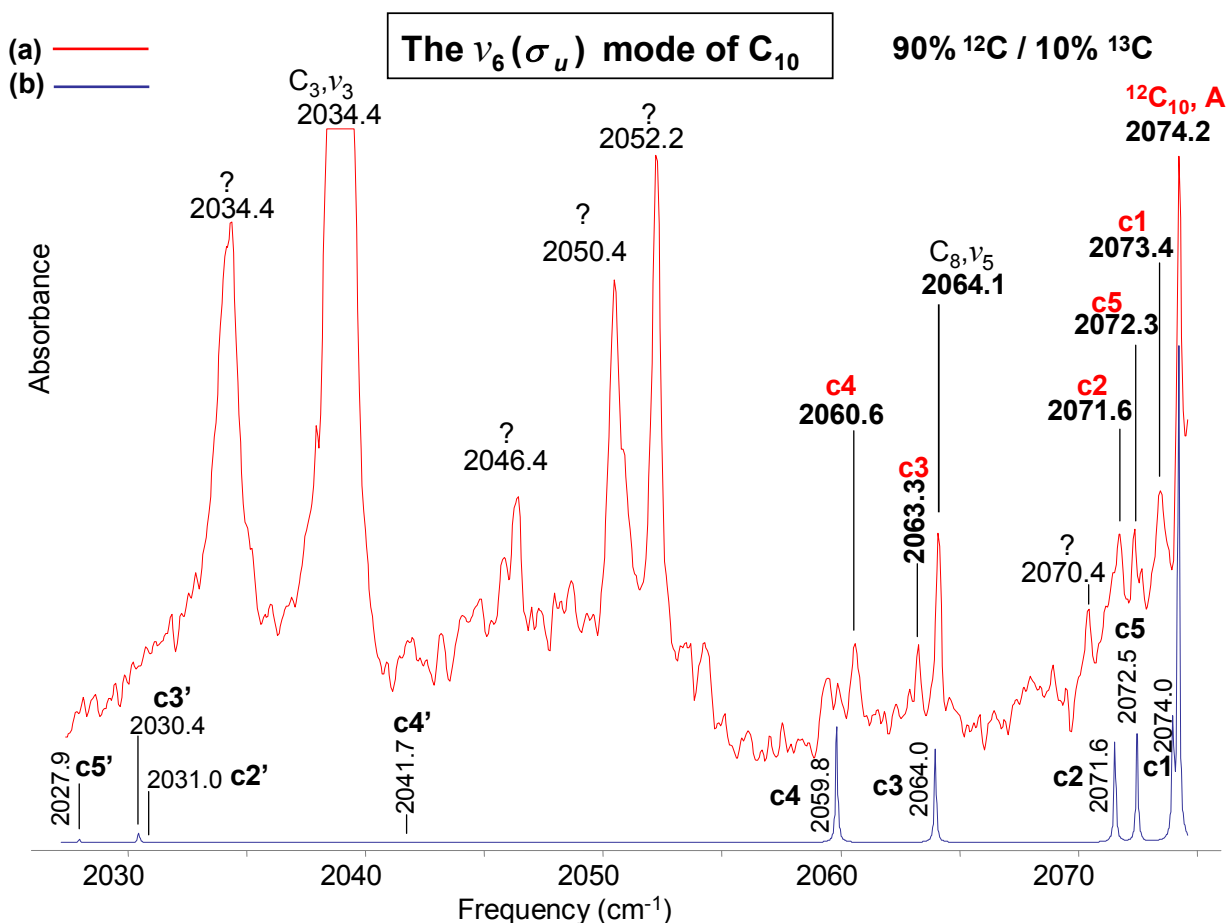


Fig. 31. Comparison of the observed FTIR spectrum of the $\nu_6(\sigma_u)$ mode of the linear C_{10} and its single ^{12}C and ^{13}C isotopic shifts with carbon enrichments (a) 90% ^{13}C and 10% ^{12}C and a simulation (b) derived from the DFT calculations at the B3YLP/cc-pVDZ level for the same enrichment values. The lower case letter c in the labels c1, c2..., indicates a single ^{12}C or ^{13}C carbon isotope and the number 1, 2... stands for the location (starting from left to right) where the carbon isotope is positioned. c1, c2... belong to the $\nu_6(\sigma_u)$ mode of the linear $^{13}\text{C}_{10}$ and c1', c2'... belong to the infrared active shifts of the $\nu_1(\sigma_g)$ mode of the linear $^{12}\text{C}_{10}$.

We can see from Fig. 31 that, if there are any observed bands that might be assigned to the c2', c3', c4' and c5' isotopomers, would have such a low intensity that they would be at the level of the noise, rendering them unobservable. This situation will lead us to consider whether the DPM can be applied to analyze the now IR-allowed isotopomers or not. Let us recall that in order to apply the DPM it is of fundamental importance to have both observed isotopic shift-sets, corresponding to a vibrational fundamental, including the observed frequency of the main bands of a particular molecule. In the case of the non-infrared active modes of a molecule the main band will remain unobservable upon isotopic substitution, therefore is not possible to apply the DPM.

Nevertheless, the single ^{13}C -substituted $^{13}\text{C}^{12}\text{C}_9$ isotopomers for the $\nu_2(\sigma_g)$ cannot be observed, it is possible that in the mirrored side some of the single ^{12}C -substituted $^{12}\text{C}^{13}\text{C}_9$ isotopomers of the $\nu_2(\sigma_g)$ can be observed; for example, in Fig. 31(b) we can see that it is not possible to observe a band candidate corresponding to the calculated frequency 2027.9 cm^{-1} (c5') although, as we will see later in this chapter, in the mirror spectrum a frequency is calculated at 1977.1 cm^{-1} (c5') for which a possible candidate has been observed. Conclusively the now IR-allowed cannot be eliminated nor ignored, however, in this particular molecule most of the not IR-allowed shifts cannot be observed and they will not be taken in to consideration. Hence, in order to continue with the identification of the main $\nu_6(\sigma_u)$ band proposed at 2074.2 cm^{-1} and its single ^{13}C -substituted $^{13}\text{C}^{12}\text{C}_9$ isotopomers, we will be considering the frequency interval from 2058.0 to 2075.0 cm^{-1} in Fig. 31(a), where the infrared active shifts for $\nu_6(\sigma_u)$ are expected to lie. A preliminary selection of shifts named SSC12, 2073.4 (c1), 2071.6 (c2), 2063.3(c3), 2060.6(c4) and 2072.3 cm^{-1} (c5) was made and is shown in Fig. 32 for more clarity.

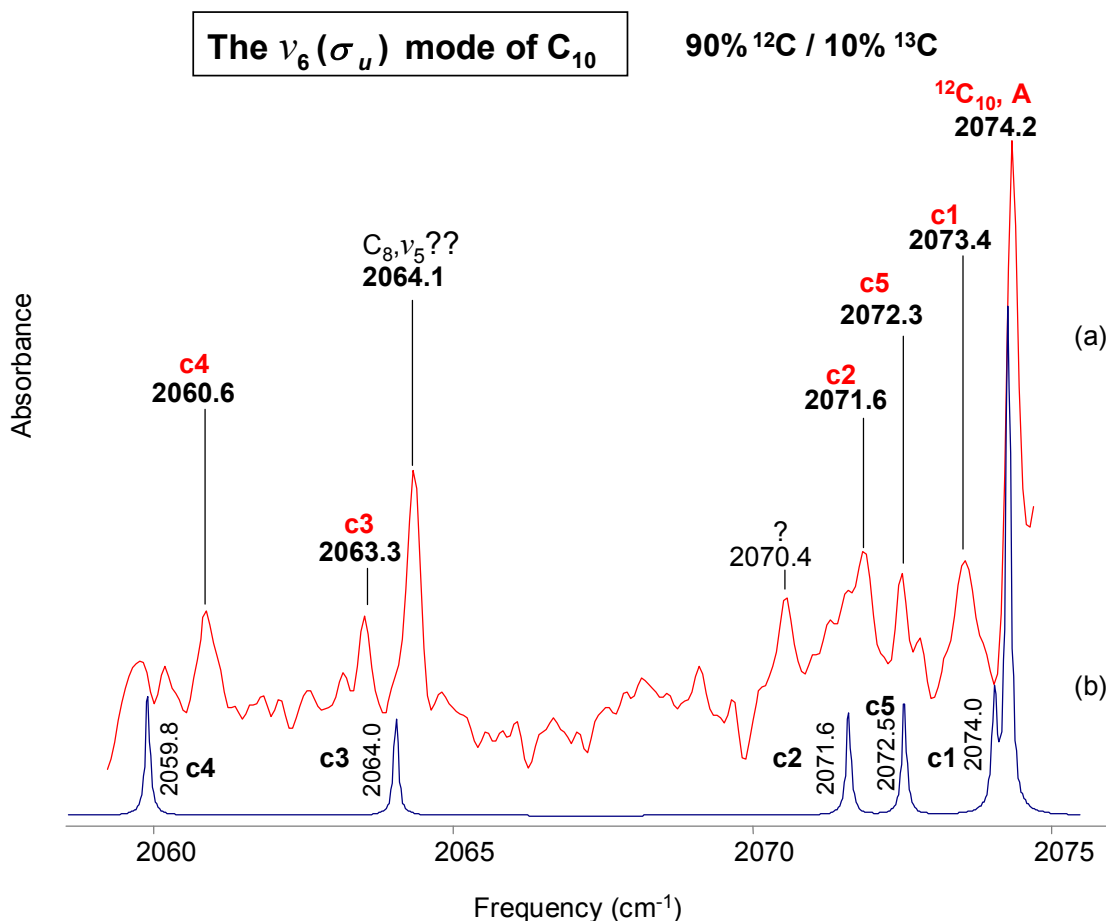


Fig. 32. Comparison of observed FTIR of the of the $\nu_6(\sigma_u)$ mode of the linear C_{10} and its single ^{12}C and ^{13}C isotopic shifts with carbon enrichments (a) 90% ^{13}C and 10% ^{12}C and a simulation (b) derived from the DFT calculations at the B3YLP/cc-pVDZ level for the same enrichment values.

The observed band at 2073.4 cm^{-1} seems to matches well the closest calculated frequency at 2074.0 cm^{-1} corresponding to the 13-12-12-12-12-12-12-12-12-12(c1) isotopomer, thus it will be assigned to the c1 isotopomer. The observed bands at 2070.4 and 2071.6 cm^{-1} can be candidates to match the calculated band at 2071.5 cm^{-1} for the 13-12-13-12-12-12-12-12-12-12-12(c2) isotopomer, although the 2071.6 cm^{-1} agrees closely in frequency. Complicating its possible assignment is the fact that other features are growing on the low frequency shoulder of

the 2071.6 cm^{-1} band. However, the band at 2070.4 cm^{-1} , must be dismissed, under the application of the DPM. We thus assign the band at 2071.6 cm^{-1} to the c2 isotopomer. A band is observed at 2064.1 cm^{-1} close to the 2063.9 cm^{-1} value reported by Maier *et al.*⁹¹ and listed in the compilation of Jacox⁹² as the $\nu_5(\sigma_u)$ mode of the linear C_8 . Vala *et al.*⁹³ have reported a frequency of 2071.5 cm^{-1} for the same mode. Without pass judgment on this discrepancy, we can conclude that our observed band at 2063.3 cm^{-1} is too intense to be a shift of the 2064.1 cm^{-1} band. On the other hand, it is close to the calculated band at 2064.0 corresponding to the 12-12-13-12-12-12-12-12-12(c3) isotopomer and it behaves correctly under the DPM method. The observed band at 2060.6 cm^{-1} is well separated from the other shifts and matches relatively well the calculated frequency at 2059.8 corresponding to the 12-12-12-13-12-12-12-12-12-12(c4) isotopomer. The observed band at 2072.3 cm^{-1} is really close to the calculated band 2072.5 cm^{-1} for the 1313-12-12-12-12-13-12-12-12-12(c5) isotopomer matches and is thus assigned to the c5 isotopomer. The final frequency shift-set for the infrared $\nu_6(\sigma_u)$ mode of the linear C_{10} is then 2073.4(c1), 2071.6(c2), 2063.3(c3), 2060.6(c4) and 2072.3 cm^{-1} (5) named SSC12.

A frequency of 1993.4 cm^{-1} , which is a factor $\sim \sqrt{12/13}$ of the 2074.2 cm^{-1} frequency, is the calculated for the fully ^{13}C -substituted isotopomer. In this as in many cases, the immediate frequency neighborhood of where a potential vibrational fundamental can be located is quite congested like in this case, where our 1993.4 cm^{-1} can be founded with in the interval from 1980.0 to 2098.0 cm^{-1} [see Fig. 33 (a)].

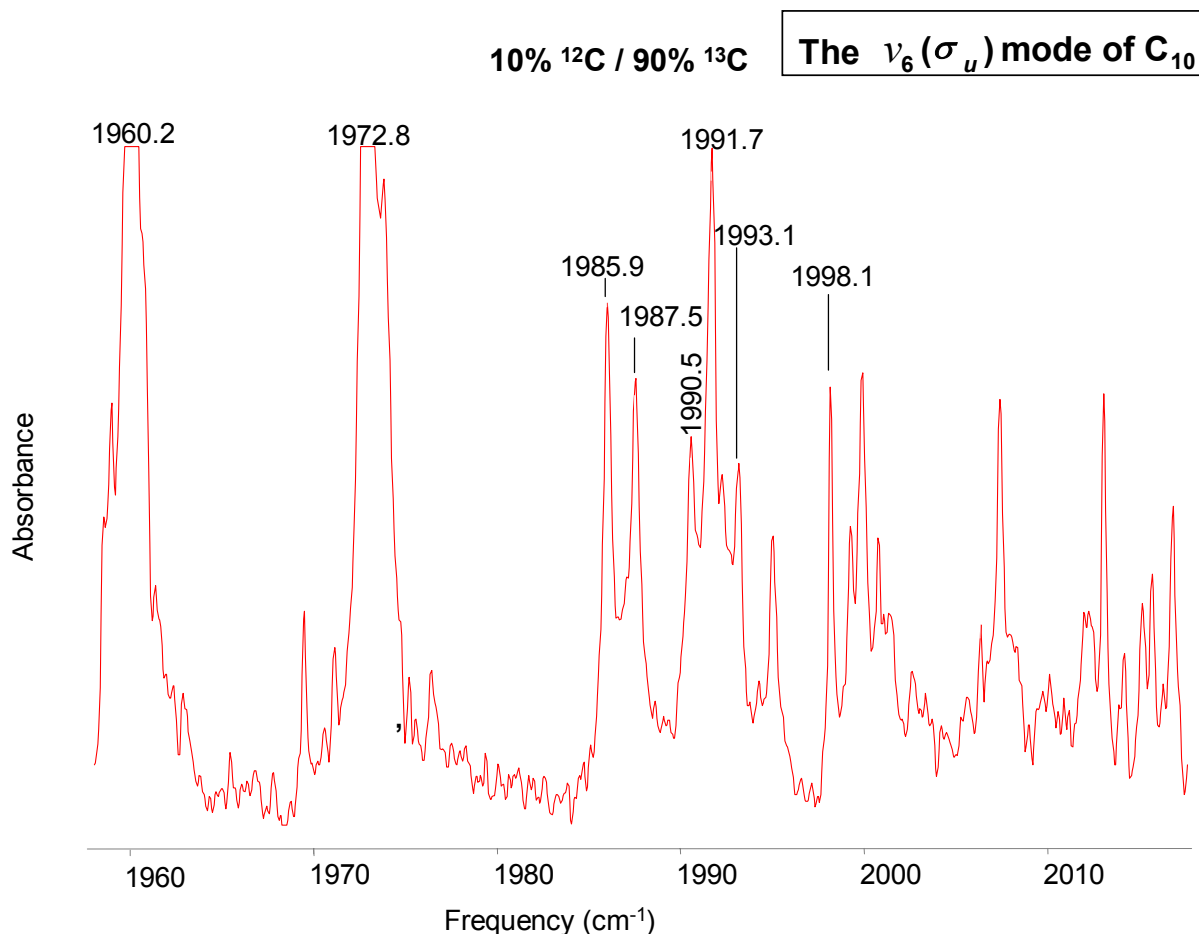


Fig. 33. FTIR spectra obtained with 90% ^{13}C and 10% ^{12}C carbon enrichment, where the $\nu_6(\sigma_u)$ mode of the linear C_{10} and its single ^{12}C -isotopic shifts suppose to lie.

As shown in Fig. 34 several absorptions have been identified as isotopomer bands of C_3 and C_9 . Of the remaining the strongest band is at 1991.7 cm^{-1} which is chosen in the present work. Previously the band at 1994.9 cm^{-1} was proposed³⁹ for assignment to the $\nu_6(\sigma_u)$ mode of $^{13}\text{C}_{10}$ but as a result of our most recent studies this band is now proposed as a shift of the $\nu_{14}(\sigma_u)$ mode of *c*- C_{10} (under current investigation by the authors of this work).

In our present work, if, we consider the 1991.7 cm^{-1} band as our candidate for the ν_6

mode of $^{13}\text{C}_{10}$ the band at 1993.1 cm^{-1} then is more likely to be one of its possible shifts (see Figure 34). Of the remaining bands in this region we suggest that the set of single ^{12}C substituted $^{12}\text{C}^{13}\text{C}_9$ isotopomers (named SSC13) comprises the bands for the IR-allowed shifts at $1993.1(\text{c}1)$, $1999.8(\text{c}2)$, $2014.1(\text{c}3)$, $2012.2(\text{c}4)$ and $1999.1\text{ cm}^{-1}(\text{c}5)$ [overlapped by the $\text{c}2$ isotopomer] and the isotopomer bands of the infrared inactive $\nu_1(\sigma_g)$ mode are at $1971.1(\text{c}2')$, $1967.7(\text{c}3')$, $1960.7(\text{c}4')$ (overlapped by the $\nu_3(\sigma_u)$ band of C_3), and $1976.3(\text{c}5')$ [see Fig. 34].

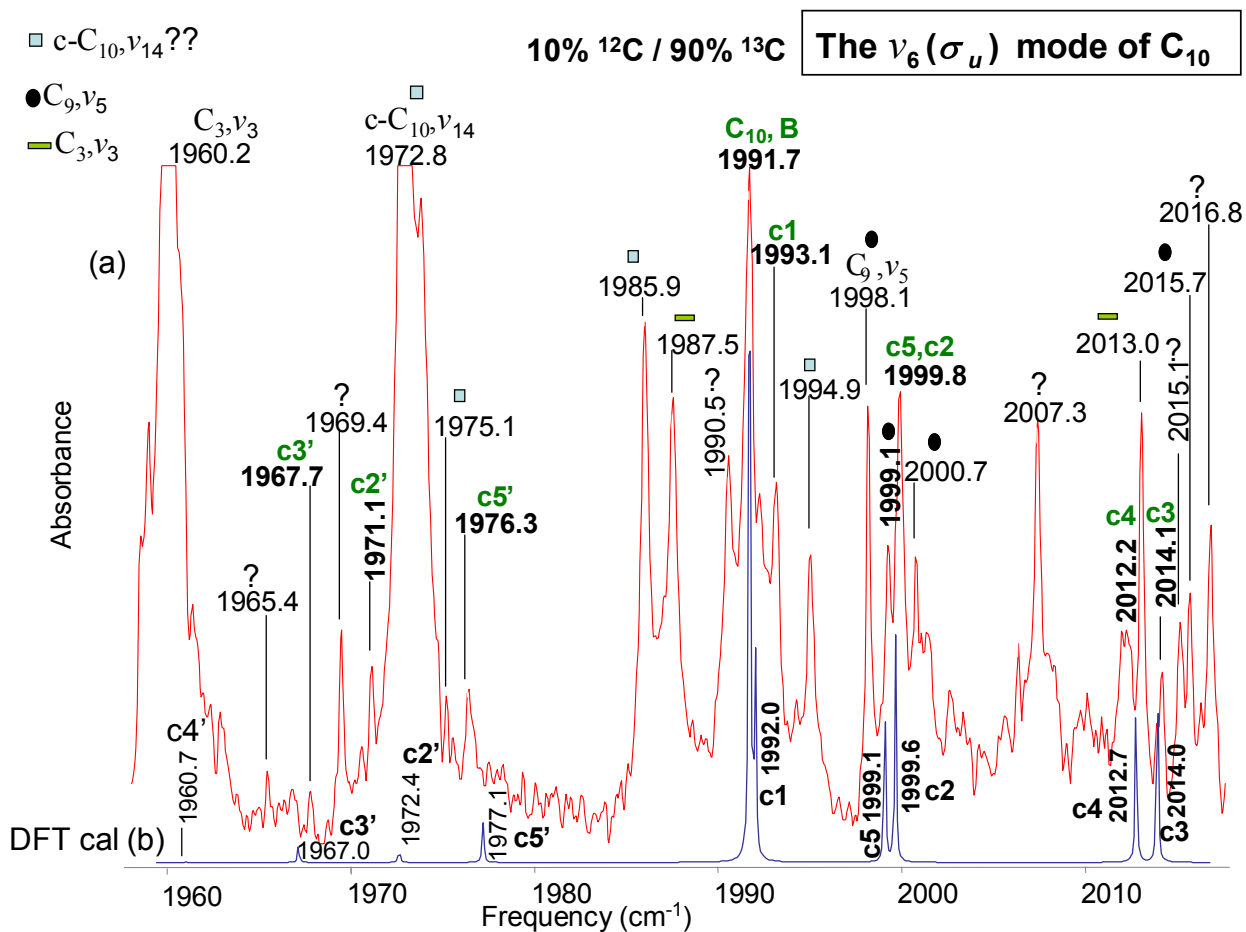


Fig. 34. Comparison of the FTIR spectra of the $\nu_6(\sigma_u)$ mode of the linear $^{13}\text{C}_{10}$ and its isotopic shifts with (a) 10% ^{12}C and 90% ^{13}C mixture and (b) a DFT calculations at the B3YLP/cc-pVDZ level simulation using the same enrichment. The label B will be used only for the vibrational fundamentals of $\nu_6(\sigma_u)$ mode of the linear $^{13}\text{C}_{10}$. The lower case letter c in the labels c1, c2..., indicates a single ^{12}C or ^{13}C carbon isotope and the number 1, 2... stands for the location (starting from left to right) where the carbon isotope is positioned. c1, c2... belong to the $\nu_6(\sigma_u)$ mode of the linear $^{13}\text{C}_{10}$ and c1', c2'... that belong to the infrared active shifts of the $\nu_1(\sigma_g)$ mode of the linear $^{13}\text{C}_{10}$. The square, dot and rectangle corresponds to the $\nu_{14}(\sigma_u)$ mode of the $c\text{-}^{13}\text{C}_{10}$, $\nu_5(\sigma_u)$ mode of the linear $^{13}\text{C}_9$ and $\nu_3(\sigma_u)$ mode of the linear $^{13}\text{C}_3$ respectively.

The complete SSC13 ^{12}C shift set for the infrared active $\nu_6(\sigma_u)$ for the inactive $\nu_1(\sigma_g)$ modes of $^{13}\text{C}_{10}$ is shown in the two sections at the bottom half of Table IX.

TABLE IX. Comparison of observed and predicted DFT (B3LYP/cc-pVDZ) frequencies for single ^{13}C -substituted isotopomers of $^{12}\text{C}_{10}$, and single ^{12}C -substituted isotopomers of $^{13}\text{C}_{10}$, for the ν_6 mode.

Isotopomer	ν_{obs}	B3LYP/cc-pVDZ		$\Delta \nu$ $\nu_{\text{obs}} - \nu_{\text{scaled}}$
		ν	ν_{scaled}	
12-12-12-12-12...(A) ¹	2074.2	2196.6	2074.2 ²	0.0
13-12-12-12-12...(c1)	2073.4	2196.4	2074.0	-0.6
12-13-12-12-12...(c2)	2071.6	2193.8	2071.6	0.0
12-12-13-12-12...(c3)	2063.3	2185.8	2064.0	-0.7
12-12-12-13-12...(c4)	2060.6	2181.4	2059.8	0.8
12-12-12-12-13...(c5)	2072.3	2194.8	2072.5	-0.2
12-13-12-12-12...(c2') ³	---	2150.8	2031.0	---
12-12-13-12-12...(c3')	---	2150.2	2030.4	---
12-12-12-13-12...(c4')	---	2162.2	2041.7	---
12-12-12-12-13...(c5')	---	2147.6	2027.9	---
13-13-13-13-13...(B) ⁴	1991.7	2110.2	1991.7 ⁵	0.0
12-13-13-13-13...(c1)	1993.1	2110.5	1992.0	1.1
13-12-13-13-13...(c2)	1999.8	2118.6	1999.6	0.2
13-13-12-13-13...(c3)	2014.1	2133.8	2014.0	0.1
13-13-13-12-13...(c4)	2012.2	2132.5	2012.7	-0.5
13-13-13-13-12...(c5)	Overlapped ⁶	2118.0	1999.1	---
13-12-13-13-13...(c2') ⁷	1971.1	2089.8	1972.4	-1.3
13-13-12-13-13...(c3')	1967.7	2084.0	1967.0	0.7
13-13-13-12-13...(c4')	Overlapped ⁸	2077.4	1960.7	---
13-13-13-13-12...(c5')	1976.3	2094.7	1977.1	-0.8

¹Single substituted ^{12}C -isotopomers for the $\nu_6(\sigma_u)$ mode of the linear $^{12}\text{C}_{10}$

²Scaling factor $\nu_{\text{obs}}/\nu \sim 0.94428$

³Single substituted ^{12}C -isotopomers for the $\nu_1(\sigma_g)$ mode of the linear $^{12}\text{C}_{10}$

⁴Single substituted ^{12}C -isotopomers for the $\nu_6(\sigma_u)$ mode of the linear $^{13}\text{C}_{10}$

⁵Scaling factor $\nu_{\text{obs}}/\nu \sim 0.94384$

⁶Overlapped by the c2 isotopomer

⁷Single substituted ^{12}C -isotopomers for the $\nu_1(\sigma_g)$ mode of the linear $^{13}\text{C}_{10}$

⁸Overlapped by the $\nu_3(\sigma_u)$ mode of the linear $^{13}\text{C}_3$

The top two sections of Table IX, have the shift-set SSC12, for the single ^{13}C -substituted $^{13}\text{C}^{12}\text{C}_9$ isotopomers of the $\nu_6(\sigma_u)$ and the $\nu_1(\sigma_g)$ modes. In this case, however, the shifts that belong to the non infrared active $\nu_1(\sigma_g)$ mode are, as demonstrated earlier, unobservable. For analysis via the DPM the SSC12 and SSC13 sets of isotopomers for the $\nu_6(\sigma_u)$ mode have been

used. Although the ^{13}C shifts belonging to infrared inactive $\nu_1(\sigma_g)$ mode of the linear $^{12}\text{C}_{10}$ are not observed, proposed ^{12}C shifts belonging to the infrared inactive $\nu_1(\sigma_g)$ mode of $^{13}\text{C}_{10}$ are reported in the 4th section of Table IX.

In Table IX the first column lists the isotopomer bands under consideration for the $\nu_6(\sigma_u)$ and $\nu_1(\sigma_g)$ modes of C_{10} with their abbreviated isotopomer labels in parentheses. The predicted frequencies for the single ^{13}C -substituted $^{13}\text{C}^{12}\text{C}_{n-1}$ isotopomers are scaled by a factor of ~ 0.94428 obtained by taking the ratio of the observed main frequency 2074.2 cm^{-1} with the corresponding DFT calculated main frequency of 2196.6 cm^{-1} of the ν_6 mode of $^{12}\text{C}_{10}$. By similarly taking the ratio of the predicted and observed frequencies for the ν_6 mode of $^{13}\text{C}_{10}$ we obtain a scaling factor of ~ 0.94384 for the ^{12}C substituted $^{12}\text{C}^{13}\text{C}_9$ isotopomers of the $\nu_6(\sigma_u)$ and $\nu_1(\sigma_g)$ modes of linear C_{10} . The remaining columns contain the same information as in similar tables in previous Chapters.

The observed band at 1993.1 cm^{-1} appears to be at 1.1 cm^{-1} away to the high frequency side of the calculated band at 1992.0 cm^{-1} for the 12-13-13-13-13-13-13-13-13(c1) isotopomer due to the “push” induced by $\nu_1(\sigma_g)$ mode. The observed band at 1999.8 cm^{-1} is close to the calculated bands at 1999.6 and 1999.1 cm^{-1} corresponding to the 13-12-13-13-13-13-13-13-13 (c2) and the 13-13-13-13-12-13-13-13-13 (c5) isotopomers.. This band is more intense than the already selected c1 isotopomer, the band at 1999.8 cm^{-1} will therefore be considered to be the result of the c2 and c5 isotopomer overlap. The two bands observed at 2012.2 and 2014.1 cm^{-1} matches well with the calculated bands at 2012.7 and 2014.0 cm^{-1} corresponding to the 13-13-13-12-13-13-13-13-13(c4) and 13-13-12-13-13-13-13-13-13(c3) isotopomers, respectively. Nevertheless, the band at 2015.1 was also considered as an alternative assignment to form a second shift-set called ‘SSC13’’ and test with the DPM. We have then the set of shifts

SSC13 formed by the 1993.1(c1), 1999.8(c2), 2014.1(c3), 2012.2(c4) and 1999.1(c5) [overlapped by the c2 isotopomer] that belong to the $\nu_6(\sigma_u)$ mode of linear $^{13}\text{C}_{10}$.

Continuing with our analysis of this molecule, we will look at the low frequency side of the 1991.7 cm^{-1} to look for evidence of the shifts from the infrared inactive $\nu_1(\sigma_g)$ mode of linear $^{13}\text{C}_{10}$ which become allowed on single ^{13}C substitution. The observed band at 1971.1 cm^{-1} is relatively away to the calculated band at 1972.5 corresponding to the c2' isotopomer as a result of the interaction of the ν_6 and ν_1 modes. For the shift predicted at 1967.0 cm^{-1} corresponding to the (c3') isotopomer there is a possible candidate at 1967.7 cm^{-1} . Even though it is well isolated, it is barely above the noise level and its assignment to the c3' isotopomer ought to be taken with caution. The calculated band at 1960.7 cm^{-1} for the c4' occurs where experimentally there is a very strong absorption by the $\nu_3(\sigma_u)$ mode of linear $^{13}\text{C}_3$. The observed band at 1976.3 cm^{-1} is close to the calculated band at 1977.1 corresponding to the c5' isotopomer which is by far the most intense of all of the isotopomers of the $\nu_1(\sigma_g)$ mode and is therefore assigned to the c5' isotopomer.

In summary, as shown in Table IX we have a complete shift-sets formed by the absorptions at 1993.1(c1), 1999.8(c2), 2014.1(c3), 2012.2(c4) and 1999.1 cm^{-1} (c5) [overlapped by the c2 isotopomer] that belong to the $\nu_6(\sigma_u)$ mode of linear $^{13}\text{C}_{10}$ with single ^{12}C substitutions at $1971.1(\text{c2}')$, $1967.7(\text{c3}')$, $1960.7(\text{c4}')$ [overlapped by the $\nu_3(\sigma_u)$ mode of linear $^{13}\text{C}_3$] and 1976.3 cm^{-1} (c5') constituting the single ^{12}C substitutions for the $\nu_1(\sigma_g)$ mode. In the cartoon presented Fig. 35 we can see the calculated spectra for the $\nu_6(\sigma_u)$ and $\nu_1(\sigma_g)$ modes of C_{10} .

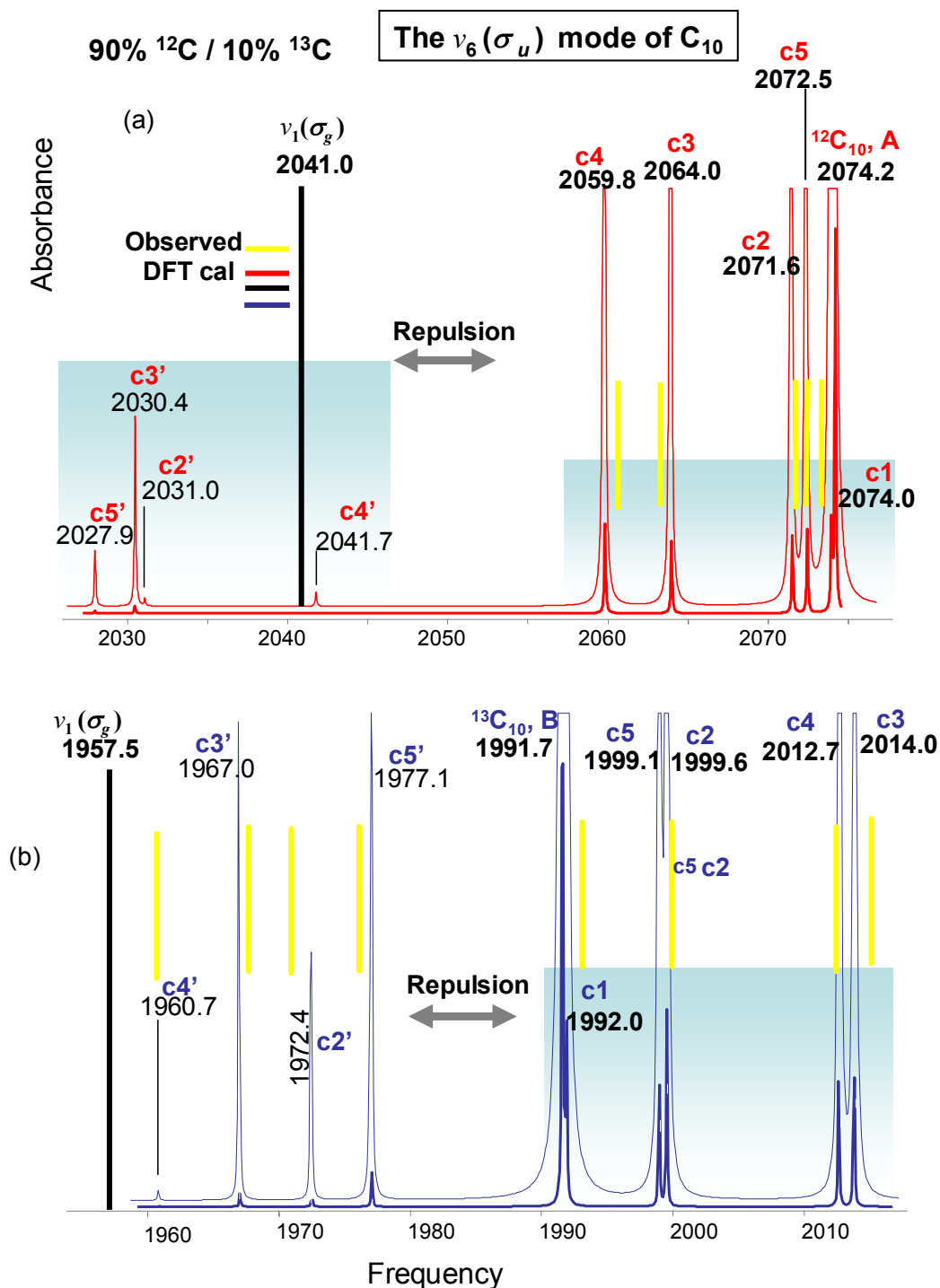


Fig. 35. Both (a)(red) and (b)(blue) are spectra derived from the DFT calculations at the B3YLP/cc-pVDZ level and its isotopic shifts with (a) 10% ^{12}C and 10% ^{13}C mixture (b) 90% ^{13}C and 10% ^{12}C . The bars in black and yellow are only for the purpose of illustrate where the interacting non infrared active $\nu_1(\sigma_g)$ mode and the observed single ^{12}C (a) and ^{13}C (b) isotopic shifts would appear. We can see also the repulsion between the shifts of the interacting ν_1 and ν_6 modes.

5.5 Conclusions

The results of Fourier transform infrared ^{13}C isotopic study have been presented for the linear $\nu_6(\sigma_u)$ and $\nu_7(\sigma_u)$ fundamentals of linear C_{10} in solid Ar at 10 K produced by the laser ablation of graphite. The analysis has relied on the much improved spectra obtained for both 90/10 and 10/90 isotopic measurements and also on taking into consideration the interaction with the $\nu_1(\sigma_g)$ and $\nu_2(\sigma_g)$ modes [by the $\nu_6(\sigma_u)$ and $\nu_7(\sigma_u)$ modes, respectively] through the use of DPM, which has been particularly useful in accurately assigning isotopic shifts. This work confirms the assignment of the vibrational fundamentals $\nu_6(\sigma_u)=2074.2\text{ cm}^{-1}$ and $\nu_7(\sigma_u)=1915.7\text{ cm}^{-1}$. These assignments are important in the analysis of the vibrational spectrum of C_{10} and also provide us with a useful insight on molecules for which interaction with a nearby infrared inactive mode results in extra isotopomer bands.

CHAPTER VI

FTIR SPECTROSCOPIC STUDY OF THE $\nu_7(\sigma_u)$ AND $\nu_8(\sigma_u)$, AND $\nu_9(\sigma_u)$ MODES OF LINEAR C_{11}

6.1 Introduction

One of the most complicated molecules encountered so far in our isotopic studies of large linear C_n species ($n \geq 6$) is the linear C_{11} carbon molecule. It has been a challenge due to the complexity of some of its vibrational fundamentals. Vala *et al.*⁹⁴ using infrared spectroscopy of matrix-isolated carbon clusters in Ar proposed assignments for the $\nu_7(\sigma_u)=1945.7\text{cm}^{-1}$ and $\nu_8(\sigma_u)=1856.6\text{ cm}^{-1}$ modes of C_{11} , but no isotopic information was reported to support these assignments. New experimental data incorporating the extensive isotopic shift data that we have obtained, has allowed us to continue with the analysis of these vibrational modes by applying the experimental technique of the mirror isotopic shift spectra, combined with theoretical analysis using DFT and the *deperturbation method* (DPM) theoretical approach described in previous chapters. In addition we will present new information on the $\nu_9(\sigma_u)=1360.0\text{ cm}^{-1}$ mode of linear C_{11} .

6.2 Results and discussion

Let us start with the $\nu_7(\sigma_u)$ mode of linear C_{11} which we consider a very good example to show the action of the coupling effects between nearby modes and the inherent experimental difficulties that underlie the studies of long carbon molecules. The $\nu_7(\sigma_u)$ vibration has a singular experimental behavior; it is the most intense mode of C_{11} and it has on ^{13}C isotopic substitution, a very strong interaction with the $\nu_2(\sigma_g)$ mode located at 12.2 cm^{-1} to the low frequency side (see Table X). This is the smallest difference between two interacting modes so far found (12.2 cm^{-1}). It results in a strong coupling and a problematical isotopic shift analysis, which makes the identification of the vibrational mode using isotopic shift analysis very difficult. In spite of this possibly problematic behavior, it is clear now (see CHAPTERS III, IV and V), that a complete isotopic characterization through an isotopic analysis via the combination of experimental measurements and theoretical calculations (DFT, DPM) may be complicated, but possible.

TABLE X. DFT B3LYP/cc-pVDZ predicted vibrational frequencies and band intensities for (ℓ -C₁₁)

Vibrational mode	Frequency (cm ⁻¹)	Infrared intensity (km/mol)
$\nu_1(\sigma_g)$	2275.7	0.0
$\nu_2(\sigma_g)$	2113.9	0.0
$\nu_3(\sigma_g)$	1709.7	0.0
$\nu_4(\sigma_g)$	1084.6	0.0
$\nu_5(\sigma_g)$	381.9	0.0
$\nu_6(\sigma_u)$	2238.4	209.7
$\nu_7(\sigma_u)$	2126.1	15161.5
$\nu_8(\sigma_u)$	1946.8	2469.8
$\nu_9(\sigma_u)$	1404.4	128.3
$\nu_{10}(\sigma_u)$	744.8	2.9
$\nu_{11}(\pi_g)$	686.9	(0.0)2
$\nu_{12}(\pi_g)$	490.6	(0.0)2
$\nu_{13}(\pi_g)$	247.5	(0.0)2
$\nu_{14}(\pi_g)$	91.3	(0.0)2
$\nu_{15}(\pi_u)$	780.3	(8.2)2
$\nu_{16}(\pi_u)$	583.2	(0.2)2
$\nu_{17}(\pi_u)$	310.2	(3.6)2
$\nu_{18}(\pi_u)$	166.3	(8.7)2
$\nu_{19}(\pi_u)$	134.8	(5.3)2

Simulated spectra from DFT calculations at the B3LYP/cc-pVDZ level using 90% ¹²C and 10% ¹³C (a) and 90% ¹³C and 10% ¹²C (b) mixture for the coupled $\nu_7(\sigma_u)$ and $\nu_2(\sigma_g)$ modes of linear ¹²C₁₁ and ¹³C₁₁, are shown in Fig. 36.

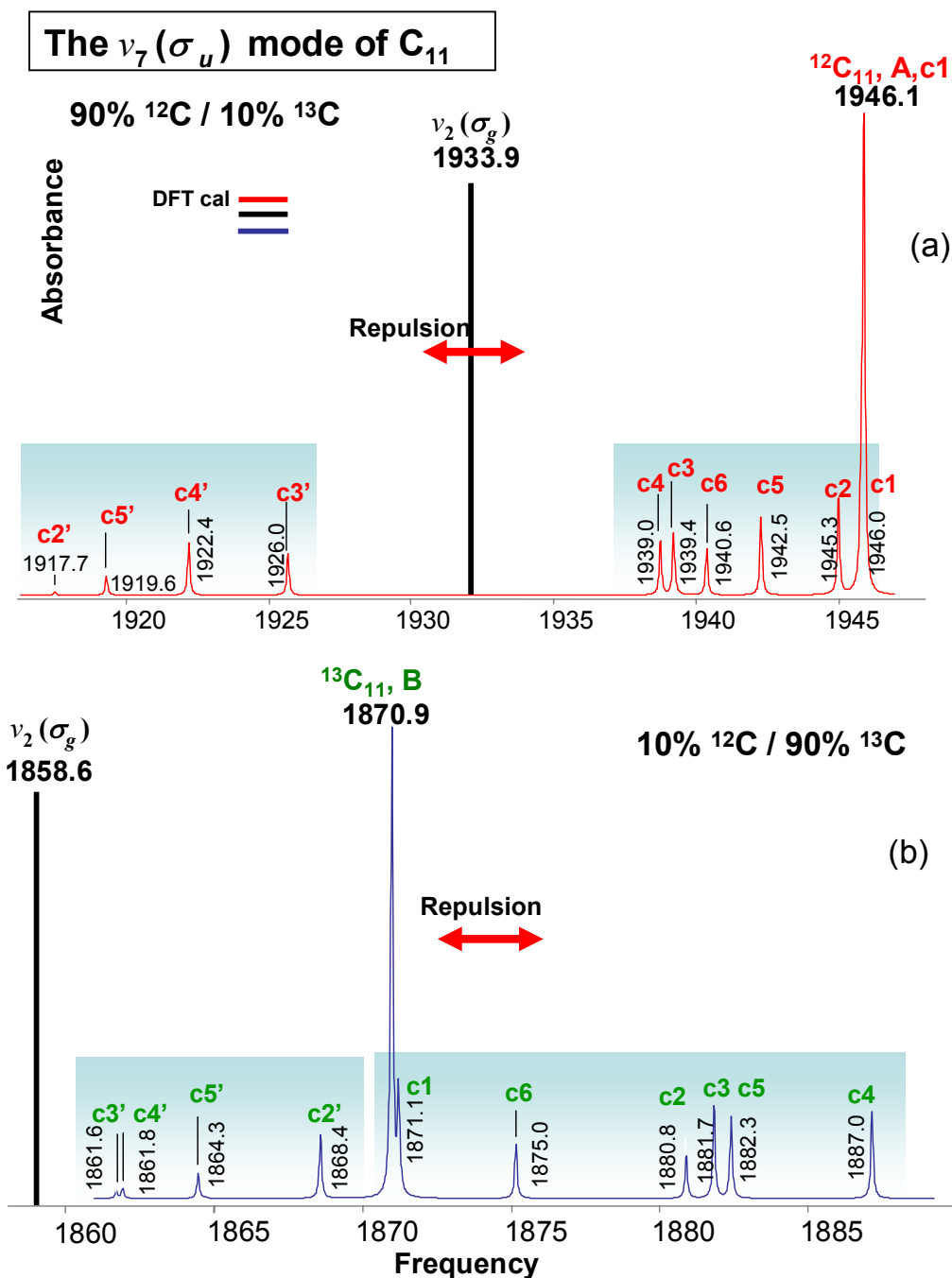


Fig. 36. Both (a)(red) and (b)(blue) are spectra derived from the DFT calculations at the B3YLP/cc-pVDZ level and its isotopic shifts with (a) 10% ^{12}C and 90% ^{13}C mixture (b) 90% ^{13}C and 10% ^{12}C . The bar in black is only for the purpose of illustrate where the interacting non infrared active $\nu_2(\sigma_g)$ mode would appear. We can see also a representation of the repulsion between the shifts of the interacting ν_2 and ν_7 modes.

In the part (a) of Fig. 36(red) we can see that the IR-allowed shifts for the $\nu_7(\sigma_u)$ mode of linear $^{12}\text{C}_{11}$ are restricted to a small frequency interval from 1938.0 to 1947.0 cm^{-1} . The bar (black) at $\sim 1933.9 \text{ cm}^{-1}$ is only as a representation of where the main frequency for the IR-forbidden $\nu_2(\sigma_g)$ mode of linear $^{12}\text{C}_{11}$ would be located. To the low frequency side we can see the shifts the $\nu_2(\sigma_g)$ mode of linear $^{12}\text{C}_{11}$ in the interval from 1915.0 to 1930.0 cm^{-1} . In contrast, the corresponding shifts for the $\nu_7(\sigma_u)$ mode of linear $^{13}\text{C}_{11}$ [see Fig. 36 (b)](blue) are spread over a larger frequency interval from 1870.0 to 1888.0 cm^{-1} and the shifts for the $\nu_2(\sigma_g)$ mode of linear $^{13}\text{C}_{11}$ are located within the interval from 1869.0 to 1860.0 cm^{-1} . The coupling between the ν_2 and ν_7 modes may result in relatively large discrepancies, between the calculated and observed band frequencies on both mirrored frequency sides for the single ^{12}C and ^{13}C -substituted isotopomers. We represent a specific isotopomer with the labels c1,c2... *etc.* for the $\nu_7(\sigma_u)$ mode and c2',c3'...*etc.* for the $\nu_2(\sigma_g)$ mode. The lower case letter c in the labels c1, c2..., and c2', c3' indicates a single ^{12}C or ^{13}C carbon isotope and the number 1, 2... stands for the location (starting from left to right) where the carbon isotope is positioned for the complementary spectra [see Fig. 36 (a) and (b)].

6.3 Assignment of the isotopomers for the $\nu_7(\sigma_u)$ mode of C_{11}

We can see in Fig. 37 (a) the experimental results obtained, before and after annealing with the purpose of finding a possible correlation, between bands for our preliminary isotopic shift selection. A prominent band at 1946.1 cm^{-1} (A) is proposed for assignment to the $\nu_7(\sigma_u)$ mode of linear C_{11} . Also, we can see to the lower frequency side of this band a series of peaks that can be utilized to propose a preliminary set of shifts for the single ^{13}C -substituted $^{13}\text{C}^{12}\text{C}_{10}$

isotopomers: the 1946.0(c1)[overlapped by the mean band at 1946.1cm⁻¹(A)], 1945.4(c2), 1939.9 (c3), 1938.6 (c4), 1942.6 (c5) and 1940.6 cm⁻¹ bands, called *SSC12*. Also, it is possible to observe further to the low frequency side bands that belongs to the IR-forbidden $\nu_2(\sigma_g)$ mode of C₁₁: the bands at 1919.7 (c2'), 1926.5(c3') and 1922.7 (c4') and 1917.4 (c5') cm⁻¹ [see Fig. 37(a)] making up the set called *SSC12'*.

We note that in the interval 1915.0-1926.0 cm⁻¹ in Fig. 37 (c) and 36(a), two calculated shifts the 1922.3 (c4') and 1925.5 cm⁻¹ (c3') from the $\nu_2(\sigma_g)$ mode for the now infrared allowed isotopomers have an intensity similar to that of the shifts for infrared allowed $\nu_7(\sigma_u)$ mode at 1938.9(c4), 1939.3(c3) and 1940.5 cm⁻¹(c6), and therefore should be possible to observe.

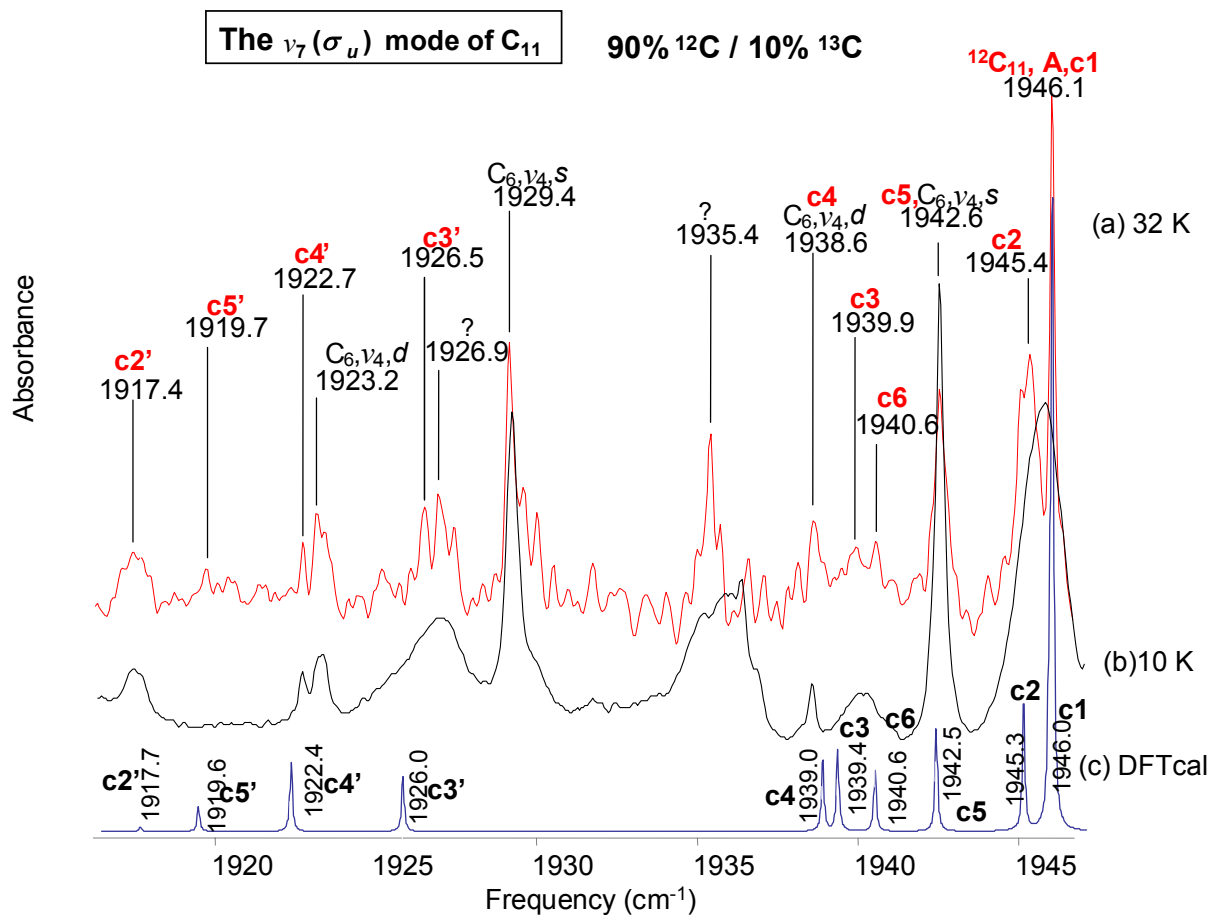


Fig. 37. Comparison of observed FTIR annealed spectra (a) 32 K and (b) 10 K of the linear C_{11} and its single ^{12}C and ^{13}C isotopic shifts with carbon enrichments (a) 90% ^{12}C and 10% ^{13}C and a simulation (c) derived from the DFT calculations at the B3YLP/cc-pVDZ level for the same enrichment values.

Moving to the analysis, we start with the 13-12-12-12-12-12-12-12-12-12-12 (c1) isotopomer calculated to be located at 1946.0 cm^{-1} . The frequency is only 0.1 cm^{-1} from the main band at 1946.1 cm^{-1} , and is thus within its envelope of the main band, rendering it unobservable. The 12-13-12-12-12-12-12-12-12-12-12 (c2) isotopomer calculated to be at 1945.3 cm^{-1} is overlapped by an unknown prominent band at 1945.4 cm^{-1} . The 12-12-13-12-12-12-12-12-12-

12-12 (c3) and the 12-12-12-13-12-12-12-12-12-12 (c4) and 12-12-12-12-12-13-12-12-12-12-12 (c6) calculated to be at 1939.4, 1939.0 and 1940.6 cm^{-1} respectively, are concentrated within a small frequency region from 1938.0 to 1941.0 cm^{-1} , due to the repulsion caused by the coupling with $\nu_2(\sigma_g)$ mode calculated to be to the lower frequency side (see Table VII) that “repels” all the isotopomers of $\nu_7(\sigma_g)$ to the high frequency side of the spectrum. This observed part of the spectrum has a difficult line profile; however it is possible to clearly observe potential shifts in Fig. 37(a) in the spectrum observed after annealing at 32 K. The observed band at 1939.9 cm^{-1} is close the calculated band at 1939.4 cm^{-1} (c3) thus it will be assigned to the c3 isotopomer. The observed band at 1938.6 cm^{-1} , which is more intense than the band assigned to the c3 isotopomer because it is overlapped by the double substituted 13-12-12-13-12-12 isotopomer of the $\nu_4(\sigma_u)$ mode of the linear C_6 (Ref.⁹⁵) is close to the calculated band at 1939.0 cm^{-1} (c4). The observed band at 1940.6 cm^{-1} is of similar characteristics to the c3 isotopomer is matches perfectly with the calculated frequency at 1940.5 cm^{-1} corresponding to the 12-centrosymmetric (c6) isotopomer, therefore, it will be assigned to the c6 isotopomer. The calculated band at 1942.5 cm^{-1} (c5) is overlapped by the c3 isotopomer of the $\nu_4(\sigma_u)$ mode of the linear C_6 (Ref.95). Finally, we have a set of shifts called SSC12, formed by the bands at 1946.0(c1) [overlapped by the main band at 1946.1 cm^{-1}], 1945.3 (c2) [overlapped by a band at 1945.4 cm^{-1}], 1939.9(c3), 1938.6 (c4) [overlapped with the double 13-12-12-13-12-12 isotopomer of the $\nu_4(\sigma_u)$ mode of the linear C_6], 1942.5 (c5) [overlapped with the c3 isotopomer of the $\nu_4(\sigma_u)$ mode of the linear C_6 at 1938.6 cm^{-1}] and 1940.6 cm^{-1} (c6). This set of shifts and its mirrored isotopomers (yet to be presented) was confirmed by the application of the *deperturbation method*. Moving to the low frequency side we can see the shifts for the IR-forbidden $\nu_2(\sigma_g)$ mode. It is important to mention that such bands cannot be processed through

deperturbation method for following reasons. The application of the DPM depends upon having both isotopic mirrored shift sets, including the observed frequencies of the main $^{12}\text{C}_n$ and $^{13}\text{C}_n$. In the case of the infrared inactive modes of a molecule, the main band will remain unobservable upon isotopic substitution and with out this piece of information it will not be valid to apply it the DPM. Nevertheless it is important to analyze them since they form part of the molecular structure of this particular vibrational fundamental.

Moving on with our isotopic analysis we found two observed bands at 1926.5 and 1926.9 cm^{-1} . Both are close to the calculated band at 1926.0 cm^{-1} corresponding to the c3' isotopomer. It is difficult determine which band is the correct choice and it cannot be tested with the DPM for the reasons discussed before. Since the band at 1926.5 cm^{-1} is the closest, it is assigned to the c3' isotopomer. The band at 1926.9 cm^{-1} will remain an unidentified band. The observed band at 1922.7 cm^{-1} is close to the c4' isotopomer band calculated at 1922.4 cm^{-1} . The relatively weaker band calculated at 1919.6 cm^{-1} is close to a peak in the measured spectrum barely above the noise that has emerged after annealing [see Fig. 36(a)]. It is well insolated from other shifts and is assigned to the c2' isotopomer. The band calculated at 1917.7 cm^{-1} for the c5' isotopomer is overlapped by an unidentified band at 1917.4 cm^{-1} . We thus have a set of shifts called SSC12 formed by 1946.0(c1) [overlapped with the main band at 1946.1 cm^{-1}], 1945.3 (c2), [overlapped by a band at 1945.4 cm^{-1}], 1939.9(c3), 1939.0 (c4) [overlapped with the double 13-12-12-13-12-12 isotopomer of the $\nu_4(\sigma_u)$ mode of the linear C_6], 1942.6 (c5) [overlapped with the c3 isotopomer of the $\nu_4(\sigma_u)$ mode of the linear C_6 at 1938.6 cm^{-1}] and 1940.6 cm^{-1} (c6) isotopomers corresponding to $\nu_7(\sigma_u)$ mode of the linear C_{11} and in addition the isotopomers corresponding to the $\nu_2(\sigma_g)$ mode of the linear C_{11} ; that includes the 1917.4 (c2') [overlapped by

a wide band at 1917.4 cm^{-1}], 1926.5 (c3') , 1922.7 (c4') and $1919.7 \text{ cm}^{-1} \text{ (c5')}$ that we can named SSC12'.

Figure 38(a), shows the mirror spectrum corresponding to the single ^{12}C substitutions in $^{13}\text{C}_{11}$ for the $\nu_7 (\sigma_u)$ mode produced by the evaporation of a rod with a 90% of ^{13}C /10% ^{12}C mixture. The absorption at 1870.9 cm^{-1} , which is a factor $\sim \sqrt{12/13}$ of the 1945.8 cm^{-1} frequency, is identified as belonging to the fully ^{13}C -substituted isotopomer $^{13}\text{C}_{11}$. In Fig. 38(a), to the high and low frequency side of the 1870.9 cm^{-1} band, we can see shift patterns for the single ^{12}C -substituted $^{12}\text{C}^{13}\text{C}_{10}$ isotopomers of the $\nu_7(\sigma_u)$ and $\nu_2(\sigma_g)$ modes of C_{11} respectively.

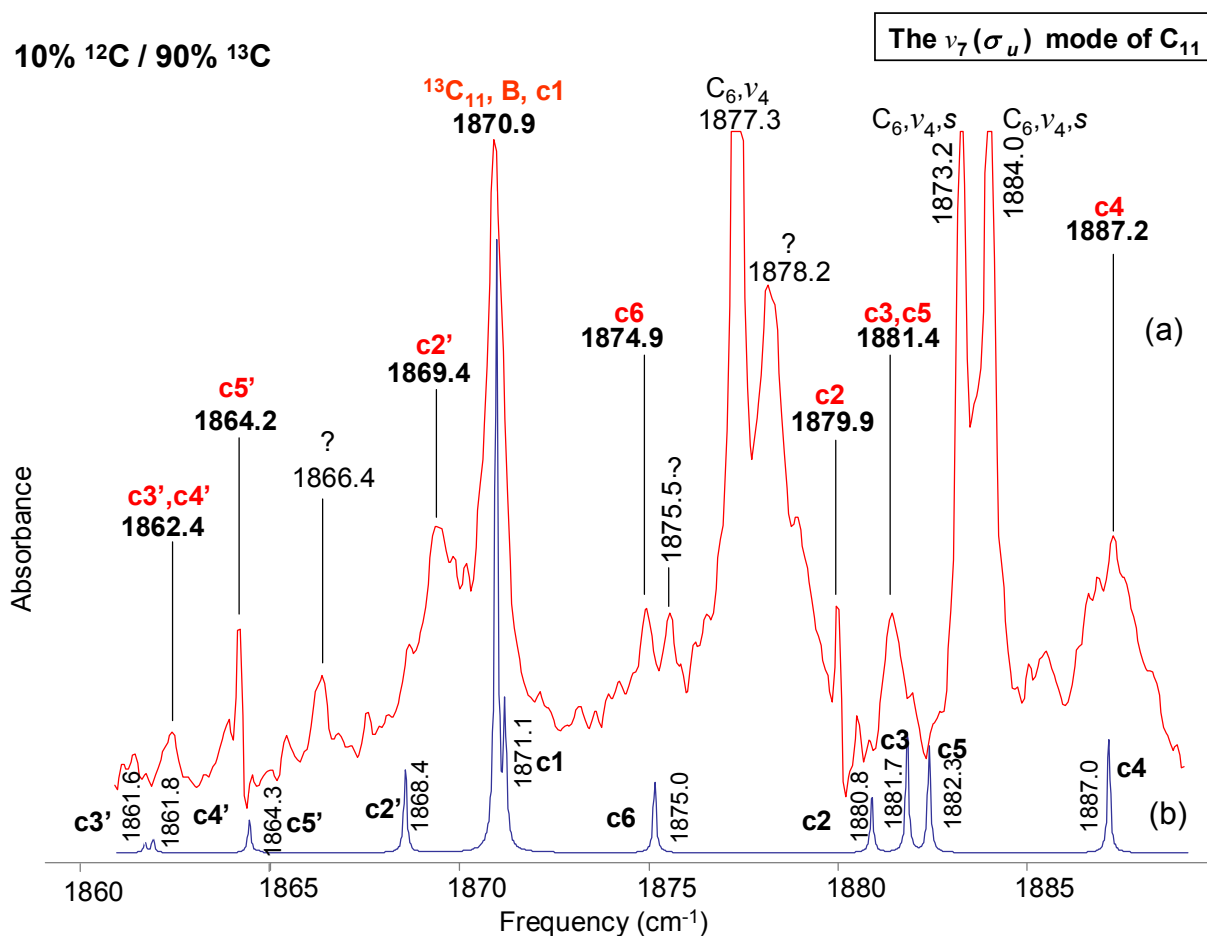


Fig. 38. Comparison of the FTIR spectra of the $\nu_7(\sigma_u)$ mode of the linear C_{11} and its isotopic shifts with (a) 90% ^{13}C and 10% ^{12}C mixture and (b) a DFT calculations at the B3YLP/cc-pVDZ level simulation using the same enrichment.

Bands are observed to the higher frequency side of the band at 1870.9 cm^{-1} [see Fig. 38(a)], that can potentially match the calculated shifts for the single ^{12}C -substituted $^{12}\text{C}^{13}\text{C}_{10}$ isotopomers of the $\nu_7(\sigma_u)$ mode. The proposed set of shifts called SSC13 include a band at 1871.1 cm^{-1} (c1) [overlapped by the main band at 1870.9 cm^{-1} (A)], 1879.9 (c2), 1881.4 (c3), 1882.3 (5) [overlapped by the c3 isotopomer], 1887.2 (c4) and 1874.9 cm^{-1} (c6). Also, by looking to the low frequency side of the main band we can form a preliminary set of shifts SSC13', for

the ^{12}C -substituted $^{12}\text{C}^{13}\text{C}_{10}$ isotopomers of the $\nu_2(\sigma_g)$ mode with the bands at 1869.4 (c2'), 1862.4 (c4') 1861.6(c3')[overlapped by the c4' isotopomers] and 1864.2 cm^{-1} (c5'). Both preliminary shift-sets appear in the two bottom sections of Table XI.

TABLE XI. Comparison of observed and predicted DFT (B3LYP/cc-pVDZ) frequencies for single ^{13}C -substituted isotopomers of $^{12}\text{C}_{11}$, and single ^{12}C -substituted isotopomers of $^{13}\text{C}_{11}$, for the ν_7 mode

Isotopomer	ν_{obs}	B3LYP/cc-pVDZ		$\Delta\nu$
		ν	ν_{scaled}	$\nu_{\text{obs}} - \nu_{\text{scaled}}$
12-12-12-12-12-12...(A) ¹	1946.1	2126.2	1946.1 ²	0.0
13-12-12-12-12-12...(c1)	Overlapped ³	2126.1	1946.0	----
12-13-12-12-12-12...(c2)	1945.4	2125.3	1945.3	0.1
12-12-13-12-12-12...(c3)	1939.9	2118.9	1939.4	0.5
12-12-12-13-12-12...(c4)	1938.6	2118.4	1939.0	-0.4
12-12-12-12-13-12...(c5)	Overlapped ⁴	2122.3	1942.5	----
12-12-12-12-12-13...(c6)	1940.6	2120.2	1940.6	0.0
12-13-12-12-12-12...(c2') ⁵	1917.6	2095.2	1917.7	-0.1
12-12-13-12-12-12...(c3')	1926.5	2104.2	1926.0	0.5
12-12-12-13-12-12...(c4')	1922.7	2100.3	1922.4	0.3
12-12-12-12-13-12...(c5')	1919.5	2097.2	1919.6	-0.1
13-13-13-13-13-13...(B) ⁵	1870.9	2042.6	1870.9 ⁶	0.0
12-13-13-13-13-13...(c1)	Overlapped ⁷	2042.8	1871.1	---
13-12-13-13-13-13...(c2)	1879.9	2053.4	1880.8	-0.9
13-13-12-13-13-13...(c3)	1881.4	2054.4	1881.7	-0.3
13-13-13-12-13-13...(c4)	1887.2	2060.2	1887.0	0.2
13-13-13-13-12-13...(c5)	Overlapped ⁸	2055.0	1882.3	---
13-13-13-13-13-12...(c6)	1874.9	2047.1	1875.0	-0.1
13-12-13-13-13-13...(c2') ⁹	1869.4	2039.9	1868.4	1.0
13-13-12-13-13-13...(c3')	Overlapped ¹⁰	2032.4	1861.6	---
13-13-13-12-13-13...(c4')	1862.4	2032.7	1861.8	0.6
13-13-13-13-12-13...(c5')	1864.2	2035.4	1864.3	-0.1

¹Single substituted ^{12}C -isotopomers for the $\nu_7(\sigma_u)$ mode of the linear $^{12}\text{C}_{11}$

²Scaling factor $\nu_{\text{obs}}/\nu \sim 0.91511$

³Overlapped by an unknown band at 1945.4 cm^{-1}

⁴Overlapped by the c3 isotopomer of the $\nu_4(\sigma_u)$ mode of the linear C_6

⁵Single substituted ^{12}C -isotopomers for the $\nu_2(\sigma_g)$ mode of the linear $^{12}\text{C}_{11}$

⁶Scaling factor $\nu_{\text{obs}}/\nu \sim 0.91594$

⁷Overlapped by the main band at 1870.9 cm^{-1}

⁸Overlapped by the band at 1881.4 cm^{-1} (c3)

⁹Single substituted ^{12}C -isotopomers for the $\nu_2(\sigma_g)$ mode of the linear $^{13}\text{C}_{11}$

¹⁰Overlapped by the band at 1881.4 cm^{-1} (c4')

The top two sections of Table XI, shows the already assigned shifts for the single ^{13}C -substituted ($^{13}\text{C}^{12}\text{C}_{10}$) isotopomers of the $\nu_7(\sigma_u)$ and $\nu_2(\sigma_g)$ modes of the linear $^{13}\text{C}_{11}$, respectively. The bottom two halves show the potential shifts for the single ^{12}C -substituted $^{12}\text{C}^{13}\text{C}_{10}$ isotopomers. The first column lists the isotopomers under consideration for the $\nu_7(\sigma_u)$ and $\nu_2(\sigma_g)$ modes of C_{11} with their abbreviated isotopomer labels in parentheses as c1,c2... etc for the $\nu_7(\sigma_u)$ mode and c2',c3'...etc for the $\nu_2(\sigma_g)$ mode. The predicted frequencies for the single ^{13}C -substituted $^{13}\text{C}^{12}\text{C}_{10}$ isotopomers in the third column (labeled ν) are scaled by a factor of ~ 0.91511 obtained by taking the ratio of the observed main frequency 1945.8 cm^{-1} with the corresponding DFT calculated main frequency of 2126.3 cm^{-1} of the ν_7 mode of $^{12}\text{C}_{11}$. By similarly taking the ratio of the predicted and observed frequencies for the ν_7 mode of $^{13}\text{C}_{11}$ we obtain a scaling factor of ~ 0.91594 for the ^{12}C substituted $^{12}\text{C}^{13}\text{C}_9$ isotopomers.

The band for the 12-13-13-13-13-13-13-13-13-13-13 (c1) isotopomer calculated to be at 1871.1 cm^{-1} is overlapped by the main band. The observed band at 1879.9 cm^{-1} is close to the calculated band at 1880.8 cm^{-1} for the 13-12-13-13-13-13-13-13-13-13-13 (c2) isotopomer. The observed band at 1881.4 cm^{-1} appears to be wide enough to contain at least two bands of the same intensity as the c2 isotopomer band; is close to the calculated bands at 1881.7 and 1882.3 cm^{-1} corresponding to the 13-13-12-13-13-13-13-13-13-13-13 (c3) and 13-13-13-13-12-13-13-13-13-13-13 (c5) isotopomers separated by only 0.6 cm^{-1} , therefore, it is assumed that the c3 (slightly more intense) and the c5 isotopomers are collapsed in this single band. Thus the observed band at 1879.9 cm^{-1} will be assigned to the c3 isotopomer while the c5 isotopomers will be consider to be overlapped by this band. The observed band at 1887.2 cm^{-1} has a wide line profile growing in to both frequency sides. This broad band may be overlapped by bands of other C_n species, growing as well as by the contribution of double substituted isotopomers it is

actually close to the calculated band at 1887.0 cm^{-1} corresponding to the 13-13-13-12-13-13-13-13-13-13 (c4), which is well isolated from any other isotopomer and is actually close to an. Analysis with the DPM and indicates that it behaves well with the corresponding mirrored band at 1938.6 cm^{-1} . Therefore the band at 1887.2 cm^{-1} will be assigned to the (c4) isotopomer. In the observed spectrum we have two bands of similar characteristics at 1874.9 and 1875.5 cm^{-1} and close to the calculated band at 1875.0 cm^{-1} corresponding to the centrosymmetric 13-13-13-13-13-12-13-13-13-13 (c6) isotopomer which is also well isolated. It is then difficult to choose the correct isotopomer. Nevertheless, the band at 1875.5 cm^{-1} was used to form an alternative set of shifts called SSC13", for testing with the DPM. It was founded that the poor behavior of the 1875.5 cm^{-1} frequency indicates that the band at 1874.9 cm^{-1} should be assigned to the (c6) isotopomer. Thus, we have shift-set SSC13, corresponding to the $\nu_7(\sigma_u)$ mode of $^{13}\text{C}_{11}$ comprising the observed bands at 1871.1 cm^{-1} (c1) [overlapped with the main band at 1870.9 cm^{-1} (B), 1879.9 (c2), 1881.4 (c3), $1882.3(5)$ [overlapped by the c3 isotopomer], 1887.2 (c4) and 1874.9 cm^{-1} (c6).

We continue the analysis with the assignment of the shifts for the $\nu_2(\sigma_g)$ mode of $^{13}\text{C}_{11}$. The band observed at 1869.4 cm^{-1} , has a wing to its low frequency side due to extra contributions from double substituted isotopomers and other C_n bands contribute to its intensity. This band is relatively close to the calculated to be at 1868.4 cm^{-1} corresponding to the c2' isotopomer. The observed band at 1864.2 cm^{-1} and is very close to the calculated band at 1864.3 cm^{-1} therefore assigned to the c5' isotopomer. The observed band at 1862.4 cm^{-1} is close to the calculated bands at 1861.6 and 1861.8 cm^{-1} corresponding to the c3' and c4' isotopomers, which are separated by only 0.2 cm^{-1} . Nevertheless, the (c4') isotopomer it is a little more intense than the 1861.6 cm^{-1} (c3') isotopomer, thus the observed band at 1862.4 will be assigned to the c4'

isotopomer and the c3' will be considered to be overlapped. The observed band at 1864.2 is too intense to sustain a single shift indicating that contribution of another unknown band. It is close to the calculated band at 1864.3 cm^{-1} corresponding to the c5' isotopomer. We thus have a shift set for the $\nu_2(\sigma_g)$ mode of $^{13}\text{C}_{11}$: the 1869.4 (c2'), 1862.4 (c3') [overlapped by the c4' isotopomer], 1862.4(c4') and 1864.2 cm^{-1} (c5') bands. In Fig. 39, similar to Fig. 36, are shown the spectra calculated at the B3YLP/cc-pVDZ level for (a) 90% ^{12}C and 10% ^{13}C and (b) 10% ^{12}C and 90% ^{13}C mixtures, where we now include bars in yellow to represent where the observed frequencies are located. This summary provides good evidence that the foregoing analysis of the isotopic shift patterns corresponding to the $\nu_2(\sigma_g)$ and $\nu_7(\sigma_u)$ modes of C_{11} is correct.

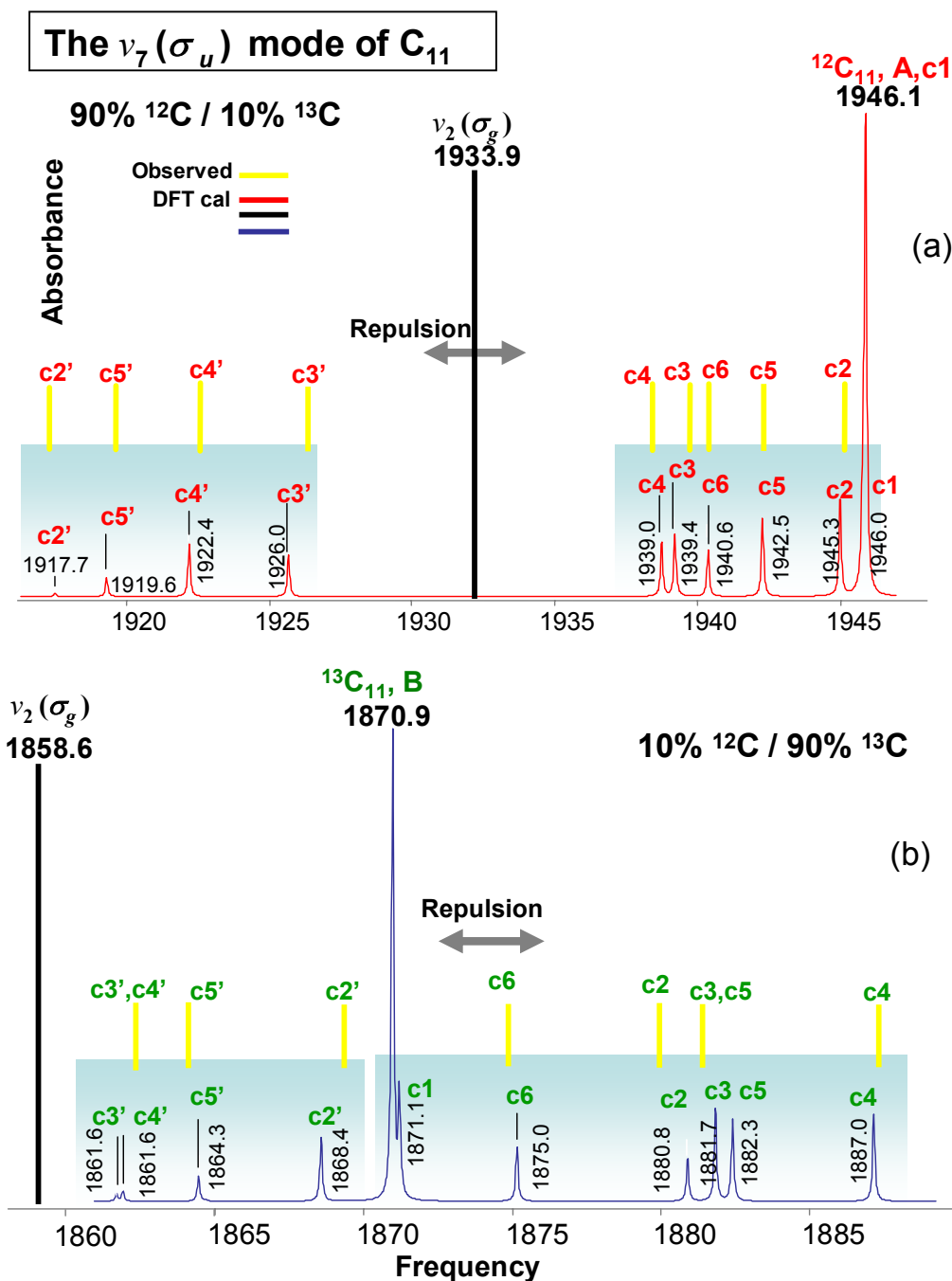


Fig. 39. Both (a)(red) and (b)(blue) are spectra derived from the DFT calculations at the B3YLP/cc-pVDZ level and its isotopic shifts with (a) 10% ^{12}C and 10% ^{13}C mixture (b) 90% ^{13}C and 10% ^{12}C . The bars in black and yellow are only for the purpose of illustrate where the interacting non infrared active $\nu_2(\sigma_g)$ mode and the observed single ^{12}C (a) and ^{13}C (b) isotopic shifts would appear. We can see also the repulsion between the shifts of the interacting ν_2 and ν_7 modes.

6.4 Assignment of the isotopomers for the $\nu_8(\sigma_u)$ mode of C_{11}

Unlike the mode just discussed, here is no evidence from the analysis of the isotopomer shift patterns for $\nu_8(\sigma_u)$ mode of C_{11} , the third most intense mode, that there is significant coupling with the IR forbidden $\nu_2(\sigma_g)$ mode located at 167.1 cm^{-1} . The spectrum in Fig. 40 shown before and after annealing, exhibits a prominent band at 1856.7 cm^{-1} that is proposed as the main band of the $\nu_8(\sigma_u)$ mode of C_{11} . To the low frequency side, we have potential set of shifts named SSC12 at $1851.0(\text{c1})$, $1840.0(\text{c2})$, $1846.5(\text{c4})$, $1842.1(\text{c6})$ and $1856.1(\text{c5})$ and $1856.4(\text{c3})\text{ cm}^{-1}$, the latter overlapped by the main band at 1856.7 cm^{-1} (A) for the $\nu_8(\sigma_u)$ mode of C_{11} [see Fig. 40(a)]. Those bands seem to be correlated under annealing at 35.0 and 10.0 K as can be seen in Fig. 40 (a) and (b) respectively.

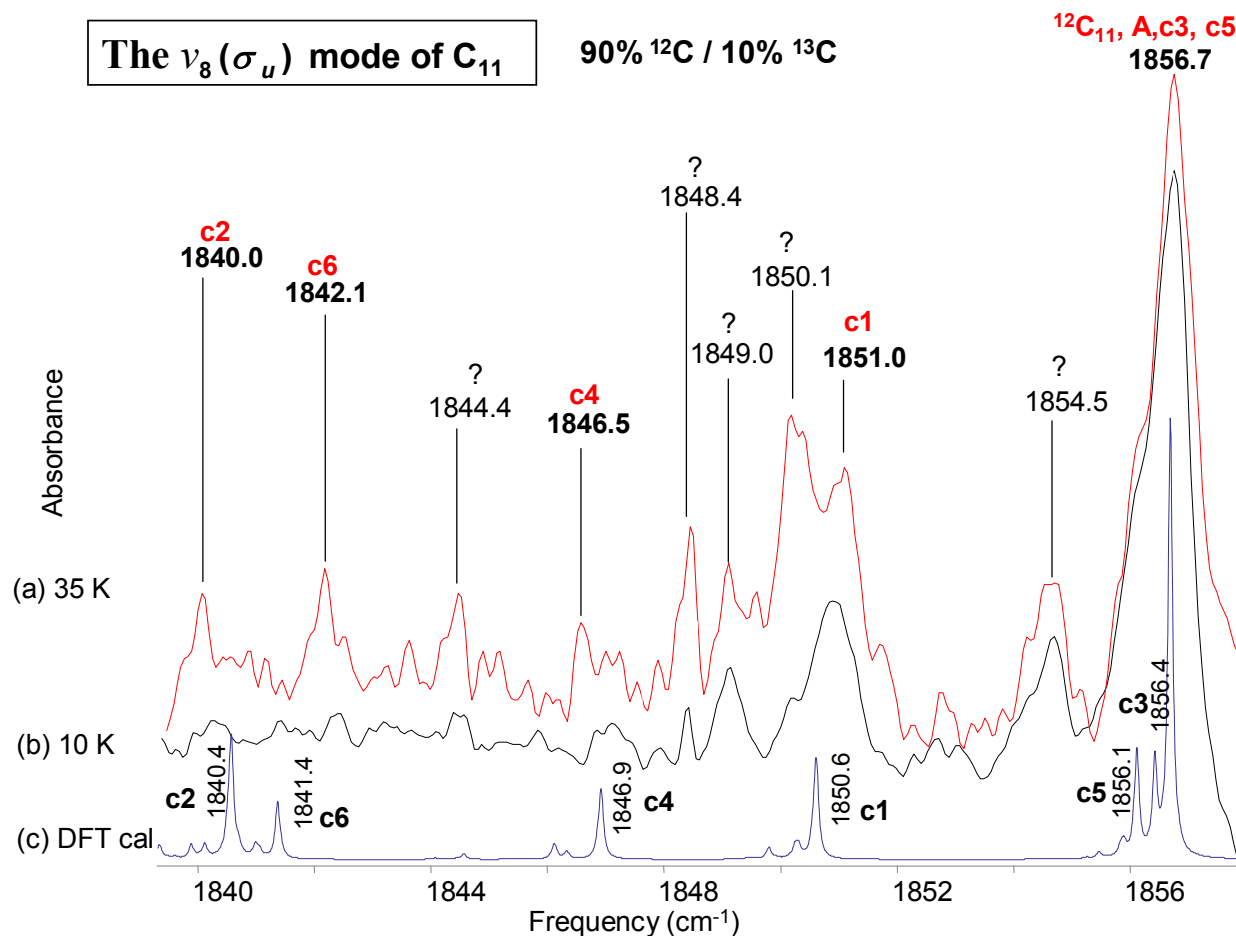


Fig. 40. Comparison of observed FTIR annealed spectra (a) 35 K and (b) 10 K of the $\nu_6(\sigma_u)$ mode of linear C_{11} and its single ^{13}C isotopic shifts using 90% ^{12}C and 10% ^{13}C carbon enrichments, and (c) a simulated spectrum derived from the DFT calculations at the B3YLP/cc-pVDZ level using the same enrichment values.

The absorption at 1851.0 cm^{-1} grows in on annealing. It is close to the calculated band at 1850.6 for the 13-12-12-12-12-12-12-12-12-12-12 (c1) isotopomer. Such a big band is probably overlapping the corresponding observed band for the c1 isotopomer. Close to the 1851.0 cm^{-1} band another strong absorption at 1850.1 cm^{-1} belonging to another C_n species has suddenly appeared but it is clearly not related to the 1851.0 cm^{-1} absorption nor to the bands at 1849.0 and 1849.0 cm^{-1} , since all three bands all existed before annealing. The latter two are probably

related to the band 1851.0 cm^{-1} that is overlapping the c1 isotopomer. The absorption at 1840.0 cm^{-1} is close to the calculated band 1840.4 cm^{-1} corresponding to the 12-13-12-12-12-12-12-12-12-12 (c2) isotopomer. The observed wide shoulder growing in to the lower side of the main band is probably overlapping corresponding observed shifts for the 12-12-13-12-12-12-12-12-12-12 (c3) and 12-12-12-12-5-12-12-12-12-12 (c5) isotopomers calculated to be at 1856.4 and 1856.1 cm^{-1} . There is an unidentified absorption at 1854.5 cm^{-1} . The observed absorption at 1846.5 cm^{-1} is close to the 1846.9 cm^{-1} band calculated for the 12-12-12-13-12-12-12-12-12-12 (c4) isotopomer. Since the unidentified observed band at 1844.4 cm^{-1} is far away from any of our already identified shift and it will not be taken into consideration. The observed at 1842.1 cm^{-1} is relatively close to the calculated band at 1841.4 cm^{-1} corresponding to the centrosymmetric 12-12-12-12-12-13-12-12-12-12 (c4) isotopomer. This band can be reasonably assigned to a band. The SSC12 set of shifts for the single ^{12}C -substituted $^{12}\text{C}^{13}\text{C}_{10}$ isotopomers is, $1850.1(\text{c1})$, $1840.0(\text{c2})$, $1856.4(\text{c3})$ and $1856.1(\text{c5})$ [overlapped by the main band at $1856.7\text{ cm}^{-1}(\text{A})$], $1846.5(\text{c4})$ 1842.1 cm^{-1} (c6), testing with the *deperturbation method* reinforced these assignments.

Figure 41, shows the mirror spectra corresponding to the single ^{12}C substitutions in $^{13}\text{C}_{11}$ for the $\nu_8 (\sigma_u)$ mode produced using a rod with a 90% ^{13}C / 10% ^{12}C mixture. The frequency of the absorption at 1784.7 cm^{-1} , which is a factor $\sim\sqrt{12/13}$ of the 1856.7 cm^{-1} frequency, is identified as belonging to the fully ^{13}C -substituted isotopomer $^{13}\text{C}_{11}$. To the high frequency side of this band, we can select a potential set of shifts, SSC13 with isotopomer frequencies $1790.0(\text{c1})$, 1797.9 (c2) $1797.3(\text{c6})$ [overlapped by the c2 isotopomer] and 1792.9 cm^{-1} (c4). The measured frequencies are compared with the results of the scaled DFT calculations in Table XII.

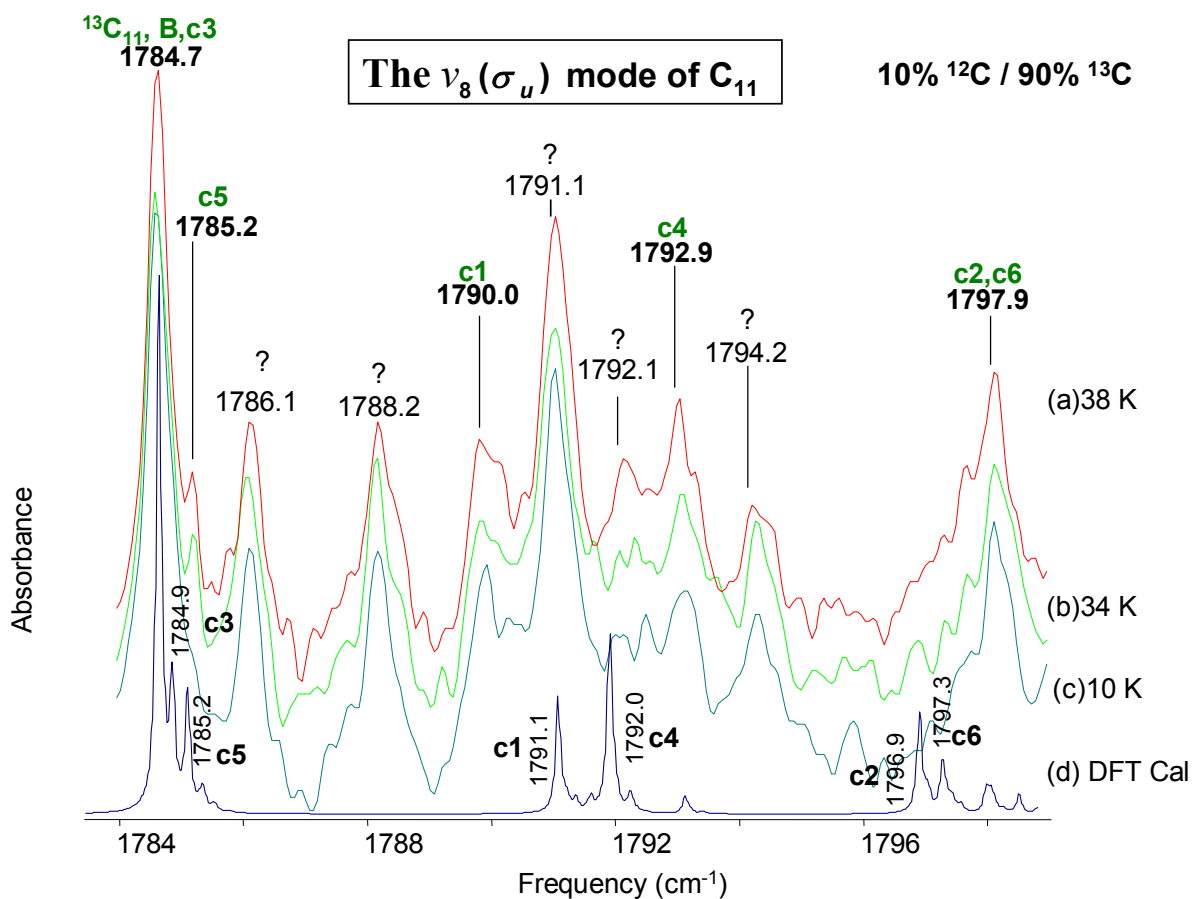


Fig. 41. Comparison of observed FTIR annealed spectra (a) 38 K (b) 34 K and (c) 10 K of the $\nu_8(\sigma_u)$ mode of linear C_{11} and its single ^{13}C isotopic shifts using 10% ^{12}C and 90% ^{13}C carbon enrichments, and (d) a simulated spectrum derived from the DFT calculations at the B3YLP/cc-pVDZ level using the same isotopic enrichments.

TABLE XII. Comparison of observed and predicted DFT (B3LYP/cc-pVDZ) frequencies for single ^{13}C -substituted isotopomers of $^{12}\text{C}_{11}$, and single ^{12}C -substituted isotopomers of $^{13}\text{C}_{11}$, for the ν_7 mode.

Isotopomer	ν_{obs}	B3LYP/cc-pVDZ		$\Delta\nu$ $\nu_{\text{obs}} - \nu_{\text{scaled}}$
		ν	ν_{scaled}	
12-12-12-12-12-12... (A)	1856.7	1946.9	1856.7 ¹	0.0
13-12-12-12-12-12...(c1)	Overlapped ²	1940.5	1850.6	---
12-13-12-12-12-12...(c2)	1840.0	1930.0	1840.6	-0.6
12-12-13-12-12-12...(c3)	Overlapped ³	1946.6	1856.4	---
12-12-12-13-12-12...(c4)	1846.5	1936.7	1846.9	-0.4
12-12-12-12-13-12...(c5)	Overlapped ⁴	1946.3	1856.1	---
12-12-12-12-12-13...(c6)	1842.1	1930.8	1841.3	0.8
13-13-13-13-13-13...(B)	1784.7	1870.3	1784.7 ⁵	0.0
12-13-13-13-13-13...(c1)	1790.0	1877.0	1791.1	-1.1
13-12-13-13-13-13...(c2)	1797.9	1883.1	1796.9	1.0
13-13-12-13-13-13...(c3)	Overlapped ⁶	1870.5	1784.9	---
13-13-13-12-13-13...(c4)	1792.9	1877.9	1792.0	0.9
13-13-13-13-12-13...(c5)	1785.2	1870.8	1785.2	0.0
13-13-13-13-13-12...(c6)	Overlapped ⁷	1883.5	1797.3	---

¹Scaling factor $\nu_{\text{obs}}/\nu \sim 0.95423$

²Overlapped by unknown band at 1851.0 cm^{-1}

^{3,4}Overlapped by the main band at 1856.7 cm^{-1}

⁵Scaling factor $\nu_{\text{obs}}/\nu \sim 0.95366$

⁶Overlapped by the main band at 1784.6 cm^{-1}

⁷Overlapped by the (c2) isotopomer at 1797.9 cm^{-1}

The top half of Table XII, shows the selection *SSC12* for the single ^{13}C -substituted $^{13}\text{C}^{12}\text{C}_{10}$ isotopomers, and in the bottom half the selection *SSC13*, for the single ^{12}C -substituted $^{12}\text{C}^{13}\text{C}_{10}$ isotopomers. The scaled predicted frequencies reported in the fourth column labeled ν_{scaled} for the single ^{13}C -substituted $^{13}\text{C}^{12}\text{C}_{10}$ isotopomers are scaled by a factor of ~ 0.95423 obtained by taking the ratio of the observed main frequency 1784.7 cm^{-1} with the corresponding DFT calculated main frequency of 1870.3 cm^{-1} of the ν_8 mode of $^{12}\text{C}_{11}$. By similarly taking the ratio of the predicted and observed frequencies for the ν_8 mode of $^{13}\text{C}_{11}$ we obtain a scaling factor

of ~ 0.95366 for the ^{12}C substituted $^{12}\text{C}^{13}\text{C}_{11}$ isotopomers. The measured frequencies are compared with the results of the scaled DFT calculation given in the Table XI (lower half).

The observed prominent band located at 1791.1 cm^{-1} and the unidentified band at 1792.1 cm^{-1} the first matches the calculated band at 1791.1 for the 12-13-13-13-13-13-13-13-13-13 (c1) and second is close to the calculated band at 1792.1 cm^{-1} that corresponds to 13-13-13-12-13-13-13-13-13-13 (c4). However when those two bands were tested in an alternative shift-set called SSC13' with the *deperturbation method*, it was found that neither of the bands at 1791.1 and 1792.1 cm^{-1} behaved correctly and they were eliminated from consideration. An alternative assignment of the observed bands at 1790.0 and 1792.9 cm^{-1} to the c1 and c4 isotopomers as part of the first shift-set SSC13 was confirmed by the DPM. An observed band at 1794.2 cm^{-1} is far away from any of the shifts and it was eliminated from any consideration. The observed band at 1797.9 cm^{-1} has a wide line profile and broadens sufficiently on annealing for it to contain within its envelope the two bands. It is close to the calculated bands at 1796.9 and 1797.3 cm^{-1} for the 13-12-13-13-13-13-13-13-13-13(c2) and the centrosymmetric 13-13-13-13-13-12-13-13-13-13(c6) isotopomers respectively. The calculated band at 1784.9 corresponding to the 13-13-12-13-13-13-13-13-13-13(c3) is overlapped by the main band at $1784.7\text{ (B)}\text{ cm}^{-1}$. The observed band at 1785.2 cm^{-1} matches the calculated band at 1785.2 cm^{-1} corresponding to the 13-13-13-13-15-13-13-13-13-13 (c5) isotopomer. Several unidentified bands at 1786.1 and 1788.2 cm^{-1} are C_n species but their identities are still under investigation. The final SSC13 set of shifts is formed by the single ^{12}C -substituted $^{12}\text{C}^{13}\text{C}_{10}$ isotopomers at 1790.0 (c1), 1797.9 (c2), 1796.6 (c6) [overlapped by the c2 isotopomer], 1785.2 (c3)[overlapped by the main band at 1784.7 (B)] and 1792.9 (c4) cm^{-1} (see Fig. 41).

6.5 Assignment of the isotopomers for the ν_9 (σ_u) mode of C_{11}

The single ^{13}C shift pattern for the $\nu_9(\sigma_u)$ mode of C_{11} , its fourth most intense vibrational fundamental, is calculated to lie within an frequency interval at $1345\text{-}1365\text{ cm}^{-1}$ [see Fig. 42(a), (b) and (c)]. This vibrational fundamental has been one of the most elusive to find. The closest non infrared active $\nu_4(\sigma_g)$ mode is at 319.8 cm^{-1} to the low frequency side, which would suggest no coupling with the ν_9 mode. Our proposed band is located at 1360.0 cm^{-1} and to the low frequency side, we observe a potential set of bands for the single ^{13}C -substituted $^{13}\text{C}^{12}\text{C}_{10}$ isotopomers at 1353.2 (c1), 1359.6 (c2) [overlapped by the main band at 1360.0 cm^{-1} (A)], 1350.4 (c3), 1350.0 (c6) [overlapped by c3 isotopomer], 1356.0 (c4) and 1357.5 cm^{-1} (c5). The proposed bands appear to be correlated with each other and with the main band under annealing.

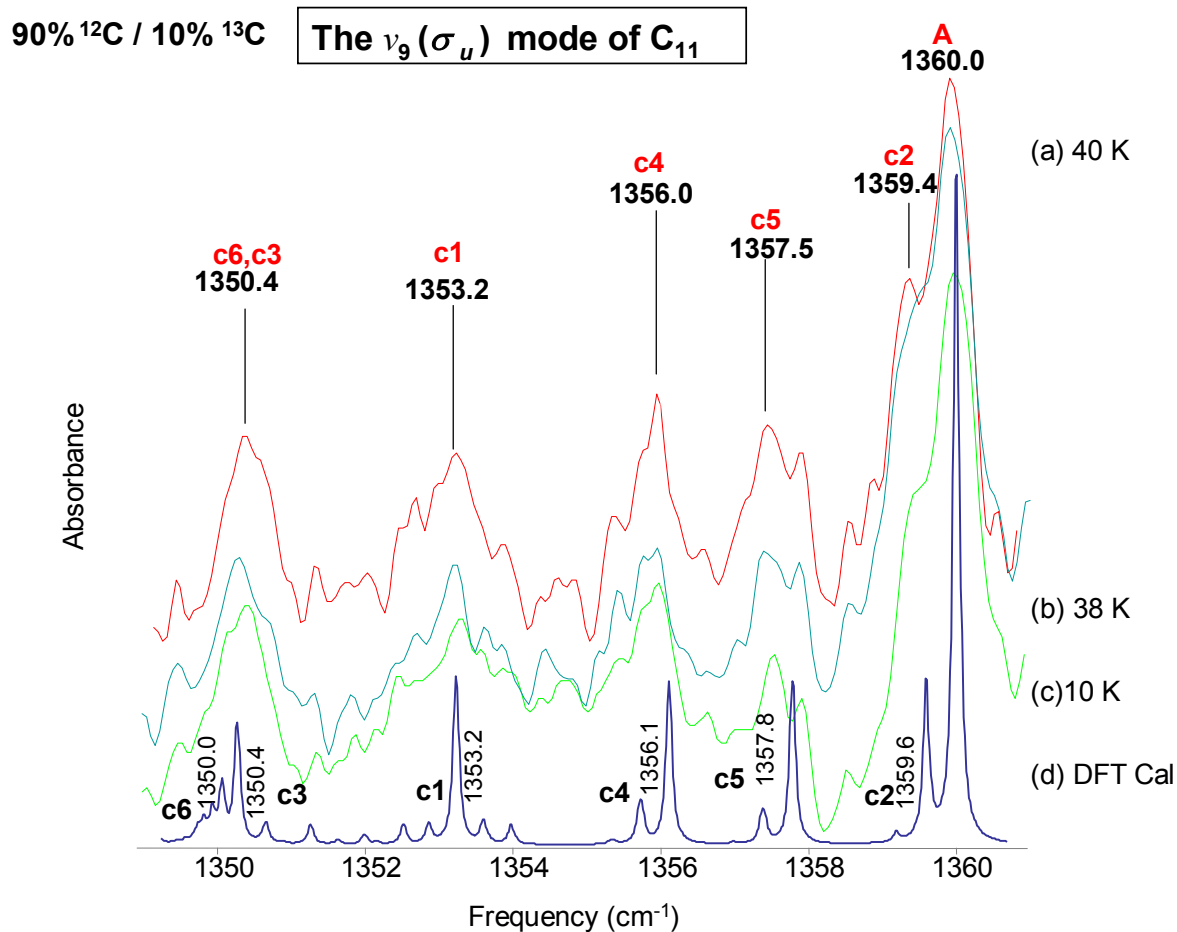


Fig. 42. Comparison of observed FTIR annealed spectra (a) 40 K (b) 38 K and (c) 10 K of the $\nu_9(\sigma_u)$ mode of linear C_{11} and its single ^{13}C isotopic shifts using 90% ^{12}C and 10% ^{13}C carbon enrichments, and (d) a simulated spectrum derived from the DFT calculations at the B3YLP/cc-pVDZ level using the same enrichment values.

The observed band at 1353.2 cm^{-1} coincides exactly with the calculated band at 1353.2 cm^{-1} corresponding to the 13-12-12-12-12-12-12-12-12-12-12 (c1) isotopomer coincides exactly with the. This band is somewhat broadened due to other double substituted isotopomers bands growing on both sides of its profile. At the lower frequency side of the main band at 1360.0 cm^{-1} (A) there is a band at 1359.4 cm^{-1} that grew in after annealing, more intense than the other potential shifts, due to the overlap with other C_n shifts. It is close to the calculated band at

1359.6 cm^{-1} corresponding to the 12-13-12-12-12-12-12-12-12-12 (c2) isotopomer. The observed band at 1350.4 cm^{-1} that appears to grow under annealing as it shown in Fig. 41 (a), (b) and (c). It is close to the calculated frequencies at 1350.4 and 1350.0 cm^{-1} for the 12-12-13-12-12-12-12-12-12-12 (c3) and centrosymmetric 12-12-12-12-12-13-12-12-12-12 (c6) isotopomers. Therefore the band at 1350.4 cm^{-1} will be assigned to the c3 isotopomer and the centrosymmetric c6 isotopomer which is only 0.4 cm^{-1} lower in frequency will be considered to be under its envelope. The observed band at 1356.0 cm^{-1} seems to be related to the (c1) and (c3) isotopomers under annealing. It is very close to the calculated band at 1356.1 cm^{-1} for the 12-12-12-13-12-12-12-12-12-12 (c4) isotopomers. Similarly, the observed band at 1357.5 cm^{-1} has an intensity that is correlated with the intensities of (c1), (c3) and (c4) isotopomer bands. It is close to the calculated band at 1357.8 cm^{-1} corresponding to the 12-12-12-12-15-12-12-12-12-12 (c5). Therefore, we have a complete set of shifts for the single ^{12}C -substituted $^{12}\text{C}^{13}\text{C}_{10}$ isotopomers consists of the 1353.2(c1), 1359.4(c2), 1350.4 (c3), 1350.0 (c6) [overlapped with the (c3) isotopomer], 1356.0 (c4) and 1357.5 cm^{-1} (c5) isotopomers for the $\nu_8(\sigma_u)$ mode of $^{12}\text{C}_{11}$ [see Table XIII].

TABLE XIII. Comparison of observed and predicted DFT (B3LYP/cc-pVDZ) frequencies for single ^{13}C -substituted isotopomers of $^{12}\text{C}_{11}$, and single ^{12}C -substituted isotopomers of $^{13}\text{C}_{11}$, for the ν_9 mode.

Isotopomer	ν_{obs}	B3LYP/cc-pVDZ		$\Delta\nu$ $\nu_{\text{obs}} - \nu_{\text{scaled}}$
		ν	ν_{scaled}	
12-12-12-12-12-12...(A)	1360.0	1404.5	1360.0 ¹	0.0
13-12-12-12-12-12...(c1)	1353.2	1397.5	1353.2	0.0
12-13-12-12-12-12...(c2)	Overlapped ²	1404.1	1359.6	0.0
12-12-13-12-12-12...(c3)	1350.4	1394.6	1350.4	0.0
12-12-12-13-12-12...(c4)	1356.0	1400.5	1356.1	-0.1
12-12-12-12-13-12...(c5)	1357.5	1402.2	1357.8	-0.3
12-12-12-12-12-13...(c6)	Overlapped ³	1394.2	1350.0	0.0

¹Scaling factor $\nu_{\text{obs}}/\nu \sim 0.96831$

²Overlapped (c6) isotopomer

³Overlapped by the main band at 1784.6 cm^{-1}

It is usually helpful, as has been demonstrated through this entire work, to have both mirrored sides of any vibrational fundamental in order to study a possible assignment and to allow the use of the *deperturbation method* to reinforce any definite assignment. In this particular case, however, it is not possible to apply this methodology, since it has not been possible, so far to obtain the mirrored single ^{12}C -substituted $^{12}\text{C}^{13}\text{C}_{10}$ isotopomers. For this reason the proposed assignment should be taken as tentative, until mirrored side is presented.

6.6 Conclusions

Results have been presented for the linear $\nu_7(\sigma_u)$, $\nu_8(\sigma_u)$ and $\nu_9(\sigma_u)$ fundamentals of linear C_{11} in solid Ar at 10 K produced by the laser ablation of graphite. The analysis has relied on the

much improved spectra obtained for both 90/10 and 10/90 isotopic measurements and also on taking into consideration the interaction with the $\nu_2(\sigma_g)$ and $\nu_1(\sigma_g)$ modes by the $\nu_7(\sigma_u)$ and $\nu_8(\sigma_u)$ modes, respectively, using the DPM, which has been particularly helpful in accurately assigning isotopic shifts. This work confirms the assignment of the vibrational fundamentals $\nu_7(\sigma_u)=1946.1$, $\nu_8(\sigma_u)=1856.7$ with a complete isotopic shift-sets in the first two cases and partial isotopic information for the tentatively assigned $\nu_8(\sigma_u)=1360.0 \text{ cm}^{-1}$ fundamental. These assignments are important in the analysis of the vibrational spectrum of C_{11} and also provide us with a useful insight on long C_n chain molecules for interactions with nearby infrared inactive mode are strong, resulting in extra isotopomer bands that provide us with useful information and experience for subsequent isotopic investigations of C_n species longer than C_{11} .

CHAPTER VII

FTIR SPECTROSCOPIC STUDY OF THE ν_5 (σ_u), AND ν_6 (σ_u) MODES OF LINEAR C₈ AND THE ν_7 (σ_u), ν_8 (σ_u) AND ν_9 (σ_u) MODES OF LINEAR C₁₂

7.1 Introduction

There have been earlier published studies^{96, 97, 98, 99, 100} pursuing the identification of the linear C₈^{97,98} and C₁₂.¹⁰⁰ The work by Vala *et al.*⁹⁷ reported the most intense $\nu_5=2071.5$ and $\nu_6=1710.5$ cm⁻¹ modes of C₈ produced by the laser ablation of graphite in Ar. Maier *et al.*⁹⁸ proposed the $\nu_5=2063.9$ and $\nu_6=1705.6$ cm⁻¹ modes based on mass-selection and by interpreting Mosinger's infrared data¹⁰¹. Nevertheless, none of these works presented an isotopic analysis to support the assignments. Ding *et al.*¹⁰⁰ performed a series of studies on the $\nu_7=2140.6$, $\nu_8=1997.2$ and $\nu_9=1818.0$ cm⁻¹ modes of linear C₁₂ in the TCU Molecular Physics Lab. In this investigation carbon deposition in Ar matrices was used to measure the absorptions of the single ¹³C-substituted (¹³C¹²C₁₀) isotopomers. They were able to assign the ν_8 and ν_9 modes although an assignment for ν_7 remained tentative.

New experimental measurements obtained during this dissertation research have given us the opportunity to present ¹³C/¹²C isotopic spectra for the ν_7 , ν_8 , ν_9 modes of linear C₁₂ that confirms the assignments. We have also utilized the *deperturbation method* to assist in the selection of the possible isotopomers and reinforce our assignments. Another, more recent, study by Krätschmer *et al.*⁹⁹ has suggested different assignments in the frequency interval where the ν_9 mode of C₁₂ has been previously identified; however, the error in their proposed reassignment,

which is apparent in the light of further evidence from the present work that reaffirms Ding *et al.*'s assignments, will be presented later in this Chapter.

7.2 Results and discussion for C₈

Let us start with the $\nu_5=2071.4\text{ cm}^{-1}$ vibration of linear C₈ that has an interaction with the nearby $\nu_1(\sigma_g)$ mode, calculated to be only 23.7 cm^{-1} lower in frequency (see TABLE XIV). Although the strong interaction may permit the appearance of some of the isotopomer bands of the IR forbidden $\nu_1(\sigma_g)$ mode in the spectrum, complicating the isotopic analysis, it is clear from discussions in CHAPTERS III and IV, that a complete isotopic characterization may still be possible.

TABLE XIV. DFT B3LYP/cc-pVDZ predicted vibrational frequencies and band intensities for (ℓ -C₈)

Vibrational mode	Frequency (cm ⁻¹)	Infrared intensity (km/mol)
$\nu_1(\sigma_g)$	2144.4	0.0
$\nu_2(\sigma_g)$	2032.9	0.0
$\nu_3(\sigma_g)$	1404.3	0.0
$\nu_4(\sigma_g)$	516.4	0.0
$\nu_5(\sigma_u)$	2168.2	1991.1
$\nu_6(\sigma_u)$	1770.1	735.3
$\nu_7(\sigma_u)$	979.3	17.7
$\nu_8(\pi_g)$	706.1	(0.0)2
$\nu_9(\pi_g)$	302.9	(0.0)2
$\nu_{10}(\pi_g)$	412.6	(0.0)2
$\nu_{11}(\pi_u)$	584.1	(0.11)2
$\nu_{12}(\pi_u)$	263.5	(10.8)2
$\nu_{13}(\pi_u)$	64.9	(9.0)2

The cartoon in Fig. 43 is shown in order to better visualize the shift patterns prediction by the DFT calculations at the B3LYP/cc-pVDZ level using (a) 90%¹²C/10%¹³C and (b) 90%¹³C/10%¹²C mixtures for the coupled $\nu_1(\sigma_u)$ and $\nu_5(\sigma_u)$ modes of linear ¹²C₈ and ¹³C₈. Fig. 43(a) we can see that the IR-allowed shifts for the $\nu_5(\sigma_u)$ mode of linear ¹²C₈ are restricted to a small frequency interval 2060.0 - 2071.5 cm⁻¹. The black bar at ~2048.7 cm⁻¹ represents the position of the main frequency for the IR-forbidden $\nu_1(\sigma_g)$ mode of linear ¹²C₈. On the low frequency side we can see the IR-allowed shifts for the IR-forbidden $\nu_1(\sigma_g)$ mode of linear ¹²C₈, lying in the interval 2024.0 - 2049.0 cm⁻¹. The corresponding shifts for the $\nu_5(\sigma_u)$ mode of linear ¹³C₈ [see Fig. 43(b)] are spread over a wider frequency range 1988.0 - 2020.0 cm⁻¹ and the shifts

for the $\nu_1(\sigma_g)$ mode of linear $^{13}\text{C}_8$ are located in the interval 1960.0 - 1982.0 cm^{-1} . The labeling in Fig. 43 (a) and (b) follows the convention used in the previous chapters.

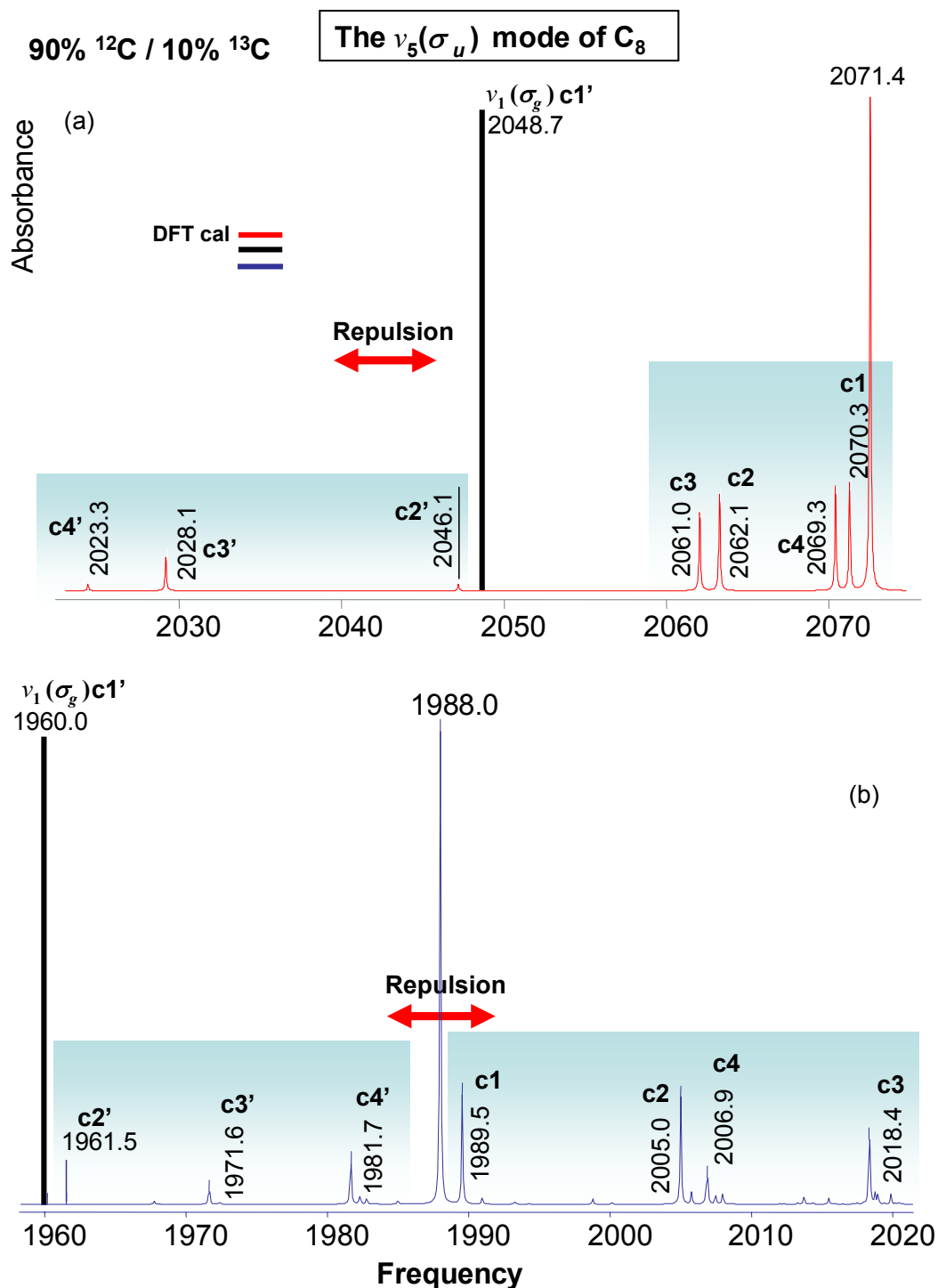


Fig. 43. The spectra are derived from DFT calculations at the B3YLP/cc-pVDZ level of the isotopic shifts with a (a) 10% ^{12}C /10% ^{13}C mixture (b) 90% ^{13}C /10% ^{12}C mixture. The bar in black is only for the purpose of illustrating where the interacting infrared forbidden $\nu_1(\sigma_g)$ mode would appear. We can see also a representation of the repulsion between the shifts of the interacting ν_1 and ν_5 modes.

The interaction between the $\nu_1(\sigma_g)$ and $\nu_5(\sigma_u)$ modes of linear C_8 enables the observation of the 2046.1(c2'), 2028.1(c3'), and 2023.3 cm^{-1} (c4') isotopomer bands for the ν_1 mode of linear $^{12}C_8$; however, they are not as intense as the mirrored 1961.5 (c2') 1971.6 (c3') and 1981.7 cm^{-1} (c4') isotopomers for the $\nu_5(\sigma_u)$ mode of linear $^{13}C_8$. We proceed with the analysis considering the shift-sets corresponding to the $\nu_5(\sigma_u)$ mode for linear $^{12}C_8$ and $^{13}C_8$. In Fig. 40(a) a prominent band is located at 2071.4 cm^{-1} (A), which Vala *et al*⁹⁷. have suggested for the $\nu_5(\sigma_u)$ mode of linear C_8 without, however, offering any supporting isotopic shifts. To the lower frequency side of this band, are four absorptions that are candidates for the single ^{12}C -substituted $^{12}C^{13}C_7$ isotopomers at 2070.3, 2067.9, 2061.7 and 2059.3 cm^{-1} , forming the set SSC12. These shift candidates seem to be correlated under annealing as shown in the spectra in Fig. 44(a), (b) and (c).

7.3 Assignment of the isotopomers for the $\nu_5(\sigma_u)$ mode of C_8

In Fig. 44 the observed bands at 2070.3 and 2061.7 cm^{-1} agree respectively, with the 2070.3 cm^{-1} calculated for the 13-12-12-12-12-12-12-12 (c1) isotopomer and the 2062.1 cm^{-1} frequency predicted for the 12-13-12-12-12-12-12-12 (c2) isotopomer.

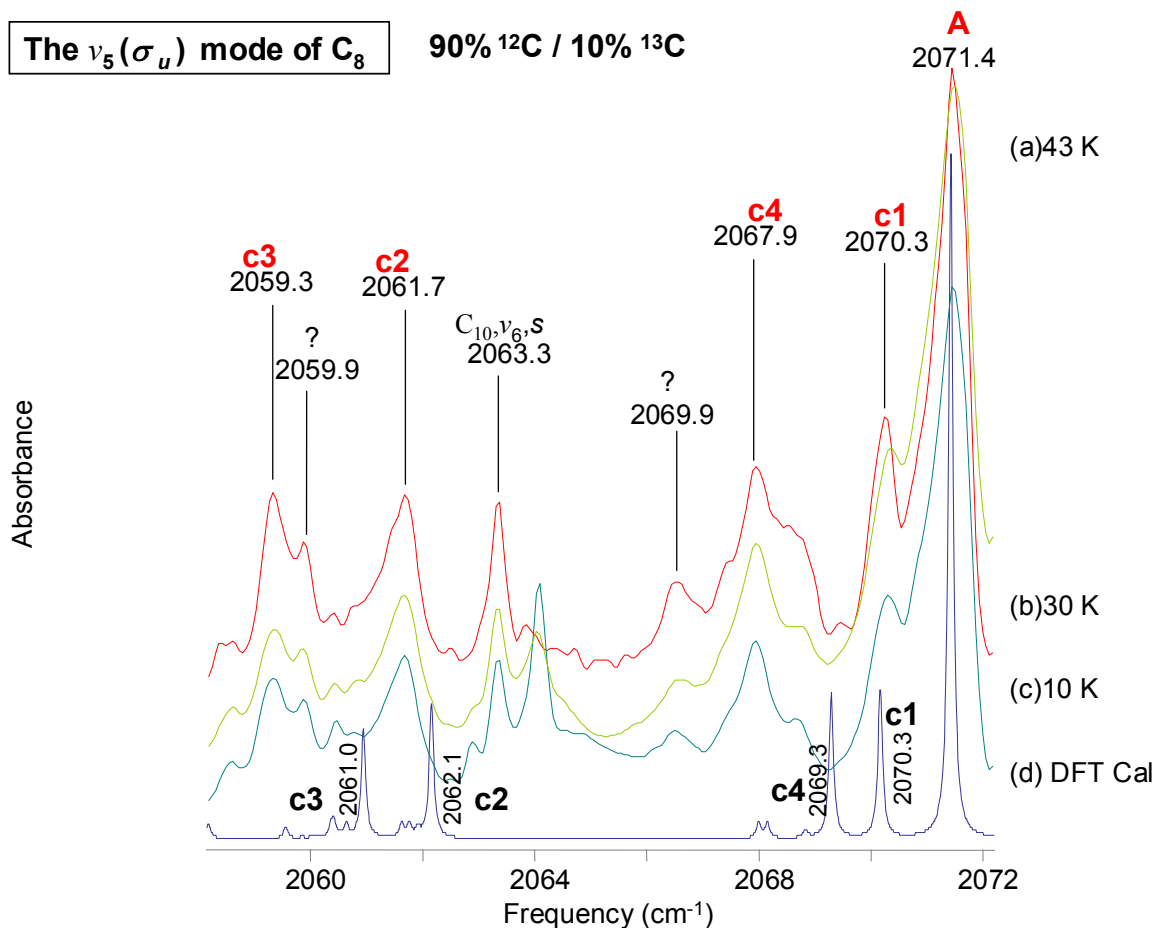


Fig. 44. Comparison of observed FTIR annealed spectra (a)43 K (b) 30 K and (c) 10 K of the $\nu_5(\sigma_u)$ mode of linear C_8 and its single ^{13}C -isotopic shifts using 90% ^{12}C and 10% ^{13}C carbon enrichments, and (d) a simulated spectrum derived from the DFT calculations at the B3YLP/cc-pVDZ level using the same enrichment values.

The observed band at 2059.3 cm^{-1} is 1.7 cm^{-1} away from the 2061.0 cm^{-1} frequency calculated for the 12-12-13-12-12-12-12-12 (c3) isotopomer. This is a relatively large difference but results from the repulsion to high frequency caused by coupling with the infrared inactive $\nu_1(\sigma_g)$ mode. This band has a broadened profile in its wings probably due to overlap by other double substituted isotopomers. The 2059.3 cm^{-1} absorption (c3) has a band growing to its high frequency side at 2059.9 cm^{-1} but it is considerably weaker than the c1 isotopomer absorption

and will be assigned to another shift. The isotopomer absorption observed at 2067.9 cm^{-1} is similarly 1.4 cm^{-1} lower than the calculated frequency at 2069.3 cm^{-1} for the 12-12-12-13-12-12-12-12 (c4) isotopomer; however, its behavior under annealing is clearly correlated with the already assigned (c1), (c2), and (3) isotopomers. It is a relatively broad band at its base because of bands growing in on both sides, probably resulting from the overlap of doubly substituted isotopomers or shifts possibly belonging to other C_n species. We now have a SSC12 shift set composed of the $2070.3(\text{c1})$, $2061.7(3)$, $2059.3(\text{c2})$, and $2067.9(\text{c4})\text{ cm}^{-1}$ isotopomer bands as shown in Table XV.

In Fig. 41 the spectra for 90% ^{12}C / 10% ^{13}C are shown. The absorption at 1988.0 cm^{-1} (B), which is a factor of $\sim\sqrt{12/13}$ of the 2071.4 cm^{-1} frequency for $^{12}\text{C}_8$ is identified as belonging to the fully ^{13}C -substituted isotopomer. In Fig. 41 (a) to the high frequency side of the 1988.0 cm^{-1} band, we can see the shift pattern for the single ^{13}C -substituted ($^{12}\text{C}^{13}\text{C}_7$) isotopomers of the $\nu_5(\sigma_u)$ mode of C_8 . The band observed at 1990.6 cm^{-1} is close to the 12-13-13-13-13-13-13-13(c1) isotopomer band calculated to be at 1989.5 cm^{-1} and is well isolated. The band at 1992.7 cm^{-1} , which is much weaker than the proposed shifts, is an unidentified C_n absorption. The band at 1995.1 cm^{-1} is a potential shift that may belong to the cyclic- C_{10} molecule currently under investigation. The band at 2016.8 cm^{-1} is close to the 2018.4 cm^{-1} frequency predicted for the 13-13-12-13-13-13-13-13(c3) isotopomer. Three bands at 2003.2 , 2006.4 and 2009.6 cm^{-1} occur in the vicinity of the bands calculated at 2005.0 and 2006.9 cm^{-1} for the 13-12-13-13-13-13-13-13(c2) and 13-13-13-12-13-13-13-13(c4) isotopomers. A shift set formed by assigning the 2003.2 , and 2006.4 cm^{-1} absorptions to the c2 and c4 isotopomers, did not behave as well under the analysis of the *deperturbation method* as the set formed by assigning the 2006.4 cm^{-1} absorption to the c2 isotopomer and the 2009.6 cm^{-1} , to the c4 isotopomer, in spite of the latter

being 2.7 cm^{-1} higher than its predicted frequency. Although this is a large frequency difference it originates with the repulsion between $\nu_5(\sigma_u)$ and $\nu_1(\sigma_g)$ modes. The final SSC13 set of shifts is thus $1990.6(\text{c}1)$, $2006.4(\text{c}2)$, $2016.8(\text{c}3)$ and $2009.6(\text{c}4) \text{ cm}^{-1}$, and we can see from Fig. 41 that they are well correlated under annealing.

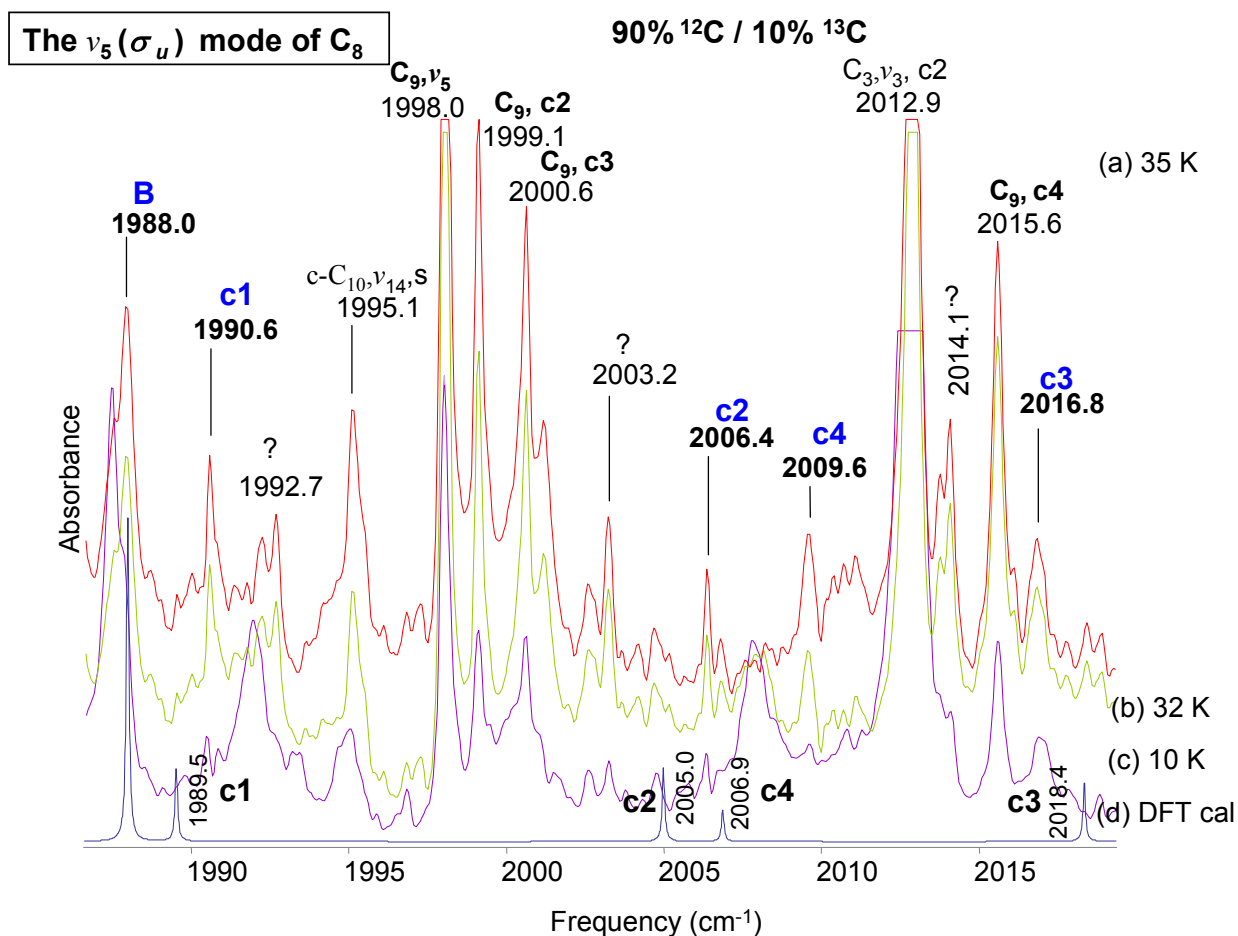


Fig. 45. Comparison of observed FTIR annealed spectra (a) 35 K (b) 32 K and (c) 10 K of the $\nu_5(\sigma_u)$ mode of linear C_8 and its single ^{12}C -isotopic shifts using 10% ^{12}C and 90% ^{13}C carbon enrichments, and (d) a simulated spectrum derived from the DFT calculations at the B3YLP/cc-pVDZ level using the same enrichment values.

TABLE XV. Comparison of observed and predicted DFT (B3LYP/cc-pVDZ) frequencies for single ^{13}C -substituted isotopomers of $^{12}\text{C}_8$, and single ^{12}C -substituted isotopomers of $^{13}\text{C}_8$, for the ν_5 mode.

Isotopomer	ν_{obs}	B3LYP/cc-pVDZ		$\Delta\nu$ $\nu_{\text{obs}} - \nu_{\text{scaled}}$
		ν	ν_{scaled}	
12-12-12-12-12-12... (A)	2071.4	2168.2	2071.4 ¹	0.0
13 -12-12-12-12-12... (c1)	2070.3	2167.0	2070.3	0.0
12- 13 -12-12-12-12... (c2)	2061.7	2158.5	2062.1	-0.4
12-12- 13 -12-12-12... (c3)	2059.3	2157.3	2061.0	-1.7
12-12-12- 13 -12-12... (c4)	2067.9	2166.0	2069.3	-1.4
13-13-13-13-13-13... (B)	1988.0	2082.9	1988.0 ²	0.0
12 -13-13-13-13-13... (c1)	1990.6	2084.5	1989.5	1.1
13- 12 -13-13-13-13... (c2)	2006.4	2100.7	2005.0	1.4
13-13- 12 -13-13-13... (c3)	2016.8	2114.7	2018.4	-1.6
13-13-13- 12 -13-13... (c4)	2009.6	2102.7	2006.9	2.7

¹Scaling factor $\nu_{\text{obs}}/\nu \sim 0.95535$

²Scaling factor $\nu_{\text{obs}}/\nu \sim 0.95443$

The foregoing discussion is summarized in Table XV. The first column lists the isotopomers and the labeling of the isotopomers follows the convention used in earlier discussion. The top section of the table shows the shifts for the single ^{13}C -substituted $^{13}\text{C}^{12}\text{C}_7$ isotopomers for the $\nu_5(\sigma_u)$ of linear $^{13}\text{C}_8$ and in the bottom section, the shifts for the single ^{12}C -substituted $^{12}\text{C}^{13}\text{C}_7$ isotopomers. The predicted frequencies for the single ^{13}C -substituted $^{13}\text{C}^{12}\text{C}_7$ isotopomers in the third column labeled ν , are scaled by a factor of ~ 0.95535 obtained by taking the ratio of the observed main frequency 2071.4 cm^{-1} with the corresponding DFT calculated main frequency of 2168.2 cm^{-1} of the ν_5 mode of $^{12}\text{C}_8$. By similarly taking the ratio of the predicted and observed frequencies for the ν_5 mode of $^{13}\text{C}_8$ we obtain a scaling factor of ~ 0.95443 for the ^{12}C substituted $^{12}\text{C}^{13}\text{C}_7$ isotopomers. In summary, Fig. 46, presents a cartoon representing the calculated and observed isotopic frequencies for the $\nu_5(\sigma_u)$ and $\nu_1(\sigma_g)$ modes of linear C_8 .

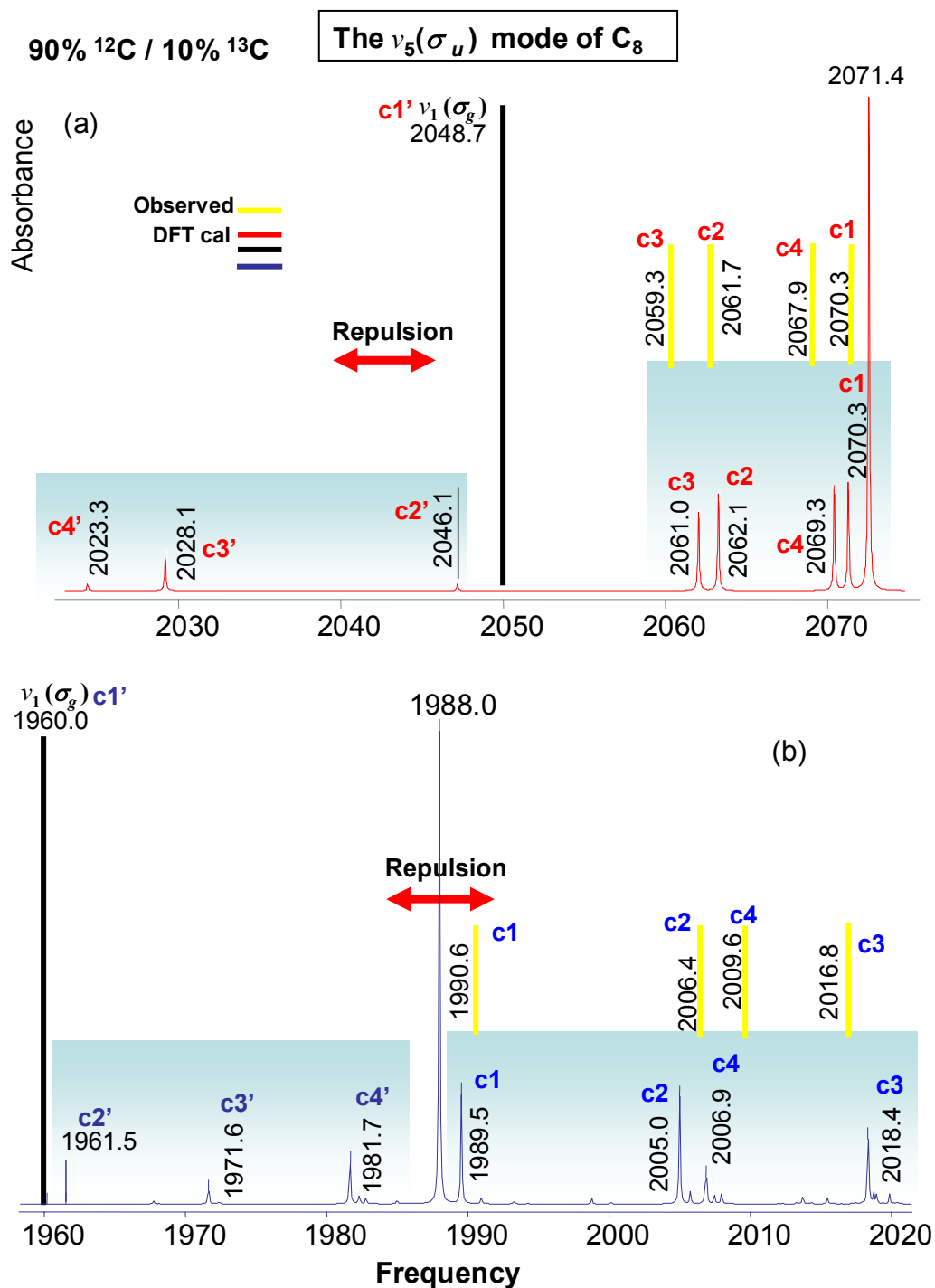


Fig. 46. Both (a)(red) and (b)(blue) are spectra derived from the DFT calculations at the B3YLP/cc-pVDZ level and its isotopic shifts with (a) 10% ^{12}C and 10% ^{13}C mixture (b) 90% ^{13}C and 10% ^{12}C , in comparison with the observed shifts, obtained by using the same isotopic mixtures. The bar in black is only for the purpose of illustrate where the interacting non infrared active $\nu_1(\sigma_g)$ mode would appear. We can see also a representation of the repulsion between the shifts of the interacting ν_1 and ν_5 modes.

7.4 Assignment of the isotopomers for the $\nu_6(\sigma_u)$ mode of C_8

In this case there are no nearby infrared inactive modes to interact with $\nu_6(\sigma_u)$ on isotopic substitution. We can see in Figure 47 (a) a prominent band located at 1710.5 cm^{-1} (A) which Vala previously identified as the $\nu_6(\sigma_u)$ mode of linear C_8 . In the present work we can readily identify the shifts bands for the single ^{12}C -substituted $^{12}C^{13}C_7$ isotopomers: $1702.4(\text{c1})$, $1696.2(\text{c2})$, $1705.7(\text{c3})$, and 1701.9 cm^{-1} (c4). As can be seen by comparison the DFT calculated spectrum in Fig. 47(b) there is excellent agreement with the DFT simulated spectrum.

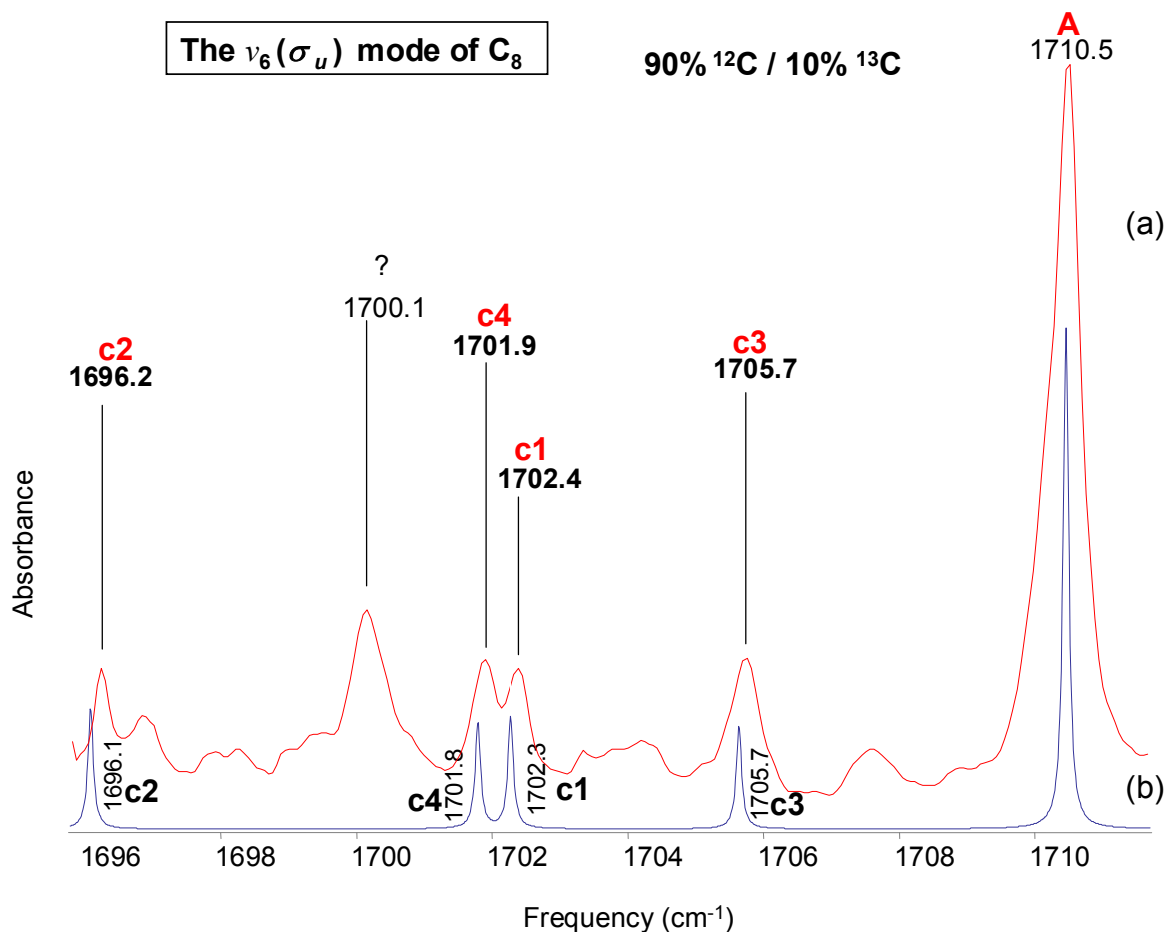


Fig. 47. Comparison of observed FTIR annealed spectra (a) the $\nu_5(\sigma_u)$ mode of linear C_8 and its single ^{13}C -isotopic shifts using 90% ^{12}C and 10% ^{13}C carbon enrichments, and (b) a simulated spectrum derived from the DFT calculations at the 3YLP/cc-pVDZ level using the same enrichment values.

There is also a band at 1700.1 cm^{-1} that is clearly more intense than any of the already assigned c1, c2, c3 and c4, isotopomer bands showing that there is no correlation between them, and it remains an unknown C_n species

The absorption observed at 1644.2 cm^{-1} (see Fig. 48), which is a factor $\sim \sqrt{12/13}$ of the 2071.4 cm^{-1} frequency, is identified as belonging to the fully ^{13}C -substituted isotopomer, which was produced by the evaporation of a carbon mixture of 10% ^{12}C /90% ^{13}C . In Fig. 48 (c) to the

high frequency side of the 1644.2 cm^{-1} (B) band we can see the shift pattern for the single ^{12}C -substituted $^{12}\text{C}^{13}\text{C}_7$ isotopomers of the $\nu_6(\sigma_u)$ mode of C_8 . Prominent isotopic shifts appear at 1652.7 (c1) 1655.3 (c2), 1648.2 (c3) and 1651.1cm^{-1} (c4) and are listed in Table XVI.

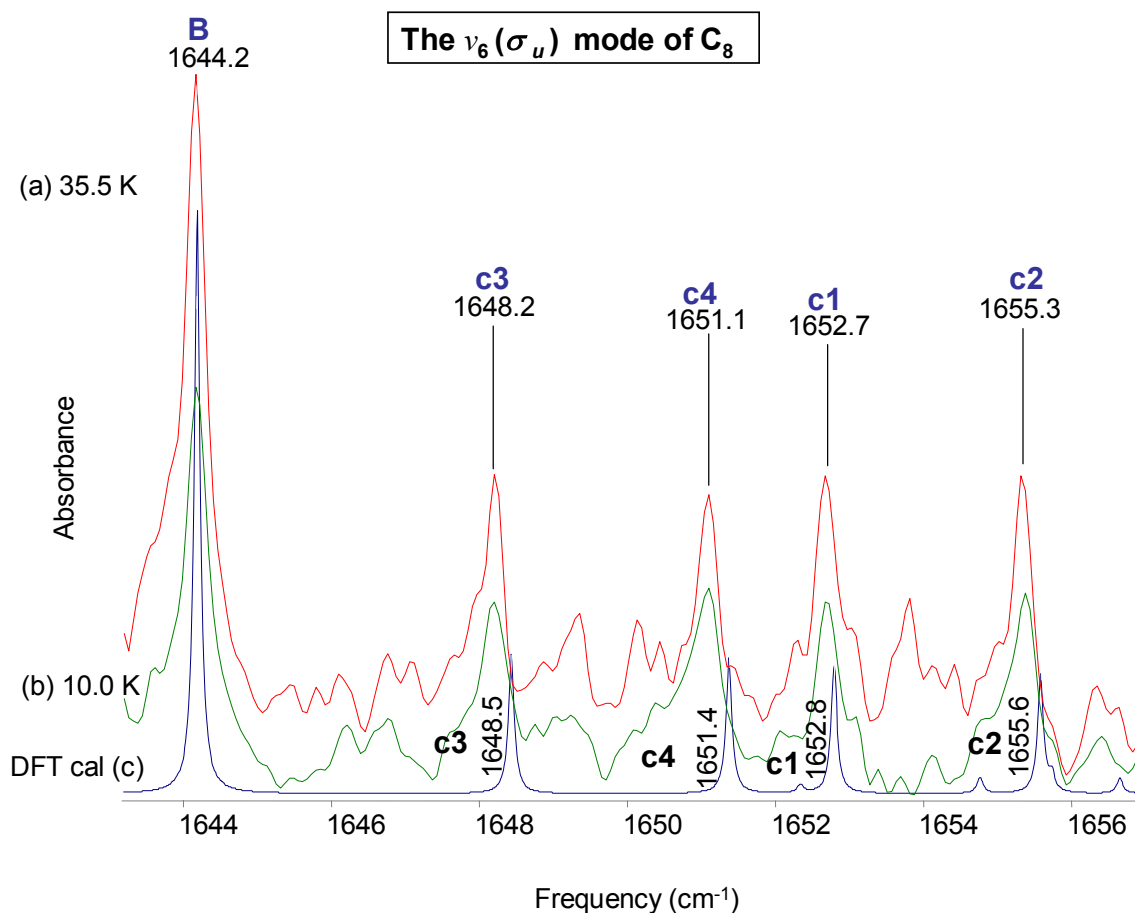


Fig. 48. Comparison of observed FTIR annealed spectra (a)35.5 K and (b) 10.0 K of the $\nu_6(\sigma_u)$ mode of linear C_8 and its single ^{13}C isotopic shifts using 90% ^{12}C and 10% ^{13}C carbon enrichments, and (c) a simulated spectrum derived from the DFT calculations at the B3YLP/cc-pVDZ level using the same enrichment values.

The top half of Table XVI, shows the set of shifts for the single ^{13}C -substituted $^{13}\text{C}^{12}\text{C}_7$ isotopomers for the $\nu_6(\sigma_u)$ mode of the linear $^{13}\text{C}_8$ and in the bottom half the shifts for the single ^{12}C -substituted $^{12}\text{C}^{13}\text{C}_7$ isotopomers. The predicted frequencies for the single ^{13}C -substituted

$^{13}\text{C}^{12}\text{C}_8$ isotopomers in the third column (labeled ν) of Table XVI, are scaled by a factor of ~ 0.96627 obtained by taking the ratio of the observed main frequency 1710.5 cm^{-1} with the corresponding DFT calculated main frequency of 1770.2 cm^{-1} of the ν_5 mode of $^{12}\text{C}_8$. By similarly taking the ratio of the predicted and observed frequencies for the ν_6 mode of $^{13}\text{C}_8$ we obtain a scaling factor of ~ 0.96689 for the ^{12}C substituted $^{12}\text{C}^{13}\text{C}_7$ isotopomers. Agreement is excellent. This is the first confirmation by isotopic measurement of the identification of the $\nu_5(\sigma_u)$ and $\nu_6(\sigma_u)$ vibrational fundamentals of C_8 .

TABLE XVI. Comparison of observed and predicted DFT (B3LYP/cc-pVDZ) frequencies for single ^{13}C -substituted isotopomers of $^{12}\text{C}_8$, and single ^{12}C -substituted isotopomers of $^{13}\text{C}_8$, for the ν_6 mode.

Isotopomer	ν_{obs}	B3LYP/cc-pVDZ		$\Delta\nu$ $\nu_{\text{obs}} - \nu_{\text{scaled}}$
		ν	ν_{scaled}	
12-12-12-12-12-12... (A)	1710.5	1770.2	1710.5^1	0.0
13 -12-12-12-12-12... (c1)	1702.4	1761.7	1702.3	0.1
12- 13 -12-12-12-12... (c2)	1696.2	1755.3	1696.1	0.1
12-12- 13 -12-12-12... (c3)	1705.7	1765.2	1705.7	0.0
12-12-12- 13 -12-12... (c4)	1701.9	1761.2	1701.8	0.1
13-13-13-13-13-13... (B)	1644.2	1700.5	1644.2^2	0.0
12 -13-13-13-13-13... (c1)	1652.7	1709.4	1652.8	-0.1
13- 12 -13-13-13-13... (c2)	1655.3	1712.3	1655.6	-0.3
13-13- 12 -13-13-13... (c3)	1648.2	1704.9	1648.5	-0.3
13-13-13- 12 -13-13... (c4)	1651.1	1707.9	1651.4	-0.3

¹Scaling factor $\nu_{\text{obs}}/\nu \sim 0.96627$

²Scaling factor $\nu_{\text{obs}}/\nu \sim 0.96689$

7.5 Results and discussion for C₁₂

The first study of the C₁₂ carbon chain was done by Ding *et al.*¹⁰⁰ in the TCU Molecular Physic Lab. They reported the identification of two vibrational fundamentals $\nu_8(\sigma_u) = 1999.7$ and $\nu_9(\sigma_u) = 1818.0$ cm⁻¹ and the tentative identification of a third, $\nu_7(\sigma_u) = 2140.6$ cm⁻¹. Because of the lack of isotopic data for the single ¹³C-substituted ¹³C¹²C₁₁ isotopomers a definite assignment for the $\nu_7(\sigma_u)$ mode was not possible. Experimental data obtained in the present work give the complete ¹³C and ¹²C isotopic spectra for the ν_7 , which can be tested with the *deperturbation method* in order to provide better insight during the selection of candidates for the isotopic shifts that will reinforce our assignments.

Recently, Krätschmer *et al.*⁹⁹ have presented results challenging the C₁₂ vibrational assignments of Ding *et al.*¹⁰⁰ and attributing the absorptions to carbon-oxygen species. In referring to the strategy of basing assignments on comparisons between observed and calculated ¹²C and ¹³C isotopic data in Ar matrices they claim that “the complexity of the matrix spectra leads to great uncertainties”. Unfortunately they do not define either the nature or the size of these uncertainties. Their assertion is remarkable since their own results on C_nO species were obtained by a similar strategy using ¹⁶O and ¹⁸O isotopic shifts, combined with carbon vapor deposition with a matrix gas mixture of Ar and O₂ and making comparisons with theoretical calculations. Specifically, they reassign the absorption at 1818.0 cm⁻¹, which Ding *et al.*¹⁰⁰ showed with ¹³C isotopic shifts is the $\nu_9(\sigma_u)$ mode of C₁₂, to C₁₃ without any evidence either against the C₁₂ assignment or in favor of their new assignment. Since research conducted for this dissertation has employed both single ¹³C shifts in ¹²C_n molecules and the mirror ¹²C shifts in

$^{13}\text{C}_n$, it seemed worthwhile to further strengthen the C_{12} assignment for the $\nu_9(\sigma_u)$ mode as well as try to test the assignment for $\nu_7(\sigma_u)$ mode, mentioned earlier, which was considered tentative by *Ding et al.*¹⁰⁰ In addition because of the development of the deperturbation method by Garcia and Rittby, possible effects of mode interactions could be considered.

7.6 Assignment of the isotopomers for the $\nu_7(\sigma_u)$ mode of C_{12}

The $\nu_7(\sigma_u)$ mode is close to the IR inactive $\nu_1(\sigma_g)$ mode that lies 24.3 cm^{-1} to its high frequency side (see Table XVII), and is expected to interact strongly with $\nu_7(\sigma_u)$.

Table XVII. DFT B3LYP/cc-pVDZ predicted vibrational frequencies and band intensities for ($\ell\text{-C}_{12}$)

Vib mode	Freq (cm^{-1})	IR Int (km/mol)	Vib mode	Freq (cm^{-1})	IR Int (km/mol)
$\nu_1(\sigma_g)$	2212.4	0.0	$\nu_{15}(\pi_u)$	696.0	(0.5)2
$\nu_2(\sigma_g)$	2003.4	0.0	$\nu_{16}(\pi_u)$	503.9	(0.6)2
$\nu_3(\sigma_g)$	1984.2	0.0	$\nu_{17}(\pi_u)$	295.2	(5.8)2
$\nu_4(\sigma_g)$	1568.3	0.0	$\nu_{18}(\pi_u)$	222.3	(0.0)2
$\nu_5(\sigma_g)$	996.6	0.0	$\nu_{19}(\pi_u)$	146.5	(8.9)2
$\nu_6(\sigma_g)$	349.7	0.0	$\nu_{20}(\pi_u)$	79.3	(0.0)2
$\nu_7(\sigma_u)$	2188.2	2412.6	$\nu_{21}(\sigma_u)$	29.8	(4.8)2
$\nu_8(\sigma_u)$	2112.7	4798.5			
$\nu_9(\sigma_u)$	1815.3	1191.4			
$\nu_{10}(\sigma_u)$	1290.1	120.9			
$\nu_{11}(\sigma_u)$	682.7	0.0			
$\nu_{12}(\pi_g)$	791.7	(0.0)2			
$\nu_{13}(\pi_g)$	595.9	(0.0)2			
$\nu_{14}(\pi_u)$	395.4	(0.0)2			

The simulations from DFT calculations at the B3YLP/cc-pVDZ level using (a) 90%¹²C/10%¹³C and (b) 90%¹³C/10%¹²C mixtures for the coupled $\nu_1(\sigma_u)$ and $\nu_7(\sigma_u)$ modes of linear ¹²C₁₂ and ¹³C₁₂ are shown in Fig. 49. In Fig. 45(a) we can see that the IR active shifts for the $\nu_7(\sigma_u)$ mode of linear ¹²C₁₂ are located to the low frequency side of the main frequency band at 2140.3 cm⁻¹(A) in the frequency interval 2123.0 - 2141.0 cm⁻¹. The bar in black at ~2164.6 cm⁻¹ represents the IR inactive $\nu_1(\sigma_g)$ mode of linear ¹²C₁₂ with the shifts lying in the interval 2154.0 - 2164.0 cm⁻¹. The corresponding frequency for the $\nu_7(\sigma_u)$ mode of fully substituted ¹³C₁₂ is calculated to be at 2188.2 (see Table XVII , scaled to be at 2058.6 cm⁻¹ (see Table XVIII) and the infrared inactive $\nu_1(\sigma_g)$ mode of linear ¹³C₁₂ is calculated to be at 2082.6 cm⁻¹, as can be seen in the cartoon in Fig. 49 (b). Their corresponding shift sets are in the intervals 2058.0 to 2076.0 cm⁻¹ and 2082.0 to 2102.0 cm⁻¹ respectively. Unfortunately, the shifts for the $\nu_1(\sigma_g)$ mode are not intense enough to be observed above the noise level so only the $\nu_7(\sigma_u)$ shifts will be considered.

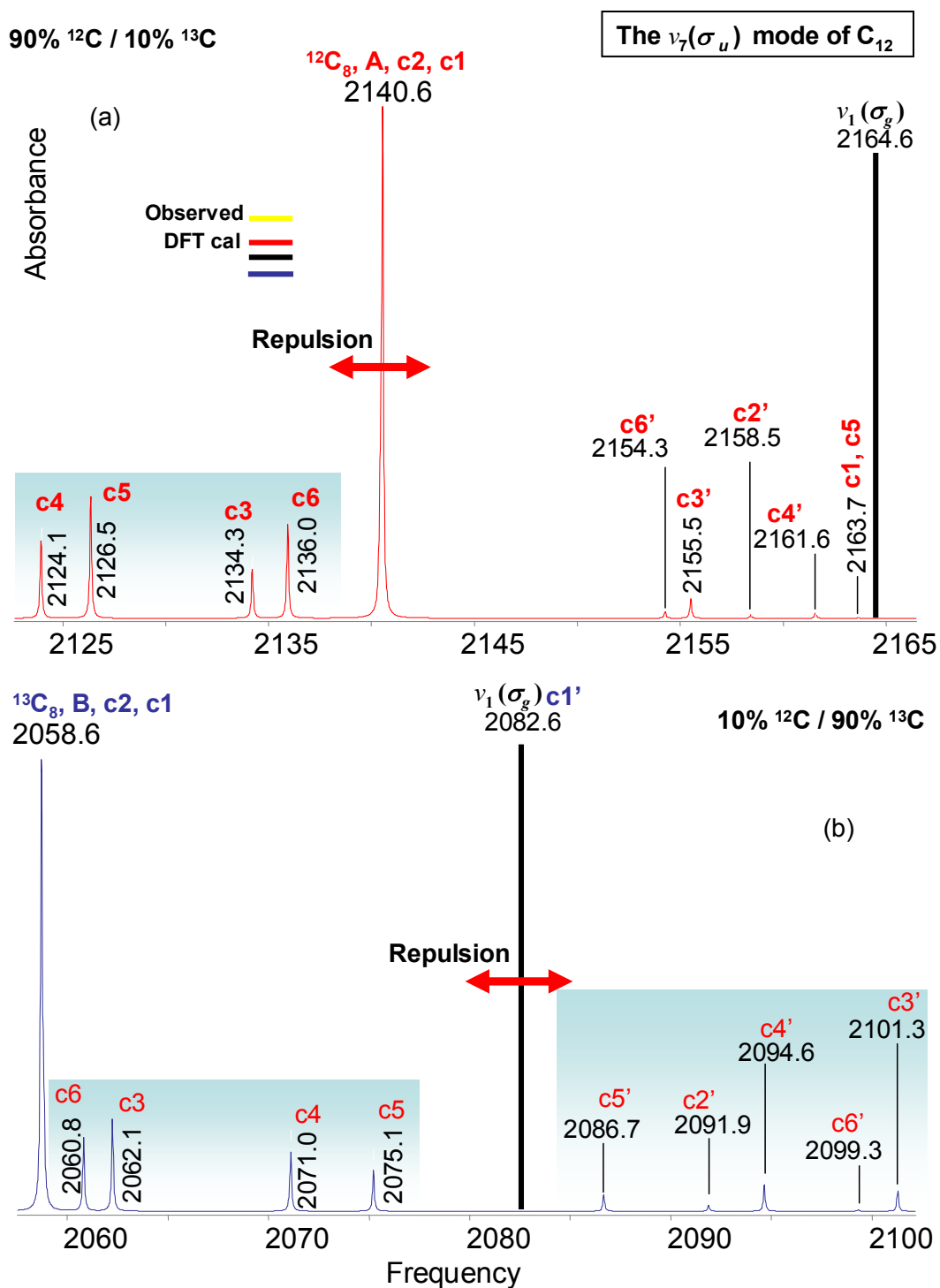


Fig. 49. Both (a)(red) and (b)(blue) are spectra derived from the DFT calculations at the B3YLP/cc-pVDZ level and its isotopic shifts with (a) 10% ^{12}C and 10% ^{13}C mixture (b) 90% ^{13}C and 10% ^{12}C . The bar in black is only for the purpose of illustrate where the interacting non infrared active $\nu_1(\sigma_g)$ mode would appear. We can see also a representation of the repulsion between the shifts of the interacting ν_1 and ν_7 modes.

In Fig. 50 (a) the prominent band located at 2140.6 cm^{-1} (A) is the $\nu_7(\sigma_u)$ mode of linear C_{12} . To the low frequency side of this band are the candidates $2136.7(\text{c6})$, $2134.5(\text{c3})$, $2126.3(\text{c5})$, and $2123.8(\text{c4}) \text{ cm}^{-1}$, for the single ^{12}C -substituted $^{12}\text{C}^{13}\text{C}_{11}$ isotopomer shifts called SSC12. Two other isotopomer bands predicted at $2140.6(\text{c1})$ and $2140.5(\text{c2}) \text{ cm}^{-1}$ would be overlapped by the main band at 2140.6 cm^{-1} . A similar set of isotopomers were reported by X.D. Ding *et al.*¹⁰⁰ in their earlier work using a spectrum with substantially greater noise levels. Nevertheless, there is a discrepancy with our selected isotopomers and Ding *et al.* in the identification of the c3 and c6 isotopomers, reported by them at $2133.4(\text{c3})$ and $2134.7 \text{ cm}^{-1}(\text{c6})$, respectively, which do not appear in our spectrum (see Fig. 50). In order to settle the matter the mirror shift set measured for the single ^{12}C -substituted $^{12}\text{C}^{13}\text{C}_{11}$ isotopomers together with our set of isotopomers was submitted to the *deperturbation method*. The revised assignments are found to be the correct ones.

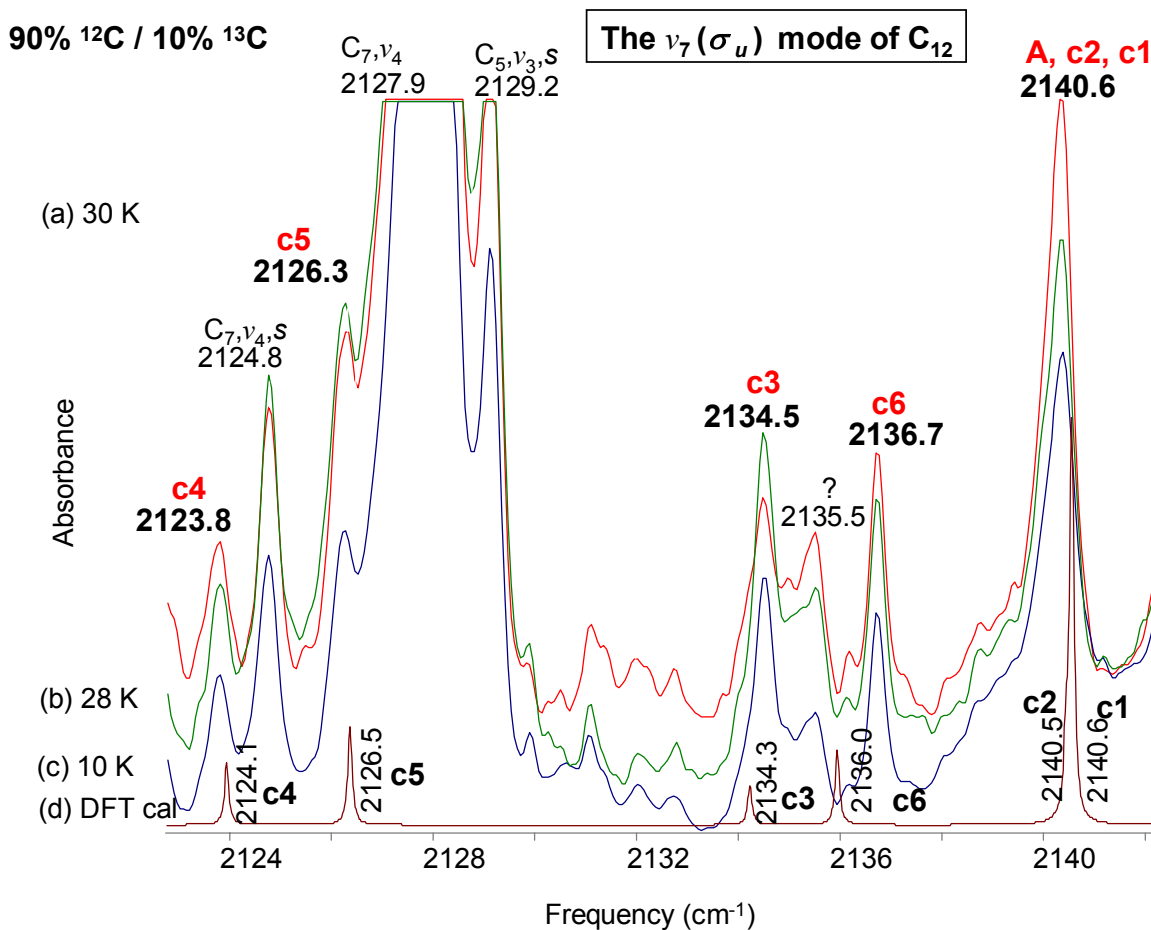


Fig. 50. Comparison of observed FTIR annealed spectra (a) 30 K, 28 K (b) and (c) 10 K of the $\nu_6(\sigma_u)$ mode of linear C_{12} and its single ^{13}C isotopic shifts using 90% ^{12}C and 10% ^{13}C carbon enrichments, and (c) a simulated spectrum derived from the DFT calculations at the B3YLP/cc-pVDZ level using the same enrichment values.

In looking at the details of assigning the frequency candidates for isotopomer bands (see Fig. 50), we note that the main band $\nu_6(\sigma_u)$ mode of linear C_{12} observed at 2140.6 cm^{-1} overlaps the bands at 2140.6 and 2140.5 cm^{-1} calculated for the 13-12-12-12-12-12-12-12-12-12-12-12 (c1) and 12-13-12-12-12-12-12-12-12-12-12-12 (c2) isotopomers respectively. The bands observed at 2134.5 and 2136.7 cm^{-1} are very close to the frequencies 2134.3 and 2136.0 cm^{-1} calculated for the 12-12-13-12-12-12-12-12-12-12-12-12 (c3) and 12-12-12-12-12-13-12-12-12-

12-12-12 (c6) isotopomers respectively. Their behavior under annealing shows them to be related. The intensity of the weaker band at 2135.5 cm^{-1} , although not consistent with the other shift candidates was tested by the *deperturbation method* as an alternative assignment for c3 and c6; however, its behavior forced us to dismiss it, leaving it as an unidentified C_n band. The bands observed at 2123.8 and 2126.3 cm^{-1} are close to the calculated bands at 2124.1 and 2126.5 cm^{-1} for the 12-12-13-12-12-12-12-12-12-12-12-12-12(c4) and 12-12-12-12-13-12-12-12-12-12-12-12-12 (c5) isotopomers. Thus we have set of shifts called SSC12 formed by the 2140.6 (c1), 2140.5 (c2) [overlapped by main band at 2140.6 cm^{-1} (A)], 2134.5 (c3), 2123.8 cm^{-1} (c4), 2126.3 (c5) and 2136.7 cm^{-1} (c6).

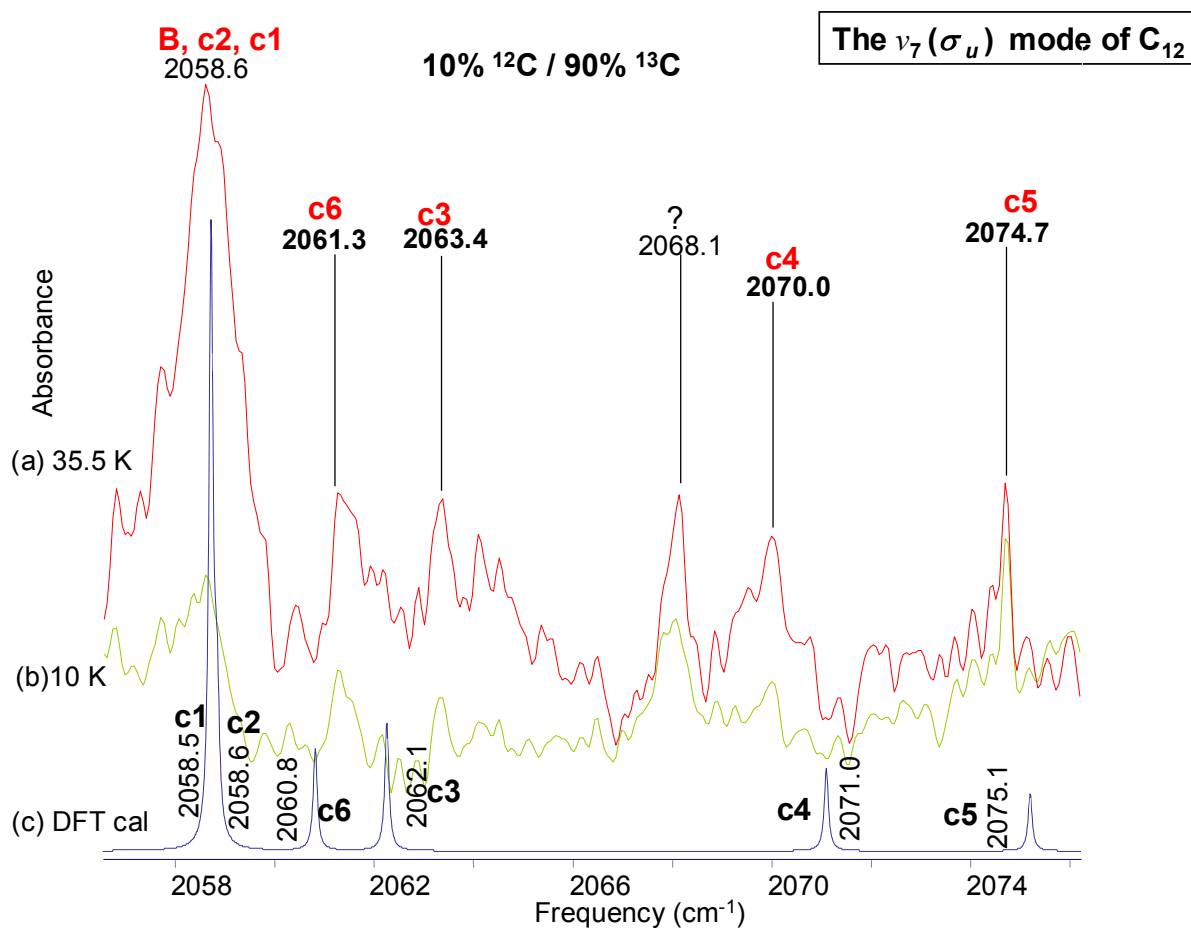


Fig. 51. Comparison of observed FTIR annealed spectra (a) 35.5 K and (b) 10.0 K of the $\nu_7(\sigma_u)$ mode of linear C_{12} and its single ^{13}C isotopic shifts using 90% ^{12}C and 10% ^{13}C carbon enrichments, and (c) a simulated spectrum derived from the DFT calculations at the B3YLP/cc-pVDZ level using the same enrichment values.

The absorption at 2058.6 (B) cm^{-1} (see Fig. 51), which is a factor $\sim \sqrt{12/13}$ of the 2140.6 cm^{-1} frequency, is identified as belonging to the fully ^{13}C -substituted isotopomer, which was produced by the evaporation of a carbon mixture of 10% $^{12}C/90\%$ ^{13}C . To the high frequency side of the 2058.6 cm^{-1} (B) band we can see the shift pattern named *SSC13* for the observed single ^{12}C -substituted $^{12}C^{13}C_{11}$ isotopomers of the $\nu_7(\sigma_u)$ mode of C_{12} at 2058.5 (c1) and 2058.6

(c2) [overlapped by the main band at 2058.6 (B)], 2063.4(c3), 2070.0 (c4), 2074.7 (c5) and 2061.3 (c6) cm^{-1} . The main $^{13}\text{C}_{12}$ bands at 2058.5 and 2058.6 cm^{-1} would overlap the 2058.6 cm^{-1} (B) calculated for the 12-13-13-13-13-13-13-13-13-13-13(c2) and 13-12-13-13-13-13-13-13-13-13-13(c2) isotopomer respectively. This shift set is in good agreement with the calculated as shown in Fig. 51 and Table XVIII, and tested well with the *deperturbation method*. The band at 2068.1 appears unrelated to the isotopomer candidates under annealing and it remains an unidentified C_n species.

TABLE XVIII. Comparison of observed and predicted DFT (B3LYP/cc-pVDZ) frequencies for single ^{13}C -substituted isotopomers of $^{12}\text{C}_{12}$, and single ^{12}C -substituted isotopomers of $^{13}\text{C}_{12}$, for the ν_7 mode.

Isotopomer	ν_{obs}	B3LYP/cc-pVDZ		$\Delta\nu$ $\nu_{\text{obs}} - \nu_{\text{scaled}}$
		ν	ν_{scaled}	
12-12-12-12-12-12...(A)	2140.6	2188.2	2140.6 ¹	0.0
13-12-12-12-12-12...(c1)	Overlapped ²	2188.2	2140.6	0.0
12-13-12-12-12-12...(c2)	Overlapped ³	2188.1	2140.5	0.0
12-12-13-12-12-12...(c3)	2134.5	2181.8	2134.3	0.2
12-12-12-13-12-12...(c4)	2123.8	2171.3	2124.1	-0.3
12-12-12-12-13-12...(c5)	2126.3	2173.8	2126.5	-0.2
12-12-12-12-12-13...(c6)	2136.7	2183.5	2136.0	0.7
13-13-13-13-13-13...(B)	2058.6	2102.1	2058.6 ⁴	0.0
12-13-13-13-13-13...(c1)	Overlapped ⁵	2102.1	2058.5	0.0
13-12-13-13-13-13...(c2)	Overlapped ⁶	2102.0	2058.6	0.0
13-13-12-13-13-13...(c3)	2063.4	2105.7	2062.1	1.3
13-13-13-12-13-13...(c4)	2070.0	2114.8	2071.0	-1.0
13-13-13-13-12-13...(c5)	2074.7	2118.9	2075.1	-0.4
13-13-13-13-13-12...(c6)	2061.3	2104.3	2060.8	0.5

¹Scaling factor $\nu_{\text{obs}}/\nu \sim 0.97824$

^{2,3}Overlapped by the main band at 2140.6 cm^{-1}

⁴Scaling factor $\nu_{\text{obs}}/\nu \sim 0.97940$

^{5,6}Overlapped by the main band at 2058.6 cm^{-1}

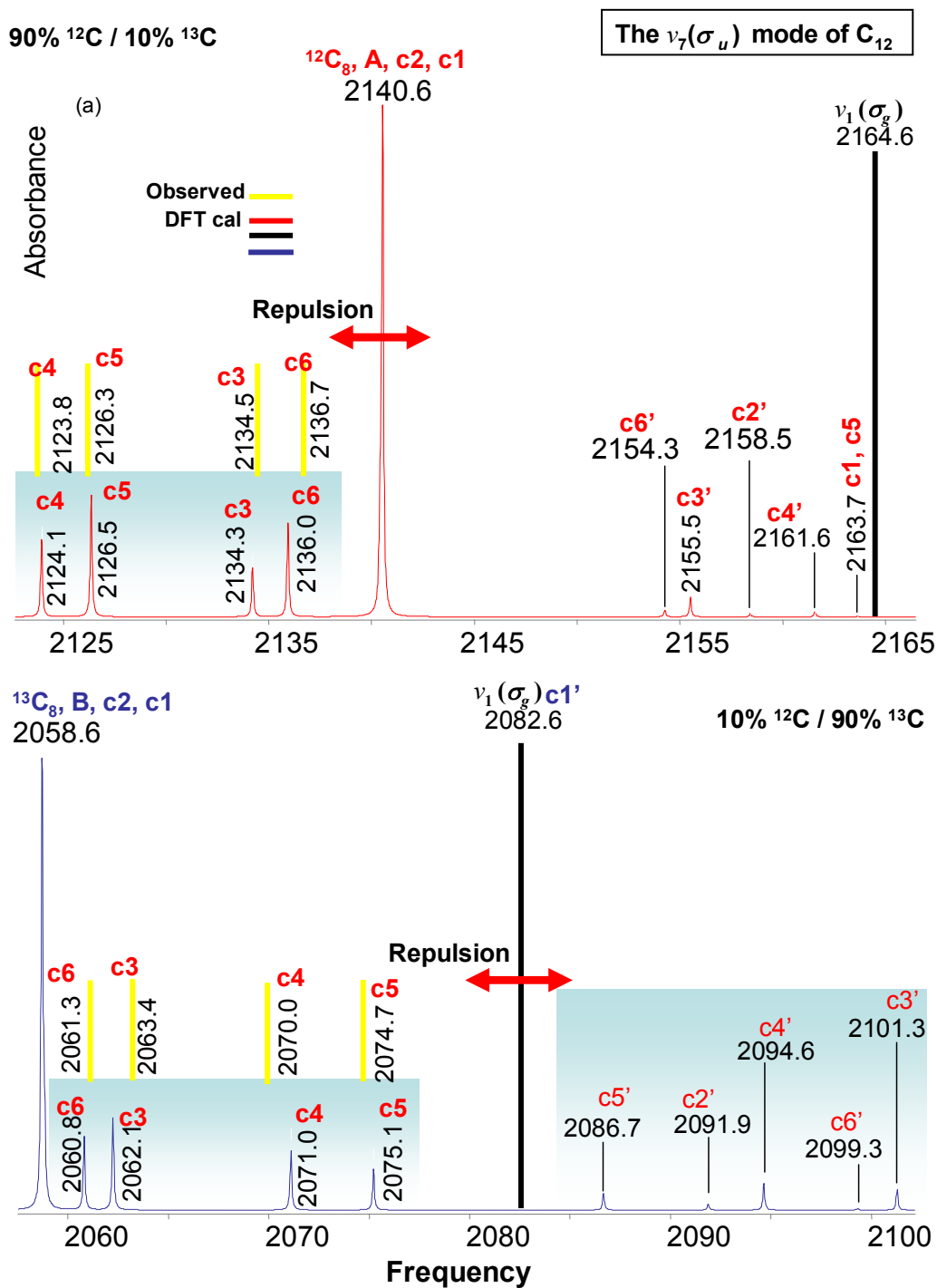


Fig. 52. Both (a)(red) and (b)(blue) are spectra derived from the DFT calculations at the B3YLP/cc-pVDZ level and its isotopic shifts with (a) 10% ^{12}C and 10% ^{13}C mixture (b) 90% ^{13}C and 10% ^{12}C . The bars in yellow are to show where the observed frequencies would be located. The bar in black is only for the purpose of illustrate where the interacting non infrared active $\nu_1(\sigma_g)$ mode would appear. We can see also a representation of the repulsion between the shifts of the interacting ν_1 and ν_7 modes.

7.7 Assignment of the isotopomers for the $\nu_8(\sigma_u)$ mode of C_{12}

Ding *et al.*¹⁰⁰ reported $\nu_8(\sigma_u)$ the second most intense mode to be located at 1997.2 cm^{-1} with an isotopic analysis performed on the single ^{12}C -substituted $^{12}\text{C}^{13}\text{C}_{11}$ isotopomers. New experimental data recently obtained give us the opportunity to observe with both the mirrored shift sets, the single ^{12}C -substituted $^{12}\text{C}^{13}\text{C}_{11}$ and the single ^{13}C -substituted $^{13}\text{C}^{12}\text{C}_{11}$ isotopomers. Both shift sets were processed through the *deperturbation method* to support our assignments. The closest IR-inactive $\nu_1(\sigma_g)$ mode lies at 99.7 cm^{-1} to the higher frequency side [see Table XVII] and is expected to have very weak interaction.

This particular mode appears in one of the most congested frequency intervals $1980.0\text{--}2000.0\text{ cm}^{-1}$ where the $\nu_8(\sigma_u)=1997.3\text{ cm}^{-1}$ mode of linear C_9 , which was analyzed earlier in Chapter IV is also located. The set of isotopomers reported by Ding *et al.*¹⁰⁰ coincide, with our own assignments except for the assigned frequencies for the c1 and c6 isotopomers. The c1 and c6 were considered by Ding to have collapsed into the band observed at 1995.0 cm^{-1} . Using our new data, it appears more likely that the c1 and c6 isotopomers correspond to the observed band at 1995.7 cm^{-1} (see Fig. 53). The proposed set of isotopomer shift bands SSC12, are 1995.7 (resulting from the overlap of the c1 and c6), $1983.6(\text{c}2)$, $1981.6(\text{c}3)$, $1996.8(\text{c}4)$ and $1991.5(\text{c}5)$ called. In order to clarify the discrepancy for the c1 and c6 isotopomers these isotopomers are analyzed in detail.

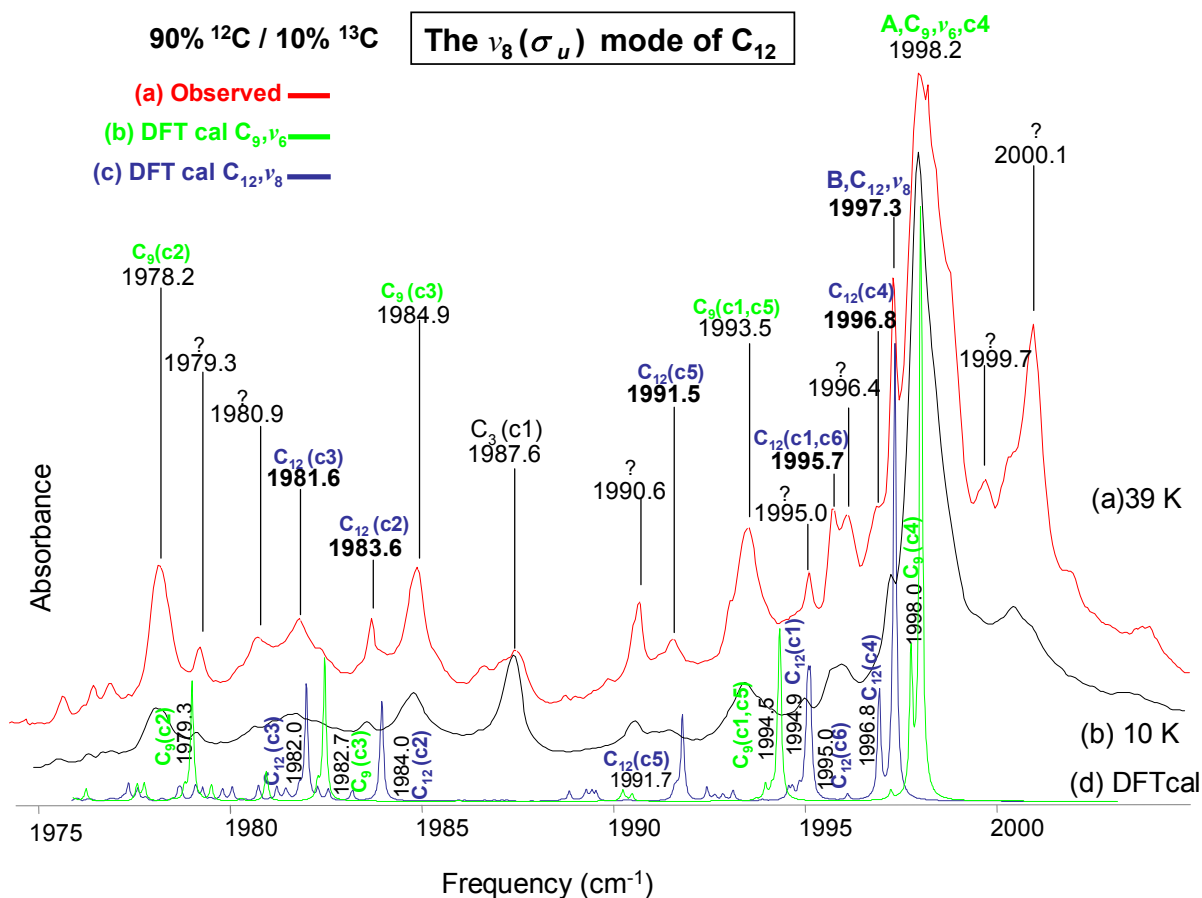


Fig. 53. Comparison of observed FTIR annealed spectra (a) 39.5 K and (b) 10.0 K of the (a) the $\nu_8(\sigma_u)$ mode of linear C_{12} and its single ^{13}C -isotopic shifts using 90% ^{12}C and 10% ^{13}C carbon enrichments, and (b) and (c) are simulated spectra derived from the DFT calculations at the B3YLP/cc-pVDZ level using the same enrichment values, for the $\nu_8(\sigma_u)$ mode of linear C_9 and $\nu_8(\sigma_u)$ mode of linear C_{12} in that order.

An observed band at 1995.7 cm^{-1} appears to be intense enough to contain two isotopomers. Nearby, we have the observed band at 1995.0 cm^{-1} assigned by Ding *et al.* to the c1 and c6 isotopomers, although its intensity is similar to the intensity of that of c2, c3, c4 and c5 bands that correspond to only one isotopomer. Our band at 1995.7 cm^{-1} is close to the calculated bands at 1994.9 and 1995.0 cm^{-1} corresponding to 13-12-12-12-12-12-12-12-12-12-12-12 (c1) and 12-12-12-12-12-13-12-12-12-12-12-12-12 (c6), and is intense enough to be the carrier of both

the c1 and c6 isotopomers. Finally, the shift set called SSC12, formed from the bands at 1994.9(c1) and 1995.0(c6) [both bands are collapsed to a single band observed at 1995.7 cm^{-1}], 1983.6 (c2), 1981.6 (c3), 1996.8(c4) and 1991.5(c5) was tested with the *deperturbation method*, which supported the revised isotopomer band assignments. The remainder of the unknown bands at 1979.3, 1980.9, 1990.6 1995.0, 1996.4 and 1999.7 cm^{-1} are probably related to the unknown prominent band at 2000.1 cm^{-1} , which is believed by the author to belong to a long C_n and will be presented subsequently in this work.

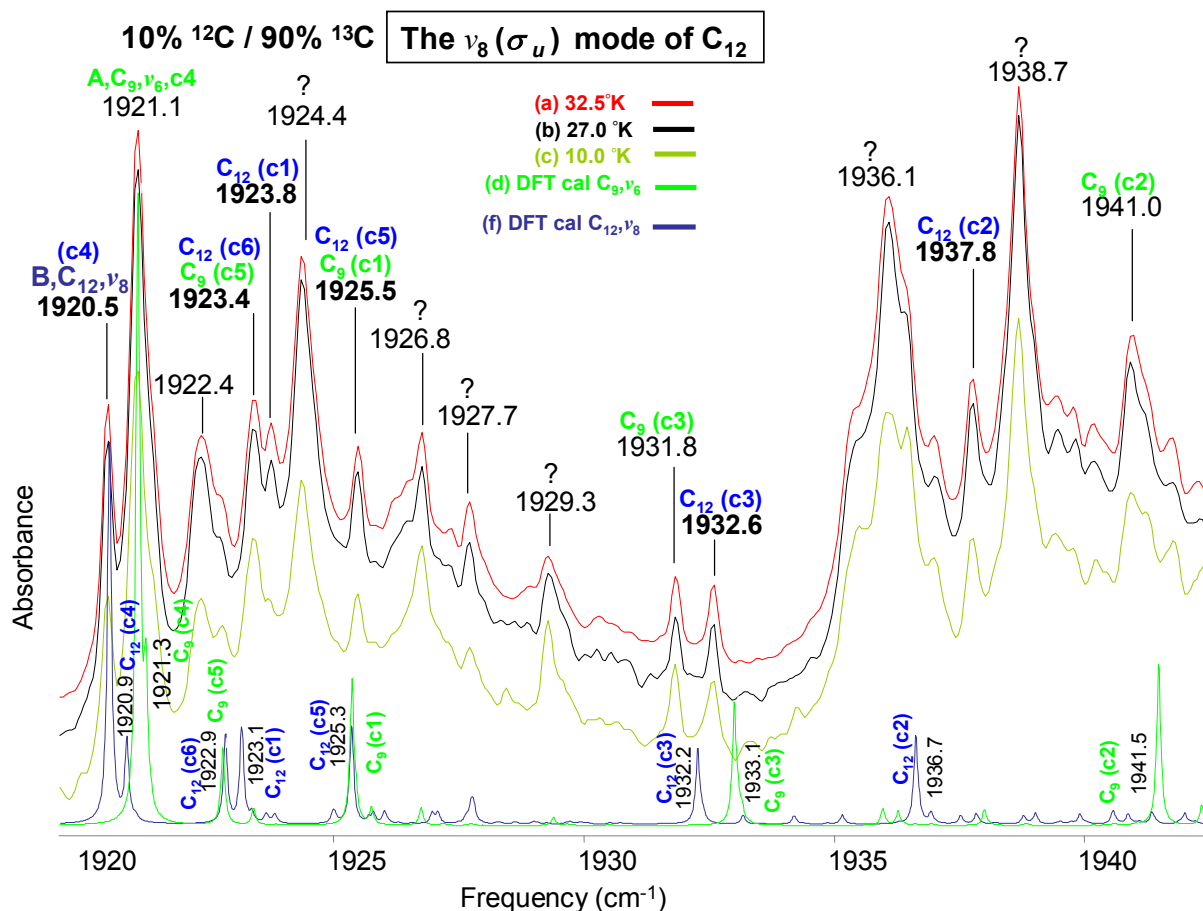


Fig. 54. Comparison of observed FTIR annealed spectra (a)32.5 K and (b) 27.0 K and (c)10.0 K of the $\nu_8(\sigma_u)$ mode of linear C_{12} and its single ^{13}C isotopic shifts using 90% ^{12}C and 10% ^{13}C carbon enrichments, and (d) and (f) a simulated spectrum derived from the DFT calculations at the B3YLP/cc-pVDZ level using the same enrichment values for the $\nu_6(\sigma_u)$ mode of linear C_9 and $\nu_8(\sigma_u)$ mode of linear C_{12} in that order.

The absorption at 1920.5 cm^{-1} (B) in Fig. 54, which is a factor $\sim \sqrt{12/13}$ of the 1997.3 cm^{-1} frequency, is identified as belonging to the fully ^{13}C -substituted isotopomer, produced by the evaporation of a carbon mixture of 10% $^{12}C/90\%$ ^{13}C . To the high frequency side of the 1920.5 cm^{-1} (B) band is the corresponding shift pattern for the single ^{12}C -substituted $^{12}C^{13}C_{11}$ isotopomers of the $\nu_8(\sigma_u)$ mode of C_{12} named SSC13, formed by the bands at 1923.8(c1), 1937.8(c2), 1932.6(c3), 2020.9(c4) [overlapped by the main band at 1920.5(B)], 1925.5(c5) [overlapped by the c1 isotopomer $\nu_6(\sigma_u)$ mode of linear C_9] and 1923.4(c6) [overlapped by the c5

isotopomer $\nu_6(\sigma_u)$ mode of linear C_9] This shift set has a consistent behavior under annealing [see Fig. 50 (a), (b) and (c)]. The observed shifts agree well with the calculated shifts as is seen in Table XIX.

TABLE XIX. Comparison of observed and predicted DFT (B3LYP/cc-pVDZ) frequencies for single ^{13}C -substituted isotopomers of $^{12}\text{C}_{12}$, and single ^{12}C -substituted isotopomers of $^{13}\text{C}_{12}$, for the ν_8 mode.

Isotopomer	ν_{obs}	B3LYP/cc-pVDZ		$\Delta\nu$ $\nu_{\text{obs}} - \nu_{\text{scaled}}$
		ν	ν_{scaled}	
12-12-12-12-12-12...(A)	1997.3	2112.8	1997.3 ¹	0.0
13-12-12-12-12-12...(c1)	Overlapped ²	2110.3	1994.9	0.0
12-13-12-12-12-12...(c2)	1983.6	2098.7	1984.0	-0.4
12-12-13-12-12-12...(c3)	1981.6	2096.6	1982.0	-0.4
12-12-12-13-12-12...(c4)	1996.8	2112.3	1996.8	0.0
12-12-12-12-13-12...(c5)	1991.5	2106.9	1991.7	-0.2
12-12-12-12-12-13...(c6)	1995.7	2110.4	1995.0	0.7
13-13-13-13-13-13...(B)	1920.5	2029.6	1920.5 ³	0.0
12-13-13-13-13-13...(c1)	1923.8	2032.4	1923.1	0.7
13-12-13-13-13-13...(c2)	1937.8	2046.7	1936.7	1.1
13-13-12-13-13-13...(c3)	1932.6	2042.0	1932.2	0.4
13-13-13-12-13-13...(c4)	Overlapped ⁴	2030.0	1920.9	0.0
13-13-13-13-12-13...(c5)	1925.5	2034.7	1925.3	0.2
13-13-13-13-13-12...(c6)	1923.4	2032.1	1922.9	0.5

¹Scaling factor $\nu_{\text{obs}}/\nu \sim 0.94533$

²Overlapped by the main band at 1995.7 cm^{-1}

³Scaling factor $\nu_{\text{obs}}/\nu \sim 0.94624$

⁴Overlapped by the main band at 1920.5 cm^{-1}

The band observed at 1922.4 cm^{-1} seems not to be related to any of our selected bands, but it is believed by the author to be a new C_n species that is the subject of a subsequent discussion. An absorption at 1925.5 cm^{-1} has earlier been assigned to the c1 isotopomer of the $\nu_6(\sigma_u)$ mode of linear C_9 . It grows in after annealing in relation to the main band at 1920.5 cm^{-1} (B) as can be seen in Fig. 54 overlapping where the c5 isotopomer band is calculated to appear. A band observed at 1926.8 cm^{-1} is also reasonably close to the calculated c5 isotopomer and it was taken to form an alternate shift set that was tested by the *deperturbation method* but with unsatisfactory results. It was, consequently, dismissed from consideration. However, the 1926.8 cm^{-1} band and

the unknown bands at 1927.7 and 1929.3 cm^{-1} may in fact, be related to the so far unidentified, prominent band at 1924.4 cm^{-1} . The band observed at 1932.6 cm^{-1} is well isolated and close to the calculated band at 1932.2 cm^{-1} for the 13-13-12-13-13-13-13-13-13-13-13-13(c3). The observed band at 1937.8 cm^{-1} appears to be somewhat more intense than the already assigned c3 isotopomer but it is close to the calculated band at 1936.7 cm^{-1} corresponding to the 13-12-13-13-13-13-13-13-13-13-13-13(c3) isotopomer. The unknown observed C_n species at 1936.1 cm^{-1} and 1938.7 cm^{-1} are currently under investigation by the author of this work. We finally have a shift-set formed by the isotopomers located at 1923.8(c1), 1937.8(c2), 1932.6(c3), 1920.9(c4) [overlapped by the main band at 1920.5(B)], 1925.5(c5) (overlapped by the c5 isotopomer $\nu_6(\sigma_u)$ mode of linear C_9) 1923.4 cm^{-1} (c6) (overlapped by the c1 isotopomer $\nu_6(\sigma_u)$ mode of linear C_9) named SSC13. This shift set was submitted together with the SSC12 set to the test of the *deperturbation method* and the results were consistent with the isotopic analysis presented here.

7.8 Assignment of the isotopomers for the $\nu_9(\sigma_u)$ mode of C_{12}

The proposed main band is at $\nu_9(\sigma_u)=1817.9 \text{ cm}^{-1}$ mode and is the third most intense mode of the linear C_{12} and within experimental error it agrees with the assignment of Ding *et al.*¹⁰⁰ of $\nu_9(\sigma_u)=1818.0 \text{ cm}^{-1}$. The closest IR-inactive mode is the $\nu_3(\sigma_g)$ mode located at 168.9 cm^{-1} to the high frequency side, which presumably introduce little or no perturbation (see Table XVII).

The experimental data obtained (see Fig. 55) are very similar to the results obtained by Ding *et al.* The observed set of isotopomers bands that we call SSC12 [see Fig. 55] is located at 1811.8(c1), 1805.1(c2), 1814.7 (c3) 1811.0(c4), 1813.4(c5) and 1812.6(c6) cm^{-1} . It is

unnecessary to further analyze these shifts but instead will consider in detail the mirrored single ^{12}C -substituted $^{12}\text{C}^{13}\text{C}_{11}$ isotopomers found in the present work.

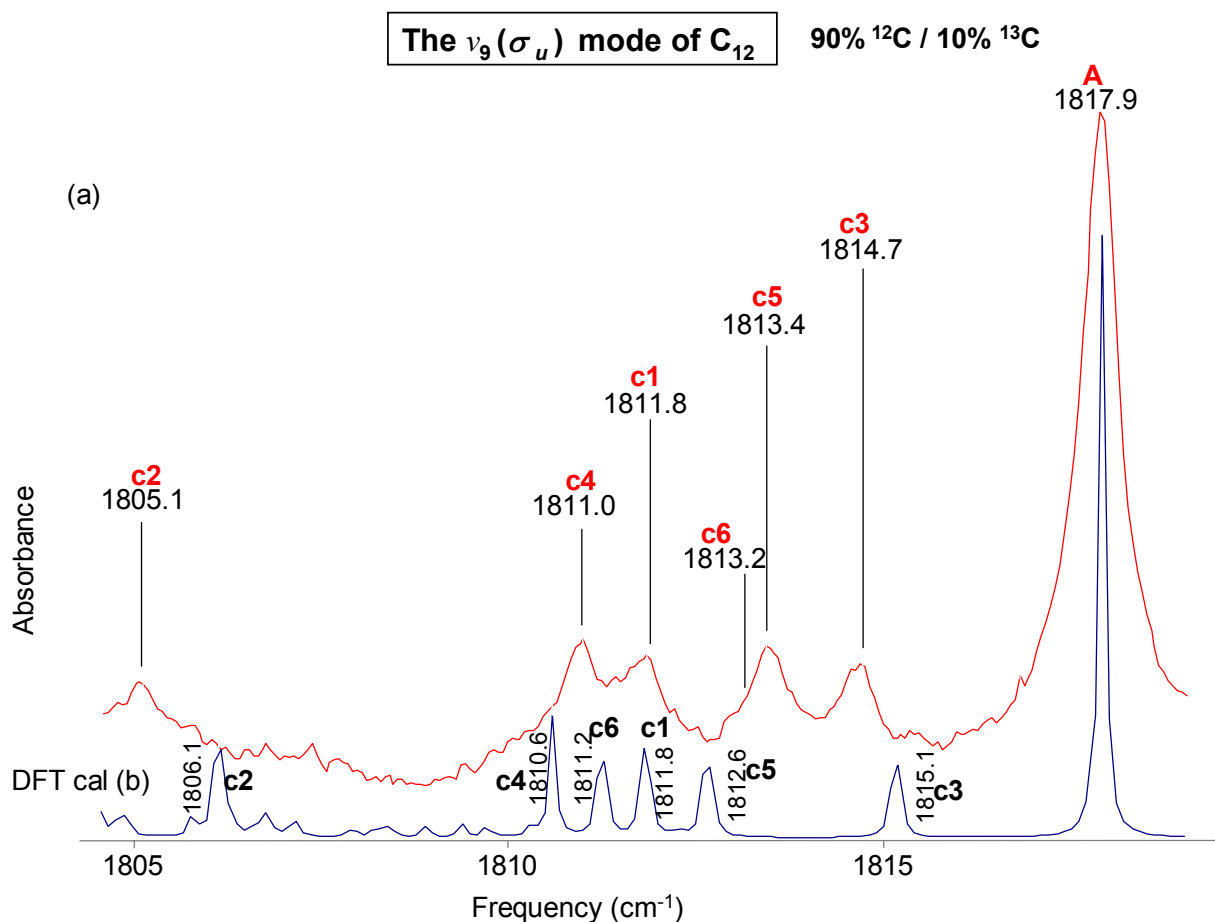


Fig. 55. Comparison of observed FTIR (a) the $\nu_9(\sigma_u)$ mode of linear C_{12} and its single ^{13}C -isotopic shifts using 90% ^{12}C and 10% ^{13}C carbon enrichments, and (b) is a simulated spectra derived from the DFT calculations at the B3YLP/cc-pVDZ level using the same enrichment values.

The absorption at 1748.2 cm^{-1} (B) (see Fig. 56), which is a factor $\sim\sqrt{12/13}$ of the 1817.9 cm^{-1} frequency, is identified as belonging to the fully ^{13}C -substituted isotopomer, produced by the evaporation of a carbon mixture of 10% ^{12}C /90% ^{13}C . To the high frequency side of the

1748.2 cm^{-1} (B) band we can see a isotopic shifts for the single ^{12}C -substituted $^{12}\text{C}^{13}\text{C}_{11}$ isotopomers of the $\nu_9(\sigma_u)$ mode of C_{12} at 1754.7 (c1), 1757.3(c2) 1750.0(c3), 1755.4(c4) 1752.4(c5) and 1753.6(c6) which appear to have consistent behavior under annealing [see Fig. 56 (a) and (b)]. The shifts appear in Table XX.

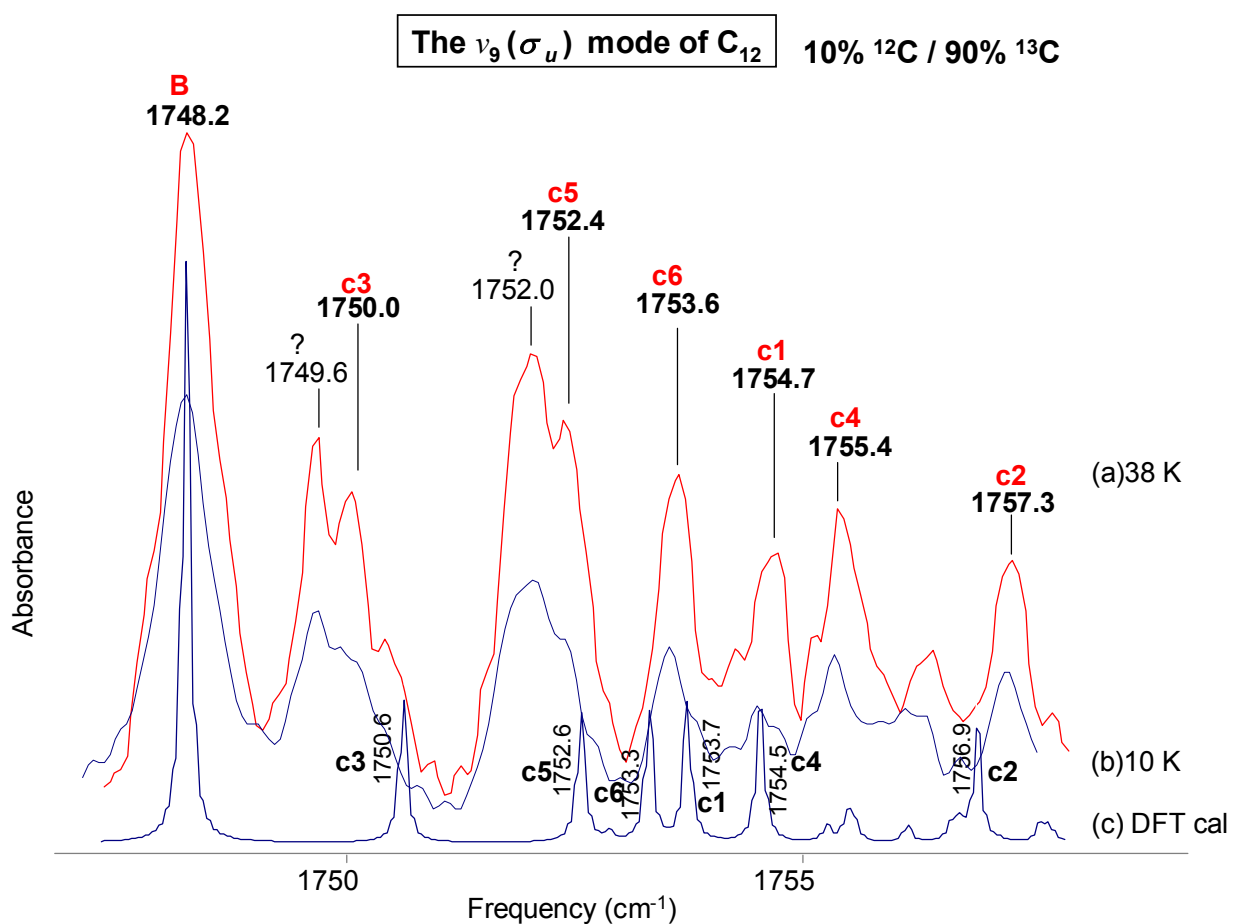


Fig. 56. Comparison of observed FTIR spectra (a) 38 K and (b) 10 K and for the $\nu_9(\sigma_u)$ mode of linear C_{12} and its single ^{13}C isotopic shifts using 90% ^{12}C and 10% ^{13}C carbon enrichments, and (c) is a simulated spectrum derived from the DFT calculations at the B3YLP/cc-pVDZ level using the same enrichment values.

TABLE XX. Comparison of observed and predicted DFT (B3LYP/cc-pVDZ) frequencies for single ^{13}C -substituted isotopomers of $^{12}\text{C}_{12}$, and single ^{12}C -substituted isotopomers of $^{13}\text{C}_{12}$, for the ν_9 mode.

Isotopomer	ν_{obs}	B3LYP/cc-pVDZ		$\Delta\nu$ $\nu_{\text{obs}} - \nu_{\text{scaled}}$
		ν	ν_{scaled}	
12-12-12-12-12-12... (A)	1817.9	1815.1	1817.9 ¹	0.0
13 -12-12-12-12-12... (c1)	1811.8	1809.0	1811.8	0.0
12- 13 -12-12-12-12... (c2)	1805.1	1803.3	1806.1	-1.0
12-12- 13 -12-12-12... (c3)	1814.7	1812.3	1815.1	-0.4
12-12-12- 13 -12-12... (c4)	1811.0	1807.8	1810.6	0.4
12-12-12-12- 13 -12... (c5)	1813.4	1809.8	1812.6	0.8
12-12-12-12-12- 13 ... (c6)	1812.6	1808.4	1811.2	1.4
13-13-13-13-13-13... (B)	1748.2	1743.9	1748.2 ²	0.0
12 -13-13-13-13-13... (c1)	1754.7	1749.4	1753.7	1.0
13- 12 -13-13-13-13... (c2)	1757.3	1752.6	1756.9	0.4
13-13- 12 -13-13-13... (c3)	1750.0	1746.3	1750.6	-0.6
13-13-13- 12 -13-13... (c4)	1755.4	1750.2	1754.5	0.9
13-13-13-13- 12 -13... (c5)	1752.4	1748.3	1752.6	-0.2
13-13-13-13-13- 12 ... (c6)	1753.6	1749.0	1753.3	0.3

¹Scaling factor $\nu_{\text{obs}}/\nu \sim 1.00154$

²Scaling factor $\nu_{\text{obs}}/\nu \sim 1.00246$

Starting at the high frequency side from the main band at 1748.2 cm^{-1} (B) in Fig. 56, we observe two broad pairs of peaks. The first is composed of the bands at 1749.6 and 1750.0 cm^{-1} and the second by the bands at 1752.0 and 1752.4 cm^{-1} . Both sets have additional features growing in on the wings. These pairs of bands are relatively close also to the calculated bands at 1750.6 cm^{-1} and 1752.6 cm^{-1} corresponding to the 13-13-12-13-13-13-13-13-13-13-13(c3) and 13-13-13-13-12-13-13-13-13-13-13(c5) isotopomers, respectively. The first choice is to assign the observed bands at 1750.0 and 1752.4 cm^{-1} to the c3 and c5 isotopomers, respectively. An alternative assignment of c3 and c5 is to 1749.6 and 1752.0 cm^{-1} . Testing with the the *deperturbation method*, indicated that the 1750.0 and 1752.4 cm^{-1} bands should be assigned to

the c3 and c5 isotopomers, respectively. The bands at 1749.6 and 1752.0 cm^{-1} remain unidentified. The bands at 1753.6, 1754.7 and 1755.4 cm^{-1} behave well on annealing, showing that they are related. The observed band at 1757.3 cm^{-1} is well isolated and close to the calculated frequency 1756.9 cm^{-1} corresponding to the 13-12-13-13-13-13-13-13-13-13-13(c2) isotopomer. The shifts are thus formed by the 1754.7 (c1), 1757.3 (c2), 1750.0 (c3), 1755.4 (c4), 1752.4(c5) and 1753.6 (c6) cm^{-1} bands.

7.9 Conclusions

The results of Fourier transform infrared ^{13}C study have been presented for the $\nu_5(\sigma_u)$ and $\nu_6(\sigma_u)$ fundamentals of linear C_8 and the $\nu_7(\sigma_u)$, $\nu_8(\sigma_u)$ and $\nu_9(\sigma_u)$ fundamentals of linear C_{12} in solid Ar at 10 K. The analysis is based on the greatly enhanced spectra acquired for both 90/10 and 10/90 isotopic measurements and also the interaction of nearby modes assisted by using the *deperturbation method*. This work further strengthens the assignment of the vibrational fundamentals of the $\nu_5=2071.4$ and $\nu_6=1710.5$ cm^{-1} of linear C_8 and the $\nu_7=2140.6$, $\nu_8=1997.3$ and $\nu_9=1817.9$ cm^{-1} of linear C_{12} by Ding *et al.*¹⁰⁰ The isotopic data for the ν_8 and ν_9 modes of C_8 will be of particular help in identifying the shifts of other C_n species located within the same highly congested frequency region, facilitating the application of our experimental and theoretical line of analysis, described in previous chapters, to the analysis of even larger molecules [$\text{C}_n, n > 12$].

CHAPTER VIII

FTIR SPECTROSCOPIC STUDY OF THE $\nu_{10}(\sigma_u)$ MODE OF LINEAR C₁₅ AND THE $\nu_{12}(\sigma_u)$ MODE OF LINEAR C₁₈

8.1 Introduction

The identification of large C_n species ($n > 12$) has been a goal for a long period of time because of a variety of practical applications, from chemical and engineering applications^{1,2,3} to the contributing to the understanding of astronomical observations, particularly, the unidentified infrared bands (UIB).^{6,8,9,10,11,12,13} In the course of this work we have been investigating experimental measurements on the C_n ($n=6, 7 \dots 12$) species. The study of these molecules has been a complex endeavor that has challenged our experimental and theoretical procedures. The fact that we have a high population of bands within small frequency intervals, frequently requires us to consider several possible sets of isotopomer shifts. In identifying vibrational fundamentals the application of DFT calculations as well as the recently developed *deperturbation method*. This approach has been of critical importance during the analysis of complex spectra recorded during the identification of the vibrational fundamentals of C₉ and C₁₂ reported in this work. This systematic process of identification has been of critical importance in the assignment of the stretching fundamentals $\nu_{10}(\sigma_u)=1999.3 \text{ cm}^{-1}$ and $\nu_{12}(\sigma_u)=2001.0 \text{ cm}^{-1}$, for the linear C₁₅ and C₁₈, respectively.

8.2 Results and discussion

In the last 5 years the challenge has been to produce C_n ($n \geq 12$) molecules. It has been suspected that spectra of molecules as large the linear C_n ($n = 15, 18$) could be lying in the densely populated interval 1990.0 - 2010.0 cm^{-1} shown in Fig. 57.

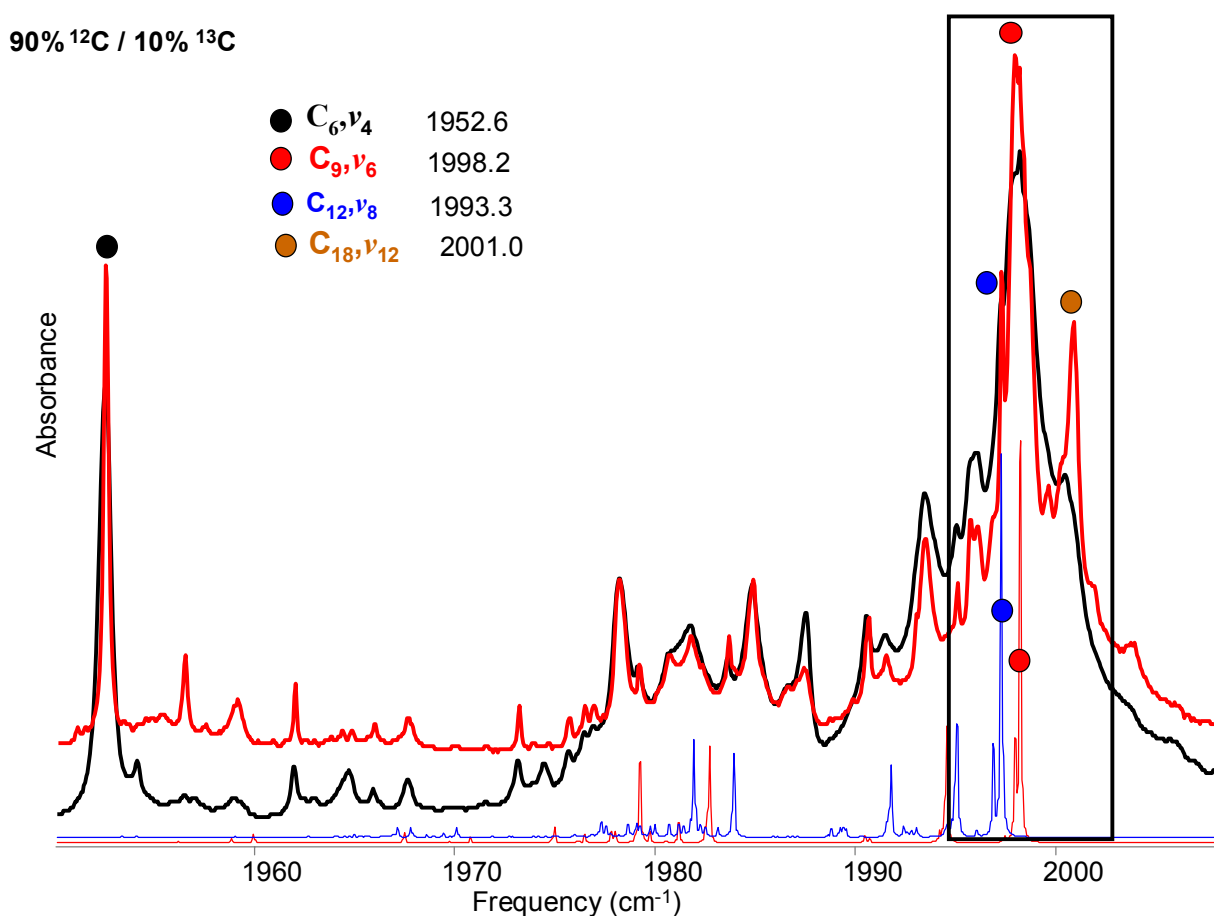


Fig. 57. Comparison of observed FTIR spectra (a) and (b) obtained through different experiments using same 90% ^{12}C and 10% ^{13}C carbon enrichments, and (c) DFT calculations at the B3YLP/cc-pVDZ level using the same enrichment values of different C_n molecules.

The spectra in bold presented in Fig. 58 (d) and (e) are the observed spectra shown in Fig. 57(a) and (b) obtained using previous experimental conditions compared with the recently

spectra obtained following changes in the experimental conditions in the present research, which have been discussed earlier.

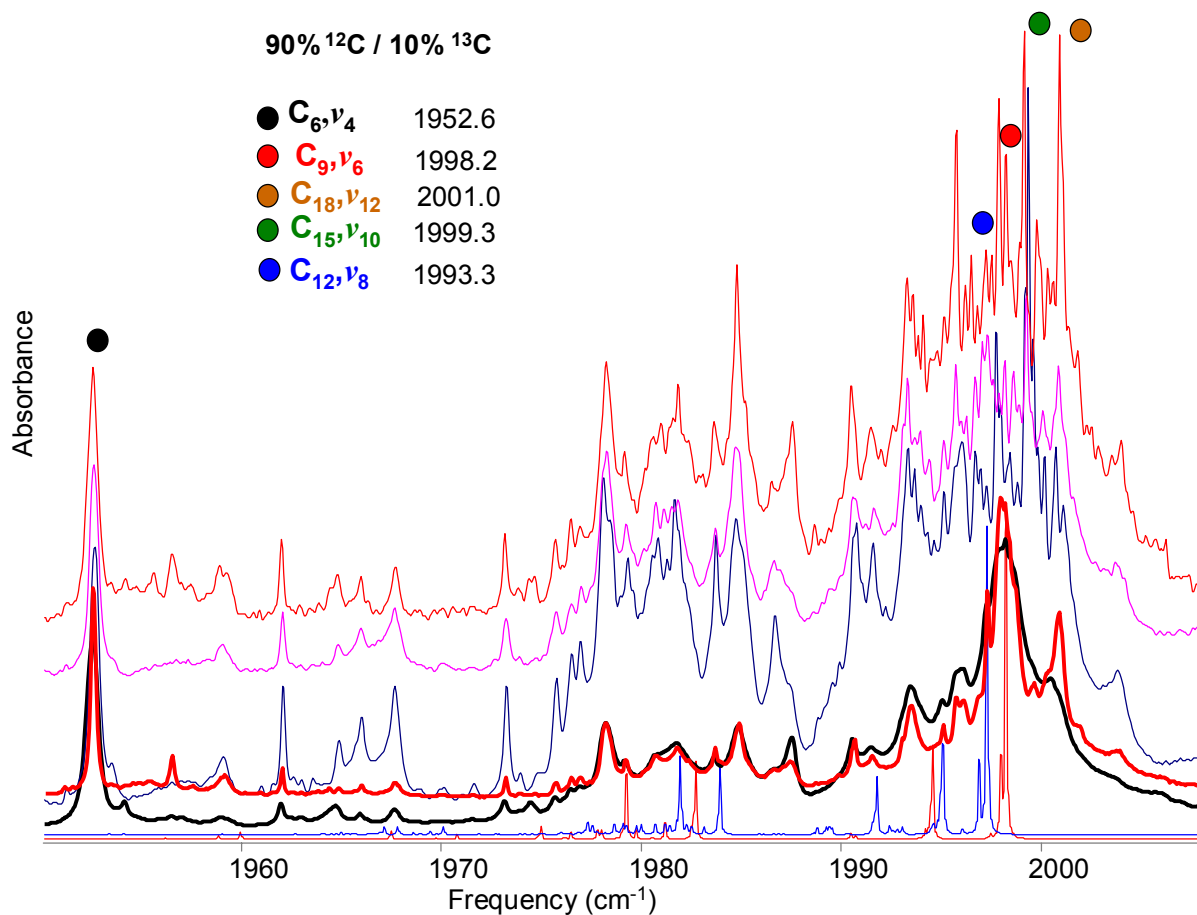


Fig. 58. Comparison of a collection of different observed FTIR spectra (a)...(e) obtained through different experiments using 90% ^{12}C and 10% ^{13}C carbon enrichments, (d) and (e) are results obtained with certain experimental conditions (rods “cooking time”, laser power, annealing processes...etc). The (a), (b), and (c) are results obtained after the improvement of those mentioned conditions.

Because of these changes, it is possible to experimentally induce the growth of several prominent bands in the 1990.0-2010.0 cm^{-1} interval as can be seen in Fig. 58 (a), (b) and (c). It is suspected that some of these unidentified bands are potential new vibrational fundamentals of long carbon C_n chains.

Theoretical calculations done by Rittby¹⁰² (see Fig. 59 and 60) point out as well, that when the number of carbon atoms augments in a linear C_n species the number of vibrational fundamentals increases; indicating that the most of the stretching fundamentals of large linear C_n ($n \geq 6$) species will be located in the interval 1900.0-2100.0 cm^{-1} .

Calculated and observed linear C_n chains (odd n)

- Predicted stretching frequencies were obtained with DFT-B3LYP/cc-pVDZ
 - Predicted σ_u antisymmetric modes **red (IR- allowed).**
 - Predicted σ_g symmetric modes **blue (IR- forbidden).**
- Observed stretching frequencies were obtained with FTIR studies
 - Observed σ_u antisymmetric modes **green (IR- allowed).**

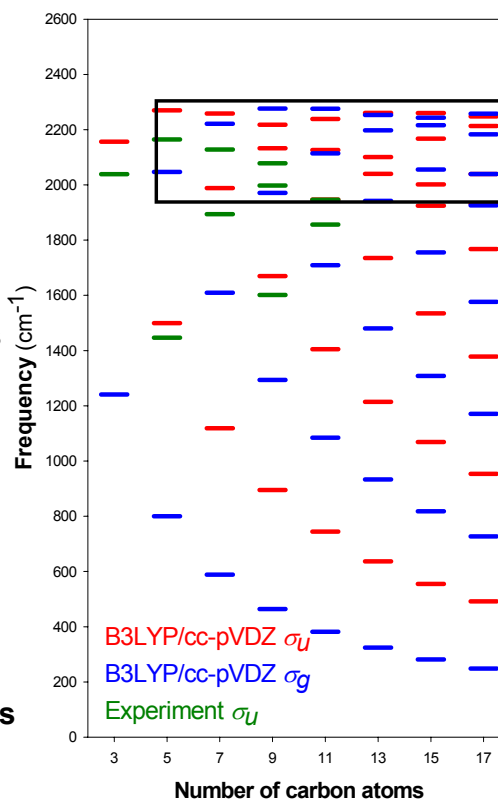


Fig. 59. Comparison of observed FTIR and DFT calculated vibrational fundamentals at the B3LYP/cc-pVDZ level for linear C_n chains with an odd number of atoms. (Courtesy of C. M. L. Rittby)

Calculated and observed linear C_n chains (even n)

- 🌿 Predicted stretching frequencies were obtained with DFT-B3LYP/cc-pVDZ
 - Predicted σ_u antisymmetric modes **red (IR- allowed).**
 - Predicted σ_g symmetric modes **blue (IR- forbidden).**
- 🌿 Observed stretching frequencies were obtained with FTIR studies
 - Observed σ_u antisymmetric modes **green (IR- allowed).**

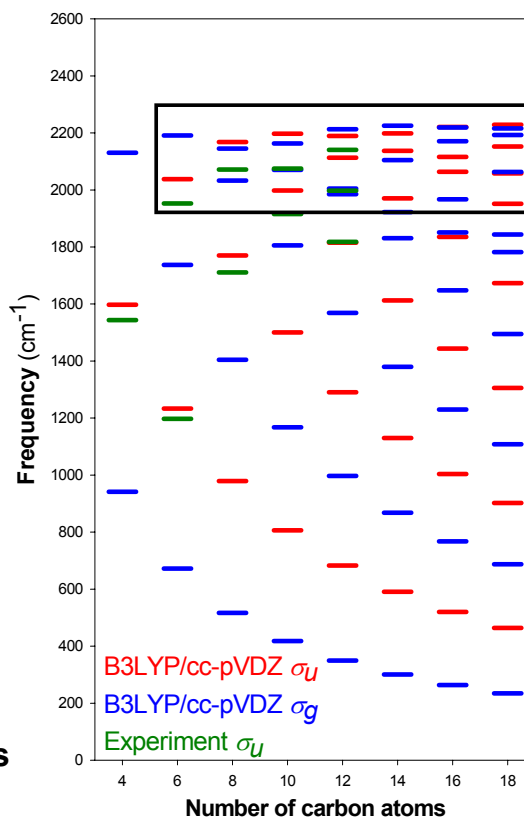


Fig. 60. Comparison of observed FTIR and DFT calculated vibrational fundamentals at the B3LYP/cc-pVDZ level for linear C_n chains with an even number of atoms. (Courtesy of C. M. L Rittby)

The new observations may lead for the first time to the possibility of identifying long molecules C_n ($n \geq 12$) such $\nu_{10}(\sigma_u)$ and $\nu_{12}(\sigma_u)$ modes of C_{15} and C_{18} , which it will be shown are located among the new features located within the same frequency interval $1990.0\text{-}2004.0\text{cm}^{-1}$ in Fig. 58.

TABLE XXI. DFT B3LYP/cc-pVDZ predicted vibrational frequencies and band intensities for (ℓ -C₁₅).

Vib mode	Freq (cm ⁻¹)	IR Int (km/mol)	Vib mode	Freq (cm ⁻¹)	IR Int (km/mol)
$\nu_1(\sigma_g)$	2242.8	0.0	$\nu_{16}(\pi_g)$	592.7	(0.0)2
$\nu_2(\sigma_g)$	2215.5	0.0	$\nu_{17}(\pi_g)$	459.1	(0.0)2
$\nu_3(\sigma_g)$	2055.4	0.0	$\nu_{18}(\pi_g)$	275.2	(0.0)2
$\nu_4(\sigma_g)$	1754.7	0.0	$\nu_{19}(\pi_g)$	153.7	(0.0)2
$\nu_5(\sigma_g)$	1307.9	0.0	$\nu_{20}(\pi_g)$	51.6	(0.0)2
$\nu_6(\sigma_g)$	817.7	0.0	$\nu_{21}(\pi_u)$	857.7	(8.5)2
$\nu_7(\sigma_g)$	281.5	0.0	$\nu_{22}(\pi_u)$	676.0	(0.5)2
$\nu_8(\sigma_u)$	2259.6	2685.8	$\nu_{23}(\pi_u)$	523.1	(0.2)2
$\nu_9(\sigma_u)$	2167.3	594.9	$\nu_{24}(\pi_u)$	320.6	(2.4)2
$\nu_{10}(\sigma_u)$	2001.1	27554.5	$\nu_{25}(\pi_u)$	216.1	(6.7)2
$\nu_{11}(\sigma_u)$	1924.3	7743.2	$\nu_{26}(\pi_u)$	97.5	(5.9)2
$\nu_{12}(\sigma_u)$	1534.6	322.7	$\nu_{27}(\pi_u)$	19.0	(3.5)2
$\nu_{13}(\sigma_u)$	1068.6	11.8			
$\nu_{14}(\sigma_u)$	555.1	17.4			
$\nu_{15}(\sigma_u)$	760.6	(0.0)2			

8.3 Assignment of the isotopomers for the $\nu_{10}(\sigma_u)$ mode of C₁₅

We begin the analysis of the new absorptions with the most intense $\nu_{10}(\sigma_u)$ mode of C₁₅. This mode has a moderate interaction with the $\nu_3(\sigma_g)$ mode that lies at 54.3 cm⁻¹ to the high frequency side as shown in Table XXI. The potential isotopomer shifts are in the spectra shown in Fig. 61. As can be appreciated from Fig. 61(b) it is difficult to establish the base line and a large number of absorptions appear in the 1995.0 to 2001.0 cm⁻¹ interval. At first glance the features appearing in the interval might be confused with noise, but they are not, and are highly reproducible. The set of absorptions that in the spectrum in Fig. 61(b) are C_n bands that sharpen and increase in intensity on annealing as can be seen in Fig. 61(a). From this set of bands is a

main band is chosen at $1999.3 \text{ cm}^{-1}(\text{A})$ and a preliminary set of isotopomer shifts located to the low frequency side at $1999.2(\text{c1})$ [overlapped by the main band], $1998.7 (\text{c2})$, $1993.4(\text{c3})$ [overlapped by the c1 and c5 isotopomers of $\nu_6(\sigma_u)$ mode of linear of C_9], $1990.6 (\text{c4})$, $1995.2 (\text{c5})$, $1996.7(\text{c6})$, $1986.7 (\text{c7})$, and $1980.8 \text{ cm}^{-1} (\text{c8})$ that we name *SSC12*. This set of isotopomer absorptions seems to grow in with the main band at $1999.3 \text{ cm}^{-1}(\text{A})$ on annealing, which indicates they may be correlated.

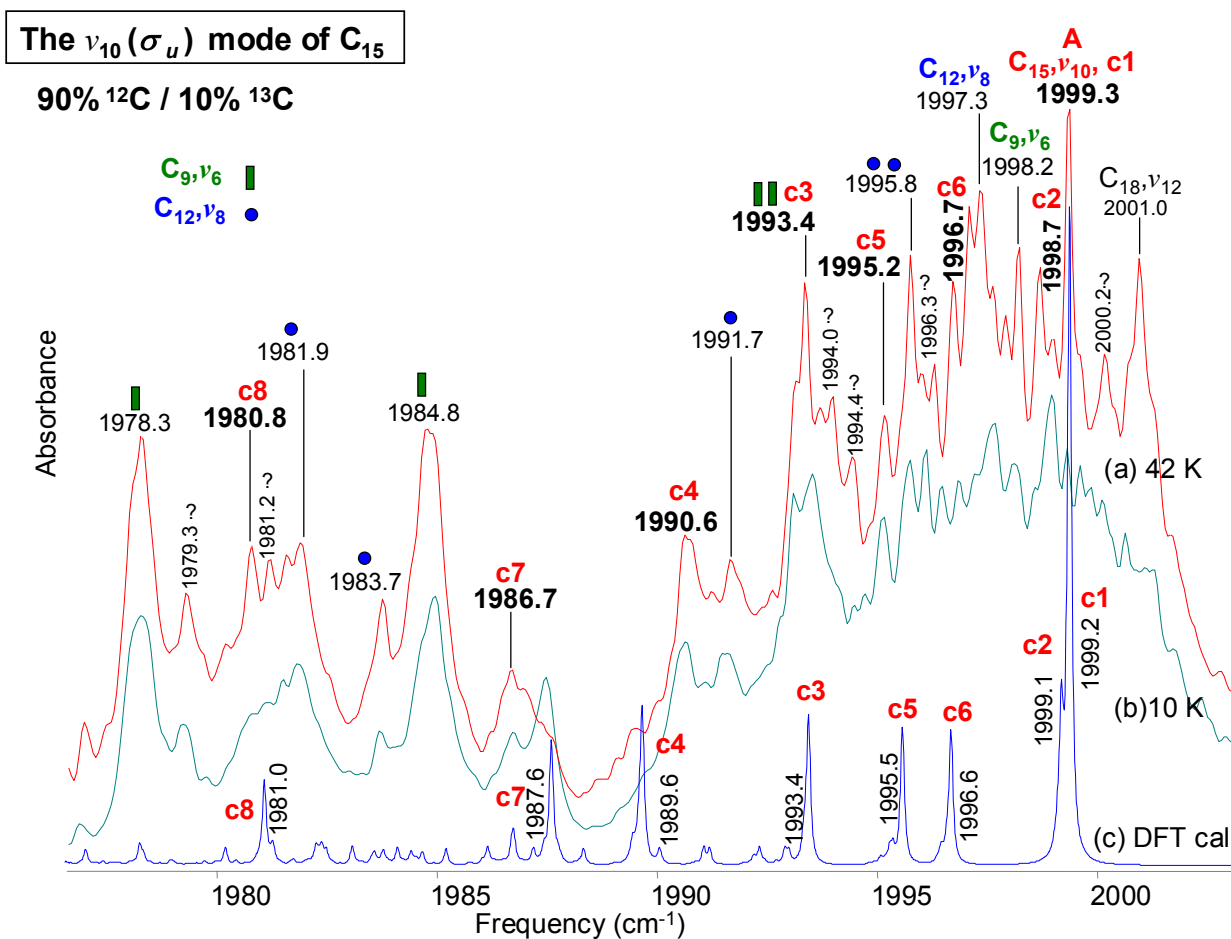


Fig. 61. Comparison of observed FTIR annealed spectra (a) 42 K and (b) 10 K of the $\nu_{10}(\sigma_u)$ mode of linear of C_{15} and its single ^{13}C isotopic shifts using 90% ^{12}C and 10% ^{13}C carbon enrichments, and (c) a simulated spectrum derived from DFT calculations at the B3YLP/cc-pVDZ level using the same enrichment values.

Examining the proposed assignments in detail we begin with the 13-12-12-12-12-12-12-12-12-12-12-12-12-12-12-12(c1) isotopomer, calculated to at 1999.2 cm^{-1} is overlapped by the main mode at 1999.3 cm^{-1} . The bands at 1998.7 and 1996.7 cm^{-1} grow in on annealing [see Fig. 61 (b)] together with main band. They are close to respectively, the calculated bands at 1999.1 cm^{-1} for the 12-13-12-12-12-12-12-12-12-12-12-12-12-12-12-12(c2) isotopomer and the 1996.7 cm^{-1} for the 12-12-12-12-12-12-13-12-12-12-12-12-12-12-12-12(c6) isotopomer. There is, however another unknown bands at 1996.3 cm^{-1} whose intensity does not correlate with the c2 and c6 isotopomers

and is probably related to an unidentified C_n band appearing at 2001.0 cm^{-1} . A band at 1993.4 cm^{-1} has already been assigned to the overlap of the c1 and c5 isotopomers of the $\nu_8(\sigma_u)$ mode of linear of C_9 and unfortunately, also matches the calculated frequency for the 12-12-13-12-12-12-12-12-12-12-12-12-12-12-12-12 (c3) isotopomer. The band observed at 1990.6 cm^{-1} seems to grow in together with the c2 and c6 isotopomer bands and is close to the band at 1989.6 cm^{-1} predicted for the 12-12-12-13-12-12-12-12-12-12-12-12-12-12-12-12 (c4) isotopomer. The bands at 1994.4 and 1995.2 cm^{-1} , are both candidates for the calculated frequency of 1995.5 cm^{-1} for the 12-12-12-12-13-12-12-12-12-12-12-12-12-12-12-12 (c5) isotopomer; however both were tested with the *deperturbation method* and the best behaved band is the 1995.2 cm^{-1} absorption. The band observed at 1986.7 cm^{-1} actually grows in on annealing with the c2, c6 and c4 isotopomer bands and is close to the frequency calculated at 1987.6 cm^{-1} for the 12-12-12-12-12-12-13-12-12-12-12-12-12-12-12-12 (c7) isotopomer. There two observed bands at 1980.8 and 1981.2 cm^{-1} , which could fit the 1981.0 cm^{-1} frequency calculated for the centrosymmetric 12-12-12-12-12-12-13-12-12-12-12-12-12-12-12-12 (c8) isotopomer. Using the *deperturbation method* indicated that the band at 1980.8 cm^{-1} behaves the best. We thus have a shift set formed by $1999.2(\text{c1})$ [overlapped by the main band at 1999.3], $1998.7(\text{c2})$, $1993.4(\text{c3})$ (overlapped by the c1 and c5 isotopomer of the $\nu_8(\sigma_u)$ mode of linear of C_9), $1990.6(4)$, $1995.2(5)$, $1996.7(6)$, $1986.7(7)$ and 1980.8 cm^{-1} (c8) absorptions, called SSC12.

Fig. 62 shows spectra from another experiment performed under different experimental conditions from those used for the spectrum in Fig. 61 but demonstrating the reproducibility of the data. Again, we see the same spectrum of the $\nu_{10}(\sigma_u)$ vibrational fundamental of linear of C_{15} located at 1999.3 cm^{-1} and its corresponding single ^{13}C -substituted $^{12}\text{C}^{13}\text{C}_{14}$ isotopomers.

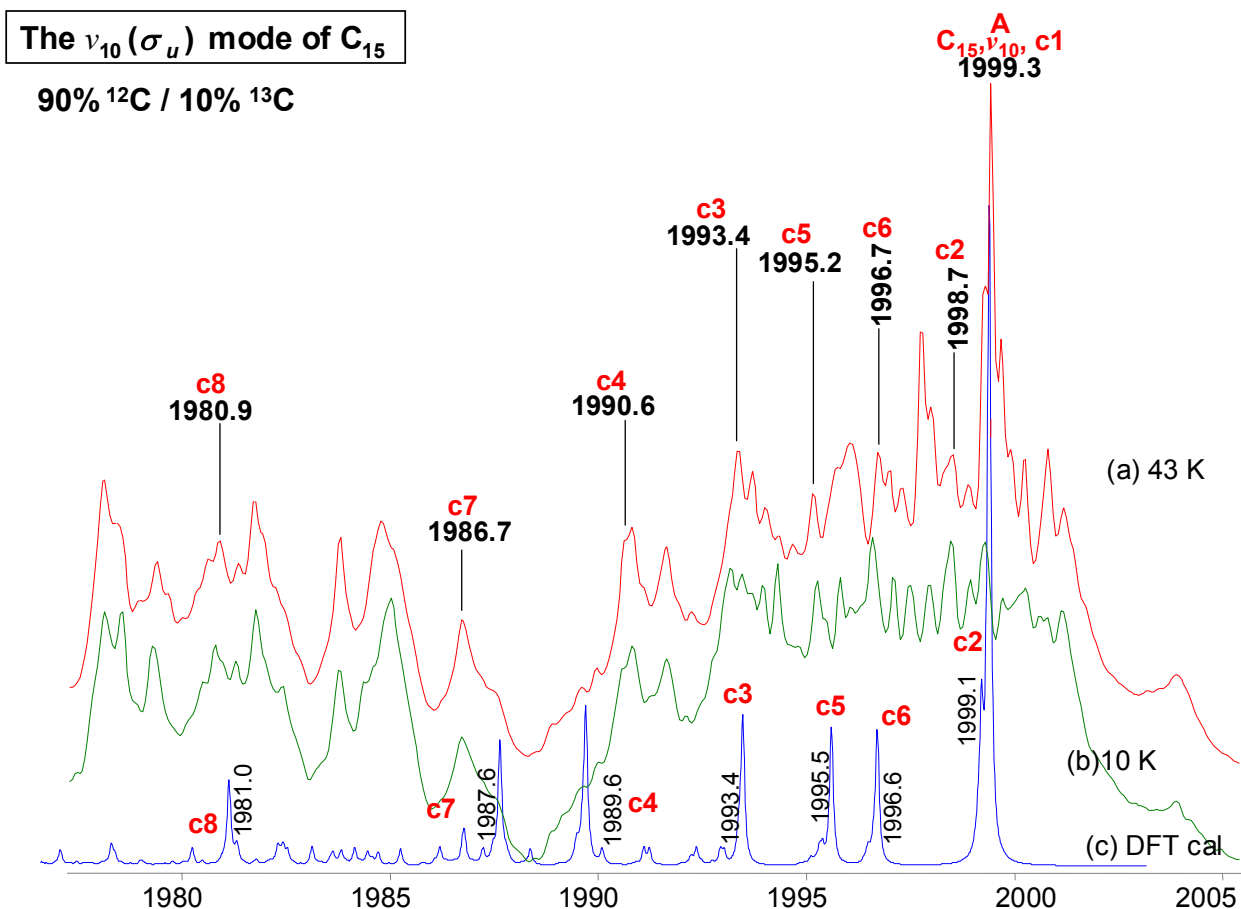


Fig. 62. Comparison of observed FTIR annealed spectra (a) 43 K and (b) 10 K of the $\nu_{10}(\sigma_u)$ mode of linear of C_{15} and its single ^{13}C isotopic shifts using 90% ^{12}C and 10% ^{13}C carbon enrichments, and (c) a simulated spectrum derived from the DFT calculations at the B3YLP/cc-pVDZ level using the same enrichment values.

In Fig. 63, the absorption at 1922.3 cm^{-1} (B), which is a factor of $\sim\sqrt{12/13}$ of the 1999.3 cm^{-1} frequency, is identified as belonging to the fully ^{13}C -substituted isotopomer $^{13}C_{15}$, which was produced by the evaporation of a carbon mixture of 10% ^{12}C /90% ^{13}C . In Fig. 63 (a) to the high frequency side of the 1922.3 cm^{-1} band, we can see the calculated shift pattern for the single ^{12}C -substituted $^{12}C^{13}C_{14}$ isotopomers of the $\nu_{10}(\sigma_u)$ mode of C_{15} .

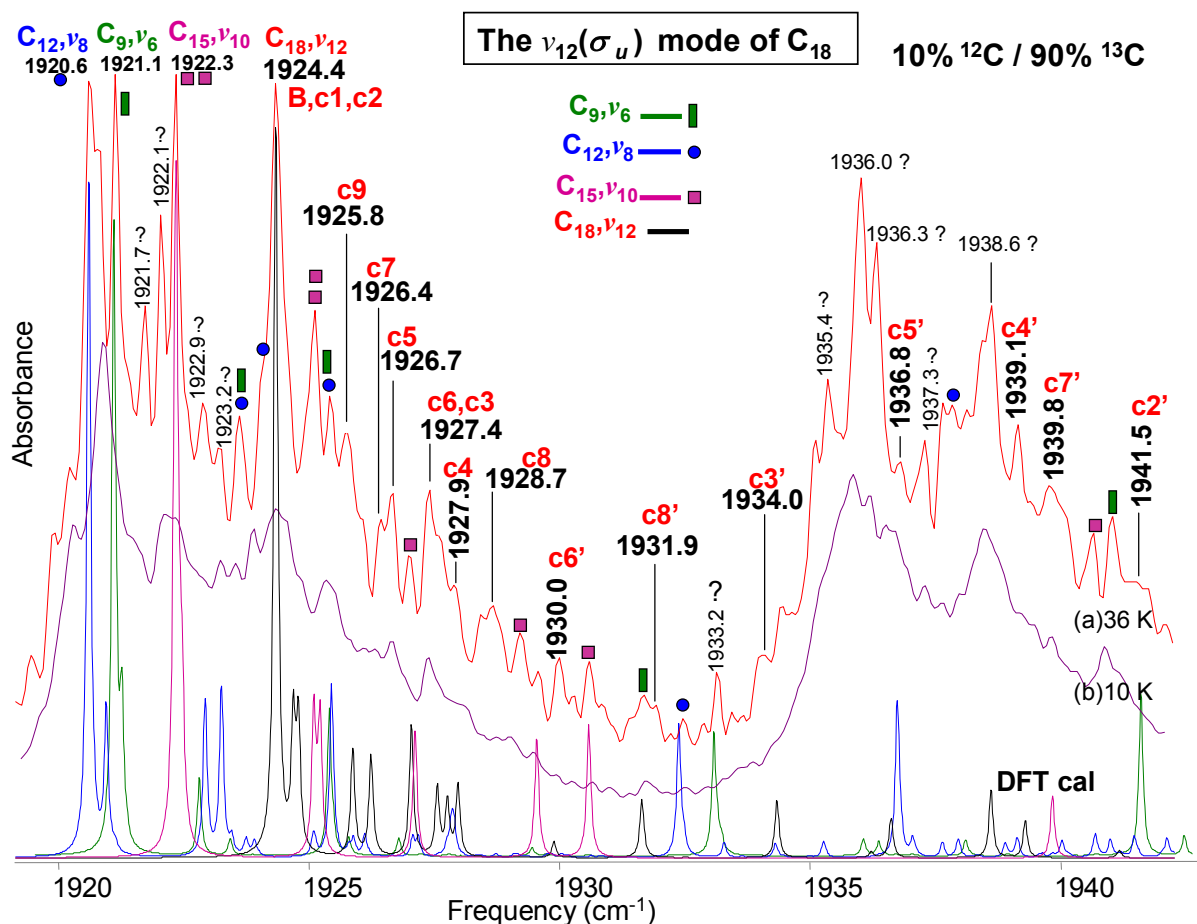


Fig. 63. Comparison of observed FTIR annealed spectra (a) 36 K and (b) 10 K of the $\nu_8(\sigma_u)$ mode of linear C_{12} and its single ^{13}C isotopic shifts using 90% ^{12}C and 10% ^{13}C carbon enrichments and a simulated spectrum derived from the DFT calculations at the B3YLP/cc-pVDZ level using the same enrichment values for the $\nu_{10}(\sigma_u)$ mode of linear C_{10} .

Before continuing with the analysis, it is necessary to note the large number of assigned and unassigned absorptions in the spectra in Fig. 63(a). Nevertheless, it is possible to choose a preliminary shift-set SSC13, formed with the bands at 1922.4 and [is overlapped by the main band at 1922.3 cm^{-1} (B)], 1922.9 (c2), 1927.0 (c3), 1929.2 (c4), 1925.1 (c5) [overlapped by the c6 isotopomer], 1925.2 (c6), 1930.6 (c7), and 1940.7 cm^{-1} (c8) [see Table XXII]. Those bands appear to grow in as the main band at 1922.3 cm^{-1} increases its intensity during annealing.

The bands at 1921.7 and 1922.1 cm^{-1} are unrelated to the 1922.3 cm^{-1} (B) band or to the $\nu_8(\sigma_u)$ mode of linear C_{12} and to the $\nu_6(\sigma_u)$ mode of linear C_9 occurring in the same region. Those bands are probably C_n species and are under current investigation by the author. The unidentified prominent band at 1924.4 cm^{-1} appears to be related to possible shifts at 1925.8, 1926.4, 1926.7, 1927.4, 1928.7, 1929.6, 1930.0, 1933.2, 1936.8, 1937.3, 1939.1 and 1939.8 cm^{-1} , and will be important in the study of the $\nu_{12}(\sigma_u)$ mode of linear C_{18} , to be discussed later in this chapter. The peak at 1935.4 cm^{-1} is an unknown C_n species. The prominent peaks at 1936.0, 1936.3 and 1938.6 are unknown C_n species under current investigation.

TABLE XXII. Comparison of observed and predicted DFT (B3LYP/cc-pVDZ) frequencies for single ^{13}C -substituted isotopomers of $^{12}\text{C}_{12}$, and single ^{12}C -substituted isotopomers of $^{13}\text{C}_{15}$, for the ν_{10} mode.

Isotopomer	ν_{obs}	B3LYP/cc-pVDZ		$\Delta \nu$ $\nu_{\text{obs}} - \nu_{\text{scaled}}$
		ν	ν_{scaled}	
12-12-12-12-12-12-12-12... (A)	1999.3	2001.3	1999.3 ¹	0.0
13-12-12-12-12-12-12-12... (c1)	Overlapped ²	2001.2	1999.2	---
12-13-12-12-12-12-12-12... (c2)	1998.7	2001.1	1999.1	-0.4
12-12-13-12-12-12-12-12... (c3)	Overlapped ³	1995.4	1993.4	---
12-12-12-13-12-12-12-12... (c4)	1990.6	1991.6	1989.6	1.0
12-12-12-12-13-12-12-12... (c5)	1995.2	1997.5	1995.5	-0.3
12-12-12-12-12-13-12-12... (c6)	1996.7	1998.6	1996.6	0.1
12-12-12-12-12-12-13-12... (c7)	1986.7	1989.6	1987.6	-0.9
12-12-12-12-12-12-12-13... (c8)	1980.8	1983.0	1981.0	-0.2
13-13-13-13-13-13-13-13... (B)	1922.3	1922.5	1922.3 ⁴	0.0
12-13-13-13-13-13-13-13... (c1)	Overlapped ⁵	1922.6	1922.4	---
13-12-13-13-13-13-13-13... (c2)	1922.9	1922.7	1922.5	0.4
13-13-12-13-13-13-13-13... (c3)	1927.0	1927.3	1927.1	-0.1
13-13-13-12-13-13-13-13... (c4)	1929.2	1929.8	1929.6	-0.4
13-13-13-13-12-13-13-13... (c5)	Overlapped ⁶	1925.4	1925.2	---
13-13-13-13-13-12-13-13... (c6)	1925.1	1925.3	1925.1	0.0
13-13-13-13-13-13-12-13... (c7)	1930.6	1930.8	1930.6	0.0
13-13-13-13-13-13-13-12... (c8)	1940.7	1940.1	1939.9	0.8

¹Scaling factor $\nu_{\text{obs}}/\nu \sim 0.99900$

²Overlapped by the main band at 1999.3 cm^{-1}

³Overlapped by the c1 and c5 isotopomer of the $\nu_8(\sigma_u)$ mode of linear of C_9

⁴Scaling factor $\nu_{\text{obs}}/\nu \sim 0.99989$

⁵Overlapped main band at 1922.3 cm^{-1}

⁶Overlapped by the c5 isotopomer

In considering the detailed assignments, it is noted that the main band at 1922.3 cm^{-1} overlaps the 12-13-13-13-13-13-13-13-13-13-13-13-13-13-13-13-13-13-13-13(1) isotopomer calculated to be 1922.4 cm^{-1} . An observed band at 1922.9 cm^{-1} is close to the band at 1922.5 cm^{-1} calculated for the 12-13-13-13-13-13-13-13-13-13-13-13-13-13-13-13-13-13-13-13(2) isotopomer. A band at 1927.0 cm^{-1} that actually grows together with the main band on annealing and is very close to the predicted 1927.1 cm^{-1} frequency for the 13-13-12-13-13-13-13-13-13-13-13-13-13-13-13-13-13-13-13-13(3) isotopomer. The 1927.0 cm^{-1} band is located between two other bands at 1926.7 and 1927.4 cm^{-1} , which are

both more intense. These bands at 1926.7 and 1927.4 cm^{-1} were tested for alternative assignments to c3 using the *deperturbation method*; however, were there behavior was not consistent with this assignment. The bands at 1929.2, and 1930.6 cm^{-1} are of similar intensity to the already assigned c2 and c3 isotopomers. The absorption at 1929.2 is actually close to the corresponding to the 13-13-13-12-13-13-13-13-13-13-13-13-13-13-13-13-13(4) isotopomer and the absorption at 1930.6 cm^{-1} matches to the calculated band at 1930.6 cm^{-1} for the 13-13-13-13-13-13-12-13-13-13-13-13-13-13-13(7) isotopomers. Both absorptions tested the best with the *deperturbation method*. The band at 1925.1 cm^{-1} which emerge with the main band at 1922.3 cm^{-1} on annealing is more intense than the already assigned c2, c3, c4 and c7 isotopomer bands. It is actually close to the frequencies 1925.2 and 1925.1 cm^{-1} calculated respectively, for the 3-13-13-13-12-13-13-13-13-13-13-13-13-13-13-13(5) and 13-13-13-13-13-13-12-13-13-13-13-13-13-13-13-13(6) isotopomers. The observed band at 1939.8 cm^{-1} is broad and more intense than the c2, c3, c4 and c7 isotopomers already assigned, possibly due to the overlap of other bands. The other nearby bands are the 1939.1 and 1940.7 cm^{-1} . Testing with the *deperturbation method*, supported assignment of the 1940.7 cm^{-1} band to the centrosymmetric 13-13-13-13-13-13-13-12-13-13-13-13-13-13-13(8) isotopomer. The final set of shifts is thus 1922.4 (c1) [overlapped by the main band at 1922.3], 1922.9(c2), 1927.0 (c3), 1929.2(c4) 1925.2 (c5) [overlapped by the c6 isotopomer] 1925.1 (c6), 1930.6 (c3) and 1940.0 cm^{-1} (c8). It is necessary to mention that this is the first time that we can account with a complete set of isotopomers assigned to the vibrational fundamental the $\nu_{10}(\sigma_u)$ mode of linear C_{15} also summarized in Table XXII.

8.4 Assignment of the isotopomers for the $\nu_{12}(\sigma_u)$ mode of C_{18}

The second half of this chapter is concerned with $\nu_{12}(\sigma_u)$ the most intense mode of C_{18} . This mode has a strong interaction with the IR-inactive $\nu_3(\sigma_g)$ mode that lies only 5.4 cm^{-1} to the high frequency side (see Table XXIII). This is the smallest frequency difference between two nearby modes found during this research. The strong interaction means that the isotopomer bands for both interacting ν_{12} and ν_3 modes will be observable upon isotopic substitution as can be seen in Fig. 64.

TABLE XXIII. DFT B3LYP/cc-pVDZ predicted vibrational frequencies and band intensities for ($\ell-C_{18}$)

Vib mode	Freq (cm^{-1})	IR Int (km/mol)	Vib mode	Freq (cm^{-1})	IR Int (km/mol)	Vib mode	Freq (cm^{-1})	IR Int (km/mol)
$\nu_1(\sigma_g)$	2215.4	0.0	$\nu_{16}(\sigma_u)$	901.8	2.3	$\nu_{31}(\pi_u)$	162.3	(6.2)2
$\nu_2(\sigma_g)$	2192.5	0.0	$\nu_{17}(\sigma_u)$	464.3	17.5	$\nu_{32}(\pi_u)$	70.4	(4.7)2
$\nu_3(\sigma_g)$	2062.9	0.0	$\nu_{18}(\pi_g)$	914.5	(0.0)2	$\nu_{33}(\pi_u)$	13.4	(2.6)2
$\nu_4(\sigma_g)$	1843.3	0.0	$\nu_{19}(\pi_g)$	725.3	(0.0)2			
$\nu_5(\sigma_g)$	1781.5	0.0	$\nu_{20}(\pi_g)$	576.2	(0.0)2			
$\nu_6(\sigma_g)$	1494.6	0.0	$\nu_{21}(\pi_g)$	460.9	(0.0)2			
$\nu_7(\sigma_g)$	1108.4	0.0	$\nu_{22}(\pi_g)$	316.9	(0.0)2			
$\nu_8(\sigma_g)$	687.2	0.0	$\nu_{23}(\pi_g)$	215.7	(0.0)2			
$\nu_9(\sigma_g)$	234.6	0.0	$\nu_{24}(\pi_g)$	112.9	(0.0)2			
$\nu_{10}(\sigma_u)$	2227.9	2752.4	$\nu_{25}(\pi_g)$	36.6	(0.0)2			
$\nu_{11}(\sigma_g)$	2151.7	1066.4	$\nu_{26}(\pi_u)$	808.4	(0.0)2			
$\nu_{12}(\sigma_u)$	2057.5	15497.1	$\nu_{27}(\pi_u)$	647.7	(0.0)2			
$\nu_{13}(\sigma_u)$	1951.5	5251.6	$\nu_{28}(\pi_u)$	516.8	(0.3)2			
$\nu_{14}(\sigma_u)$	1672.8	795.9	$\nu_{29}(\pi_u)$	386.2	(1.0)2			
$\nu_{15}(\sigma_u)$	1305.7	149.0	$\nu_{30}(\pi_u)$	268.7	(5.4)2			

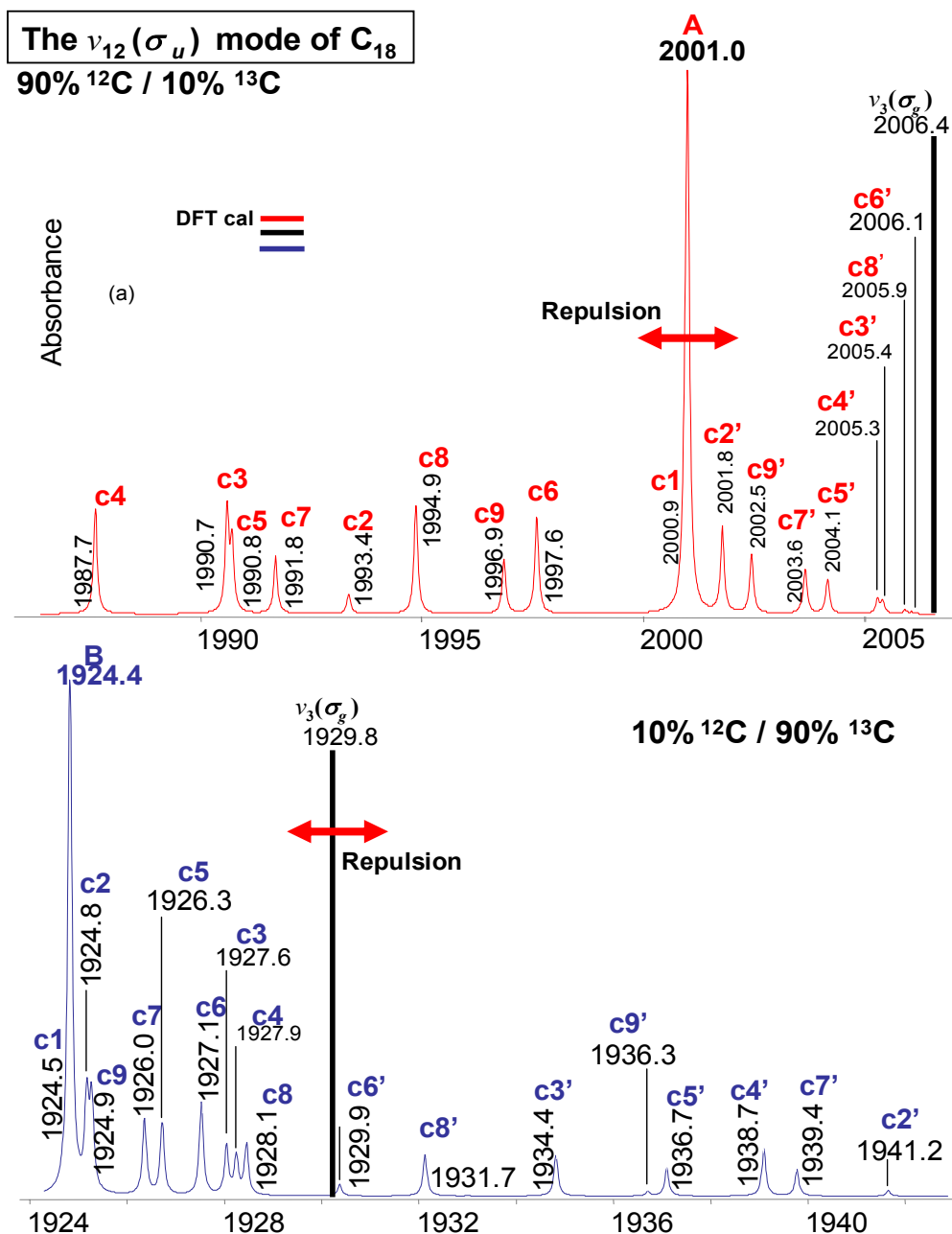


Fig. 64. Both (a)(red) and (b)(blue) are spectra derived from DFT calculations at the B3YLP/cc-pVDZ level of the isotopic shifts with a (a) 10% ^{12}C /10% ^{13}C mixture (b) 90% ^{13}C /10% ^{12}C mixture. The bar in black is only for the purpose of illustrating where the interacting IR forbidden $\nu_1(\sigma_g)$ mode would appear. A representation of the repulsion between the shifts of the interacting ν_3 and ν_{12} modes is also shown.

The frequency region containing the main band and the corresponding isotopomer shifts is shown in Fig. 65. This vibrational fundamental and its isotopic shifts, lie together with other peaks of different C_n species within a highly congested frequency interval 1985-2001.0 cm^{-1} that complicates assignments. As the number of carbon atoms increases in a carbon chain the number of vibrational fundamentals increases as can be seen in Fig. 58, 59, and 60. Predictions of the vibrational fundamental were obtained at the B3LYP/cc-PVDZ level. It is possible however, to choose a preliminary shift set formed by the single ^{13}C -substituted $^{12}\text{C}^{13}\text{C}_{17}$ isotopomers for the $\nu_{12}(\sigma_u)$ mode of linear of $^{12}\text{C}_{18}$ located to the low frequency side of the main band located at 2001.0 $\text{cm}^{-1}(\text{A})$ in Fig. 65 by taking the bands at 2000.9 (c1)[overlapped by the main band], 1993.9(c2), 1990.6(c3), 1987.6 (c3), 1990.8 (c5)[overlapped by the c3 isotopomer and the c4 isotopomer of $\nu_{10}(\sigma_u)$ mode of linear of C_{15}], 1997.5 (c6), 1991.8(c7)[overlapped by the $\nu_8(\sigma_u)$ mode of linear of C_{12}], 1994.1(c8), and 1996.2 cm^{-1} (c9). These absorptions appear to grow in when the main band increases its intensity after annealing, showing that they are correlated. Also by taking the bands located to the high frequency side of the main band at 2001.0 $\text{cm}^{-1}(\text{A})$ we can choose a preliminary shift set *SSC12*, corresponding to the infrared forbidden $\nu_3(\sigma_g)$ mode of linear of $^{12}\text{C}_{18}$. These are the absorptions at 2001.9(c2'), 2005.8(c3'), 2005.4(c4'), 2004.1(c5'), 2006.1(c6') [overlapped by the c8' isotopomer], 2003.6 (c3), 2006.3(c8') and 2002.9 $\text{cm}^{-1}(\text{c9}')$.

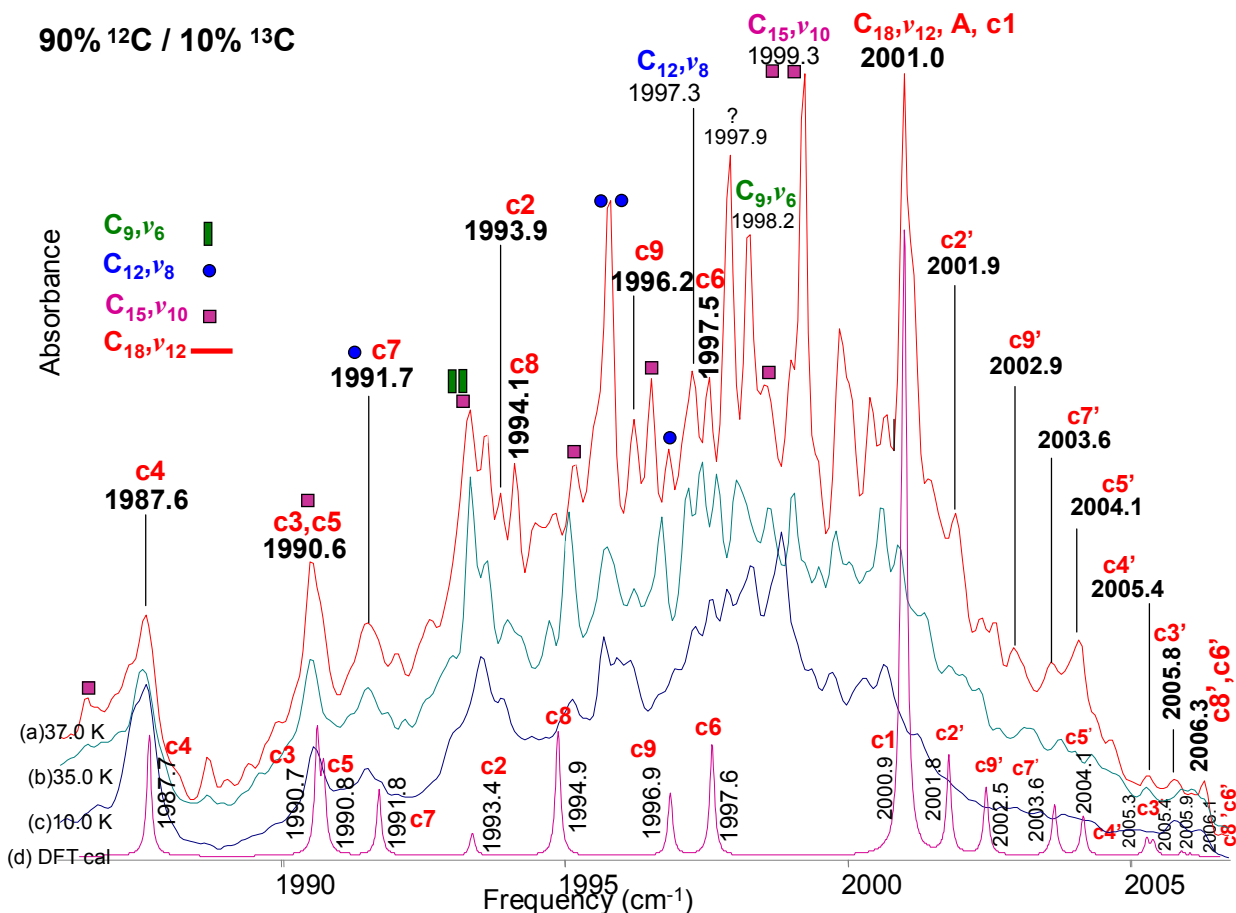


Fig. 65. Comparison of observed FTIR annealed spectra (a) 37 K, (b) 35 K and (c) 10 K of the $\nu_{12}(\sigma_u)$ mode of linear of C₁₈ and its single ¹³C isotopic shifts using 90% ¹²C and 10% ¹³C carbon enrichments, and (d) a simulated spectrum derived from the DFT calculations at the B3YLP/cc-pVDZ level using the same enrichment values.

The 13-12-12-12-12-12-12-12-12-12-12-12-12-12-12-12-12-12 (c1) isotopomer, with a calculated frequency at 2000.9 cm⁻¹ is overlapped by the main band at 2001.0 cm⁻¹ (A). The observed band at 1993.9 cm⁻¹ is close to the frequency predicted for the 12-13-12-12-12-12-12-12-12-12-12-12-12-12-12-12 (c2) isotopomer, and its low intensity is consistent with the simulated spectrum. The unknown band at 1993.6 cm⁻¹ is probably related to the unidentified

prominent band at 1997.9 cm^{-1} . The observed band at 1990.6 cm^{-1} assigned to the c4 isotopomer of the $\nu_{10}(\sigma_u)$ mode of linear of C_{15} , significantly increases its intensity after annealing, probably due to the overlap of more than one isotopomer. This band is close to the calculated bands at 1990.7 and 1990.8 cm^{-1} corresponding to the 12-12-13-12-12-12-12-12-12-12-12-12-12-12-12-12-12-12 (c3) and the 12-12-12-12-13-12-12-12-12-12-12-12-12-12-12-12-12-12 (c5) isotopomers. Therefore, the band at 1990.6 cm^{-1} is assigned to the c3 isotopomer overlapping the observed c5 isotopomer and the c4 isotopomer of the $\nu_{10}(\sigma_u)$ mode of linear of C_{15} . The band at 1987.6 cm^{-1} is well isolated from other isotopomer absorptions, and is close to the 1987.7 cm^{-1} frequency calculated for the 12-12-12-13-12-12-12-12-12-12-12-12-12-12-12-12-12-12 (c4) isotopomer. The absorptions appearing at 1997.5 and 1996.2 cm^{-1} lie in a densely populated region but they are close to the calculated bands at 1997.6 and 1996.2 cm^{-1} for the 12-12-12-12-12-13-12-12-12-12-12-12-12-12-12-12-12-12 (c6) and 12-12-12-12-12-12-12-12-12-13-12-12-12-12-12-12-12-12 (c9) isotopomers, respectively. The band observed at 1991.7 cm^{-1} is already assigned to the c5 isotopomer of the $\nu_8(\sigma_u)$ mode of linear of C_{12} . This absorption increases in intensity after annealing as can be seen in Fig. 62(a), suggesting the possibility of a contribution from another isotopomer which may be the 12-12-12-12-12-12-13-12-12-12-12-12-12-12-12-12-12-12 (c7) isotopomer with frequency calculated at 1991.8 cm^{-1} . The observed band at 1994.1 cm^{-1} is close to the calculated band at 1994.9 cm^{-1} corresponding to the 12-12-12-12-12-12-12-13-12-12-12-12-12-12-12-12-12-12 (c8) isotopomer. We thus have a set of shifts for the single substituted single ^{12}C -substituted $^{12}\text{C}^{13}\text{C}_{17}$ isotopomers for the ν_{12} mode of C_{18} with the bands at 2000.9 (c1)[overlapped by the main band], 1993.9(c2), 1990.6(c3), 1987.6(c4), 1990.8 (c5) [overlapped by the c3 isotopomer and the c4 isotopomer of $\nu_{10}(\sigma_u)$ of linear C_{15}], 1997.5(c6), 1991.8(c7) [overlapped by the $\nu_8(\sigma_u)$ mode of linear of C_{12}], 1994.1(c8), and 1996.2 cm^{-1} (c9).

To continue, to identify isotopomer bands of the IR forbidden $\nu_3(\sigma_g)$ mode of linear of C_{18} we need to move to the high frequency side of the main band at 2001.0 cm^{-1} (A) in Fig. 65 in the frequency interval $2001.0 - 2006.5\text{ cm}^{-1}$, which is shown in more detail in Fig. 66.

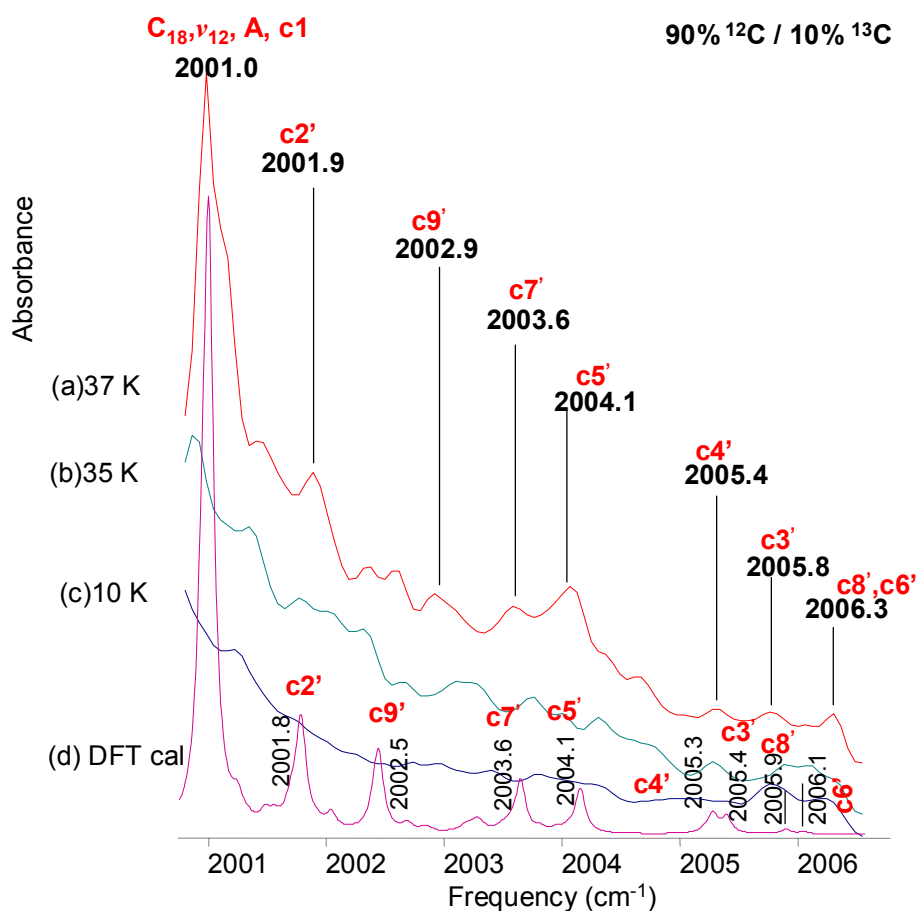


Fig. 66. A comparison of observed FTIR annealed spectra (a) 37 K, (b) 35 K and (c) 10 K of the not IR-allowed $\nu_3(\sigma_g)$ mode of linear of C_{18} and its single ^{13}C isotopic shifts using $90\%^{12}\text{C}$ and $10\%^{13}\text{C}$ carbon enrichments, and (d) a simulated spectrum derived from the DFT calculations at the B3YLP/cc-pVDZ level using the same enrichment values.

The band observed at 2001.9 cm^{-1} increases its intensity upon the appearance of the main band at 2001.0 cm^{-1} (A). The band at 2001.9 cm^{-1} is close to the calculated frequency of 2001.8 cm^{-1} for the c_2' isotopomer. The observed bands at 2005.4 and 2005.8 cm^{-1} appear somewhat less intense than the c_2' isotopomer already assigned but they are close to the calculated

frequencies at 2005.3 and 2005.4 cm^{-1} corresponding to the c4' and c3' isotopomers shown in Fig. 66(a). The observed band at 2003.6 cm^{-1} matches the frequency calculated for the c7' isotopomer. The observed band at 2004.1 cm^{-1} is more intense than the c7' isotopomer already assigned, probably due to other C_n bands, and is close to the 2004.1 cm^{-1} frequency calculated for the c5' isotopomer. The observed band at 2006.3 cm^{-1} is an isolated peak close to the bands calculated at 2005.9 and 2006.1 cm^{-1} for the c8' and c6' isotopomers which are weak in intensity. The observed band is thus intense enough to contain the absorptions of both isotopomers. Thus the 2003.6 cm^{-1} absorption will be assigned to the overlapping c8' and c6' absorptions. The observed band at 2002.9 cm^{-1} is approximately the same intensity as of the c7' isotopomer and is close to the calculated band at 2002.5 cm^{-1} for the (c9') isotopomer.

We thus have a set of IR allowed isotopomer absorptions corresponding to the infrared forbidden $\nu_3(\sigma_g)$ mode of linear of C_{18} comprised of the 2001.9(c2'), 2005.8(c3'), 2005.4(c4'), 2004.1(c5'), 2006.3(c8'), 2006.1(c6')[overlapped by the c8' isotopomer], and 2002.9 cm^{-1} (c9') absorptions.

The absorption at 1924.4 cm^{-1} (B) in Fig. 67, which is a factor $\sim \sqrt{12/13}$ of the 2001.0 cm^{-1} frequency, is recognized as belonging to the fully ^{13}C -substituted isotopomer, which was created by the evaporation of a carbon mixture of 10% ^{12}C /90% ^{13}C . In the interval 1920.0-1925.0 cm^{-1} there is a dense population of vibrational fundamentals. Most of them have been identified and presented previously in this work.

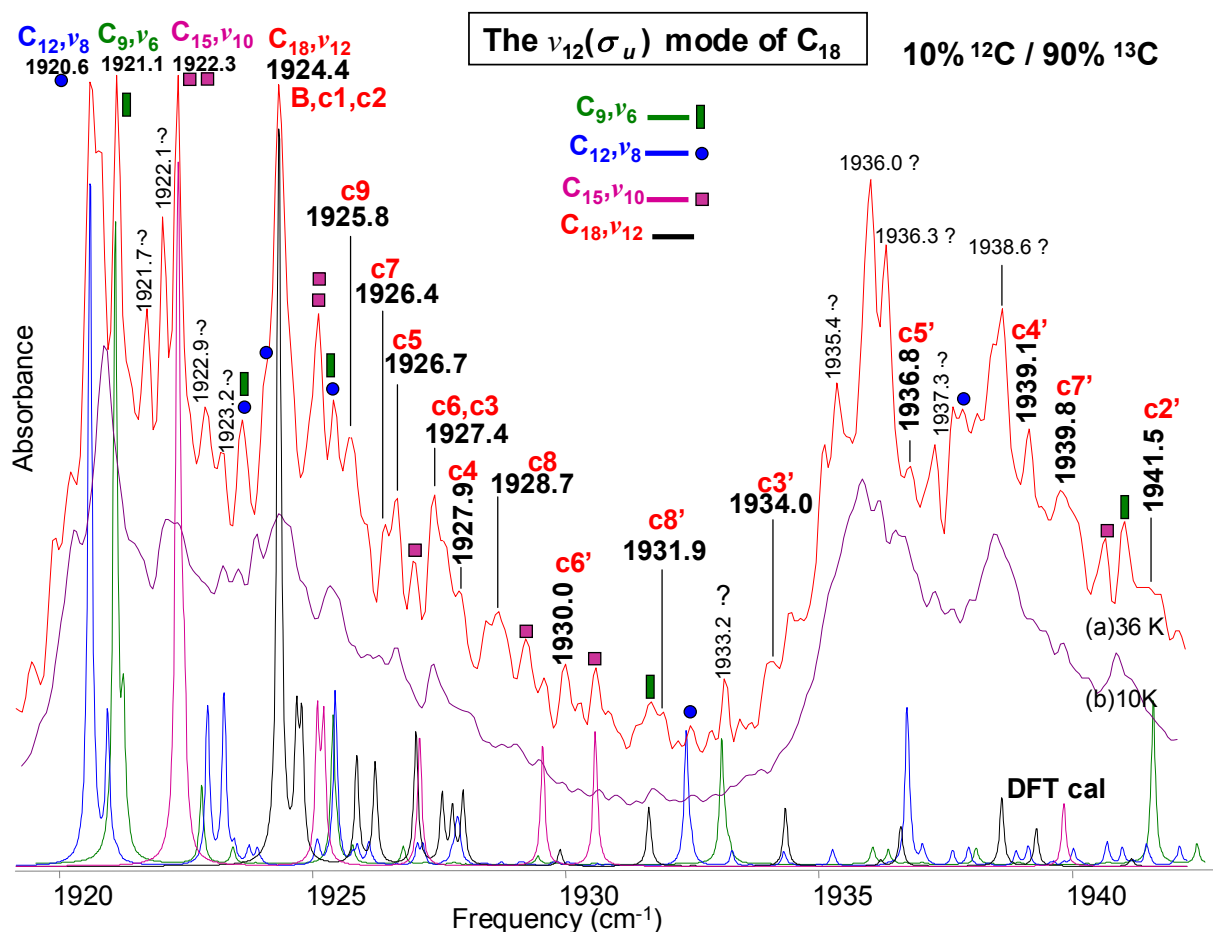


Fig. 67. Comparison of observed FTIR annealed spectra (a) 36 K and (b) 10 K of the $\nu_6(\sigma_u)$, $\nu_8(\sigma_u)$, $\nu_{10}(\sigma_u)$ and $\nu_{12}(\sigma_u)$ mode of linear C₉, C₁₂, C₁₅ and C₁₈ and its single ¹³C isotopic shifts using 90% ¹²C and 10% ¹³C carbon enrichments and a simulated spectra derived from the DFT calculations at the B3YLP/cc-pVDZ level using the same enrichment values for the $\nu_6(\sigma_u)$, $\nu_8(\sigma_u)$, $\nu_{10}(\sigma_u)$ and $\nu_{12}(\sigma_u)$ mode of linear C₉, C₁₂, C₁₅ and C₁₈.

It is possible to identify most of the observed bands in Fig. 67 which isolates the region of interest. On high frequency side of the main band at 1924.4 cm⁻¹(B) we can choose a shift set SSC13, for the single ¹²C-substituted ¹²C¹³C₁₇ isotopomers of the $\nu_{12}(\sigma_u)$ mode of C₁₈ formed with the bands at 1924.5 (c1) and 1924.8 (c2) [overlapped by the main band at 1924.4 cm⁻¹ (B)], 1927.6 (c3) [overlapped by the c6 isotopomer], 1927.9 (c4), 1926.7 (c5), 1927.4 (c6), 1926.4

(c7), 1928.7(c8) and 1925.8 cm^{-1} (c9). Those bands appear to grow in when the main band at 1924.4 cm^{-1} increases its intensity after annealing, showing they are correlated (see Table XXIV). The bands at 1921.7 and 1922.1 cm^{-1} are probably C_n species but they are not related either to the $\nu_8(\sigma_u)$ mode of linear C_{12} or to $\nu_6(\sigma_u)$ mode of linear C_9 . However the possible shifts at 1922.9 and 1923.2 cm^{-1} are probably related to them and they are under investigation. The prominent unidentified bands at 1936.0, 1936.3, and 1938.6 cm^{-1} seem not to be related to one another, although the peak at 1937.3 seems to be related to the 1936.0 band, which is under investigation. The peak at 1935.4 cm^{-1} is similarly an unidentified C_n species.

TABLE XXIV. Comparison of observed and predicted DFT (B3LYP/cc-pVDZ) frequencies for single ^{13}C -substituted isotopomers of $^{12}\text{C}_{18}$, and single ^{12}C -substituted isotopomers of $^{13}\text{C}_{18}$, for the ν_{12} mode.

Isotopomer	B3LYP/cc-pVDZ			$\Delta\nu$ $\nu_{\text{obs}} - \nu_{\text{scaled}}$
	ν_{obs}	ν	ν_{scaled}	
12-12-12-12-12-12-12-12-12... (A) ¹	2001.0	2057.5	2001.0 ²	0.0
13-12-12-12-12-12-12-12-12... (c1)	Overlapped ³	2057.4	2000.9	---
12-13-12-12-12-12-12-12-12... (c2)	1993.9	2049.7	1993.4	0.5
12-12-13-12-12-12-12-12-12... (c3)	1990.6	2046.9	1990.7	-0.1
12-12-12-13-12-12-12-12-12... (c4)	1987.6	2043.8	1987.7	-0.1
12-12-12-12-13-12-12-12-12... (c5)	Overlapped ⁴	2047.0	1990.8	---
12-12-12-12-12-13-12-12-12... (c6)	1997.5	2054.0	1997.6	-0.1
12-12-12-12-12-12-13-12-12... (c7)	Overlapped ⁵	2048.0	1991.8	---
12-12-12-12-12-12-12-13-12... (c8)	1994.1	2051.2	1994.9	-0.8
12-12-12-12-12-12-12-12-13... (c9)	1996.2	2053.3	1996.9	-0.7
12-13-12-12-12-12-12-12-12... (c2') ⁶	2001.9	2058.3	2001.8	0.1
12-12-13-12-12-12-12-12-12... (c3')	2005.8	2062.0	2005.4	0.4
12-12-12-13-12-12-12-12-12... (c4')	2005.4	2061.9	2005.3	0.1
12-12-12-12-13-12-12-12-12... (c5')	2004.1	2060.7	2004.1	0.0
12-12-12-12-12-13-12-12-12... (c6')	Overlapped ⁷	2062.7	2006.1	---
12-12-12-12-12-12-13-12-12... (c7')	2003.6	2060.2	2003.6	0.0
12-12-12-12-12-12-12-13-12... (c8')	2006.3	2062.5	2005.9	0.4
12-12-12-12-12-12-12-12-13... (c9')	2002.9	2059.0	2002.5	0.4
13-13-13-13-13-13-13-13-13... (B) ⁸	1924.4	1976.5	1924.4 ⁹	0.0
12-13-13-13-13-13-13-13-13... (c1)	Overlapped ¹⁰	1976.6	1924.5	---
13-12-13-13-13-13-13-13-13... (c2)	Overlapped ¹¹	1976.9	1924.8	---
13-13-12-13-13-13-13-13-13... (c3)	Overlapped ¹²	1979.8	1927.6	---
13-13-13-12-13-13-13-13-13... (c4)	1927.9	1980.1	1927.9	0.0
13-13-13-13-12-13-13-13-13... (c5)	1926.7	1978.5	1926.3	0.4
13-13-13-13-13-12-13-13-13... (c6)	1927.4	1979.3	1927.1	0.3
13-13-13-13-13-13-12-13-13... (c7)	1926.4	1978.1	1926.0	0.4
13-13-13-13-13-13-13-12-13... (c8)	1928.7	1980.3	1928.1	0.6
13-13-13-13-13-13-13-13-12... (c9)	1925.8	1977.0	1924.9	0.9
13-12-13-13-13-13-13-13-13... (c2') ¹³	1941.5	1993.8	1941.2	0.3
13-13-12-13-13-13-13-13-13... (c3')	1934.0	1986.8	1934.4	-0.4
13-13-13-12-13-13-13-13-13... (c4')	1939.1	1991.2	1938.7	0.4
13-13-13-13-12-13-13-13-13... (c5')	1936.8	1989.1	1936.7	0.1
13-13-13-13-13-12-13-13-13... (c6')	1929.6	1982.2	1929.9	-0.3
13-13-13-13-13-13-12-13-13... (c7')	1939.8	1991.9	1939.4	0.4
13-13-13-13-13-13-13-12-13... (c8')	1931.9	1984.0	1931.7	0.2
13-13-13-13-13-13-13-13-12... (c9')	Overlapped ¹⁴	1988.7	1936.3	---

¹Single substituted ^{13}C -isotopomers for the $\nu_{12}(\sigma_u)$ mode of the linear $^{12}\text{C}_{18}$

²Scaling factor $\nu_{\text{obs}}/\nu \sim 0.97253$

³Overlapped by the main band at 2001.0 cm^{-1}

⁴Overlapped by the c3 isotopomer

⁵Overlapped by c4 isotopomer of the $\nu_8(\sigma_u)$ mode of the linear $^{12}\text{C}_{12}$

⁶Single substituted ^{13}C -isotopomers for the not IR-allowed $\nu_3(\sigma_g)$ mode of the linear $^{12}\text{C}_{18}$

⁷Overlapped by the c8' isotopomer

⁸Single substituted ^{12}C -isotopomers for the $\nu_{12}(\sigma_u)$ mode of the linear $^{13}\text{C}_{18}$

⁹Scaling factor $\nu_{\text{obs}}/\nu \sim 0.97364$

¹⁰Overlapped by the main band at 1924.4 cm^{-1}

¹¹Overlapped by the c6 isotopomer

¹²Overlapped by the c6 isotopomer

¹³Single substituted ^{12}C -isotopomers for the not IR-allowed $\nu_3(\sigma_g)$ mode of the linear $^{13}\text{C}_{18}$

¹⁴Overlapped by an unknown band at 1936.0 cm^{-1}

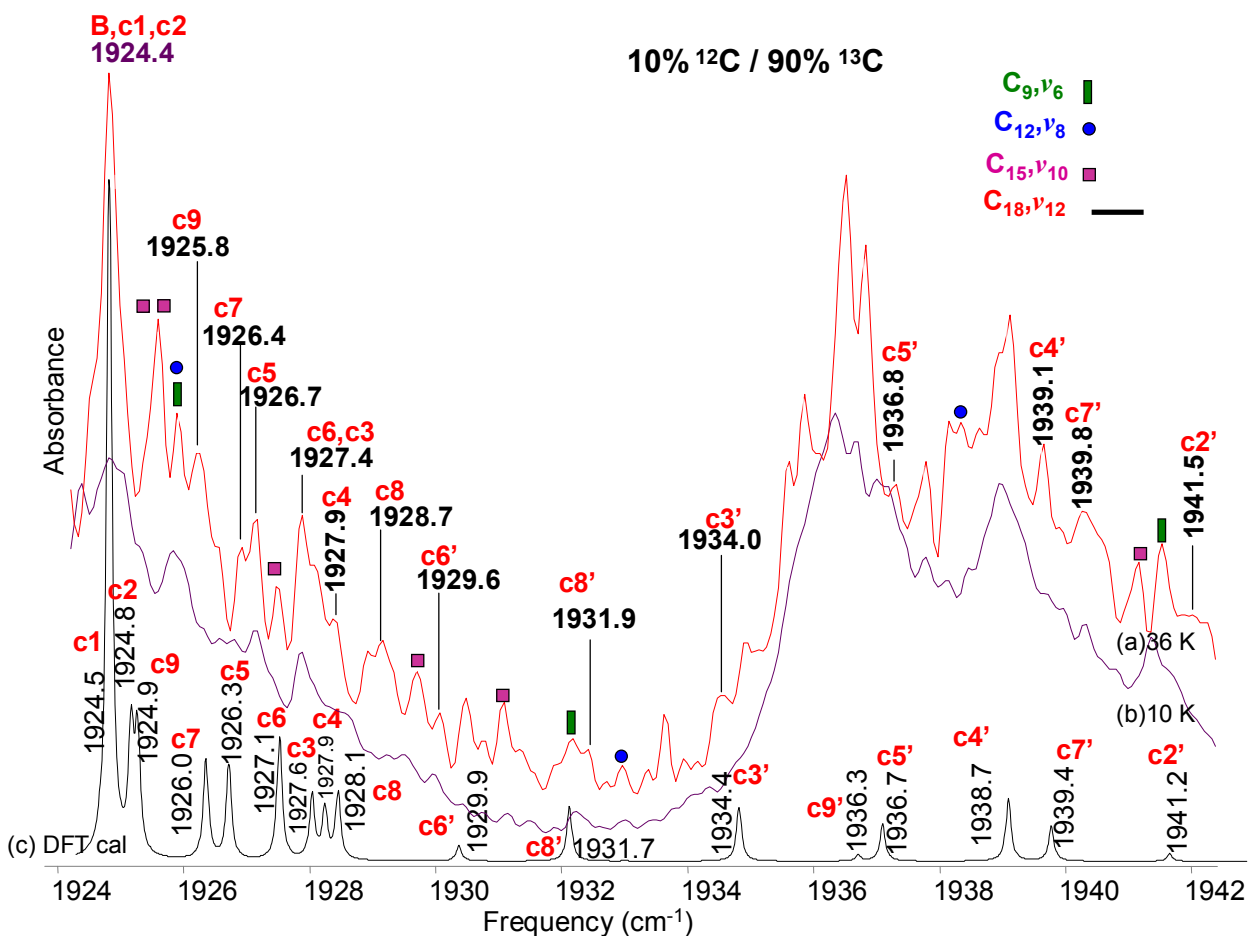


Fig. 68. Comparison of observed FTIR annealed spectra (a) 36 K and (b) 10 K of the $\nu_{12}(\sigma_u)$ mode of linear C_{18} and its single ^{13}C isotopic shifts using 90% ^{12}C and 10% ^{13}C carbon enrichments and a simulated spectra derived from the DFT calculations at the B3YLP/cc-pVDZ level using the same enrichment values for the $\nu_{12}(\sigma_u)$ mode of linear C_{18} .

In continuing with our isotopic analysis we will refer to the high frequency side of the main band at 1924.4 cm^{-1} (B) in the spectrum of Fig. 68. The bands corresponding to the 12-13-13-13-13-13-13-13-13-13-13-13-13-13-13-13-13-13-13-13 (c1) and 13-12-13-13-13-13-13-13-13-13-13-13-13-13-13-13-13-13-13-13 (c2) isotopomers calculated at 1924.5 and 1924.8 cm^{-1} seem to be overlapped by the main band. A cluster of several bands located in the frequency interval 1927.1 - 1928.5 cm^{-1} increases in intensity after annealing, as shown in Fig. 68 (a). Within this cluster, there is a

prominent band at 1927.4 cm^{-1} that is more intense than the other isotopomer bands and may result from the overlap of two isotopomer bands calculated at 1927.1 and 1927.6 cm^{-1} for the 13-13-13-13-13-112-13-13-13-13-13-13-13-13-13-13-13 (c6) and 13-13-12-13-13-13-13-13-13-13-13-13-13-13-13-13-13-13-13 (c3) isotopomers, respectively. Another absorption growing in to the high frequency side of the c6 isotopomer matches the band calculated at 1927.9 cm^{-1} for the 13-13-13-14-13-13-13-13-13-13-13-13-13-13-13-13-13-13-13 (c4) isotopomer. The observed band at 1926.7 cm^{-1} is slightly more intense than the band at 1926.4 cm^{-1} probably due to the overlap of other bands. The bands at 1926.4 and 1926.7 cm^{-1} are close to the calculated bands at 1926.0 and 1926.3 cm^{-1} corresponding to the 13-13-13-13-13-13-12-13-13-13-13-13-13-13-13-13-13-13-13 (c7) and 13-13-13-13-12-13-13-13-13-13-13-13-13-13-13-13-13-13-13 (c5) in that order. Both of the bands at 1928.4 and 1928.7 cm^{-1} are close to the calculated 1928.1 cm^{-1} corresponding to the 13-13-13-13-13-13-12-13-13-13-13-13-13-13-13-13-13-13-13 (c8) isotopomer but we choose the band at 1928.7 cm^{-1} , since its intensity of similar to the c4 isotopomer absorption and it on testing with the *deperturbation method*, it behaved well. The observed band at 1925.8 cm^{-1} seems to be related to the already assigned c4, c8, c7 and c5 isotopomers that increase their intensity after annealing processes and it is close to the 1924.9 cm^{-1} frequency calculated for the 13-13-13-13-13-13-13-12-13-13-13-13-13-13-13-13-13-13-13 (c9) isotopomer. Testing with *deperturbation method* calculations confirmed the choice.

We continue with the assignment of the isotopomer bands for the IR inactive $\nu_3(\sigma_g)$ mode of linear of $^{13}\text{C}_{18}$. Assignments are difficult here because of the presence of strong unidentified C_n bands. A bump at 1941.5 is close to the weak band at 1941.2 cm^{-1} calculated for the c2' isotopomer. An observed band at 1934.0 cm^{-1} is close to the calculated band at 1934.4 cm^{-1} for the c3' isotopomer and, thus is assigned to it. The unknown shifts at 1928.4 , 1930.0 and 1933.2

cm^{-1} are probably related but they still remain unknown. The band at 1939.1 cm^{-1} is of similar intensity of that of the $\text{c3}'$ isotopomer and it is close to the calculated band at 1938.7 cm^{-1} corresponding to the $\text{c4}'$ isotopomer. The observed band at 1929.6 cm^{-1} is weaker than the already assigned $\text{c3}'$ and $\text{c4}'$ isotopomers and even to the 1930.0 cm^{-1} band. It is close to the calculated band at 1929.9 cm^{-1} for the $\text{c6}'$ isotopomer. Bands observed at 1936.8 and 1931.9 cm^{-1} are close bands to calculated at 1936.7 and 1931.7 cm^{-1} corresponding respectively to the $\text{c5}'$ and $\text{c8}'$ isotopomers. The calculated band at 1936.3 cm^{-1} corresponding to the $\text{c9}'$ isotopomer is of small intensity and is overlapped by the prominent unknown bands at 1936.0 and 1936.3 cm^{-1} rendering the $\text{c9}'$ isotopomer unobservable.

To summarize, we have the single ^{12}C -substituted $^{12}\text{C}^{13}\text{C}_{17}$ isotopomers for the $\nu_{12}(\sigma_u)$ mode of linear of C_{18} including the shifts at 1924.5 (c1) and 1924.8 (c2) [overlapped by the main band at 1924.4 cm^{-1} (B)], 1927.6 (c3) [overlapped by the c6 isotopomer], 1927.9 (c4), 1926.7 (c5), 1927.4 (c6), 1926.4 (c7), 1928.7 (c8) and 1925.8 (c9) and for the $\nu_3(\sigma_g)$ mode, the 1941.5 (c2'), 1934.0 (c3'), 1939.1 (c4'), 1936.8 (c5'), 1929.6 (c6'), 1939.8 (c7'), 1931.9 (c8') and the 1936.3 (c9') cm^{-1} (overlapped by the unknown band at 1936.0 cm^{-1}) absorptions

A final representation of the observed and calculated isotopomers of the single ^{12}C -substituted $^{12}\text{C}^{13}\text{C}_{17}$ isotopomers for the for the $\nu_{12}(\sigma_u)$ and $\nu_3(\sigma_g)$ modes of linear of C_{18} is shown in the cartoon in Fig. 69.

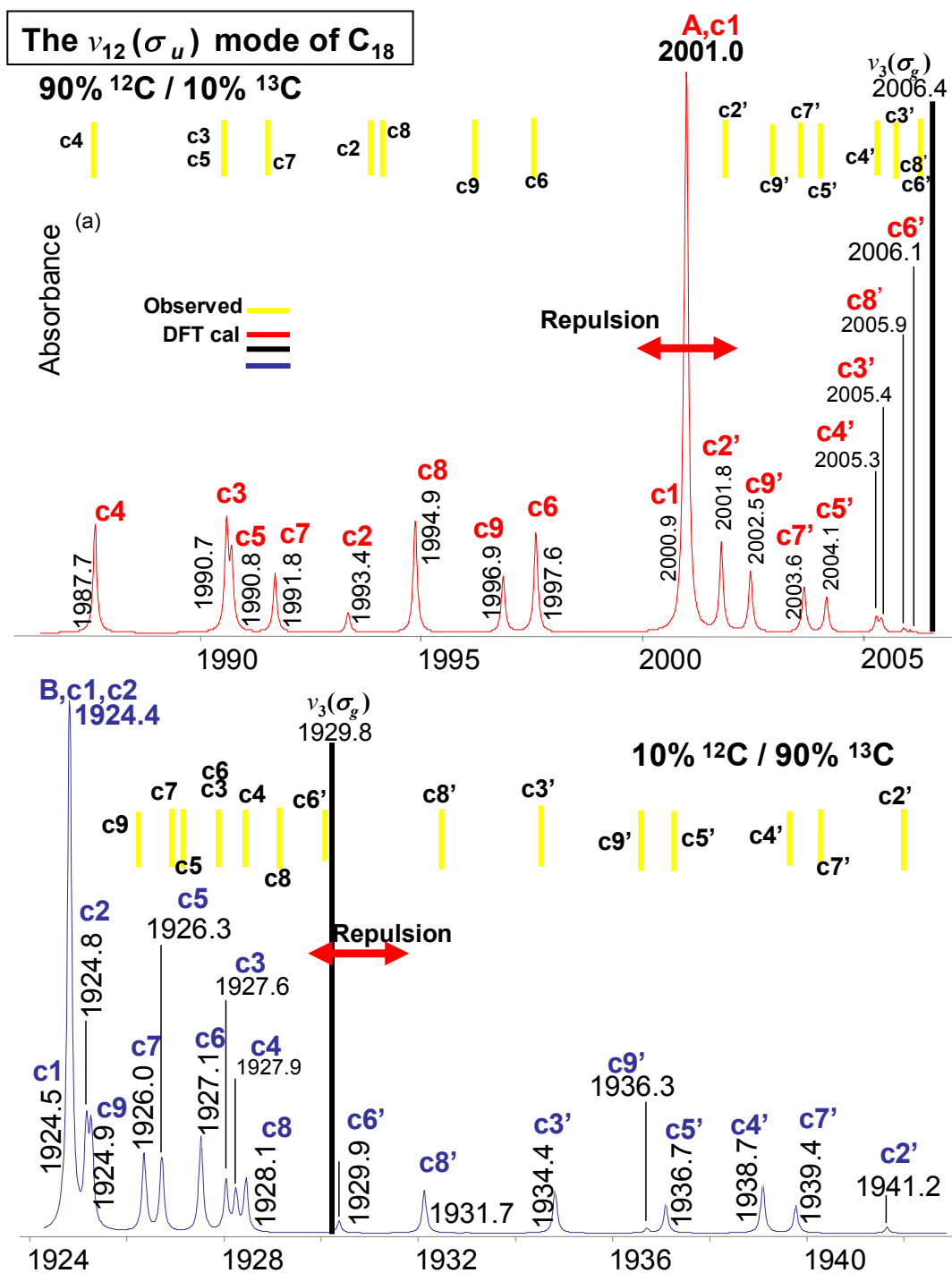


Fig. 69. Both (a)(red) and (b)(blue) are spectra derived from DFT calculations at the B3YLP/cc-pVDZ level of the isotopic shifts with a (a) 10% ^{12}C /10% ^{13}C mixture (b) 90% ^{13}C /10% ^{12}C mixture. The bars in yellow are only to represent where the observed frequencies would be located. The bar in black is also for the purpose of illustrating where the interacting infrared forbidden $\nu_1(\sigma_g)$ mode would appear. We can see also a representation of the repulsion between the shifts of the interacting ν_3 and ν_{12} modes.

8.5 Conclusions

The results of the Fourier transform infrared ^{13}C isotopic investigation have been presented for the $\nu_{10}(\sigma_u)$ and $\nu_{12}(\sigma_u)$ fundamentals of linear C_{15} and C_{18} respectively in solid Ar at 10 K produced by the laser ablation of graphite. The analysis based on the new experimental spectra acquired for both 90/10 and 10/90 isotopic measurements and also on taking into consideration the interactions between the $\nu_{10}(\sigma_u)$ and $\nu_3(\sigma_g)$ modes of linear C_{15} and the $\nu_{12}(\sigma_u)$ and $\nu_3(\sigma_g)$ modes of linear C_{18} the use of DPM to support the assignments. This work is the first assignment of the $\nu_{10}=1993.3$ and $\nu_{12}=2001.0 \text{ cm}^{-1}$ vibrational fundamentals of linear C_{15} and linear C_{18} and is a significant advance toward the identification of the spectra of even larger C_n species.

CHAPTER IX

CONCLUSIONS AND FUTURE STUDIES

9.1 Conclusions

The heart of this work has been concentrated on the quest for long C_n ($n \geq 6$) species. In pursuing this goal, several experimental and theoretical innovations were necessary. A complete characterization of C_n species using FTIR matrix isolation techniques is difficult but rewarding, as has been demonstrated by this research. In seeking to identify the vibrational fundamentals of long carbon molecules we faced several problems: 1) $^{12}C^{13}C$ isotopic carbon mixtures can produce an increasingly large number of isotopomer bands for C_n ($n \geq 6$) species. In the past it has been difficult or impossible to unambiguously identify and assign all of the single ^{13}C shifts making assignments problematic for some of the vibrational fundamentals of long C_n ($n \geq 6$) species, since it does critically depends on measuring a sufficient number of isotopic shifts. 2) It is possible to find vibrational modes of different C_n species with similar frequencies. These tend to accumulate in short frequency intervals in the infrared spectrum resulting in a collection of overlapping isotopic shifts that makes distinguishing different molecules from one another increasingly difficult. 3) An isotopic ^{13}C or ^{12}C isotopic substitution may turn a non-infrared active mode of a given linear molecule into an infrared active mode and consequently its shifts become potentially observable, complicating identifications.

In order to address the first two problems, we have in this work performed a number of substantial improvements in experimental techniques to enable the acquisition of suitable carbon mixtures restricted to $\sim 10\%$ of either ^{12}C and ^{13}C isotope to produce only single ^{13}C -substituted

($^{12}\text{C}^{13}\text{C}_{n-1}$) or single ^{12}C -substituted ($^{13}\text{C}^{12}\text{C}_{n-1}$) carbon clusters, in order to limit the number of shifts but provide a sufficient number to test assignments. We now routinely achieve experimental reproducibility, which enables better comparisons between spectra. Nevertheless the rather large number of absorptions observed in small frequency regions of the infrared spectrum, makes distinguishing different molecules from one another a challenge.

These results triggered the review of the theoretical calculations (DFT) traditionally dependent on the comparison between measured and predicted ^{12}C and ^{13}C isotopic shifts. As a result the theorists Garcia-Navarro and Rittby⁴⁷ recently developed the “deperturbation method” (DPM) in order to measure the magnitude of coupling effects on isotopic substitution and reduce or even eliminate these coupling effects from the spectrum. This development allows better comparisons with the experimental results (see Appendix A) in testing isotopic shift assignments and makes more secure the identification of vibrational fundamentals. The implementation of these experimental improvements and theoretical advances has led us to assign sixteen of the vibrational fundamentals of eight different C_n ($n \geq 7$) chains.

9.2 Summary of Results

With the measurement of a complete set of single ^{12}C and ^{13}C substituted isotopic shifts, the results of our DFT calculations, and taking into account the coupling with the $\nu_1(\sigma_g)$ mode, the $\nu_4(\sigma_u)$ fundamental of C_7 has been rigorously assigned to an absorption at 2128.1 cm^{-1} (CHAPTER III).

Similarly the measurement of single substitution shifts, DFT calculations, and taking into consideration the interaction with the IR inactive $\nu_1(\sigma_g)$ mode of C_9 , the $\nu_5(\sigma_u)$ and $\nu_6(\sigma_u)$

fundamentals of C₉ have been confirmed at 2078.2 and 1998.2 cm⁻¹ respectively. This work also confirms the assignment of the $\nu_7(\sigma_u)$ mode of C₉ at 1601.0 cm⁻¹ (CHAPTER IV).

Isotopic shift measurements, DFT calculations, and analysis of the interaction of the IR inactive $\nu_1(\sigma_g)$ and $\nu_2(\sigma_g)$ modes with the $\nu_6(\sigma_u)$ and $\nu_7(\sigma_u)$ modes has led to the confirmation of the assignment of the vibrational fundamentals $\nu_6(\sigma_u)=2074.2$ cm⁻¹ and $\nu_7(\sigma_u)=1915.7$ cm⁻¹ of C₁₀ (CHAPTER V). These assignments are important in the analysis of the vibrational spectrum of C₁₀ and also provide us with useful insights on molecules for which interaction with a nearby infrared inactive mode results in extra isotopomer bands. This work and the further work listed below marks the first time isotopic shifts for infrared inactive modes have been reported in FTIR matrix studies.

By a similar strategy this work has confirmed the assignment of the vibrational fundamentals $\nu_7(\sigma_u)=1946.1$ and $\nu_8(\sigma_u)=1856.7$ of C₁₁. Also, with a partial isotopic information the $\nu_8(\sigma_u)$ fundamental is tentatively assigned at 1360.0 cm⁻¹ (CHAPTER VI). In the case of this molecule the coupling with the nearby infrared inactive $\nu_2(\sigma_g)$ and $\nu_1(\sigma_g)$ modes is strong, inducing the observation of additional shifts bands that has provided us with valuable data and given us experience for subsequent isotopic investigations of longer C_n chains.

The analysis based on the greatly spectra acquired for both C₁₂/C₁₃ = 90%/10% and 10%/90%, isotopic measurements, makes possible for the first time the assignment on the basis of isotopic shift measurements, the vibrational fundamentals $\nu_5(\sigma_u)=2071.4$ and $\nu_6(\sigma_u)=1710.5$ cm⁻¹ of linear C₈. The previous assignments of the $\nu_7(\sigma_u)=2140.6$, $\nu_8(\sigma_u)=1997.3$ and $\nu_9(\sigma_u)=1817.9$ cm⁻¹ fundamentals of linear C₁₂, which have recently been challenged, strengthened and confirmed with the more extensive isotopic shift data obtained as a result of this dissertation research (CHAPTER VII). The isotopic data for the ν_8 and ν_9 modes of C₁₂ are

of particular help in identifying the shifts of other C_n species located within the same highly congested frequency region, facilitating the application of our strategy to even larger molecules C_n ($n > 12$) such as the $\nu_{10}(\sigma_u) = 1999.3 \text{ cm}^{-1}$ fundamental of linear C_{15} and $\nu_{12}(\sigma_u) = 2001.0 \text{ cm}^{-1}$ of linear of C_{18} (CHAPTER VIII). In the following Table XXV a summary is presented of the 16 different vibrational fundamentals corresponding to the C_7 , C_8 , C_9 , C_{10} , C_{11} , C_{12} , C_{15} and C_{18} linear molecules confirmed.

TABLE XXV. Observed results for full $^{12}C_n$ and $^{13}C_n$ and their single substituted $^{12}C_{n-1}^{13}C$ and $^{12}C^{13}C_{n-1}$ isotopomers for C_n clusters with $n \leq 12$, obtained by the laser ablation technique on carbon rods with high ^{13}C enrichment.

Species	Mode	^{12}C Band	Single ^{13}C Shifts	^{13}C Band	Single ^{12}C Shifts
C_7	ν_4	2128.1	2127.8*, 2124.7, 2118.9, 2095.5	2045.9	2046.3*, 2058.8, 2074.7, 2081.9*
C_8	ν_5	2071.4	2070.3, 2061.7, 2059.3, 2067.9	1988.0	1990.6, 2006.4, 2016.8, 2009.6
	ν_6	1710.5	1702.4, 1696.2, 1705.7, 1701.9	1644.2	1652.7, 1655.3, 1648.2, 1651.1
C_9	ν_6	1998.2	1993.5, 1978.2, 1984.9, 1997.9*, 1994.5*	1921.1	1925.5, 1941.0, 1931.7, 1921.2*, 1923.4
	ν_5	2078.2	2077.9*, 2077.1, 2075.7, 2053.7, 2048.7	1998.0	1998.4*, 1999.1, 2000.6, 2015.6, 2033.1
	ν_7	1601.0	1593.0, 1595.0, 1590.8, 1600.4, 1585.8	1538.9	1547.0, 1543.7, 1548.2, 1539.4, 1552.6
C_{10}	ν_6	2074.2	2073.4, 2071.6, 2063.3, 2060.6, 2072.3	1991.7	1993.1, 1999.8, 2014.1, 2012.2, 1999.1*
	ν_7	1915.7	1912.1, 1895.5, 1913.5*, 1906.7, 1909.8	1841.0	1846.8, 1856.8, 1842.4*, 1848.4, 1844.9

C ₁₁	v ₇	1946.1	1946.0*,1945.4, 1939.9,1938.6, 1942.5*,1940.6	1870.9	1871.1*,1879.9, 1881.4,1887.2, 1882.3,1874.9
	v ₈	1856.7	1850.6*,1840.0, 1856.4*1846.5, 1856.1*,1842.1	1784.7	1790.0,1797.9, 1784.9*1792.9, 1785.2, 1797.3
	v ₈	1360.0	1353.2,1359.6*, 1350.4,1356.0, 1357.5, 1350.0*		
C ₁₂	v ₇	2140.6	2140.6*,2140.5*, 2134.5,2123.8, 2126.3,2136.7	2058.6	2058.5*,2058.6*, 2063.4,2070.0, 2074.7,2061.3
	v ₈	1997.3	1994.9*,1983.6, 1981.6,1996.8, 1991.5,1995.7	1920.5	1923.8,1937.8, 1932.6, 1920.9* 1925.5, 1923.4
	v ₉	1817.9	1811.8,1805.1, 1814.7, 1811.0 1813.4, 1812.6	1748.2	1754.7,1757.3, 1750.0, 1755.4 1752.4, 1753.6
C ₁₅	v ₁₀	1999.3	1999.2*,1998.7, 1993.4* 1990.6 1995.2, 1996.7, 1986.7,1980.8	1922.3	1922.4*,1922.9, 1927.0,1929.2, 1925.2,1925.1, 1930.6,1940.7
C ₁₈	v ₁₂	2001.0	2000.9*,1993.91 990.6,1987.6, 1990.8*,1997.5, 1991.8*,1994.1, 1996.2	1924.4	1924.5*,1924.8* 1927.6*,1927.9, 1926.7, 1927.4, 1926.4,1928.7, 1925.8

Note 1: The frequencies marked with an * are the calculated values for which the corresponding observed value is founded to be overlapped.

9.3 Future work

It is of fundamental importance to continue with the use of the experimental techniques developed during this work, that have given as result, a much better procedure for obtaining the full substituted $^{13}\text{C}_n$ and $^{12}\text{C}_n$ carbon chains and the single ^{12}C -substituted ($^{12}\text{C}^{13}\text{C}_{n-1}$) or single ^{13}C -substituted ($^{13}\text{C}^{12}\text{C}_{n-1}$) carbon clusters. In conjunction with DFT theoretical calculations and the application of the deperturbation method it is possible to continue with the studies on linear long C_n ($n \geq 13$) species. The measurement of frequencies for both $^{13}\text{C}_n$ and $^{12}\text{C}_n$ carbon chains for long C_n ($n \geq 11$) has stimulated new theoretical studies by Rittby that take into consideration anharmonic effects¹⁰³. Those studies will help in the correct assignment of the fundamentals of a C_n molecule. There is a series of unidentified observed bands in Table XXVI that can be immediately submitted to the scrutiny of this methodology.

TABLE XXVI. Observed unknown bands (cm^{-1}) of $^{12}\text{C}_n$ species and the corresponding $^{13}\text{C}_n$ species scaled via

$$\nu(^{12}\text{C}) = \sqrt{\frac{13.0}{12.0}}[\nu(^{13}\text{C})]$$

Observed Unknown bands $^{12}\text{C}_n$	Scaled Unknown bands $^{13}\text{C}_n$
2050.6	1970.7
2050.4	1970.5
2034.4	1955.2
2011.0	1932.7
1997.9	1920.1
1969.0	1892.3
1964.7	1888.2
1803.6	1733.3
1746.2	1678.2
1282.0	1232.1
1244.1	1195.6
1206.2	1159.2
1100.1	1057.2
1064.2	1022.7
922.8	886.9
903.9	868.7
736.5	707.8
666.2	640.2

9.3.1 Future work on cyclic C_n molecules

The research on linear carbon clusters with up to 18 atoms is now more accessible because of the present fruitful investigations carried during this dissertation research. The ground state structures of many vibrational fundamentals have been firmly established experimentally by matrix isolation FTIR isotopic studies with the help of DFT calculations and the deperturbation method. However, only a few spectroscopic observations of pure cyclic carbon clusters such as cyclic C_6 (Ref.29) and cyclic C_8 (Ref.30) have ever been reported, even

though cyclic geometries are generally preferred as the lowest energy structures for C_n ($n \geq 10$) molecules. The previous identification of the vibrational fundamentals of cyclic C_6 and cyclic C_8 was accomplished with using the single ^{13}C -substituted ($^{13}\text{C}^{12}\text{C}_{n-1}$) carbon clusters. In light of the present work it is interesting to ask if it is possible to observe the “mirrored” single ^{12}C -substituted ($^{12}\text{C}^{13}\text{C}_{n-1}$) isotopomers for cyclic molecules, and furthermore, if it is possible to observe other cyclic C_n species.

The answer to these important questions is certainly a subject for a future research. Preliminary observations in the present work, however, suggest the set of frequencies recommended for further investigation Table XXVII.

TABLE XXVII. Proposed frequencies (cm^{-1}) for cyclic C_n carbon chains recommended for future study.

Species	Mode	$^{12}\text{C}_n$	$^{13}\text{C}_n$
$c\text{-C}_4$	$\nu_1(\text{b}_{1u})$	1380.8?	
$c\text{-C}_6$	$\nu_4(\text{e}^?)$	1694.9 ¹	1630.5
$c\text{-C}_8$	$\nu_{12}(\text{e}_u)$	1844.2 ²	1774.4
$c\text{-C}_{10}$	$\nu_4(\text{e}_1^?)$	2052.0	1972.9
$c\text{-C}_{15}$	$\nu_{30}(\text{b}_2)$	1473.9	1416.6
$c\text{-C}_{18}$	ν_{24}	1935.9	1862.3

^{1,2} S.L Wang *et al.*^{29,30}

Appendix A. DEPERTURBATION METHOD (DPM)

The following is a summary of the method developed by García and Rittby. (see Ref. 47). A system with two-energy level system that representing two vibrational modes has unperturbed energies $E_1^{(0)}$ and $E_2^{(0)}$ ($= \hbar\omega_2^{(0)}$) respectively and corresponding eigenvectors $|\phi_1\rangle$ and $|\phi_2\rangle$.

Then the system can be described by

$$\begin{aligned} H_0 |\phi_1\rangle &= E_1^{(0)} |\phi_1\rangle \\ H_0 |\phi_2\rangle &= E_2^{(0)} |\phi_2\rangle \end{aligned} \quad \text{A.1}$$

where H_0 is an unperturbed Hamiltonian. Introducing a positive perturbation W^+ (add mass) or a negative perturbation W^- (subtract mass), where

$$W^+ = \begin{bmatrix} W_D & W_{12} \\ W_{21} & W_D \end{bmatrix} \quad \text{A.2}$$

$$W^- = \begin{bmatrix} -W_D & -W_{12} \\ -W_{21} & -W_D \end{bmatrix} \quad \text{A.3}$$

it can be shown that the energies of the two-level system subjected to the positive perturbation W^+ (add mass) are given by:

$$\begin{aligned} E_1^+ &= E_1^{(0)} + W_D + \frac{|W_{12}|^2}{E_1^{(0)} - E_2^{(0)}} \\ E_2^+ &= E_2^{(0)} + W_D - \frac{|W_{12}|^2}{E_1^{(0)} - E_2^{(0)}} \end{aligned} \quad \text{A.4}$$

Similar expressions apply for a negative perturbation W^- (subtract mass):

$$E_1^- = E_1^{(0)} - W_D + \frac{|W_{12}|^2}{E_1^{(0)} - E_2^{(0)}}$$

A.5

$$E_2^- = E_2^{(0)} - W_D - \frac{|W_{12}|^2}{E_1^{(0)} - E_2^{(0)}}$$

The resulting energy levels are shown in Fig. 1.[†]

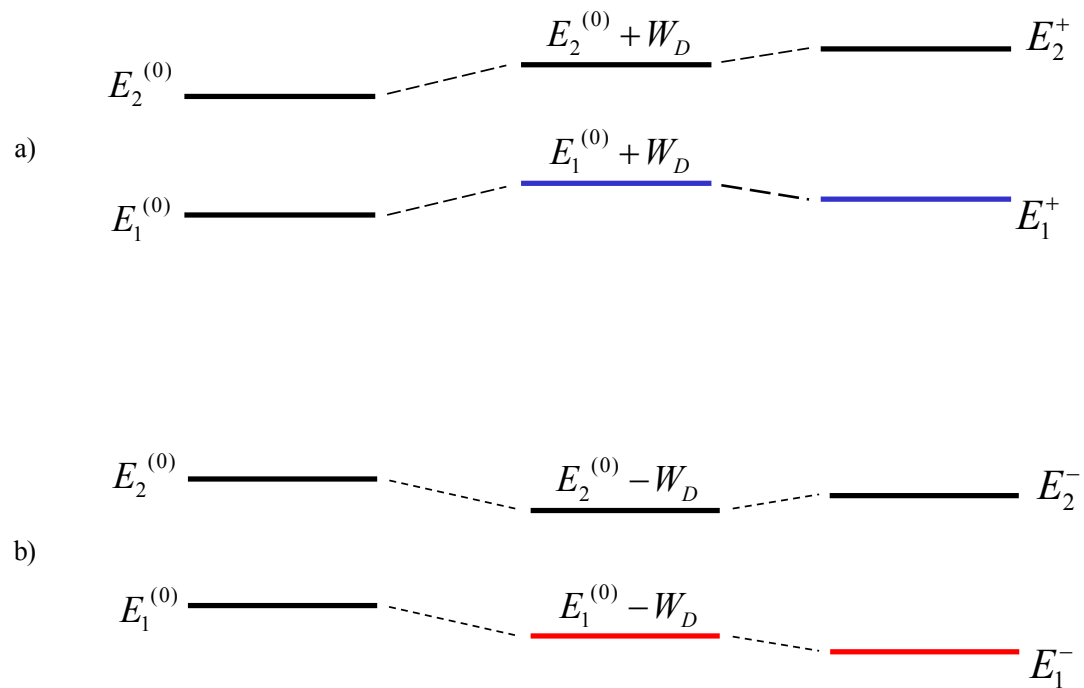


Fig. 1. Energy corrections to first (middle) and second order (right) in perturbation theory after the system is subjected to a positive perturbation (a) W^+ (adding mass) and to a negative perturbation (b) W^- (subtracting mass) (Fig. courtesy of G. García)

[†] Courtesy of G. García

The third term $\frac{|W_{12}|^2}{E_1^{(0)} - E_2^{(0)}}$ in Eq. A.4 and A.5 produces a “repulsive effect” between the perturbed energy levels E_1^+ and E_2^+ due to the coupling between the levels $E_1^{(0)}$ and $E_2^{(0)}$. The effect of the perturbation is significant when $\Delta E = E_1^{(0)} - E_2^{(0)}$ is small or the magnitude of the matrix element W_{12} is large.

If measurements of the perturbed energies E_1^+ and E_1^- have been made, the DPM uses the fact that the effects of interaction with the energy level E_2 on the energies E_1^+ and E_1^- can be eliminated by “reflecting” or “mirroring” the energy E_1^- to produce an energy $E_{1,m}^-$ and then averaging with the energy E_1^+ to give an average energy E_{AVG} (see Fig. 2).[‡]

[‡] Courtesy of G. García

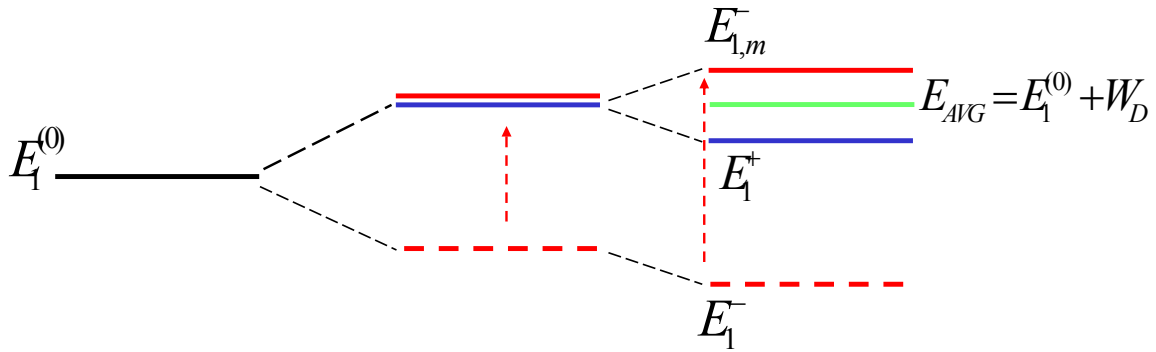


Fig. A.2. Elimination of the coupling effects of E_2 on E_1^+ and E_1^- by “mirroring” the energy E_1^- and taking the average between the “mirrored” energy $E_{1,m}^-$ and the energy E_1^+ . (Fig. courtesy of G. García)

The average energy E_{AVG} (see Eq. A.8) resulting from this process is equal to the first order energy. The interaction arising from the second order terms has been eliminated.

$$E_{AVG} = \frac{E_1^{(0)} + W_D + \frac{|W_{12}|^2}{E_1^{(0)} - E_2^{(0)}} + E_1^{(0)} + W_D - \frac{|W_{12}|^2}{E_1^{(0)} - E_2^{(0)}}}{2} = E_1^{(0)} + W_D \quad \text{A.6}$$

It is clear now that E_{AVG} has no dependence on any other nearby levels.

-
- ¹W. Weltner, Jr and R. J. Van Zee, Chem. Rev. **89**, 1713 (1989) and references therein.
- ²J. M. L. Martin, J. P. François, and R.J. Gijbels, Mol. Struct. **294**, 21 (1993)
- ³A.V. Orden, R.J.Saykally, Chem. Rev. **98**, 2313 (1998) and references therein.
- ⁴L. Začs, R.Spēlmanis, F. A. Musaev, G. A. Galazutdinov, Mon. Not. R. Astron. Soc. **339**,460(2003)
- ⁵Maier, J. P., Bguslavskiy A. E., Ding, H., Walker, G.A.H., & Bohlender, D.A. 2006 ApJ., **640**, 369
- ⁶Maier, J. P., Lankin, N. M., Walker, G.A.H., & Bohlender, D.A. 2001 ApJ. 2004, **566**, 332
- ⁷F.C. Gillett, W.J. Forrest, and K.M. Merrill, Ap.J., 183 (1973) 87
- ⁸Allamandola, L. J., Tielens, A. G. G. M., & Barker, J. R. (1985). *Astrophys. J.* **290**, 25
- ⁹Allamandola, L. J., Tielens, A. G. G. M., & Barker, J. R. (1989). *Ap.J. Suppl. Ser.* **71**, 733
- ¹⁰Allamandola, L.J., Bregman, J.D., Sandford, S.A., Tielens, A.G.G.M., Witteborn, F.C., Wooden, D.H., & Rank, D. (1989). Ap. J. **345**, L59.
- ¹¹Allamandola, L. J., Hudgins, D. M., & Sandford, S. A. (1999). *Astrophys. J. (Letters)* **511**, 115
- ¹²Allamandola, L. J., Hudgins, D. M., Bauschlicher, Jr., C. W., & Langhoff, S. R. (1999). *Astron. Astrophys.* **352**, 659-664.
- ¹³Allamandola, L. J., Bernstein, M. P., Sandford, S. A., & Walker, R. L. (1999). Evolution of Interstellar Ices. In Composition and Origin of Cometary Materials, International Space Science Institute Book Series, Vol. 8, Space Science Reviews 90, #1-2, K. Altwegg, P. Ehrenfreund, J. Geiss, & W. Huebner (eds.), (Kluwer Academic Publishers: Dordrecht), pp. 219-232.
- ¹⁴J. Hunter, J. Fye, and M.F. Jarrold, , J. Chem. Phys. **99**, 1785 (1993)
- ¹⁵G.V. Helden, N.G. Gotts, andM.T. Bowers, J. Am. Chem. Soc. **115**,4363 (1993).
- ¹⁶C.-H. Kian and W.A. Goddard III, Phys. Rev. Lett. **76**, 2515 (1996)

-
- ¹⁷ J. Karolczak, W.W. Harper, R.S. Grev, and D. J. Clouthier, *J. Chem. Phys.* **103**, 2840 (1995).
- ¹⁸ O. Leifeld, R. Hartmann, E. Miller, E. Kaxiras, K. Kern, and D. Grützmacher, *Nano.* **10**, 122 (1999).
- ¹⁹ O. Leifeld, R. Hartmann, E. Miller, E. Kaxiras, K. Kern, and D. Grützmacher, *Appl. Phys. Lett.* **74**, 994 (1999).
- ²⁰ R. Hartmann, U. Gennser, H. Sigg, K. Ensslin, and D. Grützmacher, *Appl. Phys. Lett.* **73**, 1257 (1998).
- ²¹ J. Karolczak, W.W. Harper, R.S. Grev, and D. J. Clouthier, *J. Chem. Phys.* **103**, 2840 (1995).
- ²² O. Leifeld, R. Hartmann, E. Miller, E. Kaxiras, K. Kern, and D. Grützmacher, *Nano.* **10**, 122 (1999).
- ²³ O. Leifeld, R. Hartmann, E. Miller, E. Kaxiras, K. Kern, and D. Grützmacher, *Appl. Phys. Lett.* **74**, 994 (1999).
- ²⁴ R. Hartmann, U. Gennser, H. Sigg, K. Ensslin, and D. Grützmacher, *Appl. Phys. Lett.* **73**, 1257 (1998).
- ²⁵ J. D. Presilla-Márquez, C. M. L. Rittby and W. R. M. Graham, *J. Chem. Phys.* **106**(20), 8367 (1997)
- ²⁶ S. Wang, Ph.D. Dissertation, TCU (1997)
- ²⁷ R. H. Kranze and W. R. M Graham, *J. Chem. Phys.* **98** 71 (1993)
- ²⁸ D.L Robbins, Ph.D. Dissertation, TCU (2002)
- ²⁹ S. L Wang, C. M. L. Rittby, and W. R. M Graham, *J. Chem. Phys.* **107** (16) 6032 (1997)
- ³⁰ S. L Wang, C. M. L. Rittby, and W. R. M Graham, *J. Chem. Phys.* **107** (18) 7025 (1997)
- ³¹ S. L Wang, C. M. L. Rittby, and W. R. M Graham, *J. Chem. Phys.* **112** (3) 1457 (1999)
- ³² D.L Robbins, Ph.D. Dissertation, TCU (2002) and the references therein

-
- ³³ E. Whittle, D. A. Downs, G. C. Pimentel, J. Chem. Phys. **22** 1943 (1954)
- ³⁴ I. Norman and G. Porter, *Nature*, **174**, 508 (1954)
- ³⁵ X.D. Ding, S.L. Wang, W.R.M. Graham, and C.M.L. Rittby, J. Chem. Phys. **110**, 11214 (1999), and references cited therein.
- ³⁶ D.L. Robbins, C.M.L. Rittby, and W.R.M. Graham, J. Chem. Phys. **114**, 3570 (2001)
- ³⁷ D.L. Robbins, C.M.L. Rittby, and W.R.M. Graham, J. Chem. Phys. **120**, 4664 (2004)
- ³⁸ D.L. Robbins, C.M.L. Rittby, and W.R.M. Graham, J. Chem. Phys. **117**, 3811 (2002)
- ³⁹ R. Cárdenas, Prethesis (2005)
- ⁴⁰ (Non published work by C. M. L. Rittby)
- ⁴¹ R. H. Kranze and W. R. M Graham, J. Chem. Phys. **103** 13 (1996)
- ⁴² K. R Thompson, R. L. DeKock, and W. W. Weltner, Jr., J. Am. Chem. Soc. **93**, 4688 (1971)
- ⁴³ R. H. Kranze, P.A. Whitey, C. M. L. Rittby, and W. R. M Graham, J. Chem. Phys. **103**(16) 6841 (1995)
- ⁴⁴ X.D. Ding, S. L. Wang, C. M. L. Rittby and W. R. M. Graham, J. Chem. Phys. **112**(11), 5113 (1999)
- ⁴⁵ E. Gonzalez, prethesis (2007)
- ⁴⁶ C. M. L Rittby (not published work)
- ⁴⁷ Handbook of Carbon, Graphite, Diamond and Fullerenes. By Pierson, H.O (1993) William Andrew Publishing/Noyes
- ⁴⁸ G. García, prethesis (2007)
- ⁴⁹ J.D. Presilla-Márquez and W.R.M. Graham, J. Chem. Phys. **100**, 181 (1994); C.M.L. Rittby, *ibid.*, **100**, 175 (1994)
- ⁵⁰ J.D. Presilla-Márquez, S.C. Gay, C.M.L. Rittby, and W.R.M. Graham, J. Chem. Phys. **102**,

6354 (1995)

- ⁵¹J.D. Presilla-Márquez, C.M.L. Rittby, and W.R.M. Graham, *J. Chem. Phys.* **104**, 2818 (1996)
- ⁵²X.D. Ding, S.L. Wang, C.M.L. Rittby, and W.R.M. Graham, *J. Phys. Chem. A* **104**, 3712 (2000)
- ⁵³R.E. Kinzer, C.M.L. Rittby, and W.R.M. Graham, *J. Chem. Phys.*, *submitted* (2006)
- ⁵⁴Le Bertre T., 1990, *A&A*, 236,472
- ⁵⁵F.C. Gillett, W.J. Forrest, and K.M. Merrill, *Ap.J.*, 183 (1973) 87
- ⁵⁶M. Kertsz, J. Koller, A. Ažman and W. R. M Graham, *J. Chem. Phys.* **68** (6) 2779 (1978)
- ⁵⁷W. Zhong, D. Tománek, George F. Bertsch, *Solid State Communications*, Vol. 86, No. 9, pp 607-612, 1993
- ⁵⁸A. Abdurahman, A. Shukla, M. Dolg, *Phys. Rev. B* **65**, 115106 (2002)
- ⁵⁹Á. Rusznyák, V. Zólyomi, S. Yang, M. Kertesz, *Phys. Rev. B* **72**, 155420 (2005)
- ⁶⁰J. Karolczak, W.W. Harper, R.S. Grev, and D. J. Clouthier, *J. Chem. Phys.* **103**, 2840 (1995)
- ⁶¹O. Leifeld, R. Hartmann, E. Miller, E. Kaxiras, K. Kern, and D. Grützmacher, *Nano*. **10**, 122 (1999)
- ⁶²O. Leifeld, R. Hartmann, E. Miller, E. Kaxiras, K. Kern, and D. Grützmacher, *Appl. Phys. Lett* **74**, 994 (1999)
- ⁶³R. Hartmann, U. Gennser, H. Sigg, K. Ensslin, and D. Grützmacher, *Appl. Phys. Lett.* **73**, 1257(1998)
- ⁶⁴J. Karolczak, W.W. Harper, R.S. Grev, and D. J. Clouthier, *J. Chem. Phys.* **103**, 2840 (1995)
- ⁶⁵J. Hunter, J. Fye, and M.F. Jarrold, *J. Chem. Phys.* **99**, 1785 (1993)
- ⁶⁶G.V. Helden, N.G. Gotts, and M.T. Bowers, *J. Am. Chem. Soc.* **115**, 4363 (1993)
- ⁶⁷C.-H. Kian and W.A. Goddard III, *Phys. Rev. Lett.* **76**, 2515 (1996)

-
- ⁶⁸ R. H. Kranze and W. R. M Graham, *J. Chem. Phys.* **103** 13 (1996)
- ⁶⁹ K. R Thompson, R. L. DeKock, and W. W. Weltner, Jr., *J. Am. Chem. Soc.* **93**, 4688 (1971)
- ⁷⁰ R. H. Kranze, P.A. Whitey, C. M. L. Rittby, and W. R. M Graham, *J. Chem. Phys.* **103**(16) 6841 (1995)
- ⁷¹ J. R. Heath and R. J. Saykally, *J. chem. Phys.* **94**, 1724, (1991)
- ⁷² J. R. Heath, A. van Orden, E. Kuo, and R. J Saykally, *Chem. Phys. Lett.* **182**, 17 (1991)
- ⁷³ R. H. Kranze and W. R. M Graham, *J. Chem. Phys.* **105** 13 (1996)
- ⁷⁴ Gaussian 03, Revision A.1, M. J. Frisch, G. W. Trucks, H. B. Schlegel, G. E. Scuseria, M. A. Robb, J. R. Cheeseman, J. A. Montgomery, Jr., T. Vreven, K. N. Kudin, J. C. Burant, J. M. Millam, S. S. Iyengar, J. Tomasi, V. Barone, B. Mennucci, M. Cossi, G. Scalmani, N. Rega, G. A. Petersson, H. Nakatsuji, M. Hada, M. Ehara, K. Toyota, R. Fukuda, J. Hasegawa, M. Ishida, T. Nakajima, Y. Honda, O. Kitao, H. Nakai, M. Klene, X. Li, J. E. Knox, H. P. Hratchian, J. B. Cross, C. Adamo, J. Jaramillo, R. Gomperts, R. E. Stratmann, O. Yazyev, A. J. Austin, R. Cammi, C. Pomelli, J. W. Ochterski, P. Y. Ayala, K. Morokuma, G. A. Voth, P. Salvador, J. J. Dannenberg, V. G. Zakrzewski, S. Dapprich, A. D. Daniels, M. C. Strain, O. Farkas, D. K. Malick, A. D. Rabuck, K. Raghavachari, J. B. Foresman, J. V. Ortiz, Q. Cui, A. G. Baboul, S. Clifford, J. Cioslowski, B. B. Stefanov, G. Liu, A. Liashenko, P. Piskorz, I. Komaromi, R. L. Martin, D. J. Fox, T. Keith, M. A. Al-Laham, C. Y. Peng, A. Nanayakkara, M. Challacombe, P. M. W. Gill, B. Johnson, W. Chen, M. W. Wong, C. Gonzalez, and J. A. Pople, Gaussian, Inc., Pittsburgh PA, 2003.
- ⁷⁵ X. D. Ding, S. L. Wang, C. M. L. Rittby, and W. R. M. Graham, *J. Chem. Phys.* **112**, 5113 (2000).

-
- ⁷⁶ R. H. Kranze, P. A. Withey, C. M. L. Rittby, and W. R. M. Graham, *J. Chem. Phys.* **103**, 6841 (1995).
- ⁷⁷ L.N. Shen, T.J. Doyle, and W.R.M. Graham, *J. Phys. Chem.* **93**, 1597 (1990).
- ⁷⁸ M. Vala, T. M. Chandraskhar, J. Szczepanski, R. Van Zee, and R. W. Weltner, Jr., *J. Chem. Phys.* **90**, 595 (1989)
- ⁷⁹ R. H. Kranze and W. R. M. Graham, *J. Chem. Phys.* **96** 4 (1992)
- ⁸⁰ W. Weltner, Jr and R. J. Van Zee, *Chem. Rev.* **89**, 1713 (1989) and references therein.
- ⁸¹ K. R. Thompson, R. L. DeKock, and W. W. Weltner, Jr., *J Am. Chem. Soc.* **93**, 8850 (1990)
- ⁸² J. M. L. Martin, J. P. François, and R. Gijbels, *J. Chem. Phys.* **93** 8850 (1990)
- ⁸³ P. Freivogel, M. Grutter, D. Forney, J. P. Maier, *Chem. Phys.* **216** 401 (1997)
- ⁸⁴ J. Szczepanski, S. Eckern, C. Chapo, M. Vala, *Chem. Phys.* **211** 359 (1999)
- ⁸⁵ R. H. Kranze, P.A. Whitey, C. M. L. Rittby, and W. R. M. Graham, *J. Chem. Phys.* **103**(16) 6841 (1995)
- ⁸⁶ (Dr. C. M. Rittby's non published theoretical work)
- ⁸⁷ P. Freivogel, M. Grutter, D. Forney, J. P. Maier, *Chem. Phys.* **216**, (1997)401
- ⁸⁸ R.H. Kranze, C.M.L. Rittby, and W.R.M. Graham, *J. Chem. Phys.* **98**, 71 (1993).
- ⁸⁹ R. H. Kranze and W. R. M. Graham, *J. Chem. Phys.* **105** 13 (1996)
- ⁹⁰ P. Freivogel, M. Grutter, D. Forney, J. P. Maier, *Chem. Phys.* **216**, (1997)401
- ⁹¹ D. Forney, M. Grutter, P. Freivogel, and J. P. Maier, *Proc. 10th Internat. Sympos. Atomic, Molecular, cluster. Ion, and Surface Physics*, J. P. Maier and M. Quack, Eds., Engelberg, Switzerland (1996)
- ⁹² M. E. Jacox, *J. Phys. Chem. Ref. Data*. Vol. 32, No. 1, 2003
- ⁹³ J. Szczepanski, S. Eckern, C. Chapo, M. Vala, *Chem. Phys.* **211** 359 (1999)

-
- ⁹⁴ L. Lapinsky, M. Vala, Chem. Phys. Lett **300**, (1995)195
- ⁹⁵ R.H. Kranze, C.M.L. Rittby, and W.R.M. Graham, J. Chem. Phys. **98**, 71 (1992)
- ⁹⁶ J.M.L. Martin, Peter R. Taylor, J. Phys. Chem., **100** (1996) 6047
- ⁹⁷ J. Szczepanski, S. Eckern, C. Chapo, M. Vala, Chem. Phys. **211** 359 (1999)
- ⁹⁸ P. Freivogel, M. Grutter, D. Forney, J. P. Maier, Chem. Phys. **216** 401 (1996)
- ⁹⁹ D. Strelnikov, R. Reusch, W. W. Krätschmer, J. Phys. Chem. A, **109** (2005) 7708
- ¹⁰⁰ X.D. Ding, S. L. Wang, C. M. L. Rittby and W. R. M. Graham, J. Chem. Phys. **112** (11), 5113 (1999)
- ¹⁰¹ G. Monsinger, Ph. D. Thesis, Ruprecht-Karls-Universität, Heidelberg (1995)
- ¹⁰² (C. M. L Rittby non published results)
- ¹⁰³ (C. M. L Rittby non published results)

VITA

Rafael Cárdenas

Personal Background

Born May 26, 1962, Sahuayo Michoacán
The 8th son of a family of 10 daughters and 5 sons of Rafael Cárdenas and Esperanza Espinoza de Cárdenas

Education

June, 1999
B.S., Double major in Physics and Mathematics,
UNIVERSIDAD MICHOACANA DE SAN NICOLAS DE HIDALGO (UMNSH)

May 2002
Master of Science, Physics
UNIVERSITY OF TEXAS AT EL PASO (UTEP)

December, 2007
Doctor of Philosophy, Physics
TEXAS CHRISTIAN UNIVERSITY (TCU)

Honors

May 2001
Physics Scholarship Cook Award for Outstanding Student of the year (UTEP)

May 2002
Nominated for the Outstanding Master's Thesis award (UTEP).

ABSTRACT

INFRARED STUDIES ON THE SPECTRA AND STRUCTURES OF NOVEL CARBON MOLECULES

by Rafael Cárdenas, Ph.D., 2007
Department of Physics and Astronomy
Texas Christian University

Dissertation Adviser:
Dr. W. R. M. Graham, Professor of Physics and Astronomy

Carbon clusters are formed in the laboratory by trapping the products from the Nd-YAG laser evaporation of graphite in argon matrices held at ~ 10 K. Linear carbon chains have been the subject of extensive theoretical and experimental studies over many years and are important in diverse areas as astrophysics, studies of the fullerenes, and the chemistry of fuel combustion. FTIR measurements of vibrational fundamentals and carbon-13 isotopic shifts, coupled with the predictions of theoretical density functional theory calculations and a recently developed theoretical tool, the deperturbation method have been successfully employed to identify long linear C_n ($n \geq 7$) carbon chains. The development of a process to produce carbon rods highly enriched with ^{13}C enabled the observation of well-resolved isotopic spectra of linear $^{13}\text{C}_n$ carbon clusters ($n = 3-18$). The identifications are facilitated by the measurement of both the isotopic pattern for single ^{12}C -substituted ($^{12}\text{C}^{13}\text{C}_{n-1}$) isotopomers and the “mirror” isotopic pattern for single ^{13}C -substituted ($^{13}\text{C}^{12}\text{C}_{n-1}$) isotopomers. As a result of this work it is now routinely possible to achieve experimental reproducibility of isotopic shift patterns, which enables

comparison with theoretical predictions. The combination of experimental improvements and theoretical results, has led to the identification of ^{13}C isotopic shifts for sixteen vibrational fundamentals belonging to eight different long chains, C_n ($n \geq 7$) species. The fundamentals identified include the $\nu_4(\sigma_u) = 2128.1 \text{ cm}^{-1}$ mode of C_7 ; the $\nu_5(\sigma_u) = 2078.2$, $\nu_6(\sigma_u) = 1998.2$, and $\nu_7(\sigma_u) = 1601.0 \text{ cm}^{-1}$ modes of C_9 ; the $\nu_6(\sigma_u) = 2074.2$ and $\nu_7(\sigma_u) = 1915.7 \text{ cm}^{-1}$ modes of C_{10} ; the $\nu_7(\sigma_u) = 1946.1$, $\nu_8(\sigma_u) = 1856.7$, and $\nu_9(\sigma_u) = 1360.0 \text{ cm}^{-1}$ modes of C_{11} ; the $\nu_5(\sigma_u) = 2071.4$ and $\nu_6(\sigma_u) = 1710.5 \text{ cm}^{-1}$ modes of linear C_8 ; the $\nu_7(\sigma_u) = 2140.6$, $\nu_8(\sigma_u) = 997.3$ and $\nu_9(\sigma_u) = 1817.9 \text{ cm}^{-1}$ of linear C_{12} ; the $\nu_{10}(\sigma_u) = 1999.3 \text{ cm}^{-1}$; mode of linear C_{15} ; and the $\nu_{12}(\sigma_u) = 2001.0 \text{ cm}^{-1}$ mode of linear C_{18} . In addition, isotopomer absorptions have been identified for the following modes that are normally IR inactive until isotopic substitution when they become observable: $\nu_1(\sigma_g)$ mode of C_7 , the $\nu_1(\sigma_g)$ mode of C_9 , $\nu_1(\sigma_g)$ and $\nu_2(\sigma_g)$ mode of C_{10} , $\nu_2(\sigma_g)$ and $\nu_1(\sigma_g)$ mode of C_{11} , $\nu_3(\sigma_g)$ $\nu_3(\sigma_g)$ modes C_{15} and the $\nu_3(\sigma_g)$ mode of C_{18} .